On the Prediction of Pelvic Floor Muscle Injury during Vaginal Delivery in Nullipara: Anthropometric and Viscoelastic Biomechanical Analyses

by

Paige V. Tracy

A dissertation submitted in partial fulfillment
of the requirements for the degree of
Doctor of Philosophy
(Biomedical Engineering)
in the University of Michigan
2017

Doctoral Committee:

Professor James A. Ashton-Miller, Co-Chair
Professor John O.L. DeLancey, Co-Chair
Professor Susan V. Brooks Herzog
Professor Alan S. Wineman

voigtpai@umich.edu

ORCID iD: 0000-0002-3004-099X

To my husband, Pat, and to Dip, my canine friend.

Acknowledgements

This dissertation would not have been possible without the support of my co-advisors, Professor James A. Ashton-Miller and Dr. John O.L. DeLancey. I would like to thank both for their being a constant source of inspiration for new research, and for their countless rounds of revisions for parts of this dissertation. I would also like to thank Professor Alan Wineman, for his enthusiasm in working with me through various viscoelastic theories in search of an appropriate fit for a non-traditional material. Without his guidance, the later chapters of this dissertation would not have been possible. I would also like to thank Professor Susan Brooks Herzog for her support and guidance during this dissertation process.

I would like to thank Mark Juravic, and Materna Medical, for their generous access to device distension data from which we were able to quantify for the first time the material properties of the term pregnant human birth canal. Being able to work with such data has been very exciting, and has been a very valuable asset in the development of the later chapters of this dissertation. I would also like to thank Dr. Francisco Orejuela, and the Baylor College of Medicine, for their enthusiasm in working with us to make novel measurements of the pelvic floor essential for Chapter 5 of this dissertation.

Further thanks go to Luyun Chen for her efforts in providing me with a solid foundation early on in this dissertation process. I would also like to thank Shreya Wadhwani, Lahari Nandikanti, Madeleine (Maddie) Wilson, and Elizabeth Strehl for their assistance with literature searches as well as their assistance in completing the thousands of birth simulations that contributed to this dissertation.

The members of the Pelvic Floor Research Group have provided much support and encouragement during this process. Specifically, I would like to thank Katie Kowalk and Julie Tumbarello for their patience and assistance in navigating regulations for clinical studies. I would also like to thank Drs. Jourdan (Jourdie) Triebwasser, Diana Curran, and Carolyn Swenson for contributing their clinical perspectives in helping to keep this work relevant to questions that have the potential to impact future practice.

I would also like to thank Susan Douglas and Maria Steele for their assistance in navigating departmental regulations and required paperwork.

A special thanks goes to Dan Imaizumi Krieger, Kayla Curtis, Kelly Tepper, Sasha Kapshai, Ali Attari, Payam Mirshams Shahshahani, and all of the members of the Biomechanics Research Laboratory for making graduate school an enjoyable and fulfilling experience.

Finally, I would like to thank my family for their support during my entire academic career. I would especially like to thank my parents for their encouragement and support in pursuing my doctoral research. I would also like to thank my grandparents and many younger cousins for their understanding of my absence, and for their inspiration in pursuing this work.

The person who defines my graduate school experience for me is my husband, Pat. I would like to thank him for being there for me every step of the way, with support and unique understanding having gone through much of our graduate school experience together. In addition to his unrelenting understanding and support, especially in staying late for my evening classes without complaint, I would like to thank Pat most for helping me to keep perspective, and for helping me to enjoy and explore the world around us during our time in Michigan.

I am grateful for the financial support of a Rackham Merit Fellowship and a graduate research assistantship funded by Project 1 of the Office for Research on Women's Health (ORWH) Specialized Center of Research, "Birth, Muscle Injury and Pelvic Floor Dysfunction" (P50 HD 44406) at the University of Michigan.

Please note that Chapters 2 – 7 are written in the form of papers to be submitted for publication. Therefore, please excuse any repetition that occurs in the text of these chapters. An abstract of the dissertation may be found on page xxii.

Table of Contents

List of Tables

List of Figures

List of Acronyms

ATLA	Arcus Tendineus Levator Ani
AS	Anal Sphincter
BD	Biparietal Diameter
EAS	External Anal Sphincter
EMRLD	Evaluating Maternal Recovery from Labor and Delivery
FD	Frontooccipital Diameter
ICM	Iliococcygeal Muscle
LA	Levator Ani
MI	Molding Index
MD	Mentovertical Diameter
MPa	MegaPascals
MRI	Magnetic Resonance Imaging
N	Newtons
OC	Occipitofrontal Circumference
PAM	Puboanal Muscle
PB	Perineal Body
PM	Perineal Membrane
PPM	Puboperineal Muscle
PRM	Puborectal Muscle
PVaM	Pubovaginal Muscle
PVM	Pubovisceral Muscle
QLV	Quasilinear Viscoelasticity
SC	Suboccipitobregmatic Circumference
SD	Suboccipitobregmatic Diameter
SL	Soft Tissue Loop Length
SPAA	Subpubic Arch Angle
UGH	Urogenital Hiatus
VBAC	Vaginal Birth After Cesarean Delivery

Abstract

The goal of this research was to provide clinicians with a new framework for preventing pelvic floor muscle tears during vaginal birth. Currently these tears occur in 15% of first time mothers.

In Chapter 2 we developed a theoretical anthropometric model to determine whether a fetal head could pass through the lower birth canal. In Chapter 3 we used a five parameter constitutive model to provide the first quantification of the viscoelastic behavior of the term-pregnant lower birth canal. In Chapter 4, we quantified the 400-fold variation in the longer of the two time constants among a cohort of 25 laboring nullipara. This was incorporated into the theoretical model to predict the length of the second stage of labor and the risk for pelvic floor muscle tear in these nullipara. In Chapter 5, we used secondary data from a clinical trial of the Materna device to test how well the models in Chapter 4 predicted the actual duration of the second stage of labor, and we also quantified the sensitivity and specificity of the pubovisceral muscle (PVM) tear predictions. In Chapter 6, we employed birth simulations to consider the differential effect of forceps and vacuum instrumentation, as well as episiotomy depth, on predicted PVM tear rates and duration of the active second stage of labor. In Chapter 7, we used birth simulation models to consider the effect of pre-distension of the birth canal during the first stage of labor on the predicted duration of the active second stage and on PVM tears.

This dissertation provides a foundation and tool for clinicians to better discuss delivery options antenatally with women in order to prevent pelvic muscle tears, a focus which is generally lacking at present. The next step would be a prospective clinical trial to validate the model predictions.

Chapter 1: On Injury during Vaginal Birth and the Epidemiology of Pelvic Organ Prolapse

1.1 The Epidemiology of a Common Female Pelvic Floor Disorder - Pelvic Organ Prolapse

1.1.1 General Description of Pelvic Organ Prolapse

Pelvic organ prolapse, the descent of the vagina, uterus, bladder or rectum below the pelvic floor, is the most common reason a woman will undergo surgery for adult female pelvic floor disorders. The term "Prolapse" had come into usage by 1706 through the use of terms such as "prolapsus uteri" and "prolapse of the bladder" [1], but the phenomenon was already described as early as 1835 BCE [2].

Today, the occurrence of prolapse has been assessed in three ways: lifetime need for surgery, self-report of symptoms, and physical examination findings. Of these three metrics, we are most certain of lifetime surgery rates for prolapse. A 1997 study quantified this lifetime risk for surgery for prolapse at 7% [3]. However, more recent studies suggest this value to be closer to 12 – 20% [4, 5, 6, 7]. The next most reliable metric appears to be the self-reporting of symptoms resulting in prevalence rates of 4 – 13% [8, 9, 10, 11, 12, 13, 14], which are much

lower than the values of 30 – 70% prevalence reported on physical examination [15, 16, 17, 18, 19, 14, 20].

Physical examination studies tend to over-report prolapse rates, because current classifications label some women as having prolapse (i.e., those with Stage I and some of women with Stage 2) despite these findings being within the normal range. Prolapse and its symptoms are present if the most distal portion of the prolapsing tissue is below the hymen, [21, 22], making it difficult to identify which subset of the reported women had prolapse below the hymen. Of the handful of studies which report physical examination findings, two do not specify the extent of prolapse [15, 17], while another does report stage-specific results, but does not specify location relative to the hymen [16]. The remaining show that there is a distinct cut off in prevalence when prolapse at or below the hymen is considered, with prevalence values decreasing to 7, 18, and 25% [Table 1.1] [18, 19, 14]. It is possible that these values are particularly sensitive to the precise cutoff location relative to the hymen, because the same study that reported a prevalence of 18% when the hymen was inclusively considered reported only 7% prevalence when considering only cases distinctly below the hymen, but still within the Stage II categorization [14]. Stage III prolapse, wherein the most distal portion of the prolapse lies more than 1 cm below the level of the hymen, has been shown to have the strongest correlation to self-reported symptoms [23, 24, 25].

	Threshold for Diagnosis				
Study	**Stage I**	**Stage II (inclusive)**	**≤ Hymen (inclusive)**	**Below the Hymen**	**Stage III**
Slieker-ten Hove *et al.* 2009, [14]	76%	40%	18%	7%	5%
Trowbridge *et al.* 2008, [20]	91%	70%			2%
Swift *et al*. 2005, [19]	76%	37%	7%		2%
Nygaard *et al.* 2004, [18]	98%	65%	25%		2%

Table 1.1 - Reported prolapse prevalence values corresponding to minimum threshold criteria for diagnosis based on staging system and position of the most distal portion of the prolapsing tissue relative to the hymen

1.1.2 What Causes Prolapse?

As early as 1773, "falling of the womb" was attributed to childbirth [26]. Even though the time delay between a woman's first vaginal delivery and the onset of symptoms is typically be 20 – 35 years the relationship is so strong that this fact was already obvious at that time. [27, 28].

In 1968, the hypothesized link to childbirth was first quantified through correlations between parity, fetal head size, and prolapse surgery rates [29]. Since then, it has been observed that prolapse risk continues to increase with additional vaginal births, with odds ratios for levator muscle tears relative to nulliparous of at least 1.9 for first, 2.49 for the second, from 3.55 for the third, and 4.86 – 10.8 for the fourth or greater vaginal delivery [29, 30, 31, 32, 33, 34, 15, 35, 36, 8] [9, 16, 37, 17, 38, 18, 39, 40, 19, 10] [41, 42, 11, 43, 12, 13, 44, 45, 46, 47] [48, 49, 50, 27, 51, 52, 53, 54]. Additionally, high fetal birth weights have been reported as a risk factor for later development of prolapse [29, 15, 35, 37, 19, 55], while C-sections have consistently shown a protective effect, with odds ratios of 0.1 – 0.7 relative to at least one vaginal delivery [34, 36,

56, 40, 57, 41, 11, 44, 46, 47] [48, 50, 27, 5, 58, 51, 55, 53, 59]. Although this strong relationship between prolapse and birth has been demonstrated, the mechanism by which birth results in prolapse has been unknown. This review will discuss the role of levator ani muscle tears as one of the missing links in the causal relationship between birth and prolapse.

1.2 Levator Ani Tears

1.2.1 Levator - Prolapse Link

A link between childbirth, abnormal levator muscle origin anatomy, and prolapse, was observed in 1889 and again in 1907 in anatomical studies of cadavers with prolapse [60, 61]. Whether or not levator injury played a role in prolapse was controversial during most of the 20th century. In the late 20th century, the role of levator ani muscles in supporting pelvic organs in order to prevent prolapse received renewed interest [62]. Magnetic resonance imaging (MRI) and ultrasound studies allowed the muscles to be visualized for the first time, allowing a link between levator tear and prolapse to be consistently demonstrated [63, 64, 65, 66, 67, 68, 69, 70, 71, 72] [73, 74, 75, 76, 28, 77, 78, 79, 80].

1.2.2 Levator Tear - Birth Link

The hypothesis that levator tears were a missing causal link between vaginal delivery and prolapse was further supported by studies which considered correlations between the occurrence of levator ani injuries and birth. In the mid-20th century, palpation based studies of women following delivery reported levator trauma rates of 31% in "clinic" and 12% in private patient service births, the latter involving slow delivery assisted by forceps in conjunction with early episiotomy [81, 82]. An early MR imaging study also observed levator tears in 1 of 14

recent mothers 6 months after delivery [83]. This trend was substantiated in a larger 2003 study, showing that these defects were visible on MRI after vaginal birth, but not in nulliparous women [84]. Further studies of this relationship between levator ani tears and birth reported prevalence values of 13 - 39% following vaginal delivery [85, 64, 86, 70, 87, 88, 72, 73, 89, 90] [91, 92, 93, 94, 95, 96, 97, 98, 99, 100] [101, 102, 103, 104], with 0% tear rates consistently reported for C-section groups [105, 88, 73, 89, 90]. This appears to suggest a mechanical relationship between delivery of the fetus and the levator tear. So, a primary focus of this dissertation is to try to use biomechanical models to predict and prevent levator ani tears, given the strength of the causal pathway between vaginal birth, levator injury, and subsequent prolapse.

1.2.3 Exceptions to the Levator Ani Tear - Prolapse Link

Despite the literature describing a relationship between levator tears and prolapse, not all prolapse cases can be explained by levator tears because these tears are only reported in 32 - 83% of prolapse cases [66, 68, 28, 79, 106, 77]. The strongest links to levator ani tears have been shown for prolapse of the anterior and central compartments, such as cystocele and uterine prolapse [64, 69, 70, 74]. The fact that most studies show major levator injury in only 50 to 60% of cases means that in 40% to 50% prolapse occurs despite a lack of major levator tear. Just how levator ani tears are related to the later development of prolapse therefore remains an open question, but for some at least, a levator tear appears to be important.

1.2.4 Why are Levator Ani Tears Related to Prolapse?

As early as 1889, Dickinson had proposed that the levator ani muscles play an important role in providing support to the pelvic organs [61]. This proposed supportive role for the levator ani muscles carried through studies into the mid-20th century [107, 108, 109, 60].

For example, in 1953, Berglas and Rubin used radiographic imaging to demonstrate the role of levator ani muscles in maintaining pelvic organ positioning and suggested that a change in this role may be important in explaining pelvic organ prolapse [110].

1.2.5 Anatomical Description of Birth with Relevance to Levator Ani Tears

We now turn to the anatomic relationships necessary for understanding the second stage of labor. A recent detailed review of the anatomy of female pelvic floor structures may be found in Chapter 2 of the book entitled Biomechanics of the Pelvic Floor [111].

The levator ani muscles comprise the majority of the 'U-shaped' soft tissue pelvic floor which originates from the anterior portions of the bony pelvis and the arcus tendinous levator ani [Figure 1.1] and insert centrally and more distally on structures on or near the midline to surround a central opening called the levator hiatus. The levator ani are comprised of several contiguous subdivisions; the pubovisceral muscle (also known as the pubococcygeal muscle), the puborectal muscle and the iliococcygeal muscle portions [Figure 1.1].

Stationary Anatomy

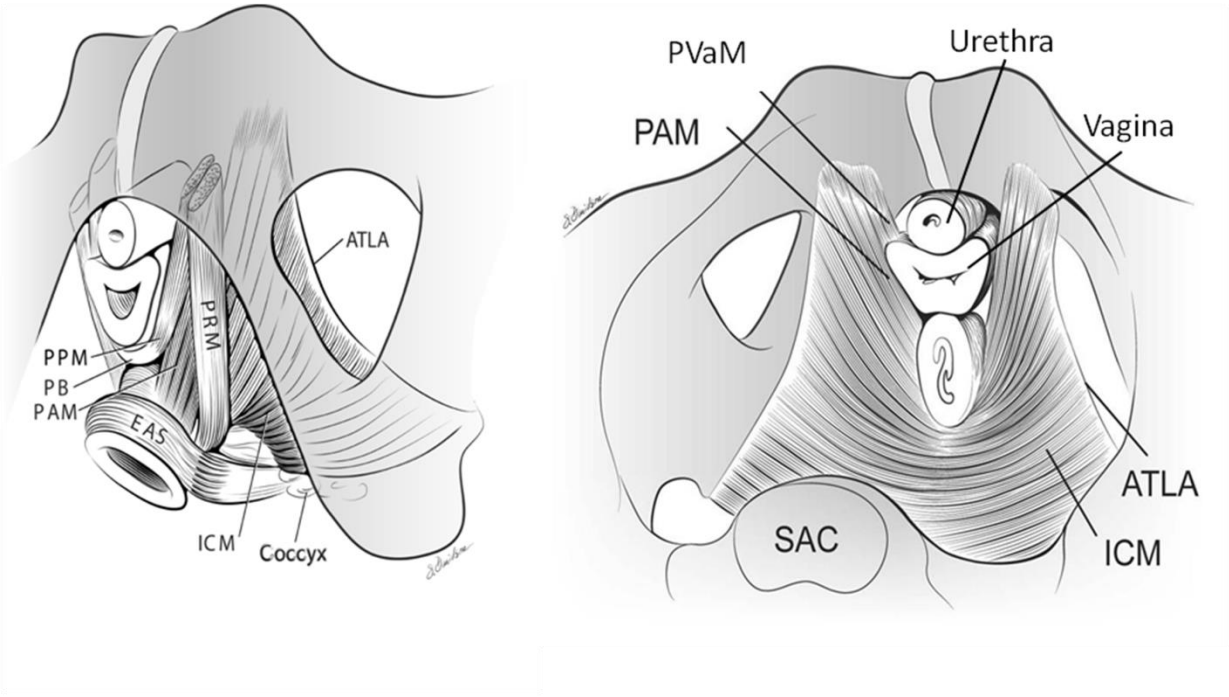

Figure 1.1 - Schematic illustration of the levator ani muscles. The subcomponents of the pubovisceral muscle (puboperineal, PPM; puboanal, PAM, and pubovaginal, PVaM) are shown. *Left:* Schematic view of the levator ani muscles from below after the vulvar structures and perineal membrane have been removed showing the arcus tendineus levator ani (*ATLA*); external anal sphincter (*EAS*); puboanal muscle (*PAM*); perineal body (*PB*) uniting the two ends of the puboperineal muscle (PPM); iliococcygeal muscle (*ICM*); puborectal muscle (*PRM*). *Right*: The LA muscle seen from above looking over the sacral promontory (*SAC*) showing the PVaM. The urethra, vagina, and rectum have been transected just above the pelvic floor. (The internal obturator muscles have been removed to clarify levator muscle origins.) Recently, it has become clear that the origin of the PRM lies more caudal than is suggested in the illustration at left, a finding will be revisited in Chapter 2 [112]. Copyright © DeLancey 2003 [113].

The pubovisceral muscle itself also has three components; the pubovaginal, puboperineal, and puboanal portions. These latter three terms reflect the multifaceted insertion of the pubovisceral muscle rather than distinct muscles. For the purposes of this dissertation, they will be considered to form a single muscle. The anterior portion of the upper 'arms' of the U-

shaped levator ani, which are comprised of the pubovisceral muscle, take origin from the pubic rami on either side of the pubic symphysis and insert on the perineal body as well as the lateral margin of the intersphincteric groove on the anterior aspect of the anal sphincter (AS) [112, 113, 114]. This U-shaped loop of tissue, along with the anterior portion of the perineal body and the puborectal muscle (PRM) form the urogenital hiatus (UGH); the UGH is the last portion of the levator ani through which the baby's head must be driven during the second stage of a vaginal birth in order for the head to be delivered.

Movement and Loading of Anatomy during Birth

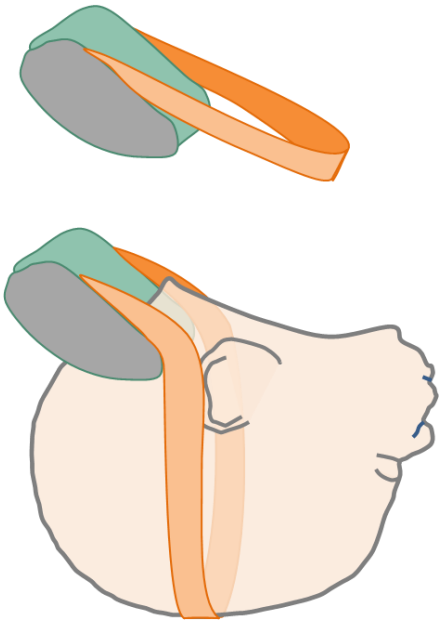

Figure 1.2 - Schematic diagram showing the possibility of the pubovisceral muscle (PVM) wrapping about the inferoposterior aspect of the pubic rami during the second stage of labor. Pubovisceral muscle (orange) originates from the anterior pelvis (green) (A) at rest and (B) stretching to accommodate a fetal head. (Redrawn from Tracy et al. 2016, [115])

When the fetal head passes through the birth canal it is bounded by the anterior pelvis, comprised of the pubic symphysis with pubic rami on either side, and partly by the loop of U-shaped soft tissue, described above, laterally and posteriorly. As the second stage of labor progresses and the baby descends through the birth canal along the curve of Carus, the fetal head comes into contact with the more inferior regions of the pubic rami as well as different regions of the levator ani. As the perineal body is pushed caudally by the fetal head and the pubovisceral muscle (PVM)[1] stretches, the loop of tissue rotates caudally much like a bucket handle would if it were pivoted about hinges placed at the PVM origins on either side of the boney pelvis above [Figure 1.2].

It is during the final moments of labor, as the fetal head "crowns" and passes through the urogenital hiatus in the levator ani muscles, when levator avulsions occur [91, 102].

Additionally, it has been consistently reported that it is this PVM portion, and not the PRM portion, which is injured during delivery [112, 116, 117, 65, 84, 118]. However, it is not currently understood why this is the case, as they both form part of the canal through which the fetal head must be delivered. This is a knowledge gap we wanted to address in Chapter 2 of this dissertation.

1.2.6 Risk Factors for Levator Ani Tears

A variety of obstetrical factors have been shown to be associated with levator tears. Of these, the use of forceps instrumentation during delivery has been identified as the strongest risk

[1] We have chosen to use the term 'pubovisceral muscle' in place of 'pubococcygeal muscle' because it more accurately describes insertion of this muscle into the walls of the vagina and rectum (as well as the intervening perineal body) than the latter term that was chosen on evolutionary grounds rather than the standard of naming muscles according to their origin and insertion.

factor for levator ani tears, with reported odds ratios ranging from 3.4 – 25.6, relative to spontaneous vaginal delivery [85, 119, 86, 105, 88, 74, 89, 90, 94, 100] [103, 120], and tear prevalence often reported to be at least 50% [68, 121, 122, 92, 93, 95]. However, it is interesting that this trend is not observed for vacuum assisted deliveries, for which odds ratios of 0.6 – 0.9 relative to spontaneous vaginal deliveries have been reported [119, 88, 89]. Additionally, early studies considering intentionally slowed forceps deliveries in conjunction with early episiotomies and conduction anesthesia to relax the muscle observed a reduction in levator tear rates [81, 82]. The reason for the observed increase in levator tears with forceps instrumentation compared to vacuum is the focus of Chapter 6 of this dissertation.

Many of the delivery variables shown to be associated with levator ani tears cannot be known before labor. Intrapartum factors such as the duration of the second stage of labor, with an odds ratio of 2.2 per hour [119, 105, 89, 95, 96, 123, 100, 120], the previously discussed forceps instrumentation, and occipito-posterior positioning, with an odds ratio of 5.05 [89] are known to contribute significantly to levator injury. It has also been shown that the odds ratio for levator tear occurrence is 4.4 in births where obstetric anal sphincter injuries occur [119, 73, 100, 104]. Additionally, one study showed a positive correlation between episiotomy use during delivery and levator tear occurrence [119], while a later study has shown the opposite trend [97].

Given the number of variables only known at the time of delivery, our goal of the antepartum prediction of levator injury is challenging. There are several factors that could be assessed prior to labor, including older maternal age [85, 119, 86, 74, 123, 103], fetal head circumference

[105, 95, 96, 78, 124, 120], and large birth weight [105, 96, 125, 124, 120], but their predictive power is low. In contrast, one study suggests that choosing to have an epidural administered may have a protective effect on the levator ani muscles, which aligns with late 19th century reports of delivery complications associated with levator ani contraction [89, 61]. Though these risk factors have been identified, the reasons why each of these individual factors affects levator tear rates remain unknown.

1.3 Previous Attempts at Levator Injury Prediction

1.3.1 Correlation Based Predictions

Early antenatal prediction attempts were unsuccessful [90]. However, a recent study has shown the ratio of the levator hiatus circumference to the fetal head circumference can be correlated to levator tear state with a correlation coefficient of 0.67 [124]. This is the first indication that the "fit" of the fetal head size with the size of the mother's pelvis is important.

Additionally, one previous commentary proposed a tool to predict future development of pelvic floor disorders based on fetal weight, maternal age, BMI, ethnicity, and family history based on previous correlative studies [126]. As of yet no metrics on the effectiveness of this proposed prediction method have been reported.

1.3.2 Previous Birth Simulations

The first simulation of how much the levator ani had to stretch to accommodate passage of the fetal head through the birth canal was the geometric simulation of Lien et al. (2004) based on the anatomy of a healthy 34 year-old nullipara, as acquired through MRI. This analysis predicted a stretch ratio of 3.4.

Study	Analysis Type	Key Assumptions	Main Results
Lehn *et al.* 2016 [127]	Experimental replication of vacuum extraction	Assumes latex to be an adequate material replica of the uterus	Increasing fluid viscosity decreases the necessary fetal removal force
Oliveria *et al.* 2016 [128]	Finite element simulation	active contraction of pelvic floor muscles and maternal anatomy based on 72 year-old cadaver	"Puborectalis" is most prone to damage
Krofta *et al.* 2016 [129]	Finite element simulation	Fits constitutive model coefficients to data from cadaver tissue	Levator ani reaches a stretch ratio of 2.5
Silva *et al.* 2015 [130]	Finite element simulation	active contraction of pelvic floor muscles and maternal anatomy based on 72 year-old cadaver	Fetal head molding reduces reaction forces by 17%
Yan *et al.* 2015 [131]	Finite element simulation	Purely elastic constitutive model fit to data from cadaver tissue	Biparietal diameter and fetal head circumference are sufficient for accurate predictions
Berardi *et al.* 2014 [132]	Finite element simulation	Fits constitutive model coefficients to data from post-menopausal women	Levator ani reaches a stretch ratio of 2.2
Jing *et al.* 2012 [133]	Finite element simulation	Fits constitutive model coefficients to data from cadaver tissue	Levator ani reaches a stretch ratio of 3.55
Yan *et al.* 2012 [134]	Finite element simulation	Purely elastic constitutive model fit to data from cadaver tissue, and 10% molding of the fetal head	Levator ani reaches a stretch ratio of 2.1 – 2.4
Li *et al.* 2011 [135]	Finite element simulation	Purely elastic constitutive model fit to data from cadaver tissue	Levator ani reaches a stretch ratio of 3.3. Tissue anisotropy has 10% effect on mechanical response.
Parente *et al.* 2010 [136]	Finite element simulation	active contraction of pelvic floor muscles and maternal anatomy based on 72 year-old cadaver	Fetal head flexion may reduce reaction forces
Li *et al.* 2010 [137]	Finite element simulation	Purely elastic constitutive model fit to data from cadaver tissue	Constitutive equation nonlinearity resulted in increased reaction forces
Parente *et al.*	Finite element	active contraction of pelvic	The pelvic floor muscles

2009 (J. Biomech.) [138]	simulation	floor muscles and maternal anatomy based on 72 year-old cadaver	reach a stretch ratio of 1.67
Parente *et al.* 2009 (Eur. J. Obstet.) [139]	Finite element simulation	active contraction of pelvic floor muscles and maternal anatomy based on 72 year-old cadaver	The pelvic floor muscles reach a stretch ratio of 1.63 for occiput anterior and 1.73 for occiput posterior
Svabik *et al.* 2009 [140]	Geometric Analysis	Maternal capacity estimated as levator hiatus circumference	Mean levator stretch ratios were 1.47 and 1.07 based on hiatus measurements taken at rest and on Valsalva respectively
Parente *et al.* 2008 [141]	Finite element simulation	active contraction of pelvic floor muscles and maternal anatomy based on 72 year-old cadaver	The pelvic floor muscles reach a stretch ratio of 1.66
Hoyte *et al.* 2008 [142]	Finite element simulation	Purely elastic constitutive model fit to data from biceps brachii	Levator ani reaches a stretch ratio of 1.6
Martins *et al.* 2007 [143]	Finite element simulation	active contraction of pelvic floor muscles and maternal anatomy based on 72 year-old cadaver	Levator ani reaches a stretch ratio of 3.5
Lien *et al.* 2004 [144]	Geometric Analysis	Assumes 20% molding of the fetal head	Levator ani reaches a stretch ratio of 3.26

Table 1.2 - Summary of key results, assumptions, and analysis techniques of previous vaginal birth simulations.

After that study, a series of finite element simulations of vaginal delivery have been carried out [Table 1.2]. The first finite element simulation relied upon a 72 year-old embalmed cadaver for its anatomical basis, and a constitutive model previously derived for the active contraction of cardiac tissue [143]. This was followed shortly by a simulation study which took its anatomical basis from MRI scans of a 21 year-old nullipara being seen for uterus didelphys, and which relied upon a purely elastic constitutive model fit to data from the biceps brachii [63]. In 2010,

the first simulation with a constitutive model based on tissues normally involved in parturition was published. However, the tissue that this model relied upon originated from a non-pregnant cadaver, and the nonlinear elastic constitutive model neglected viscous behavior [137]. In 2012, data acquired from cadaveric human pelvic floor tissue was again used as the basis for a finite element simulation; however, this time, the viscous component of mechanical behavior was taken into account through the use of Quasilinear Viscoelasticity, with *in vitro* rat and squirrel monkey data incorporated to help account for material property changes late in pregnancy [133]. Current simulations of the birthing process predict that the levator ani muscle stretches to 1.6 – 3.5 times its original length in order to accommodate the fetal head [129, 132, 133, 134, 135, 139, 142, 143, 144] [Table 1.2].

However, all these simulations lack a validated constitutive model for the term pregnant human birth canal, as well as a validated injury criterion. They are, therefore, limited in their ability to predict levator tears. Additionally, these simulations are limited in their scalability to apply to a variety of mothers in the population, as many publications take into account only one maternal and fetal head geometry pairing [143, 142, 139, 138, 137, 136, 133, 132, 130, 129] [128]. This may be due to the high computational costs for both model construction and simulation completion, as it can take up to 7 days to run a single birth simulation [131], with run times still at 3.5 hours when resolution is decreased to 10 minute increments [133]. If 10 minute increments are used, it would be impossible to account for the role of the periodic nature of contractions and pushing during labor, as three contractions with three contraction free intervals would be expected to occur during the period of time neglected between each calculation point. Therefore, multiple improvements to both the constitutive model basis and

computational methods are necessary in order to allow for accurate levator tear predictions on a population scale. This is a goal of the current dissertation.

Before this type of prediction technique can achieve feasibility for large scale implementation as a screening technique for levator injury risk, ease of use issues would have to be addressed. Due to high computational cost, and specialty software and training requirements, there would be a high burden to implementation of individualized simulations for each expecting mother. However, given a sufficient library of simulation results spanning a large variety of geometries, it may be possible to match each patient with a predicted levator tear outcome without the need to run a new simulation specifically for them. That is a goal for this dissertation. However, the development of such a tool box would still require a validated constitutive model describing the human birth canal at the time of labor as the basis for the birth simulations.

1.4 Material Properties and Changes During Pregnancy

1.4.1 Constitutive Models Previously Used for Birth Simulations

Constitutive models used in previous birth simulations have relied upon data from levator ani specimens taken from postmenopausal women [132] or cadavers [130, 129, 128, 133, 137, 135, 134, 131], or data measured for human tissues not involved in parturition [143, 142, 141].

In interpreting these data, analysis has often focused on quantifying the elastic response, neglecting the viscous component that must be present in order to allow for progress to be made on subsequent pushes during the active second stage of labor [142, 137, 135, 134, 131].

Many simulations have relied upon constitutive models originally designed to mimic actively contracting muscle, which is hopefully not the case during labor, as mothers are instructed to relax the pelvic floor [143, 141, 139, 138, 136, 130, 128]. There is therefore a real lack of reliable constitutive models for the birth canal tissue at the onset of labor, which was another goal for this dissertation.

1.4.2 Current Understanding of the Material Properties of the Birth Canal

Characterization of the mechanical properties of the tissues surrounding the birth canal has also generally been limited to analysis of tissues excised from post-menopausal or cadaveric sources [145, 146, 147].

Recently, attempts have been made to indirectly quantify the mechanical properties of the pelvic floor of a 30 year-old nullipara based on inverse finite element analysis of Valsalva on MRI [148]. However, this type of characterization during pregnancy would likely not be safe due to the increase in intra-abdominal pressure that results from Valsalva [149, 150, 151] and the impracticability of using MRI during labor.

It has, however, been possible to show in rodent and ovine models that the tissues surrounding the birth canal undergo a distinct 'softening', or increase in extensibility, in preparation for childbirth [152, 153, 154, 155, 156, 157, 158].This includes a 2.1 – 2.4 fold reduction in the elastic modulus during pregnancy [153, 156, 157] and up to a 5.4 fold increase in overall compliance by late gestation [158].

The distinct hysteresis response, or ability of the tissue to reach higher strains on each subsequent stretching cycle without increasing the force applied, can be observed even in post-

menopausal [145, 146] and some cadaveric [147] human specimens, and has been shown to increase in pregnant sheep, with the maximum strain reached increasing 4-fold when compared to virgin sheep [157]. It is this hysteresis response which allows for a laboring mother to continue to make progress on each subsequent push despite the fact that the maximum pushing efforts remain constant.

1.4.3 Changes to Maternal Anatomy and Tissue Composition during Pregnancy

Other mechanical changes observed to occur during pregnancy include increases in distensibility and compliance of the cervix throughout pregnancy in mice [159, 160], with a distinct increase in distensibility shown in late pregnant human cervix [161].

Tissue composition has also been shown to change during pregnancy, with relaxin levels shown to increase in a pregnant rat model [162] and elastin and collagen levels increasing in the human uterus during pregnancy [163]. Collagen has also been shown to increase in the cervix and extracellular matrix of the pelvic floor muscles in pregnant rat models [164, 165, 166].

A recent study demonstrated an increase in sarcomere number, but not sarcomere length, for a net increase in muscle fiber length during pregnancy in a rat model [167]. An increase in hiatal dimensions has also been shown to occur in humans during pregnancy, with one study showing a 27% increase between nulliparous and late pregnancy cohorts [168]. Several longitudinal studies also show up to a 17% increase in hiatus measurements late in pregnancy [169, 170, 171, 172, 173, 174].

It has also been shown, in rat vaginal tissue, that the smooth muscle cell phenotype changes from contractile to synthetic during pregnancy, and returns to contractile postpartum. It is postulated that this change helps to minimize trauma during delivery [175].

1.4.4 Fung Quasilinear Viscoelasticity (QLV) Model

A reasonable constitutive model for birth simulations should adequately reflect the viscoelastic behavior that must be present in the birth canal, including the hysteresis effect that allows for progress to be made on subsequent pushes. Additionally, such a model should reflect the nonlinear nature of the elastic response of pelvic floor tissues. Finally, the model should be able to be validated by comparison to the behavior of the term pregnant human birth canal.

One constitutive form that meets both the nonlinear elastic and viscous response criteria is the Quasilinear Viscoelasticity (QLV) form proposed for characterizing soft tissues [176]. QLV has been previously employed for the quantification of pelvic floor material properties in rodent and nonhuman primate models based on excised tissues [133, 154]. QLV has also been successful in characterizing a diverse array of soft tissues, including passive cardiac muscle, skin, patellar tendon, medial collateral and anterior cruciate ligaments, and hysteresis behavior in aortic valve leaflets [177, 178, 179, 180, 181, 182].

1.4.5 Failure Criteria

In order to make meaningful predictions of levator tear occurrences, it is necessary to understand how and when soft tissue tears occur. General work considering strain as a criterion for muscle injury showed damage occurred when strains exceeded 0.5 for passive muscle, while active stimulation of the tissue resulted damage at a strain of 0.3 (a 40% decrease) [183]. This

higher threshold for injury in paralyzed muscle may help to explain why lower levator tear rates have been observed in some studies of patients receiving epidurals [89].

While strain does play a role in injury occurrence, data from ovine and rodent vaginal tissue suggest that the product of stress times strain, an injury criterion previously observed in ligament studies [184, 185, 186], may be the most appropriate in predicting levator ani tissue failures [152, 155, 156, 157]. For this reason we shall employ the product of stress and strain in this dissertation.

1.5 Dissertation Structure

The overall goal of this research has been to develop an antepartum framework for predicting levator tear risk and duration of the active second stage of labor, during a vaginal birth. Our working hypothesis is that it is possible to use antenatal maternal and fetal measurements to predict those at risk for PVM tear prior to the onset of labor. This would be significant because new preventative strategies could be implemented in those few women most at risk without imposing unintended harm on those who are not destined to be injured. Those deemed likely to deliver without injury could be so informed so as to allay concern. Both outcomes would be major steps forward and are goals of this dissertation.

In Chapter 2 of this dissertation, we describe a new geometric “capacity-demand” analysis. The geometric ‘capacity’ of the maternal lower birth canal to accommodate the ‘demand’ of the fetal head for delivery without incurring maternal PVM stretch injury is assessed taking into account contributions of both variable bony and soft tissue factors.

In Chapter 3, we derive a constitutive model of the term-pregnant lower birth canal. We then validate this model using *in situ* force-displacement data from the human birth canal at the time of labor.

In Chapter 4, we build upon the constitutive model derived in Chapter 3 to test the null hypothesis that there is no significant variation in the long time constant, τ_2 among laboring women. We then test the null hypothesis that the variation in τ_2 will not affect (1) the predicted duration of the active second stage of labor, or (2) the risk of a PVM tear.

In Chapter 5, we make blinded PVM tear predictions based on ultrasound scans of nulliparous women taken at 37 weeks of pregnancy. The predictions were then compared to the subject's clinical levator tear scores, then the specificity and selectivity of the injury prediction were calculated.

In Chapter 6, we employ birth simulations based on the constitutive relations quantified in Chapter 3 in order to consider the differential effect of forceps and vacuum instrumentation, as well as episiotomy depth, on predicted PVM tear rates and duration of the active second stage of labor.

Finally, in Chapter 7, we employ birth simulations to consider the effect of pre-distension of the birth canal during the first stage of labor on the duration of the active second stage and on predicted PVM tears.

Chapters 8, 9 and 10, describe the main conclusions from the dissertation, and discuss strengths and weaknesses of the approaches, the knowledge gaps that have been filled and those that remain, and suggestions for future research.

1.6 References

[1] E. Phillips and J. Kersey, The New World of Words: Universal English Dictionary, London: J Phillips, 1706.

[2] *Kahun Papyrus,* Egypt, 1835 BCE.

[3] A. Olsen, V. Smith, J. Bergstrom, J. Colling and A. Clark, "Epidemiology of surgically managed pelvic organ prolapse and urinary incontinence," *Obstetrics and Gynecology,* vol. 89, no. 4, pp. 501-6, 1997.

[4] F. Smith, C. Holman, R. Moorin and N. Toskos, "Lifetime risk of undergoing surgery for pelvic organ prolapse," *Obstetrics and Gynecology,* vol. 116, no. 5, pp. 1096-100, 2010.

[5] M. Abdel-Fattah, A. Farnilusi, S. Fielding, J. Ford and S. Bhattacharya, "Primary and repeat surgical treatment for female pelvic organ prolapse and incontinence in parous women in the UK: a register linkage study," *BMJ Open,* vol. 1, no. 2, p. e000206, 2011.

[6] T. de Boer, M. Slieker-Ten Hove, B. CW, K. Kluivers and V. ME, "The prevalence and factors associated with previous surgery for pelvic organ prolapse and/or urinary incontinence in a cross-sectional study in The Netherlands," *European Journal of Obstetrics, Gynecology, and Reproductive Biology,* vol. 158, no. 2, pp. 343-9, 2011.

[7] J. Wu, C. Matthews, M. Conover, V. Pate and M. Jonsson Funk, "Lifetime risk of stress urinary incontinence or pelvic organ prolapse surgery," *Obstetrics and Gynecology,* vol. 123, no. 6, pp. 1201-6, 2014.

[8] S. Kumari, I. Walia and A. Singh, "Self-reported uterine prolapse in a resettlement colony of north India," *Journal of Midwifery & Women's Health,* vol. 45, no. 4, pp. 343-50, 2000.

[9] A. MacLennan, A. Taylor, D. Wilson and D. Wilson, "The prevalence of pelvic floor disorders and their relationship to gender, age, parity and mode of delivery," *BJOG: an International Journal of Obstetrics and Gynaecology,* vol. 107, no. 12, pp. 1460-70, 2000.

[10] G. Tegerstedt, M. Maehle-Schmidt, O. Nyren and M. Hammarstrom, "Prevalence of symptomatic pelvic organ prolapse in a Swedish population," *International Urogynecology Journal and Pelvic Floor Dysfunction,* vol. 16, no. 6, pp. 497-503, 2005.

[11] G. Rortveit, J. Brown, D. Thom, S. Van Den Eeden, J. Creasman and L. Subak, "Symptomatic pelvic organ prolapse: prevalence and risk factors in a population-based, racially diverse cohort," *Obstetrics and Gynecology,* vol. 109, no. 6, pp. 1396-403, 2007.

[12] I. Nygaard, M. Barber, K. Burgio, K. Kenton, S. Meikle, J. Schaffer, C. Spino, W. Whitehead, J. Wu and D. Brody, "Prevalence of symptomatic pelvic floor disorders in US women," *JAMA,* vol. 300, no. 11, pp. 1311-6, 2008.

[13] J. Lawrence, E. Lukacz, C. Nager, J. Hsu and K. Luber, "Prevalence and co-occurrence of pelvic floor disorders in community-dwelling women," *Obstetrics and Gynecology,* vol. 111, no. 3, pp. 678-85, 2008.

[14] M. Slieker-ten Hove, A. Pool-Goudzwaard, M. Eijkemans, R. Steegers-Theunissen, C. Burger and M. Vierhout, "Prediction model and prognostic index to estimate clinically relevant pelvic organ prolapse in a general female population," *International Urogynecology Journal and Pelvic Floor Dysfunction,* vol. 20, no. 9, pp. 1013-21, 2009.

[15] E. Samuelsson, F. Victor, G. Tibblin and K. Svardsudd, "Signs of genital prolapse in a Swedish population of women 20 to 59 years of age and possible related factors," *American Journal of Obstetrics and Gynecology,* vol. 180, no. 2 Pt 1, pp. 299-305, 1999.

[16] S. Swift, "The distribution of pelvic organ support in a population of female subjects seen for routine gynecologic health care," *American Journal of Obstetrics and Gynecology,* vol. 183, no. 2, pp. 277-85, 2000.

[17] S. Hendrix, A. Clark, I. Nygaard, A. Aragaki, V. Barnabei and A. McTierman, "Pelvic Organ Prolapse in the Women's Health Initiative; gravity and gravidity," *American Journal of Obstetrics and Gynecology,* vol. 186, no. 6, pp. 1160-6, 2002.

[18] I. Nygaard, C. Bradley and D. Brandt, "Pelvic organ prolapse in older women: prevalence and risk factors," *Obstetrics and Gynecology,* vol. 104, no. 3, pp. 489-97, 2004.

[19] S. Swift, P. Woodman, A. O'Boyle, M. Kahn, M. Valley, D. Bland, W. Wang and J. Schaffer, "Pelvic organ support study (POSST): the distribution, clinical definition, and epidemiologic condition of pelvic organ support defects," *American Journal of Obstetrics and Gynecology,* vol. 192, no. 3, pp. 795-806, 2005.

[20] E. Trowbridge, N. Fultz, D. Patel, J. O. L. DeLancey and D. Fenner, "Distribution of pevlic organ support measures in a population-based sample of middle-aged, community-dwelling African American and white women in southeastern Michigan," *American Journal of Obstetrics and Gynecology,* vol. 198, no. 5, pp. 548.e1-6, 2008.

[21] A. Hall, J. Theofrastous, G. Cundiff, R. Harris, L. Hamilton, S. Swift and R. Bump, "Interobserver and intraobserver reliability of the proposed international Continence Society, Society of Gynecologic Surgeons, and American Urogynecologic Society pelvic organ prolapse classification system," *American Journal of Obstetrics and Gynecology,* vol. 175, no. 6, pp. 1467-70, 1996.

[22] M. Barber, L. Brubaker, I. Nygaard, T. 2. Wheeler, J. Schaffer, Z. Chen, C. Spino and P. F. D. Network, "Defining success after surgery for pelvic organ prolapse," *Obstetrics and Gynecology,* vol. 114, no. 3, pp. 600-9, 2009.

[23] R. Ellerkmann, G. Cundiff, C. Melick, M. Nihira, K. Leffler and A. Bent, "Correlation of symptoms with location and severity of pelvic organ prolapse," *American Journal of Obstetrics and Gynecology,* vol. 185, no. 6, pp. 1332-7, 2001.

[24] S. Swift, S. Tate and J. Nicholas, "Correlation of symptoms with degree of pelvic organ support in a general population of women: what is pelvic organ prolapse?," *American Journal of Obstetrics and gynecology,* vol. 189, no. 2, pp. 372-7, 2003.

[25] C. Bradley and I. Nygaard, "Vaginal wall descensus and pelvic floor symptoms in older women," *Obstetrics and Gynecology,* vol. 106, no. 4, pp. 759-66, 2005.

[26] A. Marguerite, Abrege de l'Art des Accouchements, Paris: Debure, 1773.

[27] A. Leijonhufvud, C. Lundholm, S. Cnattingius, F. Granath, E. Andolf and D. Altman, "Risks of stress urinary incontinence and pelvic organ prolapse surgery in relation to mode of childbirth," *American Journal of Obstetrics and Gynecology,* vol. 204, no. 1, pp. 70.e1-7, 2011.

[28] V. Thomas, S. KL, R. Guzman Rojas and H. Dietz, "The latency between pelvic floor trauma and presentation for prolapse surgery," *Ultrasound in Obstetrics and Gynecology,* vol. 42, no. s1, pp. 39-39, 2015.

[29] S. Timonen, E. Nuoranne and B. Meyer, "Genital prolapse: etiological factors," *Annales Chirurgiae et Gynaecologiae Fenniae,* vol. 57, no. 3, pp. 363-70, 1968.

[30] Y. Lukman, "Utero-vaginal prolapse: A rural disability of the young," *East Aftrican Medical Journal,* vol. 72, no. 1, pp. 2-9, 1995.

[31] J. Mant, R. Painter and M. Vessey, "Epidemiology of genital prolapse: observations from the Oxford Planning Association Study," *British Journal of Obstetrics and Gynaecology,* vol. 104, no. 5, pp. 579-85, 1997.

[32] F. Chiaffarino, L. Chatenoud, M. Dindelli, M. Meschia, A. Buonaguidi, F. Amicarelli, M. Surace, E. Bertola, E. Di Cintio and F. Parazzini, "Reproductive factors, family history, occupation and risk of urogenital prolapse," *European Journal of Obstetrics, Gynecology, and Reproductive Biology,* vol. 82, no. 1, pp. 63-7, 1999.

[33] H. Gurel and S. Gurel, "Pelvic relaxation and associated risk factors: the results of logistic regression analysis," *Acta Obstetricia et Gynecologia Scandinavica,* vol. 78, no. 4, pp. 290-3, 1999.

[34] M. Carley, R. Turner, D. Scott and J. Alexander, "Obstetric history in women with surgically corrected adult urinary incontinence or pelvic organ prolapse," *The Journal of the American Association of Gynecologic Laparoscopists,* vol. 6, no. 1, pp. 85-9, 1999.

[35] K. Rinne and P. Kirkinen, "What predisposes young women to genital prolapse," *European Journal of Obstetrics, Gynecology, and Reproductive Biology,* vol. 84, no. 1, pp. 23-5, 1999.

[36] Progetto Menopausa Italia Study Group, "Risk factors for genital prolapse in non-hysterectomized women around menopause: Results from a large cross-sectional study in menopausal clinics in Italy," *European Journal of Obstetrics, Gynecology, and Reproductive Biology,* vol. 93, no. 2, pp. 135-40, 2000.

[37] S. Swift, T. Pound and J. Dias, "Case-control study of etiologic factors in the development of severe pelvic organ prolapse," *International urogynecology Journal and Pelvic Floor Dysfunction,* vol. 12, no. 3, pp. 187-92, 2001.

[38] E. Sze, G. Sherard and J. Dolezal, "Pregnancy, labor, delivery, and pelvic organ prolapse," *Obstetrics and Gynecology,* vol. 100, no. 5 Pt 1, pp. 981-6, 2002.

[39] C. Dannecker, A. Lienemann, T. Fischer and C. Anthuber, "Influence of spontaneous vaginal delivery on objective measures of pelvic organ support: assessment with the pelvic organ prolapse quantification (POPQ) technique and functional cine magnetic resonance imaging," *European Journal of Obstetrics, Gynecology, and Reproductive Biology,* vol. 115, no. 1, pp. 32-8, 2004.

[40] A. O'Boyle, J. O'Boyle, B. Calhoun and G. Davis, "Pelvic organ support in pregnancy and postpartum," *International Urogynecology Journal and Pelvic Floor Dysfunction,* vol. 16, no. 1, pp. 69-72, 2005.

[41] E. Lukacz, J. Lawrence, R. Contreras, C. Nager and K. Luber, "Parity, mode of delivery, and pelvic floor disorders," *Obstetrics and Gynecology,* vol. 107, no. 6, pp. 1253-60, 2006.

[42] G. Tegerstedt, A. Miedel, M. Maehle-Schmidt, O. Nyren and M. Hammarstrom, "Obstetric risk factors for symptomatic prolapse: a population-based approach," *American Journal of Obstetrics and Gynecology,* vol. 194, no. 1, pp. 75-81, 2006.

[43] C. Kim, M. Jeon, D. Chung, S. Kim, J. Kim and S. Bai, "Risk factors for pelvic organ prolapse," *International Journal of Gynaecology and Obstetrics,* vol. 98, no. 3, pp. 248-51, 2007.

[44] X. Fritel, N. Varnoux, M. Zinis, G. Breart and V. Ringa, "Symptomatic pelvic organ prolapse at midlife, quality of life, and risk factors," *Obstetrics and Gynecology,* vol. 113, no. 3, pp. 609-16, 2009.

[45] E. Sze and G. Hobbs, "Relation between vaginal birth and pelvic organ prolapse," *Acta Obstetricia et Gynecologia Scandinavica,* vol. 88, no. 2, pp. 200-3, 2009.

[46] C. Larsson, K. Kallen and E. Andolf, "Cesarean section and risk of pelvic organ prolapse: a nested case-control study," *American Journal of Obstetrics and Gynecology,* vol. 200, no. 3, pp. 243.e1-4, 2009.

[47] V. Handa, I. Nygaard, K. Kenton, G. Cundiff, C. Ghettic, W. Ye and H. Richter, "Pelvic Floor Disorders Network. Pelvic organ support among primiparous women in the first year after childbirth," *International Urogynecology Journal and Pelvic Floor Dysfunction,* vol. 20, no. 12, pp. 1407-11, 2009.

[48] L. Quiroz, A. Munoz, S. Shippey, R. Gutman and V. Handa, "Vaginal parity and pelvic organ prolapse," *The Journal of Reproductive Medicine,* vol. 55, no. 3-4, pp. 93-8, 2010.

[49] B. Kudish, C. Iglesia, R. Gutman, A. Sokol, A. Rodgers, M. Gass, M. L. J. O'Sullivan, M. Abu-Sitta and B. Howard, "Risk factors for prolapse development in white, black, and hispanic women," *Female Pelvic Medicine & Reconstructive Surgery,* vol. 17, no. 2, pp. 80-90, 2011.

[50] V. Handa, J. Blomquist, L. Knoepp, K. Hoskey, K. McDermott and A. Munoz, "Pelvic Floor Disorders 5-10 years after vaginal or cesarean childbirth," *Obstetrics and Gynecology,* vol. 118, no. 4, pp. 777-84, 2011.

[51] K. Elenskaia, R. Thakar, A. Sultan, I. Scheer and J. Onwude, "Effect of childbirth on pelvic organ support and quality of life: a longitudinal cohort study," *International Urogynecology Journal,* vol. 24, no. 6, pp. 927-37, 2013.

[52] A. Yeniel, A. Ergenoglu, N. Askar, I. Itil and R. Meseri, "How do delivery mode and parity affect pelvic organ prolapse?," *Acta Obstetricia et Gynecologia Scandinavica,* vol. 92, no. 7, pp. 847-51, 2013.

[53] C. Glazener, A. Elders, C. Macarthur, R. Lancashire, P. Herbison, S. Hagen, N. Dean, C. Bain, P. Toozs-Hobson, K. Richardson, A. McDonald, G. McPherson and D. Wilson, "Childbirth and prolapse: long-term associations with the symptoms and objective measurement of pelvic organ prolapse," *BJOG: an International Journal of Obstetrics and Gynaecology,* vol. 120, no. 2, pp. 161-8, 2013.

[54] I. Nilsson, S. Akervall, I. Milsom and M. Gyhagen, "Long-term Effects of Vacuum Extraction on Pelvic Floor Function: a Cohort Study in Primipara," *International Urogynecology Journal,* vol. 27, no. 7, pp. 1051-6, 2016.

[55] M. Gyhagen, M. Bullarbo, T. Nielsen and I. Milsom, "Prevalence and risk factors for pelvic organ prolapse 20 years after childbirth: a national cohort study in singleton primiparae after vaginal or caesarean delivery," *BJOG: an International Journal of Obstetrics and Gynaecology,* vol. 120, no. 2, pp. 152-60, 2013.

[56] P. Moalli, S. Jones Ivy, L. Meyn and H. Zyczynski, "Risk factors associated with pelvic floor disorders in women undergoing surgical repair," *Obstetrics and Gynecology,* vol. 101, no. 5 Pt 1, pp. 869-74, 2003.

[57] R. Uma, G. Libby and D. Murphy, "Obstetric management of a woman's first delivery and the implications for pelvic floor surgery in later life," *BJOG: an International Journal of Obstetrics and Gynaecology,* vol. 112, no. 8, pp. 1043-6, 2005.

[58] I. Diez-Itza, M. Arrue, L. Ibanez, J. Paredes, A. Murgiondo and C. Sarasqueta, "Influence of mode of delivery on pelvic organ support 6 months postpartum," *Gynecologic and Obstetric Investigation,* vol. 72, no. 2, pp. 123-9, 2011.

[59] I. Volloyhaug, S. Morkved, O. Salvesen and S. KA, "Pelvic organ prolapse and incontinence 15-23 years after first delivery: a cross-sectional study," *BJOG: an International Journal of Obstetrics and Gynaecology,* vol. 122, no. 7, pp. 964-71, 2015.

[60] J. Halban and J. Tandler, Anatomie und Aetiologie der Genitalprolapse Beim Weibe, 1 ed., Vienna: Braumueller, 1907.

[61] R. Dickinson, "Studies of the levator ani muscle," *The American Journal of Obstetrics and Diseases of Women and Children,* vol. 29, no. 9, pp. 897-916, 1889.

[62] J. O. L. DeLancey, "Anatomy and Biomechanics of Genital Prolapse," *Clinical Obstetrics and Gynecology,* vol. 36, no. 4, pp. 897-909, 1993.

[63] L. Hoyte, L. Schierlitz, K. Zou, G. Flesh and J. Fielding, "Two- and 3-Dimensional MRI Comparison of Levator Ani Structure, Volume, and Integrity in Women with Stress Incontinence and Prolapse," *American Journal of Obstetrics and Gynecology,* vol. 185, no.

1, pp. 11-9, 2001.

[64] H. Dietz and A. Steensma, "The prevalence of major abnormalities of the levator ani in urogynaecological patients," *BJOG: an International Journal of Obstetrics and Gynaecology,* vol. 113, no. 2, pp. 225-30, 2006.

[65] H. Dietz, G. AV and P. Phadke, "Avulsion of the pubovisceral muscle associated with large vaginal tear after normal vaginal delivery," *The Australian & New Zealand Journal of Obstetrics & Gynaecology,* vol. 47, no. 4, pp. 341-4, 2007.

[66] S. Athanasiou, C. Chaliha, P. Toozs-Hobson, S. Salvatore, V. Khullar and L. Cardozo, "Direct imaging of the pelvic floor muscles using two-dimensional ultrasound: a comparison of women with urogenital prolapse versus controls," *BJOG: an International Journal of Obstetrics and Gynaecology,* vol. 114, no. 7, pp. 882-8, 2007.

[67] H. Dietz, "Quantification of major morphological abnormalitities of the levator ani," *Ultrasound in Obstetrics and Gynecology,* vol. 29, no. 3, pp. 329-34, 2007.

[68] J. O. L. DeLancey, D. M. Morgan, D. E. Fenner, R. Kearney, K. Guire, J. M. Miller, H. Hussain, W. Umek, Y. Hsu and J. A. Aston-Miller, "Comparison of levator ani muscle defects and function in women with and without pelvic organ prolapse," *Obstetrics and Gynecology,* vol. 109, pp. 295-302, 2007.

[69] H. Dietz and J. Simpson, "Levator Trauma is Associated with Pelvic Organ Prolapse," *BJOG: an International Journal of Obstetrics and Gynaecology,* vol. 115, no. 8, pp. 979-84, 2008.

[70] H. Dietz and K. Shek, "Validity and reproducibility of the digital detection of levator trauma," *International Urogynecology Journal and Pelvic Floor Dysfunction,* vol. 19, no. 8, pp. 1097-101, 2008.

[71] H. Dietz and K. Shek, "Levator defects can be detected by 2D translabial ultrasound," *International Urogynecology Journal and Pelvic Floor Dysfunction,* vol. 20, no. 7, pp. 807-11, 2009.

[72] Z. Abdool, K. Shek and D. H, "The effect of levator avulsion on hiatal dimensions and function," *American Journal of Obstetrics and Gynecology,* vol. 201, no. 1, pp. 89.e1-5, 2009.

[73] M. Heilbrun, I. Nygaard, M. Lockhart, H. Richter, M. Brown, K. Kenton, D. Rahn, J. Thomas, A. Weidner, C. Nager and J. O. L. DeLancey, "Correlation Between Levator Ani Muscle Injuries on Magnetic Resonance Imaging and Fecal Incontinence, Pelvic Organ Prolapse, and Urinary Incontinence in Primiparous Women," *American Journal of Obstetrics and Gynecology,* vol. 202, no. 5, pp. 488.e1-6, 2010.

[74] H. Dietz and A. Kirby, "Modelling the Likelihood of Levator Avulsion in a Urogynaecological Population," *The Australian & New Zealand Journal of Obstetrics & Gynaecology,* vol. 50, no. 3, pp. 268-72, 2010.

[75] H. Dietz, A. Franco, K. Shek and A. Kirby, "Avulsion injury and levator hiatal ballooning: two independent risk factors for prolapse? An observational study," *Acta Obstetricia et Gynecologica Scandinavica,* vol. 91, no. 2, pp. 211-4, 2012.

[76] G. Rostaminia, D. White, A. Hegde, L. Quiroz, G. Davila and S. Shobeiri, "Levator Ani Deficiency and Pelvic Organ Prolapse Severity," *Obstetrics and Gynecology,* vol. 121, no. 5, pp. 1017-24, 2013.

[77] M. Berger, D. Morgan and J. O. L. DeLancey, "Levator Ani Defect Scores and Pelvic Organ Prolapse: is There a Threshold Effect?," *International Urogynecology Journal,* vol. 25, no. 10, pp. 1375-9, 2014.

[78] R. Laterza, L. Schrutka, W. Umek, S. Albrich and H. Koelbl, "Pelvic floor dysfunction after levator trauma 1-year postpartum: a prospective case-control study," *International Urogynecology Journal,* vol. 26, no. 1, pp. 41-7, 2015.

[79] V. Thomas, S. KL, R. Guzman Rojas and H. Dietz, "Temporal Latency Between Pelvic Floor Trauma and Presentation for Prolapse Surgery: a Retrospective Observational Study," *International Urogynecology Journal,* vol. 26, no. 8, pp. 1185-9, 2015.

[80] S. Albrich, K. Rommens, J. Steetskamp, V. Weyer, G. Hoffmann, C. Skala and E. Zahn, "Prevalence of levator ani defects in urogynecological patients," *Geburtshilfe und Frauenheilkunde,* vol. 75, no. 1, pp. 51-55, 2015.

[81] H. Gainey, "Post-partum observation of pelvic tissue damage," *American Journal of Obstetrics and Gynecology,* vol. 45, no. 1, p. 457, 1943.

[82] H. Gainey, "Post-partum observations of pelvic tissue damage: Further studies," *American Journal of Obstetrics and Gynecology,* vol. 70, no. 4, pp. 800-7, 1955.

[83] R. Tunn, J. O. L. DeLancey, D. Howard, J. Thorp, J. Ashton-Miller and L. Quint, "MR Imaging of Levator Ani Muscle Recovery Following Vaginal Delivery," *International Urogynecology Journal and Pelvic Floor Dysfunction,* vol. 10, no. 5, pp. 300-7, 1999.

[84] J. O. L. DeLancey, R. Kearney, Q. Chou, S. Speights and S. Binno, "The Appearance of Levator Ani Muscle Abnormalities in Magnetic Resonance Images After Vaginal Delivery," *Obstetrics and Gynecology,* vol. 101, no. 1, pp. 46-53, 2003.

[85] H. Dietz and V. Lanzarone, "Levator trauma after vaginal delivery," *Obstetrics and Gynecology,* vol. 106, no. 4, pp. 707-12, 2005.

[86] H. Dietz and J. Simpson, "Does delayed childbirth increase the risk of levator injury in labour?," *The Australian & New Zealand Journal of Obstetrics & Gynaecology,* vol. 47, no. 6, pp. 491-5, 2007.

[87] H. Dietz and C. Shek, "Levator avulsion and grading of pelvic floor muscle strength," *International Urogynecology Journal and Pelvic Floor Dysfunction,* vol. 19, no. 5, pp. 633-6, 2008.

[88] K. Shek and H. Dietz, "The effect of childbirth on hiatal dimensions," *Obstetrics and Gynecology,* vol. 113, no. 6, pp. 1272-8, 2009.

[89] K. Shek and H. Dietz, "Intrapartum risk factors for levator trauma," *BJOG An International Journal of Obstetrics and Gynecology,* vol. 117, no. 12, pp. 1485-1492, 2010.

[90] K. Shek and H. Dietz, "Can levator avulsion be predicted antenatally?," *American Journal of Obstetrics and Gynecology,* vol. 202, no. 6, pp. 586.e1-6, 2010.

[91] I. Blasi, I. Fuchs, R. D'Amico, V. Vinci, G. La Sala, V. Mazza and W. Henrich, "Intrapartum translabial three-dimensional ultrasound visualization of levator trauma," *Ultrasound in Obstetrics and Gynecology,* vol. 37, no. 1, pp. 88-92, 2011.

[92] J. Cassado Garriga, A. Pessarrodona Isern, M. Espuna Pons, M. Duran Retamal, A. Felgueroso Fabrega, M. Rodriguez Carballeira and I. Jorda Santamaria, "Four-dimensional sonographic evaluation of avulsion of the levator ani according to delivery mode," *Ultrasound in Obstetrics and Gynecology,* vol. 38, no. 6, pp. 701-6, 2011.

[93] J. Cassado Garriga, A. Pessarrodona Isern, M. Espuna Pons, M. Duran Retamal, A. Felgueroso Fabregas and M. Rodriguez-Carballeira, "Tridimensional sonographic anatomical changes on pelvic floor muscle according to the type of delivery," *International Urogynecology Journal,* vol. 22, no. 8, pp. 1011-8, 2011.

[94] S. Albrich, R. Laterza, C. Skala, S. Salvatore, H. Koelb and G. Naumann, "Impact of mode of delivery on levator morphology: A prospective observational study with three-dimensional ultrasound early in the postpartum period," *BJOG: an International Journal of Obstetrics and Gynaecology,* vol. 119, no. 1, pp. 51-60, 2012.

[95] S. Chan, R. Cheung, A. Yiu, L. Lee, A. Pang, K. Choy, T. Leung and T. Chung, "Prevalence of levator ani muscle injury in Chinese women after first delivery," *Ultrasound in Obstetrics and Gynecology,* vol. 39, no. 6, pp. 704-9, 2012.

[96] G. Hilde, J. Staer-Jensen, F. Siafarikas, K. Gjestland, M. Ellstrom Engh and K. Bo, "How well can pelvic floor muscles with major defects contract? A cross-sectional study 6 weeks after delivery using transperineal 3D/4D ultrasound and manometer," *BJOG: an International Journal of Obstetrics and Gynaecology,* vol. 120, no. 11, pp. 1423-9, 2013.

[97] J. Cassado, A. Pessarrodona, M. Rodriguez-Carballeira, L. Hinojosa, G. Manrique, A. Marquez and M. Marcias, "Does episiotomy protect against injury of the levator ani muscle in normal vaginal delivery?," *Neurourology and Urodynamics,* vol. 33, no. 8, pp. 1212-6, 2014.

[98] R. Guzman Rojas, V. Wong, K. Shek and H. Dietz, "Impact of levator trauma on pelvic floor muslce function," *International Urogynecology Journal,* vol. 25, no. 3, pp. 375-80, 2014.

[99] S. Chan, R. Cheung, K. Yiu, L. Lee and T. Chung, "Pelvic floor biometry in Chinese primiparous women 1 year after delivery: a prospective observational study," *Ultrasound in Obstetrics & Gynecology,* vol. 43, no. 4, pp. 466-74, 2014.

[100] K. van Delft, R. Thakar, A. Sultan, N. Schwertner-Tiepelmann and K. Kluivers, "Levator Ani Muscle Avulsion During Childbirth: a Risk Prediction Model," *BJOG: An International Journal of Obstetrics and Gynaecology,* vol. 121, no. 9, pp. 1155-63, 2014.

[101] S. Chan, R. Cheung, K. Yiu, L. Lee and T. Chung, "Effect of levator ani muscle injury on primiparous women during the first year after childbirth," *International Urogynecology Journal,* vol. 25, no. 10, pp. 1381-8, 2014.

[102] J. Garcia Mejido, C. Suarez Serrano, A. Fernandez Palacin, A. Aquise Pino, M. Bonomi Barby and J. Sainz Bueno, "Evaluation of levator ani muscle throughout the diferent stages of labor by transperineal 3D ultrasound," *Neurourology and Urodynamics,* p. Epub, 2016.

[103] P. Rahmanou, J. Caudwell-Hall, I. Kamisan Atan and H. Dietz, "The association between maternal age at first delivery and risk of obstetric trauma," *American Journal of Obstetrics and Gynecology,* vol. 215, no. 4, pp. e1-7, 2016.

[104] D. Valsky, S. Cohen, M. Lipschuetz, D. Hochner-Celnikier, H. Daum, I. Yagel and S. Yagel, "Third- or Fourth-Degree Intrapartum Anal Sphincter Tears are Associated with Levator Ani Avulsion in Primiparas," *Journal of Ultrasound in Medicine,* vol. 35, no. 4, pp. 709-15, 2016.

[105] D. Valsky, M. Lipschuetz, A. Bord, I. Eldar, B. Messing, D. Hochner-Celnikier, Y. Lavy, S. Cohen and S. Yagel, "Fetal head circumference and length of second stage of labor are risk factors for levator ani muscle injury, diagnosed by 3-dimensional transperineal ultrasound in primiparous women," *American Journal of Obstetrics and Gynecology,* vol. 201, no. 1, pp. 91.e1-7, 2009.

[106] L. Chen, S. Lisse, K. Larson, M. Berger, J. Ashton-Miller and J. O. L. DeLancey, "Structural Failure Sites in Anterior Vaginal Wall Prolapse: Identification of a Collinear Triad," *Obstetrics and Gynecology,* vol. 128, no. 4, pp. 853-62, 2016.

[107] R. Paramore, The Statistics of the Female Pelvic Viscera, London: Lewis, 1925.

[108] J. Tandler, "Anatomie und topographische Anatomie der weiblichen Genitalien," in *Stoeckel's Handbuch der Gynaekologie*, Muenchen, J F Bergmann, 1930.

[109] A. Curtis, B. Anson and F. Ashley, "Further studies in gynecological anatomy and related clinical problems," *Surg Gynecol Obstet,* 1942.

[110] B. Berglas and I. Rubin, "Study of the supportive structures of the uterus by levator myography," *Surgery, Gynecology & Obstetrics,* vol. 97, no. 6, pp. 677-92, 1953.

[111] J. O. L. DeLancey, L. Hoyte and M. Damaser, "Chapter 2 - Pelvic Floor Anatomy and Pathology," in *Biomechanics of the Pelvic Floor*, London, UK, Academic Press, 2016, pp. 13 - 51.

[112] R. Margulies, M. Huebner and J. O. L. DeLancey, "Origin and insertion points involved in levator ani muscle defects," *American Journal of Obstetrics and Gynecology,* vol. 196, no. 3, pp. 251-255, 2007.

[113] J. Kim, C. Betschart, R. Ramanah, J. Ashton-Miller and J. O. L. DeLancey, "Anatomy of the pubovisceral muscle origin: Macroscopic and microscopic findings within the injury zone," *Neurourology and Urodynamics,* vol. 34, no. 8, pp. 774-780, 2015.

[114] C. Betschart, J. Kim, J. M. Miller, J. A. Ashton-Miller and J. O. L. DeLancey, "Comparison of muscle fiber directions between different levator ani muscle subdivisions: in vivo MRI

measurements in women," *International Urogynecology Journal,* vol. 25, no. 9, pp. 1263-1268, 2014.

[115] P. V. Tracy, J. O. L. DeLancey and J. A. Ashton-Miller, "A Geometric Capacity - Demand Analysis of Maternal Levator Muscle Stretch Required for Vaginal Delivery," *Journal of Biomechanical Engineering,* pp. e1-e54, 2016.

[116] K. Lammers, K. Kluivers, M. Vierhout, M. Prokop and J. Futterer, "Inter- and intraobserver reliability for diagnosing levator ani changes on magnetic resonance imaging," *Ultrasound in Obstetrics & Gynecology,* vol. 42, no. 3, pp. 347-52, 2013.

[117] A. Derpapas, A. Digesu, M. Hamady, P. Gallo, C. Dell'Utri, G. Vijaya and V. Khullar, "Prevalence of pubovisceral muscle avulsion in a general gynecology cohort: a computed tomography (CT) study," *Neurourology and Urodynamics,* vol. 32, no. 4, pp. 359-62, 2013.

[118] J. O. L. DeLancey, H. Sorensen, C. Lewicky-Gaupp and T. Smith, "Comparison of the puborectal muscle on MRI in women with POP and levator ani defects with those with normal support and no defect," *International Urogynecology Journal,* vol. 23, no. 1, pp. 73-77, 2012.

[119] R. Kearney, J. Miller, J. Ashton-Miller and J. O. L. DeLancey, "Obstetric factors associated with levator ani muscle injury after vaginal birth," *Obstetrics and Gynecology,* vol. 107, no. 1, pp. 144-9, 2006.

[120] J. Caudwell-Hall, I. Kamisan Atan, A. Martin, R. Guzman Rojas, S. Langer, K. Shek and H. Dietz, "Intrapartum Predictors of Maternal Levator Ani Injury," *Acta Obstetricia et Gynecologica Scandinavica,* p. Epub ahead of print, 2017.

[121] L. Krofta, M. Otcenasek, E. Kasikova and J. Feyereisl, "Pubococcygeus-puborectalis trauma after forceps delivery: evaluation of the levator ani muscle with 3D/4D ultrasound," *International Urogynecology Journal and Pelvic Floor Dysfunction,* vol. 20, no. 10, pp. 1175-81, 2009.

[122] R. Kearney, M. Fitzpatrick, S. Brennan, M. Behan, J. Miller, D. Keane, C. O'Herlihy and J. O. L. DeLancey, "Levator ani injury in primiparous women with forceps delivery for fetal distress, forceps for second stage arrest, and spontaneous delivery," *International Journal of Gynaecology and Obstetrics,* vol. 111, no. 1, pp. 19-22, 2010.

[123] L. Low, R. Zielinski, Y. Tao, A. Galecki, C. Brandon and J. Miller, "Predicting Birth-Related Levator Ani Tear Severity in Primiparous Women: Evaluating Maternal Recovery from Labor and Delivery (EMRLD)," *Open Journal of Obstetrics and Gynecology,* vol. 4, no. 6, pp. 266-78, 2014.

[124] G. Rostaminia, J. D. Peck, K. Van Deft, R. Thakar, A. Sultan and S. A. Shobeiri, "New Measures for Predicting Birth-Related Pelvic Floor Trauma," *Female Pelvic Med Reconstructive Surgery,* vol. 22, no. 5, pp. 292-6, 2016.

[125] J. Garcia-Mejido, L. Gutieerez-Palomino, C. Borrero, P. Valdivieso, A. Fernandez-Palacin and J. Sainz-Bueno, "Factors that influence the development of avulsion of the levator ani muscle in eutocic deliveries: 3-4D transperineal ultrasound study," *The Journal of Maternal-Fetal & Neonatal Medicine,* vol. 29, no. 19, pp. 3183-6, 2016.

[126] D. Wilson, J. Dornan, I. Mislsom and R. Freeman, "UR-CHOICE: can we provide mothers-to-be with information about the risk of future pelvic floor dysfunction?," *International Urogynecology Journal,* vol. 25, no. 11, pp. 1449-52, 2014.

[127] A. Lehn, A. Baumer and M. Leftwich, "An experimental approach to a simplified model of human birth," *Journal of Biomechanics,* vol. 49, no. 11, pp. 2313-7, 2016.

[128] D. P. M. Oliverira, B. Calvo, T. Mascarenhas and R. Natal Jorge, "Numerical Simulation of the Damage Evolution in the pelvic floor muscles during childbirth," *Journal of Biomechanics,* vol. 49, no. 4, pp. 594-601, 2016.

[129] L. Krofta, L. Havelkova, I. Urbankova, M. Kromar, L. Hyncik and J. Feyereisl, "Finite Element Model Focused on Stress Distribution In the Levator Ani Muscle During Vaginal Delivery," *International Urogynecology Journal,* vol. 28, no. 2, pp. 275-284, 2016.

[130] M. E. T. Silva, D. A. Oliveira, T. H. Roza, S. Brandao, M. P. L. Parente, T. Mascarenhas and R. M. Natal Jorge, "Study on the influence of the fetus head molding on the biomechanical behavior of the pelvic floor muscles, during vaginal delivery," *Journal of Biomechanics,* vol. 48, no. 9, pp. 1600-1605, 2015.

[131] X. Yan, J. A. Kruger, P. M. Nielsen and M. P. Nash, "Effects of fetal head shape variation on the second stage of labour," *Journal of Biomechanics,* vol. 48, no. 9, pp. 1593-1599, 2015.

[132] M. Berardi, O. Martinez-Romero, A. Elias-Zuniga, M. Rodriguez, E. Ceretti, A. Fjorentino, G. Donzella and A. Avanzini, "Levator Ani Deformation During the Second Stage of Labour," *Proceedings of the Institution of Mechanical Engineers, Part H, Journal of Engineering in Medicine,* vol. 228, no. 5, pp. 501-508, 2014.

[133] D. Jing, J. A. Ashton-Miller and J. O. L. DeLancey, "A subject-specific anisotropic visco-hyperelastic finite element model of female pelvic floor stress and strain during the second stage of labor," *Journal of Biomechanics,* vol. 45, pp. 455-460, 2012.

[134] X. Yan, J. Kruger, P. Nielsen and M. Nash, "Effects of Levator Ani Muscle Morphology on the Mechanics of Vaginal Childbirth," in *Computational Biomechanics for Medicine*, New York, Springer, 2012, pp. 63-75.

[135] X. Li, J. Kruger, M. Nash and P. Nielsen, "Anisotropic effects of the levator ani muscle during childbirth," *Biomechanics and Modeling in Mechanobiology,* vol. 10, no. 4, pp. 485-94, 2011.

[136] M. Parente, R. Natal Jorge, T. Mascarenchas, A. Fernandes and A. Silva-Filho, "Computational Modeling Approach to Study the Effects of Fetal Head Flexion During Vaginal Delivery," *American Journal of Obstetrics and Gynecology,* vol. 203, no. 3, pp. 217.e1-6, 2010.

[137] X. Li, J. Kruger, M. Nash and P. Nielsen, "Effects of nonlinear muscle elasticity on pelvic floor mechanics during vaginal childbirth," *Journal of Biomechanical Engineering,* vol. 132, no. 11, 2010.

[138] M. Parente, R. Natal Jorge, T. Mascarenhas and A. M. J. Fernandes, "The influence of the material properties on the biomechanical behavior of the pelvic floor muscles during vaginal delivery," *Journal of Biomechanics,* vol. 42, no. 9, pp. 1301-6, 2009.

[139] M. Parente, R. Jorge, T. Mascarenhas, A. Fernandes and J. Martins, "The Influence of an Occipito-Posterior Malposition on the Biomechanical Behavior of the Pelvic Floor," *European Journal of Obstetrics, Gynecology, and Reproductive Biology,* vol. 144, no. 1, pp. S166-9, 2009.

[140] K. Svabik, K. Shek and H. Dietz, "How much does the levator hiatus have to stretch during childbirth?," *Urogynaecology,* vol. 116, no. 12, pp. 1657-62, 2009.

[141] M. Parente, R. Natal Jorge, T. Mascarenhas, A. Fernandes and J. Martins, "Deformation of the pelvic floor muscles during a vaginal delivery," *International Urogynecology Journal and Pelvic Floor Dysfunction,* vol. 19, no. 1, pp. 65-71, 2008.

[142] L. Hoyte, M. Damaser, S. Warfield, G. Chukkapalli, A. Majumdar, D. Choi, A. Trivedi and P. Krysl, "Quantitiy and Distribution of Levator Ani Stretch During Simulated Vaginal Childbirth," *American Journal of Obstetrics and Gynecology,* vol. 199, no. 2, pp. 198.e1-5, 2008.

[143] J. Martins, M. Pato, E. Pires, M. Parente and T. Mascarenhas, "Finite element studies of the deformation of the pelvic floor," *Annals of the New York Academy of Sciences,* vol. 1101, no. 1, pp. 316-34, 2007.

[144] K. Lien, B. Mooney, J. O. L. DeLancey and J. Ashton-Miller, "Levator ani muscle stretch induced by simulated vaginal birth," *Obstetrics and Gynecology,* vol. 103, no. 1, pp. 31-40, 2004.

[145] C. Rubod, M. Boukerrou, M. Brieu, C. Jean-Charles, P. Dubois and M. Cosson, "Biomechanical properties of vaginal tissue: preliminary results," *Internation Urogynecology Journal and Pelvic Floor Dysfunction,* vol. 19, no. 6, pp. 811-6, 2008.

[146] E. Pena, P. Martins, T. Mascarenhas, R. M. Natal Jorge, A. Ferreira, M. Doblare and B. Calvo, "Mechanical Characterization of the Softening Behavior of Human Vaginal Tissue," *Journal of the Mechanical Behavior of Biomedical Materials,* vol. 4, pp. 275-83, 2011.

[147] A. Nagle, M. Barker, S. Kleeman, B. Haridas and T. Mast, "Passive Biomechanical Properties of Human Cadaveric Levator Ani Muscle at Low Strains," *Journal of Biomechanics,* vol. 47, no. 2, pp. 583-6, 2014.

[148] M. Silva, S. Brandao, M. Parente, T. Mascarenhas and R. Natal Jorge, "Establishing the biomechanical properties of the pelvic soft tissues through an inverse finite element analysis using magnetic resonance imaging," *Proceedings of the Institution of Mechanical Engineers. Part H, Journal of Engineering in Medicine,* vol. 230, no. 4, pp. 298-309, 2016.

[149] G. Goldish, J. Quast, J. Blow and M. Kuskowski, "Postural effects on intra-abdominal pressure during Valsalva maneuver," *Archives of Physical Medicine and Rehabilitation,* vol. 75, no. 3, pp. 324-7, 1994.

[150] S. Madjar, M. Balzarro, R. Appell, M. Tchetgen and D. Nelson, "Baseline abdominal pressure and valsalva leak point pressures-correlation with clinical and urodynamic data," *Neurourology and Urodynamics,* vol. 22, no. 1, pp. 2-6, 2003.

[151] D. Hackett and C. Chow, "The Valsalva maneuver: its effect on intra-abdominal pressure and safety during resistance exercise," *Journal of Strength and Conditioning Research,* vol.

27, no. 8, pp. 2338-45, 2013.

[152] J. L. Lowder, K. M. Debes, D. K. Moon, N. Howden, S. D. Abramowitch and P. A. Moalli, "Biomechanical Adaptations of the Rat Vagina and Supportive Tissues in Pregnancy to Accommodate Delivery," *Obstetrics and Gynecology,* vol. 109, no. 1, pp. 136-143, 2007.

[153] D. Rahn, M. Ruff, S. Brown, H. Tibbals and R. Word, "Biomechanical properties of the vaginal wall: effect of pregnancy, elastic fiber deficiency, and pelvic organ prolapse," *American Journal of Obstetrics and Gynecology,* vol. 198, no. 5, pp. 590.e1-6, 2008.

[154] D. Jing, "Experimental and Theoretical Biomechanical Analyses of the Second Stage of Labor.," 2010. [Online]. Available: http://deepblue.lib.umich.edu/handle/2027.42/76013. [Accessed 21 August 2015].

[155] M. Alperin, A. Feola, R. Duerr, P. Moalli and S. Abramowitch, "Pregnancy- and delivery-induced biomechanical changes in rat vagina persist postpartum," *International Urogynecology Journal,* vol. 21, no. 9, pp. 1169-74, 2010.

[156] A. Feola, P. Moalli, M. Alperin, R. Duerr, R. Gandley and S. Abramowitch, "Impact of pregnancy and vaginal delivery on the passive and active mechanics of the rat vagina," *Annals of Biomedical Engineering,* vol. 39, no. 1, pp. 549-58, 2011.

[157] D. Ulrich, S. L. Edwards, K. Su, J. F. White, J. A. M. Ramshaw, G. Jenkin, J. Deprest, A. Rosamilia, J. A. Werkmeister and C. E. Gargett, "Influence of Reproductive Status on Tissue Composition and Biomechanical Properties of Ovine Vagina," *Public Library of Science,* vol. 9, no. 4, pp. 1 - 8, 2014.

[158] A. Feola, M. Endo and J. Deprest, "Biomechanics of the rat vagina during pregnancy and postpartum: a 3-dimensional ultrasound approach," *International Urogynecology Journal,* vol. 25, no. 7, pp. 915-20, 2014.

[159] K. Yoshida, C. Reeves, J. Vink, J. Kitajewski, R. Wapner, H. Jiang, S. Cremers and K. Myers, "Cervical collagen network remodeling in normal pregnancy and disrupted parturition in Antxr2 deficient mice," *Journal of Biomechanical Engineering,* vol. 136, no. 2, 2014.

[160] K. Yoshida, M. Mahendroo, J. Vink, R. Wapner and K. Myers, "Material properties of mouse cervical tissue in normal gestation," *Acta Biomaterialia,* vol. 36, no. 1, pp. 195-209, 2016.

[161] D. Liao, L. Hee, P. Sandager, N. Uldbjerg and H. Gregersen, "Identification of biomechanical properties in vivo in human uterine cervix," *Journal of the Mechanical Behavior of Biomedical Materials,* vol. 39, no. 1, pp. 27-37, 2014.

[162] O. Sherwood, V. Crnekovic, W. Gordon and J. Rutherford, "Radioimmunoassay of relaxin throughout pregnancy and during parturition in the rat," *Endocrinology,* vol. 107, no. 3, pp. 691-8, 1980.

[163] J. Woessner and T. Brewer, "Formation and breakdown of collagen and elastin in the human uterus during pregnancy and post-partum involution," *The Biochemical Journal,* vol. 89, no. 1, pp. 75-82, 1963.

[164] A. Rundgren, "Phyiscal properties of connective tissue as influenced by single and repeated pregnancies in the rat," *Acta physiologica Scandinavica. Supplementum.,* vol. 417, no. 1, pp. 1-138, 1974.

[165] M. Alperin, T. Kaddis, R. Pichika, M. Esparza and R. Lieber, "Pregnancy-induced adaptations in intramuscular extracellular matrix of rat pelvic floor muscles," *American Journal of Obstetrics and Gynecology,* vol. 215, no. 2, pp. 210.e1-7, 2016.

[166] M. Harkness and R. Harkness, "The collagen content of the reproductive tract of the rat during pregnancy and lactation," *The Journal of Physiology,* vol. 123, no. 3, pp. 492-500, 1954.

[167] M. Alperin, D. M. Lawley, M. C. Esparza and R. L. Lieber, "Pregnancy-induced adaptations in the intrinsic structure of rat pelvic floor muscles," *American Journal of Obstetrics and Gynecology,* vol. 213, no. 2, pp. 191 - 197, 2015.

[168] K. Shek, J. Kruger and H. Dietz, "The effect of pregnancy on hiatal dimensions and urethral mobility: an observational study," *International Urogynecology Journal,* vol. 23, no. 11, pp. 1561-7, 2012.

[169] J. Staer-Jensen, F. Siafarikas, G. Hilde, K. Bo and M. Engh, "Ultrasonographic evaluation of pelvic organ support during pregnancy.," *Obstetrics and Gynecology,* vol. 122, no. 2 Pt 1, pp. 329-36, 2013.

[170] G. van Veelen, K. Schweitzer and C. van der Vaart, "Ultrasound imaging of the pelvic floor: changes in anatomy during and after first pregnancy," *Ultrasound in Obstetrics & Gynecology,* vol. 44, no. 4, pp. 476-80, 2014.

[171] S. Oliphant, I. Nygaard, W. Zong, T. Canavan and P. Moalli, "Maternal adaptations in preparation for parturition predict uncomplicated spontaneous delivery outcome.," *American Journal of Obstetrics and Gynecology,* vol. 211, no. 6, pp. 630.e1-7, 2014.

[172] S. Chan, R. Cheung, K. Yiu, L. Lee, T. Leung and T. Chung, "Pelvic floor biometry during a first singleton pregnancy and the relationship with symptoms of pelvic floor disorders: a prospective observational study," *BJOG: an International Journal of Obstetrics and Gynaecology,* vol. 121, no. 1, pp. 121-9, 2014.

[173] F. Siafarikas, J. Staer-Jensen, G. Hilde, K. Bo and M. Ellstrom Engh, "The levator ani muscle during pregnancy and major levator ani muscle defects diagnosed postpartum: a three- and four- dimensional transperineal ultrasound study," *BJOG: an International Journal of Obstetrics and Gynaecology,* vol. 122, no. 8, pp. 1083-91, 2015.

[174] J. Staer-Jensen, F. Siafarikas, G. Hilde, J. Benth, K. Bo and M. Engh, "Postpartum recovery of levator hiatus and bladder neck mobility in relation to pregnancy," *Obstetrics and Gynecology,* vol. 125, no. 3, pp. 531-9, 2015.

[175] J. Daucher, K. Clark, D. Stolz, L. Meyn and P. Moalli, "Adaptations of the rat vagina in pregnancy to accommodate delivery," *Obstetrics and Gynecology,* vol. 109, no. 1, pp. 128-35, 2007.

[176] Y. C. Fung, Biomechanics: Mechanical Properties of Living Tissues, New York, NY: Springer-Verlag, 1993.

[177] M. Kwan, T. Lin and S. Woo, "On the viscoelastic properties of the anteromedial bundle of the anterior cruciate ligament," *Journal of Biomechanics,* vol. 26, no. 4-5, pp. 447-52, 1993.

[178] G. Johnson, D. Tramaglini, R. Levine, K. Ohno, N. Choi and S. Woo, "Tensile and viscoelastic properties of human patellar tendon," *Journal of Orthopaedic Research,* vol. 12, no. 6, pp. 796-803, 1994.

[179] E. Carew, E. Talman, D. Boughner and I. Vesely, "Quasi-Linear Viscoelastic theory applied to internal shearing of porcine aortic valve leaflets," *Journal of Biomechanical Engineering,* vol. 121, no. 4, pp. 386-92, 1999.

[180] J. Funk, G. Hall, J. Crandall and W. Pilkey, "Linear and Quasi-Linear Viscoelastic Characterization of Ankle Ligaments," *Journal of Biomechanical Engineering,* vol. 122, no. 1, pp. 15-22, 2000.

[181] J. Sarver, P. Robinson and D. Elliott, "Methods for quasi-linear viscoelastic modelling of soft tissue: application to incremental stress-relaxation experiments," *Journal of Biomechanical Engineering,* vol. 125, no. 5, pp. 754-8, 2003.

[182] O. Lokshin and Y. Lanir, "Viscoelasticity and preconditioning of rat skin under uniaxial stretch: microstructural constitutive characterization," *Journal of Biomechanical Engineering,* vol. 131, no. 3, 2009.

[183] S. V. Brooks, E. Zerba and J. A. Faulkner, "Injury to muscle fibers after single stretches of passive and maximally stimulated muscles in mice," *Journal of Physiology,* vol. 488, no. 2, pp. 459-469, 1995.

[184] M. Chiba and K. Komatsu, "Mechanical Responses of the Periodontal Ligament in the Transverse Section of the Rat Mandibular Incisor at Various Velocities of Loading In Vitro," *Journal of Biomechanics,* vol. 26, no. 4, pp. 561-70, 1993.

[185] M. M. Panjabi, J. J. Crisco, C. Lydon and J. Dvorak, "The Mechanical Properties of Human Alar and Transverse Ligaments at Slow and Fast Extension Rates," *Clinical Biomechanics,* vol. 13, no. 2, pp. 112-20, 1998.

[186] T. J. Bonner, N. Newell, A. Kuranaratne, A. D. Pullen, A. A. Amis, A. M. J. Bull and S. D. Masouros, "Strain-rate sensitivity of the lateral collateral ligament of the knee," *Journal of the Mechanical Behavior of Biomedical Materials,* vol. 41, pp. 261-270, 2015.

Chapter 2: A Geometric Capacity - Demand Analysis of Maternal Levator Muscle Stretch Required for Vaginal Delivery

Paige V. Tracy[1], John O. DeLancey[2], James A. Ashton-Miller[3]
[1] Department of Biomedical Engineering, University of Michigan
[2] Department of Obstetrics and Gynecology, University of Michigan
[3] Department of Mechanical Engineering, University of Michigan

This chapter has been published in the Journal of Biomechanical Engineering.

2.1 Abstract

Because levator ani muscle injuries occur in approximately 13% of all vaginal births, insights are needed to better prevent them. In Part I of this paper we conducted an analysis of the bony and soft tissue factors contributing to the geometric 'capacity' of the maternal pelvis and pelvic floor to deliver a fetal head without incurring stretch injury of the maternal soft tissue. In Part II we quantified the range in demand, represented by the variation in fetal head size and shape, placed on the maternal pelvic floor. In Part III we analyzed the capacity-to-demand geometric ratio, g, in order to determine whether a mother can deliver a head of given size without stretch injury. The results of a Part I sensitivity analysis showed that initial soft tissue loop length had the greatest effect on maternal capacity, followed by the length of the soft tissue loop above the inferior pubic rami at ultimate crowning, then subpubic arch angle and head size, and finally the levator origin separation distance. We found the more caudal origin of the

puborectal portion of the levator muscle helps to protect it from the stretch injuries commonly observed in the pubovisceral portion. Part II fetal head molding index and fetal head size revealed fetal head circumference values ranging from 253 to 351 mm, which would increase up to 11 mm upon face presentation. The Part III capacity-demand analysis of g revealed that, based on geometry alone, the 10th percentile maternal capacity predicted injury for all head sizes, the 25th percentile maternal capacity could deliver half of all head sizes, while the 50th percentile maternal capacity could deliver a head of any size without injury. If ultrasound imaging could be operationalized to make measurements of ratio g it might be used to usefully inform women on their level risk for levator injury during vaginal birth.

2.2 Introduction

The soft tissues surrounding the birth canal undergo remarkable elongation to allow a fetal head to emerge from the pelvis [1] [2] [3]. Unfortunately, the elongation can be such that approximately 13% of women delivering vaginally for the first time sustain stretch-related injuries of their levator ani (LA) muscles. These muscles partially surround the birth canal [4] and form the key soft tissue structures that must be dilated for delivery to occur. Using magnetic resonance imaging, researchers have identified the injuries as partial or complete damage of the left and/or right side pubovisceral muscle (PVM) portion of the LA [5]. These injuries are presently not treated surgically because the risks of repairing such deep structures outweigh any benefit that might derive. These injuries are found much more often in women with pelvic floor dysfunction, including pelvic organ prolapse. For example, the relative risk of prolapse compared to nulliparous women is 4 in women who have given birth to one child, and 8 in women who have given birth to two children [6]. Indeed, approximately 11% of all U.S.

women undergo surgery later in life for pelvic organ prolapse, or urinary and fecal incontinence, with the leading risk factor for developing these conditions being vaginal birth (for review, see [7]). At present it is not possible to predict which women will be injured during a vaginal birth. Furthermore, we do not know which pre-labor maternal and fetal parameters might help predict injury. The goal of this paper is to provide the conceptual and mathematical framework to consider these questions and to report the results of our first analyses.

The factor of safety for a structure like a bridge is defined as the ratio of the capacity of the structure to resist, without failure, the loads applied divided by the maximum load, or demand, that it will be called upon to resist in service. Using this capacity-demand concept, one can define the geometric capacity-demand ratio, g, for vaginal birth as the ratio of maternal geometric capacity to pass a fetal head through the birth canal divided by the demand, which is represented by the size of the fetal head. More precisely, the maternal capacity can be defined as the largest internal circumference to which the soft tissues defining the narrowest part of the maternal birth canal can stretch without failure. The fetal demand is maximum circumference of the fetal head presented to the narrowest part of the birth canal after molding of the fetal head; molding is the amount of fetal head compression needed to pass through the birth canal. If we disregard time-dependent effects for the moment, then when g is greater than unity, no levator injury will result. When g is much less than unity, levator injury will almost certainly result because the fetal head is too large to pass through the birth canal without stretching the maternal soft tissues beyond their ability to lengthen without rupture. But when g is just less than 1 there is uncertainty about whether injury will result. A goal of this paper is to determine the range of possible values for g based on the known variance in

maternal and fetal geometries. In clinical practice knowledge of the value of g might help the expectant mother better evaluate her different delivery options.

In terms of anatomy, when the fetal head passes through the birth canal it is bounded by the front of the boney pelvis, comprised of the pubic symphysis with pubic rami on either side, and partly by the "U"-shaped soft tissue forming a loop laterally and posteriorly. As the second stage of labor progresses and the baby descends through the birth canal along the curve of Carus, the fetal head comes into contact with the more inferior regions of the pubic rami and different regions of soft tissue become progressively engaged by the fetal head. There has not been a detailed analysis of which soft tissues comprise those different regions of the U-shape because there has not been a precise anatomic description of the orientation of those soft tissues until recently [8].

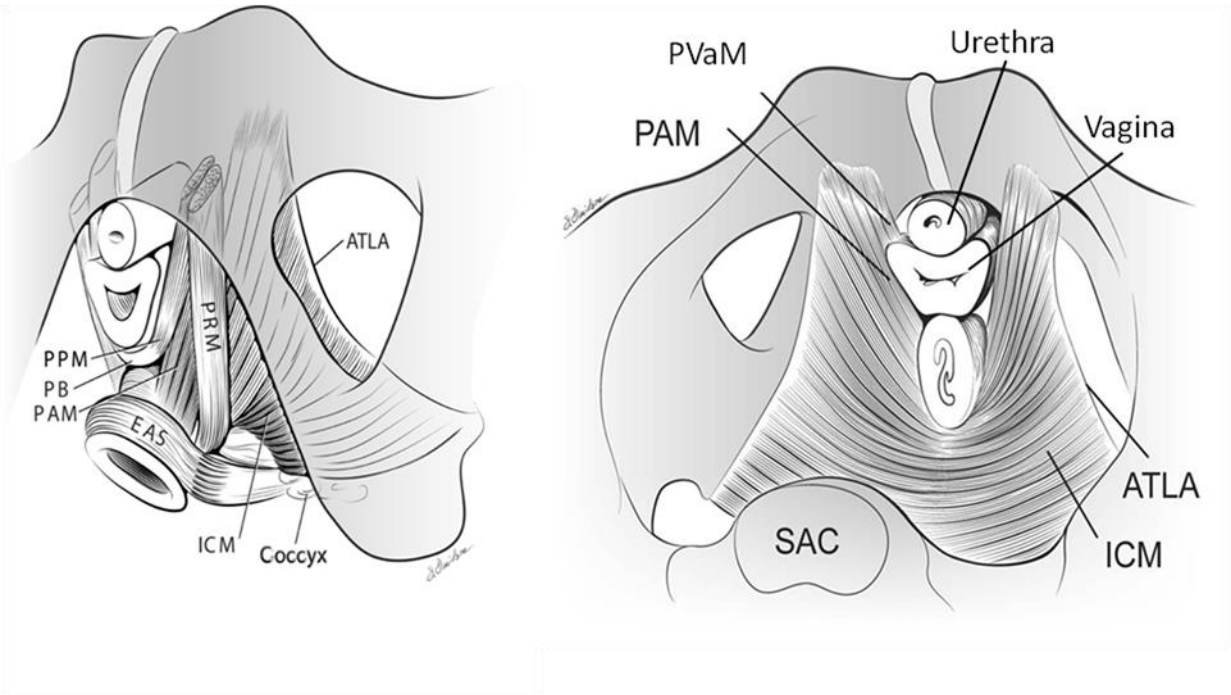

Figure 2.1 - Schematic illustration of the levator ani muscles. The subcomponents of the pubovisceral muscle (puboperineal, PPM; puboanal, PAM, and pubovaginal, PVaM) are shown. *Left:* Schematic view of the levator ani muscles from below after the vulvar structures

and perineal membrane have been removed showing the arcus tendineus levator ani (*ATLA*); external anal sphincter (*EAS*); puboanal muscle (*PAM*); perineal body (*PB*) uniting the two ends of the puboperineal muscle (*PPM*); iliococcygeal muscle (*ICM*); puborectal muscle (*PRM*). *Right:* The LA muscle seen from above looking over the sacral promontory (*SAC*) showing the PVaM. The urethra, vagina, and rectum have been transected just above the pelvic floor. (The internal obturator muscles have been removed to clarify levator muscle origins.) Recently, it has become clear that the origin of the PRM lies more caudal than is suggested in the illustration at left [8]. Copyright © DeLancey 2003 [9].

In the case of the soft tissue loop, the levator ani muscles comprise the majority of the U-shaped soft tissue loop which surrounds the central opening, called the levator hiatus, through which the baby must pass. The soft tissue is comprised of several subdivisions; the pubovisceral (also known as the pubococcygeal), the puborectal and the iliococcygeal portions (Figure 2.1). The pubovisceral muscle itself also has three components; the pubovaginal, puboperineal, and puboanal portions. These latter parts are simply aspects of the pubovisceral muscle rather than distinct muscles and will be considered here to form a single muscle. The upper arms of the "U' attach to the pubic rami on either side of the pubic symphysis. In the most important, distal, region of the U-shaped loop, the tissues which will undergo the greatest stretch are the PVM and the puborectal muscles (PRM) [1]. The PVM inserts distally onto the perineal body (PB) and lateral margins of the anal sphincter (AS). The PVM and PRM together form the narrowest part of the birth canal. It will be shown to be functionally important that the PVM originates on either side of the posterior aspect of the pubic symphysis while the PRM originates more caudally [8]. The reason this is functionally important is because when muscle injury occurs, it is the PVM on one or both sides that is injured, and not the PRM [5]; this, despite the fact that they both arise from the posterior aspect of the bone near the pubic symphysis and both encircle the levator hiatus through which birth occurs. There is presently no biomechanical

explanation for this difference in the propensity for stretch injury and that is a secondary goal of this paper.

In Part I of this paper we conduct a geometric analysis of the contributions of variations in the bony and soft tissue factors to the geometric 'capacity' of the maternal pelvic floor to accommodate fetal head delivery without incurring maternal levator muscle stretch injury. We also conduct a sensitivity analysis of the maternal factors that contribute to the 50^{th} percentile maternal pelvis capacity to deliver a fetal head of given size. The factors we considered include the subpubic arch angle (SPAA), PVM and PRM origin placement, initial soft tissue loop lengths, and the effect of the downward rotation of the PVM and PRM around the pubic symphysis. In Part II we quantify the range in demand represented by the variation in geometric size of the fetal head and variation in fetal head molding. As to the main goal of this paper, Part III, we use the results from Parts I and II to analyze the interaction between maternal capacity and fetal demand by calculating the values for g to understand whether a mother can deliver a head of given size without stretch injury. In the Discussion, we will consider the possibility of using pre-labor ultrasound imaging to measure both maternal capacity and fetal demand in order to establish g for that individual.

2.3 Methods

2.3.1 Part I: Quantification of factors contributing to the maternal capacity for the 50th percentile woman.

We hypothesized that anatomical differences between the PVM and PRM muscles help to explain why the PVM is injured but the PRM is not. It is known, that in the standing posture, the PVM fibers angle downwards from their origin high on the inside of the pelvis in a posterior direction [8]. By contrast, the PRM fibers angle upward from their origin low on the pelvis [8]. The two loops overlap one another laterally, with the PRM passing outside the PVM (Figure 2.1). As labor progresses, the posterior PRM tissue is engaged first, followed by the anterolateral portion of the PVM [10]. Then, as the head is forced downward along the Curve of Carus, we assume that both loops are pushed downwards, rotating about their origins, which lie on a mediolateral axis, much as a bucket handle about its hinges. Unlike bucket handles, however, they are stretched significantly as they rotate downward to reach the "ultimate crowning" configuration (Figure 2.2). The lower margin of the pelvic bone forms an inverted valley, the SPAA, which is deeper as the fetal head moves downwards, causing the head to ride along the boney ridges on either side, thereby bridging the inverted valley. The larger the subpubic arch angle, the further apart lie the ridge lines (Figure 2.3). The origins of the PRM and PVM lie on the sides of the valley. As the head rides along the ridges most, ~90%, of the PVM soft tissue loop actually contacts the fetal head, while the remaining 10% of the PVM lies above the inferior pubic ramus (Point '2', Figure 2.2) on either side of the valley not in contact with the fetal head. Then, as the PVM loop is drawn and rotated downwards by the descending fetal head, the percentage of PVM length above Point 2 increases and the length in contact

with the greater part of the fetal head decreases to ~70%, because the valley is deeper. This means that the PVM will have to stretch more to accommodate the passage of the fetal head. The effective length of the PVM in contact with the head decreases (Figure 2.2) because less of the loop can pass around in contact with the fetal head. In contrast, the effective length of the PRM loop is unchanged as it rotates downward because its origins lie close to the inferior pubic ramus.

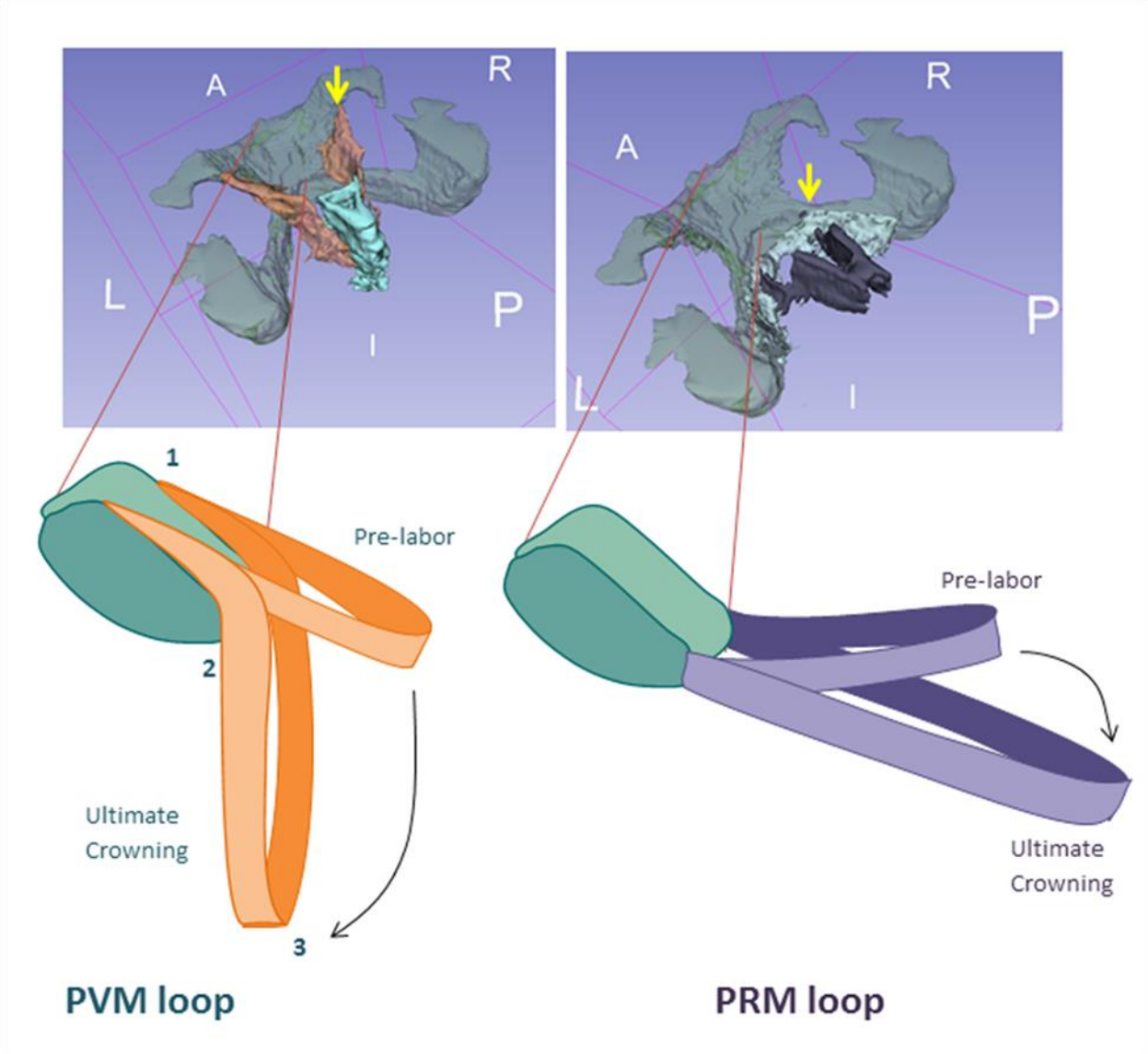

Figure 2.2 - Upper Left: Left lateral view of 3D model of the pelvis (green), showing the high origin location (yellow arrow) of the PVM (orange) and the PVM insertion on the PB/AS (blue).

Upper Right: 3D model of the pelvis (green), showing the PRM (purple) originating from the PM (white). In the upper two figures, A, P, L, R, and I denote anterior, posterior, left, right, and inferior, respectively. Lower left: The pubic symphysis is projected in the sagittal view seen in a view from the left showing a downward rotation of the PVM loop. Note the wrapping of the PVM around the inferior pubic ramus at point 2 at ultimate crowning. The portion of the PVM between points 1 and 2 lying above the inferior pubic ramus point, 2, is the "non-contact" length because it cannot contact and encircle the fetal head due to the rigidity of the pubic bone. That part of the PVM lying between points 2 and 3 lies below the pubic ramus at 2 so it can contact and encircle the fetal head to allow it to pass inside the loop formed by the PVM. Lower right: This illustrates the downward rotation of the PRM from the pre-labor to the ultimate crowning position. Note the absence of PRM wrapping.

Acquisition of Maternal MRI Data

MRI scans were acquired through the parent study "Evaluating Maternal Recovery from Labor and Delivery (EMRLD)" [11] [12], which followed primiparous women after childbirth (Institutional Review Board approval # HUM00051193). In this article, we limit our consideration to subjects who served as controls and delivered via caesarean section, and who did not attempt to push prior to delivery. This was to ensure that our geometric model represents the female pelvic floor prior to the development of delivery induced injuries. The complete MRI protocol has been described elsewhere [11] [12].

Maternal Capacity Model Generation

Axial, sagittal, and coronal images were imported into 3D Slicer 3.4.2009-10-15 (Brigham and Women's Hospital, Boston, MA, USA) imaging software. The segmentation editor module was used to create label maps of each feature. Label maps were based in the axial plane, but were traced using sagittal and coronal views as well. Anatomic features modeled include the

anterior pelvis, pubovisceral muscle (PVM), puborectal muscle (PRM), perineal membrane (PM), and the AS.

3-D models were generated for three individuals (Figure 2.2), and the individual closest to the 50th percentile was selected based on comparison to a previous 50th percentile model generated in our group [13]. Fiducial points were placed on visible PVM and PRM fibers identified in sagittal slices to establish their line-of-action [8]. These fiber lines were then extended until intersection with the pelvis (PVM) or PM (PRM) for origin identification and checked against the original scans to confirm anatomical plausibility. The posterior limit of these fibers was determined by extending their trajectory to the posterior-most point of the corresponding label map.

The subpubic arch was calculated using the right and left PRM and PVM origins, as well as a midpoint placed on the pubic septum at the level of the origins. Pythagoras' theorem was employed to calculate

Abbreviation	Description
L_{PRM}	$length\ of\ PRM, wrapped\ around\ rectum$
L_{PM}	$distance\ between\ pelvis\ and\ PRM\ origin\ on\ PM$
L_{PVM}	$combined\ length\ of\ PVM\ fibers, originating\ from\ pelvis\ and\ inserting\ or$ $/AS$
$L_{AS,PVM}$	$contact\ length\ between\ PVM\ and\ PB/AS\ at\ insertion$
d_{AS}	$diameter\ of\ AS$
t_{AS}	$AS\ thickness$
$L_{AS,max}$	$maximum\ length\ contribution\ of\ \frac{PB}{AS}, calculated\ from\ d_{AS}\ and\ t_{AS}$
$\delta_{origins,pelvis}$	$distance\ between\ origins\ along\ pelvis$
θ	$sub\ pubic\ arch\ angle$
L_{wrap}	$distance\ between\ origin\ on\ pelvis\ and\ nearest\ PVM$ $-\ head\ contact\ point$

Table 2.1 - Variables used in the 3D Slicer analysis.

Maternal Capacity Calculations

In what follows, the calculations were all performed in Microsoft Excel.

Anatomical consideration:

1) soft tissue loop length (SL)
    a. It has been observed in rat models that resting muscle fiber length can increase by 37% during pregnancy in preparation for birth [14]. This architectural elongation was incorporated as a 1.37 fiber elongation, FE.
    b. The striated muscle stretch ratio, R_{SM}, may reach up to 1.6 prior to onset of injury [15].
    c. No human data are available on PM elastic properties, it is estimated that the PM stretch ratio, R_{PM}, is able to reach up to 1.15 based on data available for the abdominal fascia [16].
    d. The loops of tissue involve three main types of tissue. The PVM and PRM are striated muscle and the AS complex has both smooth and striated muscle. PM and PB are primarily connective tissue.
        i. The PRM loop takes origin bilaterally from a short length of passive fascia, called the perineal membrane, and passes anteroposteriorly as a right and left muscle portion that decussate posteriorly behind the rectum to form the anorectal angle. We assumed that the anal sphincter is able to

deform prior to injury with the 1.6 striated muscle stretch ratio mentioned previously.

ii. The PVM takes origin from the pubic bone bilaterally at bony entheses [17] [18] and is comprised of striated muscle which inserts into the perineal body (PB) and smooth and striated muscle of the internal and external anal sphincters(AS) respectively, in the intersphincteric groove, which is located between these sphincters (Figure 2.2).

(1.1) $SL_{PRM} = FE * R_{SM} * L_{PRM} + R_{PM} * L_{PM} = soft\ tissue\ loop\ length\ for\ PRM$

(1.2) $SL_{PVM} = FE * R_{SM} * L_{PVM} - L_{AS,PVM} + L_{AS,max} = soft\ tissue\ loop\ length\ for\ PVM$

2) Maternal Capacity in the Ultimate Crowned State

a. We found that the PRM origin on the PM was so low that no wrapping of the PRM would occur about the inferior pubic rami in the downward rotation observed during birth.

b. The PVM origin lies approximately 2 cm below the pubic tubercle, necessitating up to 4 cm before it wraps around the pubic ramus on the left and right sides (Distance between 1 and 2 on Figure 2.2) [19]. This is termed the non-contact length because it reduces the muscle length available for contacting and accommodating the fetal head. The non-contact length was assumed to be a straight line. Accounting for curvature of the pelvis in this cut plane had less than a 1.5% effect on maternal capacity.

(2) $C_{M.lower} = SL + \pi * D_{head} * \left(\frac{180-\theta}{360}\right) - L_{wrap,left} - L_{wrap,right}$

3) Population variation

a. The H-line, which is the distance from the inferior posterior aspect of the pubic symphysis to the posterior rectal wall, and which represents the anteroposterior width of the levator hiatus, has been quantified, with a mean of 4.4 ± 0.7 cm in 178 Caucasian women [20] It is assumed here that percent variation in levator hiatus is proportional to variation in the soft tissue loop length.

b. The retropubic arch angle, in a study of 593 individuals, has been reported to have a mean of 109.3 ± 9.0^{o} when measured in the axial plane at the level of the PVM origins [21].

c. A study of 178 women found a mean lower pelvis SPAA of 83.7 ± 7.0^{o} [20].

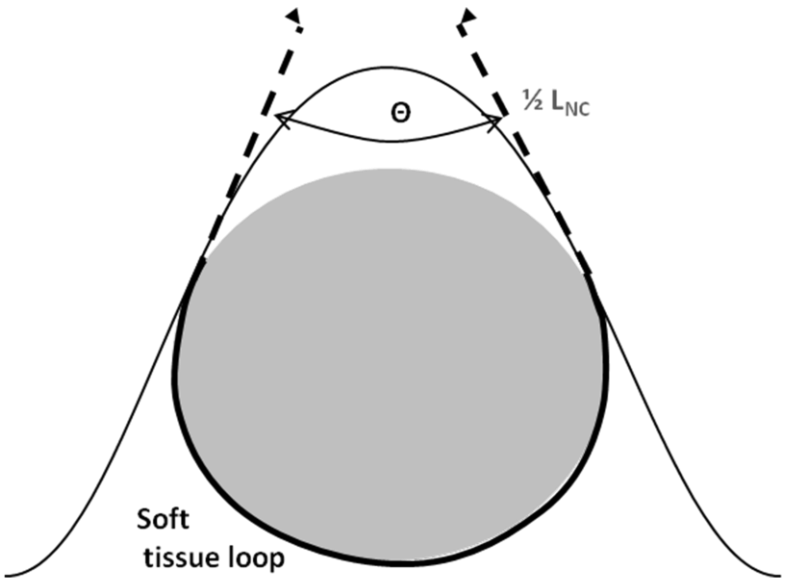

Figure 2.3 - Caudal view of anterior pelvis with variables used in the maternal capacity calculations. The soft tissue loop originates high on the pelvis (filled arrow heads) and wraps around the fetal head (grey circular structure). The portion of the soft tissue loop in contact

with the fetal head is represented by the thick black band, while the portion not in contact with the fetal head is represented by the dashed lines. Θ = subpubic arch angle. Arch = pelvis/ subpubic arch.

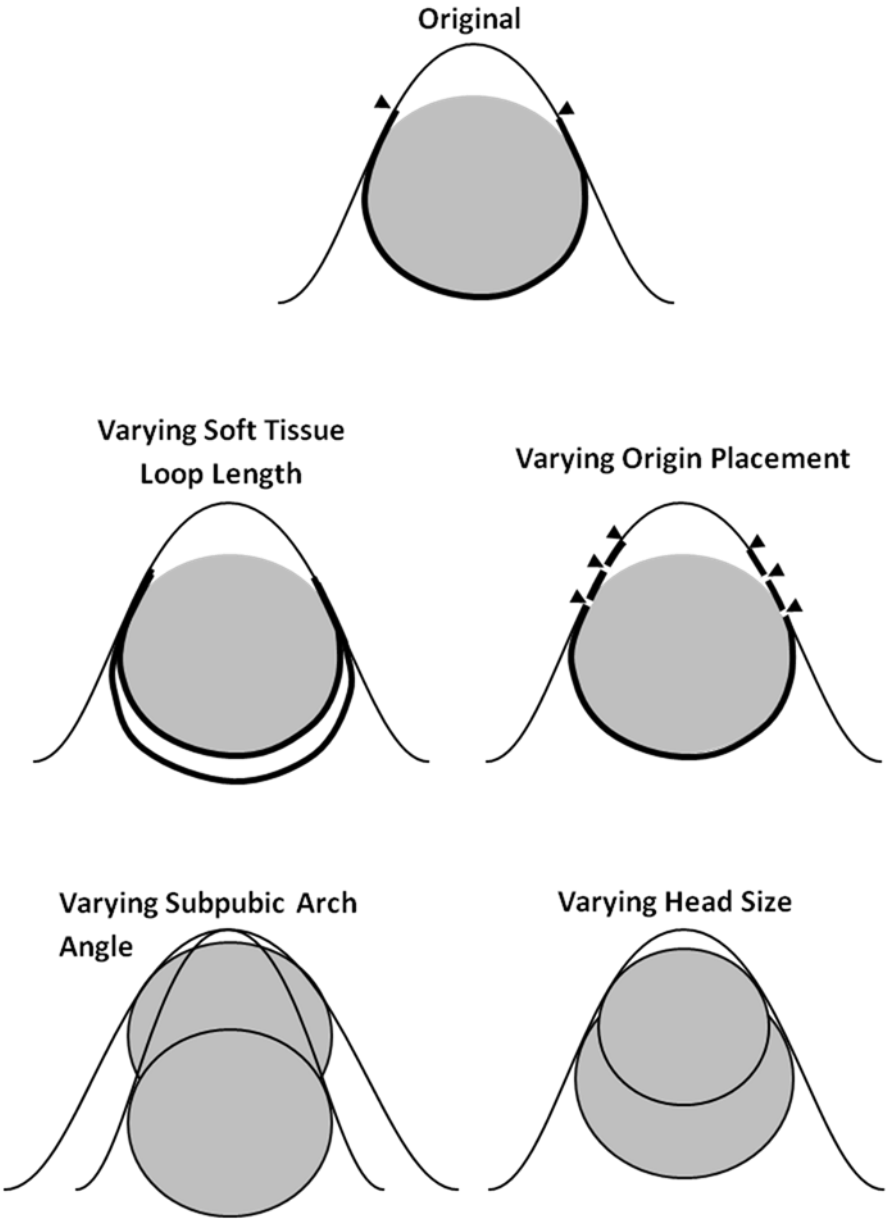

Figure 2.4 - Graphic illustration of the sensitivity analyses in caudal view. Top: Nominal configuration using the convention in Figure 2.3. Middle left: Varying soft tissue loop length (thick black band). Middle right: Varying soft tissue origin placement on pelvis (black arrow heads). Bottom left: Varying subpubic arch angle. Bottom right: Varying head size (grey circle). The variation in soft tissue length reduction in downward rotation is not shown. Factors were varied by ±10%.

Sensitivity analysis was performed by individually varying subpubic arch angle, soft tissue loop length, origin separation along pelvis, and the non-contact length (Figure 2.4). Each variable was increased and decreased by 10%.

The distribution of geometric maternal capacity values was calculated by incorporating the previously discussed quantified variation in SPAA and H-line values.

2.3.2 Part II: Quantification of Factors Affecting Fetal Head Demand

4) Approximating the Suboccipitobregmatic Circumference from the Occipitofrontal Circumference
    a) The Centers for Disease Control and Prevention has reported a mean male head circumference at birth of 344.6 mm and a mean female head circumference at birth of 338.8 mm [22] [23]. These data refer to the occipitofrontal circumference (OC), which is a function of the frontooccipital (FD) and biparietal diameters (BD) (Figure 2.5).
    b) The fetal head circumference that imposes the geometric demand on the pelvic floor during birth, the suboccipitobregmatic circumference (SC), is a function of the suboccipitobregmatic diameter (SD) and BD.
    c) Reduction of the biparietal and suboccipitobregmatic diameters and corresponding elongation of the mentovertical (maxillovertical) diameter results from compressive forces experienced during labor [24].
        i) A fetal head molding index (MI) for characterizing the degree of head deformation in the birth canal has been defined (eq 4.2, appendix), with a mean+SD value of 2.00 ± 0.22 observed clinically [25].

d) As a simplification we modeled the effective cross-section of the fetal head as circular at the time of labor (BD = SD).

e) It was also assumed that the volume of the fetal head is constant.

f) An instantaneous increase in BD of at least 0.5 cm following birth has been observed [26].

(4) $\pi * BD_L = \frac{OC\sqrt{2}}{\sqrt{1+\frac{MI}{1.2^2}}} - \frac{\pi}{2} cm = \boldsymbol{SC}$

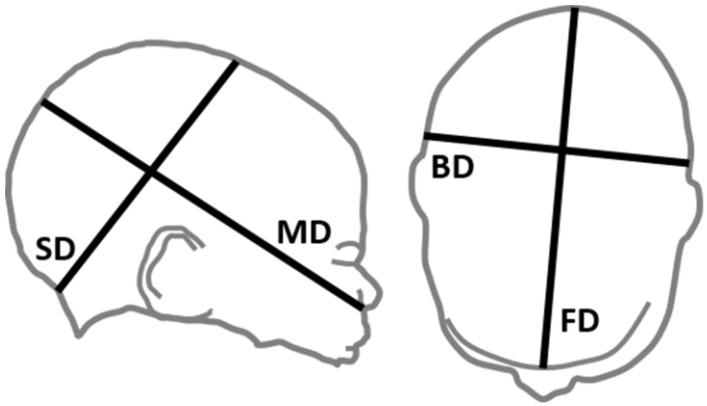

Figure 2.5 - Cranial and right side views of the fetal head showing the suboccipitobregmatic (SD), mentovertical (MD), biparietal (BD), and frontooccipital (FD) diameters. Figure adapted from Sobre et al. [27]

Functional fetal head circumferences were calculated for locations throughout reported population distributions for fetal head OC [12] [13] and molding [6] (Figure 2.6 & Figure 2.11S).

5) Usual and Abnormal Fetal Head Presentations

a) The most common fetal head position during the second stage of labor, as the head is delivered, is an occiput anterior position or 'vertex presentation', with the back of the head oriented towards the pubic symphysis, and the nose towards the sacrum.

b) In a minority of births, the fetus presents in the occiput posterior or transverse position, with the nose oriented towards the pubic symphysis and the back of the skull towards the sacrum or placed sideways.

c) This change in position does not change the head circumference itself. But it can, however, change the orientation of the head in the birth canal known as positional deflection of the head. The most extreme case of this deflection is a 'face presentation' [28] in which the presenting diameter typically becomes 7 mm longer than that experienced during the vertex presentation [29]. In our simulations, a normal occiput anterior or vertex presentation was assumed.

(5) $C_f = \sqrt{\frac{C_0^2 + (C_0 + \pi * 7mm)^2}{2}}$

2.3.3 Part III: Geometric Capacity-Demand Calculations Using the Value of g

A Capacity-Demand table for the values of g was created by using estimates of head size (SC) calculated for an average value of molding and using the minimum calculated maternal capacity for each population point which, interestingly, we shall see was always the PVM lower loop value rather than the PRM value (c.f., Figure 2.8 & Figure 2.10).

2.4 Results

2.4.1 Part I: Quantification of factors contributing to the maternal capacity for the 50th percentile woman.

Maternal circumference values for the 50th percentile female at Ultimate Crowning were 425 mm for PRM and 313 mm for PVM (Table 2.2).

	Circumference	Diameter
PRM loop	425	135
PVM without wrapping	347	110
PVM with wrapping	313	100

Table 2.2 - Effect of PVM wrapping on initial maternal capacities (in mm) for the 50th percentile female pelvis at ultimate crowning.

Our initial results assumed zero PB/AS deformation. We then investigated how reasonable geometric deformation of the PB/AS (Figure 2.11S) would contribute to maternal capacity to accommodate birth without injury (Table 2.3). We began with the shape deformation of the PB/AS from a circular sphincter to an elliptical cross section with corresponding stretch of the perineal body resulting from lateral tension, without changes in cross sectional area or wall thickness. This resulted in a maternal capacity increase to 326 mm for PVM. A 1.6x stretch without injury of the smooth muscle lining comprising the PB/AS resulted in a further increase in maternal capacity to 349 mm for PVM. All subsequent results follow from a model with PB/AS shape deformation and 1.6x levator muscle stretch.

	No Shape Deformation	Shape Deformation Only	Shape Deformation + Soft Tissue Stretch
PVM without wrapping	347	357	374
PVM with wrapping	313	326	349

Table 2.3 - Effect of incorporating PB/AS shape deformation and soft tissue stretch on maternal capacity (in mm) in the presence and absence of PVM wrapping about the inferior pubic ramus (see Figure 2.2).

Results for the sensitivity analysis (Table 2.4) showed that a 10% change in subpubic angle resulted in up to a 4% decrease or a 2% increase in circumference. Further, varying soft tissue loop length by 10% resulted in up to a 15% change in maternal capacity for the PVM loop. The same 10% change in soft tissue loop length resulted in up to an 8% change in circumference for the PRM loop. Likewise a 10% change in origin separation along the pelvis allowed for a 2 % change in circumference. Only two factors affected PVM circumference calculations: non-contact length and head diameter. A 10% change in non-contact length resulted in up to a 5% change in circumference. So, the factors with the greatest effect on maternal capacity were initial soft tissue loop length, downward bending angle and narrowing of the subpubic arch angle, in that order.

	PRM	PVM without wrapping	PVM with wrapping
Subpubic Arch Angle (-10%)	-3%	-2%	-4%
Subpubic Arch Angle (+10%)	+2%	+1%	+2%
Soft Tissue Loop Length (-10%)	-8%	-9%	-15%
Soft Tissue Loop Length (+10%)	+8%	+9%	+15%
Origin Separation Along Pelvis (-10%)	-2%	-1%	-2%
Origin Separation Along Pelvis (+10%)	+2%	+1%	+2%
Non-Contact Length (-10%)	0%	0%	+5%
Non-Contact Length (+10%)	0%	0%	-5%

Table 2.4 - Results of the sensitivity analyses (expressed as a percentage change in maternal circumference) for the four factors in the presence and absence of PVM wrapping.

Based on variations in SPAA and soft tissue loop length, the distribution in maternal capacity was calculated (Table 2.5). The 50^{th} percentile female had a capacity of 416 mm for PRM and 349 mm for PVM. The 2.3^{rd} percentile female had a capacity of 292 mm for PRM and 185 mm for PVM. The 97.7^{th} percentile female had a capacity of 543 mm for PRM and 484 mm for PVM.

From Table 2.2 and Table 2.3 we see that it is the PVM that is the levator structure that most constrains maternal geometric capacity after having rotated downward into its most inferior position at the end of the second stage. This finding corroborates and extends the results of Lien *et al.* who used a similar, but less accurate, site of PVM attachment on the pubic bone and who did not consider the downward rotation of the PVM in their analysis [1].

Maternal Percentile	PRM loop	PVM without wrapping	PVM with wrapping
2.3	292	259	185
5	313	279	216
10	336	300	248
15	351	314	269
25	374	334	298
50	416	372	349
75	458	409	397
90	497	443	438
95	521	464	462
97.7	543	483	484

Table 2.5 - Distribution of maternal geometric capacities (in mm) calculated with and without PVM wrapping about the inferior pubic rami.

2.4.2 Part II: Quantification of Factors Affecting Fetal Head Demand

Calculation of fetal head demand (SC) for population values of OC and MI revealed a SC value of 300 mm for a male head with 50^{th} percentile molding and 50^{th} percentile OC. Male fetuses having the same percentile value for both head size and molding (small head with very little molding, medium head with medium molding, large head with maximum molding) (green diagonal) ranged in SC value from 297 to 302 mm. A male head of minimum OC and maximum MI had a SC value of 257 mm, while a male head of minimum MI and maximum OC had a SC value of 351 mm. Values were slightly lower for female heads. (Appendix)

			fetal head circumference population distribution								
			2.30%	5%	10%	25%	50%	75%	90%	95%	97.70%
Molding population distribution	2.3%	-2	**277**	281	285	292	300	308	315	319	323
	5%	-1.65	271	**275**	279	286	294	301	308	312	316
	10%	-1.28	268	271	**276**	282	290	298	305	309	313
	25%	-0.68	263	266	270	**277**	285	292	299	303	307
	50%	0	257	261	265	272	**279**	286	293	297	301
	75%	0.68	252	256	260	266	273	**281**	287	291	295
	90%	1.28	248	252	255	262	269	276	**282**	286	290
	95%	1.65	245	249	253	259	266	273	280	**283**	287
	97.7%	2	241	245	248	255	261	268	275	278	**282**

Figure 2.6 - Vertex Presentation. Male fetal head circumference (in mm) presenting to the birth canal in a vertex presentation. Green indicates region of equal population distribution values for molding and head size. The intensity of the blue shading indicates the degree of maximal molding of small fetal heads, while the intensity of the red shading indicates the degree of lack of molding of large fetal heads.

			fetal head circumference population distribution								
			2.30%	5%	10%	25%	50%	75%	90%	95%	97.70%
Molding population distribution	2.3%	-2	**288**	292	296	304	311	319	326	331	335
	5%	-1.65	282	**286**	290	297	305	312	319	323	327
	10%	-1.28	279	283	**287**	294	301	309	316	320	324
	25%	-0.68	274	278	282	**288**	296	303	310	314	318
	50%	0	268	272	276	283	**290**	297	304	308	312
	75%	0.68	263	267	271	278	285	**292**	298	302	306
	90%	1.28	259	263	267	273	280	287	**294**	297	301
	95%	1.65	257	260	264	270	277	284	291	**295**	298
	97.7%	2	252	256	260	266	273	280	286	289	**293**

Figure 2.7 - Face Presentation. Male fetal head circumference (in mm) presenting to the birth canal during face presentation. Green indicates region of equal population distribution values for molding and head size. The intensity of the blue shading indicates the degree of maximal molding of small fetal heads, while the intensity of red shading indicates the degree of lack of molding of large fetal heads.

The 7 mm diameter increase that has been reported to occur with face presentation increased the predicted effective circumference by 11 mm (Figure 2.7).

2.4.3 Part III: Capacity-Demand calculations using the value of g

Here we consider the fetal head demand results from Part II within the context of the maternal capacity results from Part I by tabulating the population values of g. For the PVM loop, fetal head demand (SC) was predicted to exceed maternal capacity for every maternal capacity smaller than the 10th percentile. The 25th percentile maternal capacity met the demands represented by the 25th percentile fetal head, and was approximately equal to the demand imposed by the 50th percentile fetal head. The 50th percentile maternal capacity was predicted to be able to deliver all fetal head sizes examined without injury (Figure 2.8).

		DEMAND (Fetal Head Circumference, in Percentile)								
		2.3%	5%	10%	25%	50%	75%	90%	95%	97.7%
CAPACITY (Maternal Circumference, in Percentile)	2.3%	0.67	0.66	0.65	0.63	0.62	0.60	0.59	0.58	0.57
	5%	0.78	0.77	0.76	0.74	0.72	0.70	0.69	0.68	0.67
	10%	0.90	0.89	0.87	0.85	0.83	0.81	0.79	0.78	0.77
	15%	0.97	0.96	0.94	0.92	0.90	0.88	0.85	0.84	0.83
	25%	1.08	1.06	1.05	1.02	0.99	0.97	0.95	0.93	0.92
	50%	1.26	1.25	1.22	1.20	1.16	1.14	1.11	1.09	1.08
	75%	1.44	1.42	1.39	1.36	1.32	1.29	1.26	1.24	1.23
	90%	1.59	1.56	1.54	1.50	1.46	1.43	1.39	1.37	1.36
	95%	1.67	1.65	1.62	1.58	1.54	1.50	1.47	1.45	1.43
	97.7%	1.75	1.73	1.70	1.66	1.61	1.58	1.54	1.52	1.50

Figure 2.8 - Predicted maternal capacity – to – fetal head demand ratio, g, for the PVM loop with wrapping. The intensity of the red shading indicates the degree of cephalolevator disproportion for the PVM.

		DEMAND (Fetal Head Circumference, in Percentile)								
		2.3%	5%	10%	25%	50%	75%	90%	95%	97.7%
CAPACITY (Maternal Circumference, in Percentile)	2.3%	0.94	0.93	0.91	0.89	0.86	0.84	0.82	0.81	0.80
	5%	1.01	1.00	0.98	0.96	0.93	0.91	0.89	0.87	0.86
	10%	1.09	1.07	1.05	1.03	1.00	0.98	0.95	0.94	0.93
	15%	1.14	1.12	1.10	1.08	1.05	1.02	1.00	0.98	0.97
	25%	1.21	1.19	1.17	1.14	1.11	1.09	1.06	1.05	1.03
	50%	1.35	1.33	1.31	1.27	1.24	1.21	1.18	1.17	1.15
	75%	1.48	1.46	1.44	1.40	1.36	1.33	1.30	1.28	1.27
	90%	1.61	1.58	1.55	1.52	1.48	1.44	1.41	1.39	1.37
	95%	1.68	1.66	1.63	1.59	1.55	1.51	1.47	1.45	1.44
	97.7%	1.75	1.73	1.69	1.65	1.61	1.57	1.53	1.51	1.50

Figure 2.9 - Predicted maternal capacity – to – fetal head demand ratio, g, for the PVM loop without wrapping. The intensity of the red shading indicates the degree of cephalolevator disproportion for the PVM in this special case.

		DEMAND (Fetal Head Circumference, in Percentile)								
		2.30%	5%	10%	25%	50%	75%	90%	95%	97.70%
CAPACITY (Maternal Circumference, in Percentile)	2.30%	1.06	1.04	1.02	1.00	0.97	0.95	0.93	0.92	0.90
	5%	1.13	1.12	1.10	1.07	1.04	1.02	0.99	0.98	0.97
	10%	1.22	1.20	1.18	1.15	1.12	1.09	1.07	1.05	1.04
	15%	1.27	1.25	1.23	1.20	1.17	1.14	1.11	1.10	1.09
	25%	1.36	1.34	1.31	1.28	1.25	1.22	1.19	1.17	1.16
	50%	1.51	1.49	1.46	1.42	1.39	1.36	1.32	1.30	1.29
	75%	1.66	1.64	1.61	1.57	1.53	1.49	1.45	1.44	1.42
	90%	1.80	1.78	1.74	1.70	1.66	1.62	1.58	1.56	1.54
	95%	1.89	1.86	1.83	1.78	1.74	1.70	1.65	1.63	1.61
	97.70%	1.97	1.94	1.91	1.86	1.81	1.77	1.72	1.70	1.68

Figure 2.10 - Predicted maternal capacity – to – fetal head demand ratio, g, for the PRM loop. The intensity of red shading indicates the degree of cephalolevator disproportion for the PRM.

For the PRM loop, fetal head demand was predicted to be satisfied by all maternal capacities greater than the 5th percentile. The 5th percentile maternal capacity was predicted to satisfy up to the 75th percentile fetal head demand. Maternal capacities of 10th percentile and above were predicted to suffice for any fetal head size (Figure 2.10).

Similar results were obtained for the other two women whose models were derived from the MR scans.

2.5 Discussion

2.5.1 Part I: Quantification of factors contributing to the maternal capacity for the 50th percentile woman.

The sensitivity analysis showed that initial soft tissue loop length had the largest impact on circumference. In particular, the increase in soft tissue loop length allows the head-pelvis contact points to move farther posteriorly and laterally along the pelvis, increasing the pelvis-head arch length in addition to the portion of the circumference comprised by the soft tissue loop length. In the case of the PVM, the 10% change in soft tissue loop length that results in a 15% change in maternal capacity is a result of the non-contact PVM length remaining constant, allowing all of the gained length to contribute directly to encompassing the fetal head. Soft tissue loop length had the greatest impact on maternal capacity, followed by SPAA, which was closely followed by origin separation. In the PVM model, non-contact length had less of an effect than initial soft tissue loop length itself, but a greater effect than any other factor considered here.

2.5.2 Part II: Quantification of Factors Affecting Fetal Head Demand

Population values of SC varied from 253 mm for a female head of minimum OC and maximum MI to 351 mm for a male head of maximum OC and minimum MI. However, male fetuses having the same percentile value for OC and MI (green diagonal, Figure 2.6) ranged in SC value from 297 to 302 mm, varying by a maximum of 5 mm. As molding is the consequence of compressive forces, and the compressive forces experienced would be expected to increase with head size, it is feasible that the greatest extent of molding would occur in the largest

heads. However, it is also possible that the smallest heads would be the least developed structurally and therefore the most susceptible to deformation for a given compressive force.

The 0.7 cm diameter increase reported to occur with face presentation increased the effective circumference by 11 mm. For a mother delivering a baby close to her capacity, this could make the difference between safe delivery and a life time of complications following levator injury. It has also previously been proposed that the increase in injuries associated with occiput posterior presentation is the result of increased soft tissue resistance and poor use of the bony birth canal space during this type of delivery [30].

2.5.3 Part III: Capacity-Demand calculations using the value of g

The approach in this paper provides a new framework for considering the biomechanical reasons for maternal levator injury during vaginal delivery by relating fetal demand to maternal capacity via a simple ratio, g. The Part III values of g reveal that a 50th percentile maternal capacity can accommodate fetal heads of all sizes, a 25th percentile maternal capacity will accommodate half of all fetal head sizes, and a 15th percentile maternal capacity is insufficient to accommodate any fetal head sizes without any creep-relaxation behavior. These tissue properties are indeed known to be time dependent, with increases in compliance observed during late pregnancy [31] [32], which may provide the additional soft tissue lengthening of 8% necessary for the 15th percentile female to be able to deliver a head of average size. Alternatively, we may have underestimated the amount of molding that occurs acutely, since most measurements of molding are made post-hoc at time intervals of 1 hour or more after the baby is delivered. They do not capture the situation while the head is in the pelvic cavity. The

fetal skull is viscoelastic [33] [34] [26], so a certain degree of spring-back may have already occurred before the first measurement of fetal skull size is made in the delivery room [26]. If the amount of molding has been underestimated by 50% then the average fetal head circumference presented to the pelvic floor would be 279 mm, with minimum and maximum values of 241 mm and 323 mm respectively, or a reduction in fetal head circumference by approximately 7%.

Our geometric model provides the first biomechanical explanation for why the PVM is more likely to be injured during childbirth than the PRM (see Introduction). A 10^{th} percentile woman's PRM can accommodate any fetal head demand, while a 25^{th} percentile woman's PVM can only accommodate the demand represented by half of all fetal heads. It has not been immediately intuitive why the PVM should be more constrained than the PRM. The answer is found in the location of their origins on the pelvis. We found that the PRM origin on the PM was so low that PRM-pelvis wrapping could not occur in the downward rotation observed during birth. In contrast, the PVM origin is approximately 2 cm below the pubic tubercle, necessitating up to 4 cm in PVM-pelvis wrapping per side (8 cm total) [19]. Since this distance is required for wrapping around the pubic bone, it reduces the PVM muscle length available for accommodating the fetal head. Clearly, the greater the perineal descent which, for a given head size, would be expected to be exacerbated by less elastic soft tissues and less stress relaxation, the higher the probability of PVM wrapping.

Might Ultrasound be used to Assess PVM Injury Risk?

If acquired prior to labor, as demonstrated in the case of BD and head circumference by Ergaz *et al.* [35]., measurement of the fetal head diameters (MD, SD, and BD) would allow for calculation of the fetal head size relative to the population and relative to the mother's injury threshold. So:

(6.1) $Fetal\ Head\ Volume = \frac{1}{6}\pi MD_0 * BD_0 * SD_0 = \frac{1}{6}\pi MD_f * BD_f * SD_f = \frac{1}{6}\pi MD_f * {BD_f}^2$

The fetal head volume and MI can be simplified using the assumption BD=SD.

(6.2) $MI = \frac{{MD_f}^2}{{BD_f}^2}$

(6.3) $MD_f = \sqrt{MI} * BD_f$

This allows us to express MD_f and as a result fetal head volume as a function of BD_f.

(6.4) $MD_0 * BD_0 * SD_0 = MD_f * {BD_f}^2 = \sqrt{MI} * {BD_f}^3$

(6.5) $BD_f = \frac{(MD_0 * BD_0 * SD_0)^{1/3}}{MI^{1/6}}$

As a result, we can solve for BD_f and SC in terms of pre-labor fetal head measurements.

(6.6) $SC = \pi * BD_f = \pi \frac{(MD_0 * BD_0 * SD_0)^{1/3}}{MI^{1/6}}$

From Figure 2.8, we see that it is more important to measure maternal capacity than the fetal head demand. It is only in the region between the 15th and 25th percentile that additional insight may be gained by measuring the fetal head. It may not yet be feasible to acquire origin locations and specific PVM and PRM geometries via ultrasound. However, subpubic arch angle

and hiatus width are regularly quantified via ultrasound and can be used to identify a mother's status within the population [36] [20]. Even without fetal head measurements, these data could then be used to identify mothers who are on the border between predicted labor success and predicted cephalolevator muscle disproportion. This would equate to the situation of encountering a value of g slightly less than 1.0. In this situation, interventions such as antenatal perineal massage might be employed to try to prevent trauma at the time of labor [37]. In terms of clinical applicability, the capacity-demand ratio, g, that we have calculated could be used by clinicians to assess injury risk in the same way calculators are currently used to assess likely success with vaginal birth after cesarean delivery (VBAC) [38]. Ultimately, the goal here is to provide mothers and practitioners with information of levels of risk so that they can make better informed decisions during their labor preparation process. A woman with a very low g ratio and anticipating only one child might, for example, choose cesarean delivery before labor. At present cesarean section on maternal request is often selected because of concerns for pelvic floor injury without knowing how likely that injury is to occur.

This analysis has a series of limitations, some of which are the result of current knowledge gaps and some of which are due to simplifying assumptions. First, in the Part I maternal capacity calculations, the lack of *in vivo* viscoelastic data for the human levator ani muscle during vaginal delivery currently limits any accurate prediction of time-dependent PVM and PRM muscle loop behavior. This means the present maternal capacity calculations are conservative because time-dependent stress relaxation behavior would lead to larger maternal capacity values than presently calculated. The viscoelastic behavior has been measured *in vitro* in rat and human vaginal tissue by Jing [31] and by Lowder *et al*. in rat vaginal tissue [32]. Jing found a relaxation

behavior with time constants on the order of 31 and 40 minutes in pregnant and non-pregnant rats, respectively. If these apply to the PVM loop, and there is no evidence yet that they do, then in a 1-2 hour time window, representing the average length of the second stage of labor, one would expect to see noticeable creep lengthening of the PVM. In practice, a final stretch ratio of 1.73 after creep would be required for the 15th percentile female to be able to deliver 50% of all fetal heads, resulting in the observed injury occurrence of approximately 13% [4] .

Might it be possible that assumptions made in this analysis biased the results? The assumption for which we do not have direct experimental evidence is the wrapping of the PVM around the inferior margin of the pubic ramus as the PVM loop rotates downwards during the second stage of labor (Figure 2.2). This assumption causes the effective length of the PVM to be shortened, thereby increasing the amount of PVM stretch required. If this wrapping does not occur, then we will have overestimated the stretch of the PVM, but not the PRM (Figure 2.9). That overestimation for PVM stretch is tabulated in Table 2.2, Table 2.3, Table 2.5, and Table 2.6S). Additionally, we have made the assumption that muscle fiber elongation (growth) observed in rats during pregnancy also occurs in humans. As human studies on this question have not been conducted, and as there is not a perfect analog between rat and human pelvic floor anatomy, we have made the assumption that the rat coccygeus muscle is the closest analog to human levator ani muscles.

A limitation in the Part II fetal head demand analysis is the lack of measurements of the spring-back of the fetal head skull in the minutes after delivery and before the fetal head is measured. This means we may have underestimated the effect of molding in our calculations. Greater

molding would lead to a diminished fetal head demand and therefore a larger g value than presently predicted, so again our analysis is conservative. Variations in fetal head shape, such as the non-circular cross section observed in occiput posterior presentation, and subsequent shape changes in passage along the Curve of Carus are also expected to have an impact and should be considered in future models.

There is already evidence that pelvic floor measurements can help predict delivery outcome. In a study of 231 nulliparous women, Siafarikas *et al.* found that a smaller levator hiatus dimensions measured by ultrasound in late pregnancy had a significant association with a longer active second stage of labor and increased likelihood of the need for instrumental delivery to complete delivery [39]. It seems logical that these weak correlations (all < 0.3) can be strengthened once the other measureable parameters such as head size and subpubic arch angle are added. The theoretical framework provided in this article to organize the key geometrical factors influencing maternal capacity and fetal demand should help in the process of identifying elements that can be used for more accurate predictions and should help guide future work in this direction.

2.6 Conclusions

1) Initial soft tissue loop length had the greatest impact on maternal capacity, followed by non-contact length, then SPAA, and finally levator origin separation.

2) We conclude that the PVM and PRM loops have the capacity to accommodate 75% of births vertex presentation without injury. But for injury to occur in only 15% of births, as observed

clinically, there must be either more fetal head molding than was allowed for, or stress relaxation behavior of the PVM loop under strain, both of which are entirely possible.

3) We conclude that the more caudal origin of the PRM portion of the levator muscle reduces its stretch ratio at ultimate crowning, thereby helping to protect it from the stretch injuries commonly observed in the PVM portion.

4) Use of ultrasound to measure fetal head diameter prior to birth could provide information on the fetal head demand that will be made of the maternal levator ani muscles, and hence g, during birth. Ultrasound estimates of levator hiatus size prior to birth would provide a first estimate of maternal capacity via initial soft tissue loop length.

5) The numeric value of the capacity – demand ratio, g, indicates the level of risk for levator injury during the late stage of vaginal delivery. A g value of 1.0 or more rules out cephalolevator muscle disproportion and hence risk of levator injury due to the conservative assumptions employed in the current analysis.

6) In practice it may be most logical to first measure maternal capacity in order to establish whether it lies above the 25^{th} percentile. If it lies below the 25^{th} percentile then the fetal head should be measured to gain the additional insight provided by the value of g.

Acknowledgements: We thank Dr. Luyun Chen for her comments on reading the manuscript, and Dr. Janis Miller for access to the EMRLD MRI data. We gratefully acknowledge financial support from the Public Health Service and the Office for Research on Women and Gender grant # P50 HD044406-07 (Project 1).

2.7 Nomenclature:

AS = anal sphincter

BD = biparietal diameter

BD_0 = BD prior to molding

BD_f = BD following molding

BD_L = BD at time of labor

C_0 = original circumference

C_f = face presentation circumference

$C_{M,\ lower}$ = maternal circumference in the ultimate crowning state

D_{head} = fetal head diameter

FD = frontooccipital diameter

FE = fiber elongation

LA = levator ani

MD = mentovertical diameter

MD_0 = MD prior to molding

MD_f = MD following molding

MI = molding index

OC = occipitofrontal circumference

PB = perineal body

PM = perineal membrane

PRM = puborectal muscle

PVM = pubovisceral muscle

R_{PM} = perineal membrane stretch ratio

R_{SM} = striated muscle stretch ratio

SC = suboccipitobregmatic circumference

SD = suboccipitobregmatic diameter

SD_0 = SD prior to molding

SD_f = SD following molding

SL = soft tissue loop length

SL_{PRM} = soft tissue loop length for PRM

SL_{PVM} = soft tissue loop length for PVM

SPAA = subpubic arch angle

2.8 References

[1] K.-C. Lien, J. O. L. DeLancey and J. A. Ashton-Miller, "Biomechanical Analyses of the Efficacy of Patterns of Maternal Effort on Second-Stage Progress," *Obstetrics & Gynecology,* vol. 113, no. 4, pp. 873-880, 2009.

[2] M. E. T. Silva, D. A. Oliveira, T. H. Roza, S. Brandao, M. P. L. Parente, T. Mascarenhas and R. M. Natal Jorge, "Study on the influence of the fetus head molding on the biomechanical behavior of the pelvic floor muscles, during vaginal delivery," *Journal of Biomechanics,* vol. 48, no. 9, pp. 1600-1605, 2015.

[3] X. Yan, J. A. Kruger, P. M. Nielsen and M. P. Nash, "Effects of fetal head shape variation on the second stage of labour," *Journal of Biomechanics,* vol. 48, no. 9, pp. 1593-1599, 2015.

[4] K. Shek and H. Dietz, "Intrapartum risk factors for levator trauma," *BJOGP An International Journal of Obstetrics and Gynecology,* vol. 117, no. 12, pp. 1485-1492, 2010.

[5] R. Margulies, M. Huebner and J. O. L. DeLancey, "Origin and insertion points involved in levator ani muscle defects," *American Journal of Obstetrics and Gynecology,* vol. 196, no. 3, pp. 251-255, 2007.

[6] J. Mant, R. Painter and M. Vessey, "Epidemiology of genital prolapse: observations from the Oxford Planning Association Study," *British Journal of Obstetrics and Gynaecology,* vol. 104, no. 5, pp. 579-85, 1997.

[7] J. A. Ashton-Miller and J. O. L. DeLancey, "On the Biomechanics of Vaginal Birth and Common Sequelae," *Annual Review of Biomedical Engineering,* vol. 11, pp. 163-176, 2009.

[8] C. Betschart, J. Kim, J. M. Miller, J. A. Ashton-Miller and J. O. L. DeLancey, "Comparison of muscle fiber directions between different levator ani muscle subdivisions: in vivo MRI measurements in women," *International Urogynecology Journal,* vol. 25, no. 9, pp. 1263-1268, 2014.

[9] R. Kearney, R. Sawhney and J. O. L. DeLancey, "Levator Ani Muscle Anatomy Evaluated by Origin-Insertion Pairs," *American College of Obstetricians and Gynecologists,* vol. 104, no. 1, pp. 168-173, 2004.

[10] K. Lien, B. Mooney, J. O. L. DeLancey and J. Ashton-Miller, "Levator ani muscle stretch induced by simulated vaginal birth," *Obstetrics and Gynecology,* vol. 103, no. 1, pp. 31-40, 2004.

[11] J. M. Miller, C. Brandon, J. A. Jacobson and e. al., "MRI findings in patients considered high risk for pelvic floor injury studied serially after vaginal childbirth," *American Journal of Roentgenology,* vol. 195, no. 3, pp. 786-91, 2010.

[12] C. Brandon, J. Jacobson, L. Low, L. Park, J. O. L. DeLancey and J. Miller, "Pubic bone injuries in primiparous women: magnetic resonance imaging in detection and differential

diagonosis of structural injury," *Ultrasound in Obstetrics & Gynecology,* vol. 39, no. 4, pp. 444-51, 2012.

[13] J. Luo, J. A. Ashton-Miller and J. O. L. DeLancey, "A model patient: Female pelvic anatomy can be viewed in diverse 3-dimensional images with a new interactive tool," *American Journal of Obstetrics and Gynecology,* vol. 205, no. 4, p. 391, 2011.

[14] M. Alperin, D. M. Lawley, M. C. Esparza and R. L. Lieber, "Pregnancy-induced adaptations in the intrinsic structure of rat pelvic floor muscles," *American Journal of Obstetrics and Gynecology,* vol. 213, no. 2, pp. 191 - 197, 2015.

[15] S. V. Brooks, E. Zerba and J. A. Faulkner, "Injury to muscle fibers after single stretches of passive and maximally stimulated muscles in mice," *Journal of Physiology,* vol. 488, no. 2, pp. 459-469, 1995.

[16] M. Kirilova, S. Stoytchev, D. Pashkouleva and V. Kavardzhikov, "Experimental study of the mechanical properties of human abdominal fascia," *Medical Engineering & Physics,* vol. 33, no. 1, pp. 1-6, 2011.

[17] J. Kim, R. Ramanah, J. O. L. DeLancey and A.-M. JA, "On the anatomy and histology of the pubovisceral muscle enthesis in women," *Neurourology and Urodynamics,* vol. 30, no. 7, pp. 1366-1370, 2011.

[18] J. Kim, C. Betschart, R. Ramanah, J. Ashton-Miller and J. O. L. DeLancey, "Anatomy of the pubovisceral muscle origin: Macroscopic and microscopic findings within the injury zone," *Neurourology and Urodynamics,* vol. 34, no. 8, pp. 774-780, 2015.

[19] K. Larson, J. Luo, A. Yousuf, J. Ashton-Miller and J. O. L. DeLancey, "Measurement of the 3D geometry of the fascial arches in women with a unilateral levator defect and architectural distortion," *International Urogynecology Journal,* vol. 23, no. 1, pp. 57-63, 2012.

[20] V. L. Handa, M. E. Lockhart, J. R. Fielding, C. S. Bradley, L. Brubaker, G. W. Cundiff, W. Ye and H. E. Richter, "Racial Differences in Pelvic Anatomy by Magnetic Resonance Imaging," *Obstetrics and Gynecoiogy,* vol. 111, no. 4, pp. 914-920, 2008.

[21] S. Albrich, K. Shek, U. Krahn and H. Dietz, "Measurement of the subpubic arch angle by 3D translabial ultrasound and its impact on vaginal delivery," *Ultrasound in Obstetrics & Gynecology,* vol. 46, no. 4, pp. 496-500, 2015.

[22] Centers for Disease Control and Prevention, "Data Table for Boys Weight-for-Length and Head Circumference-for-age Charts," 9 September 2010. [Online]. Available: http://www.cdc.gov/growthcharts/who/boys_weight_head_circumference.htm. [Accessed 18 June 2015].

[23] Centers for Disease Control and Prevention, "Data Table for Girls Weight-for-Length and Head Circumference-for-age Charts," 9 September 2010. [Online]. Available: http://www.cdc.gov/growthcharts/who/girls_weight_head_circumference.htm. [Accessed 18 June 2015].

[24] J. Baxter, "Moulding of the Foetal Head: A Compensatory Mechanism," *Journal of Obstetrics and Gynaecology of the British Empire,* vol. 53, p. 212, 1946.

[25] T. J. Kriewall, S. J. Stys and G. K. McPherson, "Neonatal head shape after delivery: An index of molding," *Journal of Perinatal Medicine,* vol. 5, no. 6, pp. 260-267, 1977.

[26] H. C. Moloy, "Studies on head molding during labor," *American Journal of Obstetrics and Gynecology,* vol. 76, pp. 762-782, 1942.

[27] B. Sorbe and S. Dahlgren, "Some important factors in the molding of the fetal head during vaginal delivery - a photographic study," *International Journal of Gynaecology and Obstetrics,* vol. 21, no. 3, pp. 205-212, 1983.

[28] M. Gardberg and M. Tuppurainen, "Persistent occiput posterior presentation - a clinical problem," *Acta Obstetricia et Gynecologica Scandinavica,* vol. 73, no. 1, pp. 45-47, 1994.

[29] U. Borell and I. Fernstrom, "Die Umformung des kindlichen Kopfes wahrend normaler Entbingen in regelrechter Hinterhauptslag," *Geburtshilfe und Frauenheilkunde,* vol. 18, no. 9, pp. 1156-1166, 1958.

[30] J. Lowder, L. Burrows, M. Krohn and A. Weber, "Risk factors for primary and subsequent anal sphincter lacerations: a comparison of cohorts by parity and prior mode of delivery," *American Journal of Obstetrics and Gynecology,* vol. 196, no. 4, pp. 344-348, 2007.

[31] D. Jing, "Experimental and Theoretical Biomechanical Analyses of the Second Stage of Labor.," 2010. [Online]. Available: http://deepblue.lib.umich.edu/handle/2027.42/76013. [Accessed 21 August 2015].

[32] J. L. Lowder, K. M. Debes, D. K. Moon, N. Howden, S. D. Abramowitch and P. A. Moalli, "Biomechanical Adaptations of the Rat Vagina and Supportive Tissues in Pregnancy to Accommodate Delivery," *Obstetrics and Gynecology,* vol. 109, no. 1, pp. 136-143, 2007.

[33] T. J. Kriewall, "Structural, mechanical, and material properties of fetal cranial bone," *American Journal of Obstetrics and Gynecology,* vol. 143, no. 6, pp. 707-714, 1982.

[34] S. S. Margulies and K. L. Thibault, "Infant Skull and Suture Properties: Measurements and Implications for Mechanisms of Pediatric Brian Injury," *J Biomech Eng,* vol. 122, no. 4, pp. 364-371, 2000.

[35] U. Ergaz, I. Goldstein, M. Divon and Z. Weiner, "A Preliminary Study of Three-dimensional Sonographic Measurements of the Fetus," *Rambam Maimonides Medical Journal,* vol. 6, no. 2, p. e0019, 2015.

[36] D. Maharaj, "Assessing cephalopelvic disproportion: back to the basics," *Obstetrical & Gynecoogicall Survey,* vol. 65, no. 6, pp. 387-395, 2010.

[37] M. M. Beckmann and O. M. Stock, "Antenatal perineal massage for reducing perineal trauma," *Cochrane Database of Systematic Reviews,* vol. 4, 2013.

[38] W. Grobman, Y. Lai, M. Landon, C. Spong, K. Leveno, D. Rouse, M. Varner, A. Moawad, S. Caritis, M. Harper, R. Wapner, Y. Sorokin, M. Miodovnik, M. Carpenter, M. O'Sullivan, B. Sibai, O. Langer, J. Thorp, S. Ramin, B. Mercer and NICHD, "Development of a nomogram for prediction of vaginal birth after cesarean delivery," *Obstetrics and Gynecology,* vol. 109,

no. 4, pp. 806-812, 2007.

[39] F. Siafarikas, J. Staer-Jensen, G. Hilde, K. Bo and E. M. Ellstrom, "Levator hiatus dimensions in late pregnancy and the process of labor: a 3- and 4-dimensional transperinael ultrasound study," *American Journal of Obstetrics and Gynecology,* vol. 210, no. 5, pp. 484-491, 2014.

[40] N. Schwertner-Tiepelmann, R. Thakar, A. H. Sultan and R. Tunn, "Obstetric levator ani muscle injuries: current status," *Ultrasound in Obstetrics & Gynecology,* vol. 39, no. 4, pp. 372 - 383, 2012.

[41] J. O. L. DeLancey, H. Sorensen, C. Lewicky-Gaupp and T. Smith, "Comparison of the puborectal muscle on MRI in women with POP and levator ani defects with those with normal support and no defect," *International Urogynecology Journal,* vol. 23, no. 1, pp. 73-77, 2012.

[42] T. Kriewall, N. Akkas, D. Bylski, J. Melvin and B. J. Work, "Mechanical Behavior of Fetal Dura Mater Under Large Axisymmetric Inflation," *J Biomech Eng,* vol. 105, no. 1, pp. 71-76, 1983.

[43] V. L. Handa, M. E. Lockhart, J. R. Fielding, C. S. Bradley, L. Brubakery, G. W. Cundiffy, W. Ye and H. E. Richter, "Racial Differences in Pelvic Anatomy by Magnetic Resonance Imaging," *Obstetrics and Gynecoiogy,* vol. 111, no. 4, pp. 914-920, 2008.

2.9 Appendix:

	Subject 1 (50th percentile)	Subject 2	Subject 3
PRM	425	335	356
PVM without wrapping	347	324	399
PVM with wrapping	313	268	325

Table 2.6S - Comparison of the effect of PVM wrapping on maternal capacity (in mm) at ultimate crowning for each woman.

Due to the small sample size and the nature of the parent study, both subjects 2 and 3 were below the 50th percentile in size. Results reported in Table 2.6S assume no soft tissue stretch or shape deformation of the anal sphincter.

	2.3%	5%	10%	15%	25%	50%	75%	90%	95%	97.7%
SPAA (^{o})	69.7	72.2	74.7	76.5	79	83.7	88.4	92.7	95.3	97.7
Retropubic arch angle (^{o})	91.4	94.6	97.9	100.0	103.3	109.3	115.3	120.8	124.1	127.2
Levator Hiatus (mm)	30	32	35	37	39	44	49	53	56	58

Table 2.7S - Finding the maternal capacity – Population distribution of SPAA and hiatus.

SPAA: as measured at the ischium of the pelvis

Retropubic arch angle: as measured in the axial plane found once the full length of the pubic rami is visible after drawing a perpendicular plane through the pubic symphysis [21]

Levator Hiatus: measured as the H-line, or the distance from the inferior posterior aspect of the symphysis to the posterior rectal wall [20]

			fetal head circumference population distribution								
			2.30%	5%	10%	25%	50%	75%	90%	95%	97.70%
Molding population distribution	2.3%	-2	**297**	301	305	312	320	328	335	340	344
	5%	-1.65	289	**293**	297	304	312	320	327	331	335
	10%	**-1.28**	285	289	**293**	300	308	315	322	326	330
	25%	-0.68	279	283	287	**294**	301	309	315	320	323
	50%	0	273	276	280	287	**294**	302	308	312	316
	75%	0.68	267	270	274	281	288	**295**	301	305	309
	90%	1.28	261	265	269	275	282	289	**296**	299	303
	95%	1.65	259	262	266	272	279	286	292	**296**	300
	97.7%	2	253	257	261	267	273	280	286	290	**294**

Figure 2.11S - Female Vertex Presentation. Female fetal head circumference (in mm) as presented to the pelvic floor during vertex presentation. Green indicates region of equal population distribution values for molding and head size. The intensity of the blue shading indicates the degree of maximal molding of small fetal heads. The intensity of the red shading indicates the degree of the lack of molding of large fetal heads.

2.10 Calculations

[1] Calculating soft tissue loop length (SL)

(1.1.1) $SL_{PRM} = FE * R_{SM} * L_{PRM} + R_{PM} * L_{PM}$

$$SL_{PRM} = soft\ tissue\ loop\ length\ for\ PRM$$

$$L_{PRM} = length\ of\ PRM, wrapped\ around\ rectum$$

$$L_{PM} = distance\ between\ pelvis\ and\ PRM\ origin\ on\ PM$$

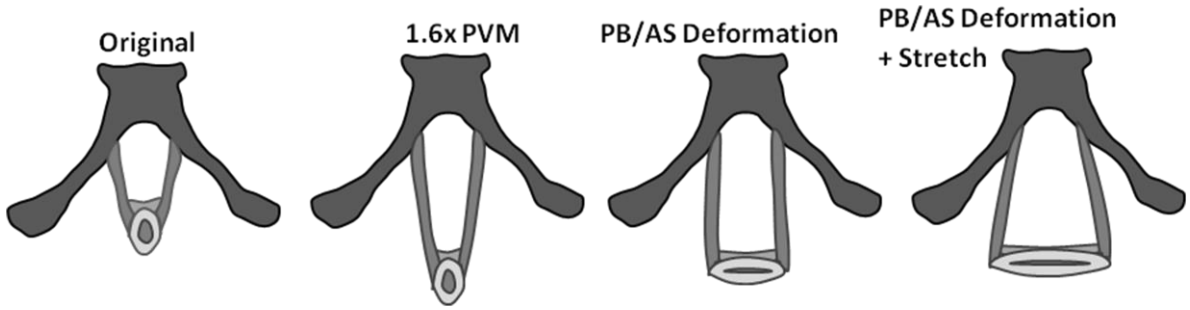

Figure 2.12S - Caudal view of a tracing of the 50 percentile female pelvic rami and soft tissue loops before and after three stages of simulated maximum non-injurious stretch. (Left) Pelvis and unstretched levator loop showing pubic rami (Dark grey), PVM (mid grey), AS (light grey ellipsoid shape), PB (intermediate grey adjacent to and above AS), and rectum (dark line around outside of AS) geometry. (Second left) Mathematically, the PVM was initially stretched by 1.6x. (Second right) PB/AS was then deformed for maximal elliptical length, conserving cross-sectional area. (Far right) The smooth muscle of the deformed PB/AS was also stretched by 1.6x.

(1.2.1) $SL_{PVM} = FE * R_{SM} * L_{PVM} - L_{AS,PVM} + L_{AS,max}$

$$SL_{PVM} = soft\ tissue\ loop\ \ length\ for\ PVM$$

$$L_{PVM} = combined\ length\ of\ PVM\ fibers, originating\ from\ pelvis\ and\ inserting\ on\ PB$$

$$/AS$$

$$L_{AS,PCM} = contact\ length\ between\ PVM\ and\ PB/AS\ at\ insertion$$

$$L_{AS,max} = maximum\ length\ contribution\ of\ PB/AS$$

The area of the internal anal sphincter was calculated by subtracting the rectal space from the circular cross-section defined by the circumference of the PB/AS.

(1.2.2) $$A_{AS} = \pi \frac{d_{AS}^{2}}{4} - \frac{\pi}{4}(d_{AS} - 2 * t_{AS})^{2}$$

$$d_{AS} = diameter\ of\ AS$$

$$t_{AS} = AS\ thickness$$

(1.2.3) $d_{AS,min} = 2 * t_{AS}$

After evacuation of the rectum, the PB/AS can be reconfigured as an ellipse with conserved cross-sectional area and ring thickness (Figure 2.11S).

(1.2.4) $A_{AS} = \frac{\pi}{4} d_{AS,max} * d_{AS,min}$

The maximum diameter of the PB/AS can be solved for in terms of original diameter and ring thickness.

(1.2.5) $d_{AS,max} = \frac{2*A_{AS}}{\pi * t_{AS}} = \frac{({d_{AS}}^2 - (d_{AS} - 2*t_{AS})^2)}{2*t_{AS}}$

After elliptical distortion, PB/AS muscle fibers run approximately linearly along the long diameter, allowing for a 1.6x stretch without injury (Figure 2.12S).

(1.2.6) $L_{AS,max} = R_{SM} * d_{AS,max}$

[2] Maternal circumference in a single plane (Figure 2.13S)

(2.1) $C_M = SL + AL_{head,pelvis} - L_{NC}$

$$C_M = maternal\ circumference$$

$$AL_{head,pelvis} = arch\ length\ along\ head, between\ contact\ points\ with\ the\ pelvis$$

$$L_{NC} = soft\ tissue\ loop\ length\ not\ in\ contact\ with\ fetal\ head$$

½ L_{NC}

(2.2) $L_{NC} = 2 * L_{head,pelvis} - \delta_{origins,pelvis}$

$$\delta_{origins,pelvis} = distance\ between\ origins\ along\ pelvis$$

$$L_{head,pelvis} = distance\ from\ origin\ of\ pelvis\ angle\ to\ head - pelvis\ contact\ point$$

(2.3) $L_{head,pelvis}=\frac{D_{head}}{2*\tan(\frac{\theta}{2})}$

$$D_{head} = BD = SD = fetal\ head\ diameter$$

$$\theta = sub\ pubic\ arch\ angle, degrees$$

(2.4) $AL_{head,pelvis} = \pi * D_{head} * (\frac{180-\theta}{360})$

(2.5) $C_M = \pi * D_{head} = SL + \pi * D_{head} * \left(\frac{180-\theta}{360}\right) + \delta_{origins,pelvis} - \frac{D_{head}}{\tan(\frac{\theta}{2})}$

(2.6) $C_M = \pi * D_{head} = \frac{SL+\delta_{origins,pelvis}}{1+\frac{\theta-180}{360}+\frac{1}{\pi\tan(\frac{\theta}{2})}}$

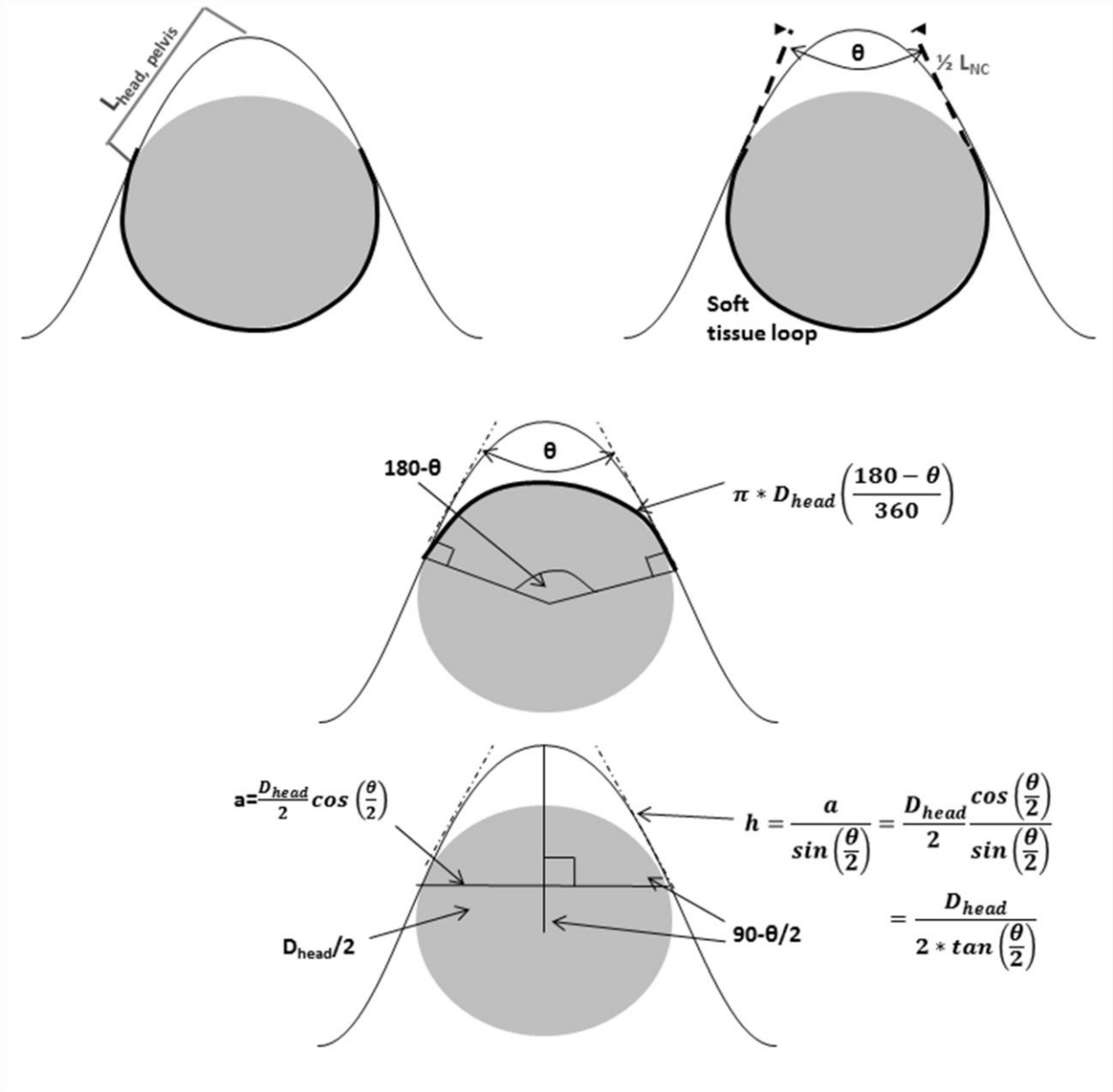

Figure 2.13S - Caudal view of anterior pelvis following the graphical convention in Figure 2.4 illustrating variables used in Part II maternal capacity calculations. Grey circular shape = fetal head. Θ = subpubic arch angle; all angles are in degrees. Arrow head = soft tissue origin. Arch = pelvis/ subpubic arch. Top row: Length of soft tissue loop in contact with the fetal head is represented by the black band. The length of soft tissue loop not in contact with the fetal head is represented by the dashed line. Second row: Calculations for the archlength of the portion of the head not in contact with the soft tissue loop. Dot-dash line: tangent to pelvis at point of contact with the fetal head. Bottom row: Calculations for the distance from the subpubic arch to the head-pelvis contact points.

[3] Maternal circumference in the lower plane

(3.1) $C_{M.lower} = SL + \pi * D_{head} * \left(\frac{180-\theta}{360}\right) - L_{wrap,left} - L_{wrap,right}$

$$L_{wrap} = distance\ between\ origin\ on\ pelvis\ and\ nearest\ PCM - head\ contact\ point$$

It was necessary to assume a value for fetal head diameter in order to solve for L_{wrap}.

Fetal Head Calculations

[4] Approximating the Suboccipitobregmatic Circumference from the Occipitofrontal Circumference

The suboccipitobregmatic circumference (SC) results from an ellipse with the biparietal (BD) and suboccipitobregmatic (SD) diameters as its axes (Figure 2.5). This was simplified by approximating SD to be equal to BD.

(4.1) $SC \approx \pi\sqrt{\frac{SD^2+{BD_L}^2}{2}} = \pi * BD_L$

$$BD_L = Biparietal\ Diameter\ during\ labor$$

Kriewall's molding index was modified by approximating SD to be equal to BD, and by approximating the mentovertical diameter (MD) to be equal to 1.2 * the frontooccipital (FD), based on values reported by Sobre *et al*. [27, 25].

(4.2) $MI = \frac{MD^2}{BD_B * SD} = \frac{1.2^2 FD^2}{{BD_B}^2} = 2.0 \pm 0.22$

$$BD_B = Biparietal\ Diameter\ post - birth$$

(4.3) $FD^2 = \frac{MI * {BD_B}^2}{1.2^2}$

The occipitofrontal circumference (OC, conventional measurement taken at time of birth) is a function of FD and BD. Equation 4.2 was solved for FD (4.3), which was used to solve for OC in terms of MI and BD (4.4).

(4.4) $OC \approx \pi \sqrt{\frac{FD^2 + {BD_B}^2}{2}} = \pi * BD_B \sqrt{\frac{(1 + \frac{MI}{1.2^2})}{2}}$

Equation 4.4 leads to the ability to write BD as a function of OC and MI, which are both commonly reported.

(4.5) $BD_B = \frac{OC\sqrt{2}}{\pi \sqrt{1 + \frac{MI}{1.2^2}}}$

It has been observed that BD increases by at least 0.5 cm between labor and measurements taken immediately after birth [26].

(4.6) $BD_L = BD_B - 0.5cm$

Equations 4.5 and 4.6 allow us to solve for BD_L, and consequently SC as a function of commonly reported variables.

(4.7) $\pi * BD_L = \frac{OC\sqrt{2}}{\sqrt{1 + \frac{MI}{1.2^2}}} - \frac{\pi}{2} cm = \boldsymbol{SC}$

[5] Face Presentation

The face presentation circumference (C_f) was calculated as the circumference of an ellipse with one axis as the unaltered circumference (d_0) and one axis as the modified diameter (d_f), observed to gain up to 7 mm at delivery. Both diameters were expressed in terms of the original circumference (C_0), allowing us to calculate C_f as a function of C_0 only (Figure 2.7).

(5.1) $C_f = \pi\sqrt{\frac{d_0^2+d_f^2}{2}}$

(5.2) $d_0 = \frac{C_0}{\pi}$

(5.3) $d_f = d_0 + 7mm$

(5.4) $C_f = \pi\sqrt{\frac{\frac{C_0^2}{\pi^2}+\left(\frac{C_0}{\pi}+7mm\right)^2}{2}}$

(5.5) $C_f = \sqrt{\frac{C_0^2+(C_0+\pi*7mm)^2}{2}}$

Chapter 3: A Constitutive Model Description of the Material Properties of Birth Canal Tissue in A Term Pregnant Woman

Paige V Tracy[1], Alan S Wineman[2], Francisco J Orejuela[3], Susan M Ramin[3], John O L DeLancey[4], James A Ashton-Miller[2]
[1] Department of Biomedical Engineering, University of Michigan
[2] Department of Mechanical Engineering, University of Michigan
[3] Department of Obstetrics and Gynecology, Baylor College of Medicine
[4] Department of Obstetrics and Gynecology, University of Michigan

3.1 Abstract

Remarkable changes must occur in the pelvic floor muscles and tissue comprising the birth canal in order to allow vaginal delivery. Despite these preparatory adaptations, approximately 13% of first time mothers sustain tears near the origin(s) of the pubovisceral muscle (PVM). In order to investigate why these tears occur, it is necessary to first quantify the viscoelastic behavior of the term pregnant human birth canal. The goal of this study was to quantify the material properties of the human birth canal, *in situ,* at the time of delivery and compare them to existing animal models. The results show that human, ovine and squirrel monkey birth canal tissue can be characterized by the same set of constitutive relations, with the differences between species primarily explained by the long time constant, τ_2, which has values of 555 seconds, 1110 seconds, and 2777 seconds, respectively. The quantification of these viscous properties should allow for improved accuracy of computer models aimed at understanding vaginal birth-related injuries.

Keywords: Levator Ani; Quasilinear Viscoelasticity; Birth; Constitutive Model

3.2 Introduction

Of the 3 million of women who give birth each year, approximately 15% experience tears to the pubovisceral (PVM) portion of the levator ani muscles [1]. These tears are linked to the later development of disorders such as pelvic organ prolapse and incontinence [2] [3]; problems that lead to approximately 10% of all US women eventually requiring corrective surgery [2].

Concerned about these types of complications, some women choose elective Cesarean Section; however, such a procedure carries its own immediate and delayed risks [4] [5]. In addition, because there is no current method to accurately predict the risk of a PVM tear prior to birth, the 85% of women who would not experience tears during vaginal delivery may be undergoing unnecessary procedures.

The ability to reliably predict PVM tear outcomes prior to delivery, as outlined theoretically by Tracy et al. 2016 [6], would represent a major advance if it could be validated using clinical data. Proof of concept results in women using antenatal hiatal diameters and postpartum fetal head data to predict injury are promising [7]. However, we believe the accuracy of such predictions is currently limited by the complete lack of viscoelastic property data of the term-pregnant human birth canal *in situ*. During labor, the human birth canal undergoes a remarkable degree of deformation in less than two hours that is unprecedented elsewhere in the body: for example, the PVM undergoes an estimated three-fold increase in length [8] [9] [10] in less than two hours.

As a result, it is not reasonable to assume the term pregnant material properties of the pelvic floor striated muscles to be similar to those of striated muscles found elsewhere. Additionally, it has been shown in ovine [11] and rat [12] models that there are remarkable pelvic floor material property changes in preparation for, and during, labor. As a result, it is important to identify the mechanical behavior of the human birth canal as proximate to the time of delivery as possible.

The goal of this study was to derive a constitutive model of the term-pregnant birth canal, based in part on pre-existing animal model data [11] [13]. We then sought to validate this model using *in situ* force-displacement data from the human birth canal at the time of labor.

3.3 Constitutive Model

We begin with a constitutive model that takes the form of Fung Quasilinear Viscoelastic Theory for soft tissues [14]. The development of this constitutive model relied on pregnant squirrel monkey and ovine birth canal data, as well as human birth canal distention data [13]. Pregnant squirrel monkey pelvic floor muscle ramp-and-hold relaxation tests were first used to determine the form of the relaxation function, including parameter C and short and long time constants τ_1 and τ_2. Pregnant ovine vaginal wall uniaxial cyclic loading data available in literature [11] were used to determine the elastic function form, including parameters A and B, as well as to characterize cyclic stress-strain hysteresis behavior, resulting in modifications to relaxation parameters C and τ_2. This elastic function form was also compared to a similar form originally fit to the squirrel monkey data (Figure 3.2). When validating with term pregnant human birth canal distension data, the estimate of parameter τ_2 was refined.

All of the following calculations and simulations were performed on a Lenovo T430 computer using MATLAB v.R2015a. Run times ranged from 1 to 120 minutes.

3.3.1 Characterization of Relaxation Form

A uniaxial relaxation function of the form previously suggested for soft tissue applications [14] was fit to previously collected squirrel monkey pelvic floor muscle tensile ramp-and-hold data [13] .

Relaxation Function Form:

(2.1.1) $$G(t) = \frac{1+C*[E_1(t/\tau_2)-E_1(t/\tau_1)]}{1+C*ln(\tau_2/\tau_1)}$$

(2.1.2) $$E_1(x) = \int_x^\infty \frac{e^{-y}}{y}\,dy$$

The elastic function form is also given here for reference:

(2.1.3) $$\sigma = A(e^{B\varepsilon^3} - 1)$$

From this relaxation function, a creep function can be derived using methods established by Fung [14] (Figure 3.6S).

Creep Function form:

(2.1.4) $$J(t) = J(\infty)\left\{1 + \frac{(1+s_0\tau_2)(1+s_0\tau_1)}{C*s_0*(\tau_2-\tau_1)}e^{s_0 t} + C\int_{1/\tau_1}^{1/\tau_2} \frac{e^{-xt}}{x*\left\{(C\pi)^2+\left[1+C*\ln\left(\frac{x\tau_2-1}{1-x\tau_1}\right)\right]^2\right\}}dx\right\}$$

$$s_0 = -\frac{e^{1/C}-1}{\tau_2 e^{1/C} - \tau_1}$$

$$J(\infty) = 1 + C * \ln\left(\tau_2/\tau_1\right)$$

3.3.2 Characterization of Hysteresis:

Using the creep function form (2.1.3), and the following creep form of the constitutive function, and using ramped stress as an input, Ulrich's ovine experiments were then simulated [11] .

Creep Form: $\varepsilon(t) = J(0)\sigma(t) + \int_0^t \sigma(t-s)\dot{J}(s)\,ds$ (2.2.1)

This revealed an elastic function of the form $\sigma = A(e^{B\varepsilon^3} - 1)$ (2.1.3)

Following parameter validation through simulation of *in vivo* human birth canal creep (constant uniaxial force distension) testing (Section 2.3), uniaxial cyclic loading was simulated in order to verify a reasonable description of the cyclic stress-strian hysteresis loops demonstrated in the pregnant ovine data.

3.3.3 Parameter Optimization:

To verify this constitutive model's ability to predict human maternal birth canal distension behavior at the time of first stage of labor, the results of simulations described below have been compared to what we believe to be the first experimental creep testing data for the term-pregnant human birth canal. The model parameters C and τ_2 were optimized by trial and error methodology in order to obtain a best-fit against the experimental data.

Human data were available from ongoing tests of a device which generates an outward radial force with the purpose of dilating the lower birth canal in the first stage of labor developed by Materna Medical, Inc. Force and displacement data collected as part of a clinical trial at Baylor College of Medicine were provided to us by Materna Medical and were analyzed as part of this

research. The analysis of these data in this way was not envisioned in the design of the trial. These data were collected continuously while the device was powered on, corresponding to the entire duration of birth canal distension by the device, as well as time required for device calibration, insertion, and removal. The force data were used as the input to the simulation once converted to tensile stress values in the direction of the line-of-action of the muscle fibers based on an assumed average anatomic cross sectional area of the healthy female PVM equal to 1.2 cm^2 [15]. Considering that the vaginal wall has one sixth the cross sectional area of the PVM [16] and one tenth the elastic modulus of striated muscle [17] [18], vaginal wall tissues were assumed to provide negligible resistance to stretch.

Simulations were run for a time step size of 0.1 seconds, with assumed soft tissue incompressibility. The geometric relationship between soft tissue length and maternal capacity (circumference of birth canal) was quantified using a previously derived mathematical relationship [6].

3.3.4 Sensitivity Analysis

Sensitivity analysis was performed by individually varying elastic function parameters A and B, relaxation coefficient C, and the short and long time constants, τ_1 and τ_2 respectively. Each variable was increased and decreased by 1 decade (factor of 10).

3.4 Results

3.4.1 Constitutive Relationships

The overall constitutive relationship is of the form:

$$\varepsilon(t) = J(0)\sigma(t) + \int_0^t \sigma(t-s)\frac{dJ}{ds}(s)\,ds \qquad (2.2.1)$$

Where, the final creep function is:

$$J(t) = J(\infty)\left\{1 + \frac{(1+s_0\tau_2)(1+s_0\tau_1)}{C*s_0*(\tau_2-\tau_1)}e^{s_0 t} + C\int_{1/\tau_1}^{1/\tau_2} \frac{e^{-xt}}{x*\left\{(C\pi)^2+\left[1+C*\ln\left(\frac{x\tau_2-1}{1-x\tau_1}\right)\right]^2\right\}}dx\right\} \qquad (2.1.4)$$

and where

$$s_0 = -\frac{e^{1/C}-1}{\tau_2 e^{1/C}-\tau_1}$$

$$J(\infty) = 1 + C * \ln\left({}^{\tau_2}/_{\tau_1}\right).$$

$$C = 13.08 \qquad \tau_1 = 0.973\ seconds \qquad \tau_2 = 555\ seconds$$

The final elastic function form is:

$$A(e^{B\varepsilon^3} - 1) \quad (2.1.3)$$

Where $A = 16.1\ MPa$ and $B = 0.081$.

The results of this constitutive model were compared to experimental distension data collected for the term pregnant human birth canal (Figure 3.1).

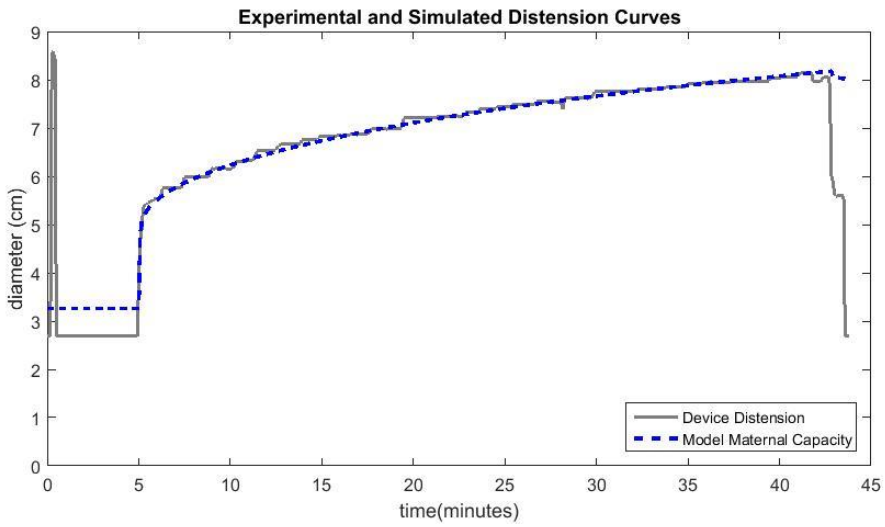

Figure 3.1 - Experimental human distension data (gray solid) and simulated maternal capacity distension/diameter (blue dashed). The initial spike in distension data represents device calibration deployment prior to insertion into the birth canal and the terminal drop is attributed to device removal.

3.4.2 Species Model Variations

The previously published pregnant squirrel monkey elastic function took on the form:

$A(e^{B\varepsilon} - 1)$ (3.2.1) [13]

In optimizing the constitutive model for the term pregnant human case, it was found that the following elastic function form provided the best fit.

$A(e^{B\varepsilon^3} - 1)$ (2.1.3)

This change in elastic function form resulted in an increased simulated elastic response for a given value of parameter B and a decreased elastic response for a given value of parameter A. As a result, it is not surprising that in the final constitutive form, the human value for parameter A is larger than its squirrel monkey counterpart while the human value for parameter B is reduced when compared to the corresponding squirrel monkey value (Table 3.1).

	Squirrel Monkey	Ovine	Human
A (MPa)	0.161*	16.1	16.1
B (unitless)	2.98*	0.081	0.081
C (unitless)	0.327	13.1	13.1
τ_1 (seconds)	0.973	0.973	0.973
τ_2 (seconds)	2777	1110	555

Table 3.1 - Parameter values for the squirrel monkey, ovine and human models. *The elastic function previously fit to squirrel monkey data takes on a different form than that fit here to ovine and human data. [13]

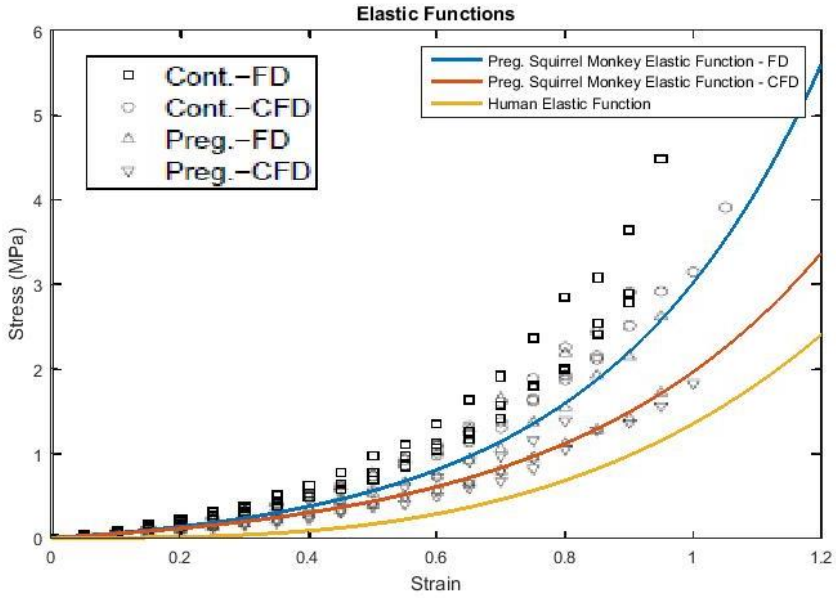

Figure 3.2 - The term pregnant human birth canal elastic function (yellow) is compared to previously published *ex vivo* mechanical data for pregnant squirrel monkey pelvic floor muscle in the circumferential fiber direction (FD, blue) and cross fiber direction (CFD, red) [13].

The relaxation function for the human birth canal constitutive model retained the same form as that fit to previously published squirrel monkey pelvic floor muscle data [13]. However, the values of the coefficient, C, and the long time constant, τ_2, varied between the two species with C increasing from 0.327 for the squirrel monkey case to 16.1 for the human case and τ_2 decreasing from 2777 seconds for the squirrel monkey case to 555 seconds for the human case

(Table 3.1, Figure 3.3). Decreasing τ_2 had the impact of decreasing the time required to reach the final relaxation state, while increasing C had the impact of decreasing the steady state stress at the final relaxation state.

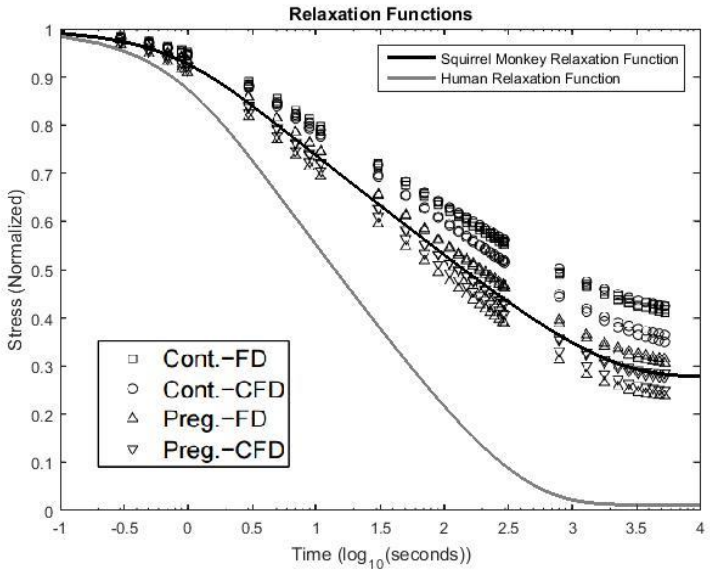

Figure 3.3 - The term pregnant human birth canal relaxation function (grey) is compared to previously published *ex vivo* mechanical data for pregnant squirrel monkey pelvic floor muscle in the circumferential fiber direction (FD, black) [13] These relaxation functions plateau at 0.278 and 0.0119 for pregnant squirrel monkey and human respectively.

τ_2 was also found to vary between human and ovine models, with the optimized fit to ovine hysteresis data occurring at a τ_2 value of 1110 seconds (Figure 3.4, Table 3.1). Considering this result, the human and ovine models did agree quite well on coefficient C, or the steady state stress at the final relaxation state.

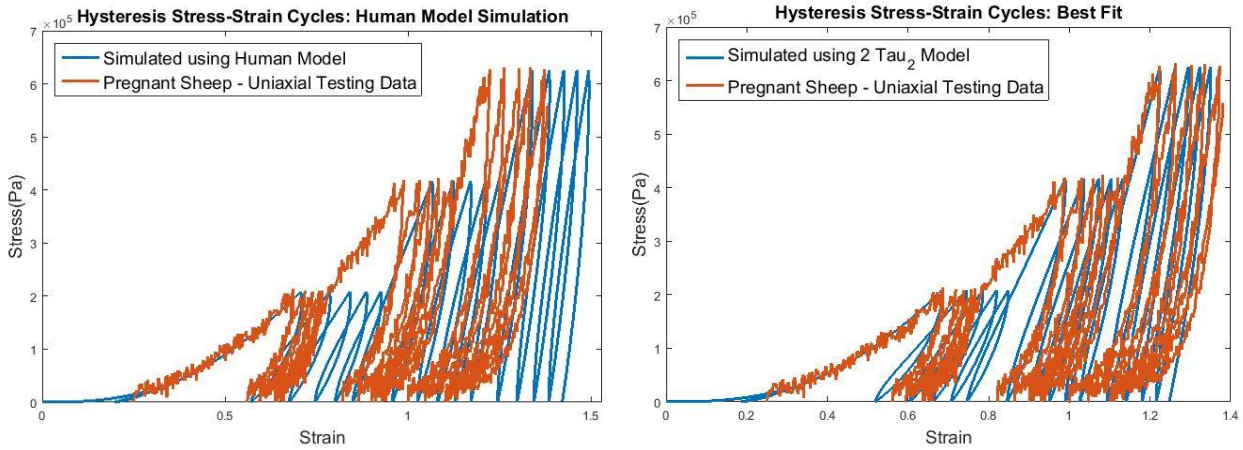

Figure 3.4 - Hysteresis stress-strain ramping simulations (blue) for the term pregnant human birth canal constitutive relationships (left) and ovine vaginal wall tissue model optimized constitutive relationships (right) are compared to previously published *ex vivo* mechanical data for pregnant ovine vaginal wall tissue (red) [11].

3.4.3 Sensitivity Analysis

Results for the sensitivity analysis (Figure 3.5) showed that a 1 decade variation in elastic function parameter B had the greatest impact on the magnitude of the distension response. However, a 1 decade variation in elastic function parameter A resulted in a response of a similar magnitude. Of the viscous (creep and relaxation) parameters, the long time constant, τ_2, had the greatest effect on magnitude of response. Variations in the short time constant, τ_1, and coefficient C had smaller effects on the magnitude of response, with the smallest effect being observed for a 1 decade increase in parameter C.

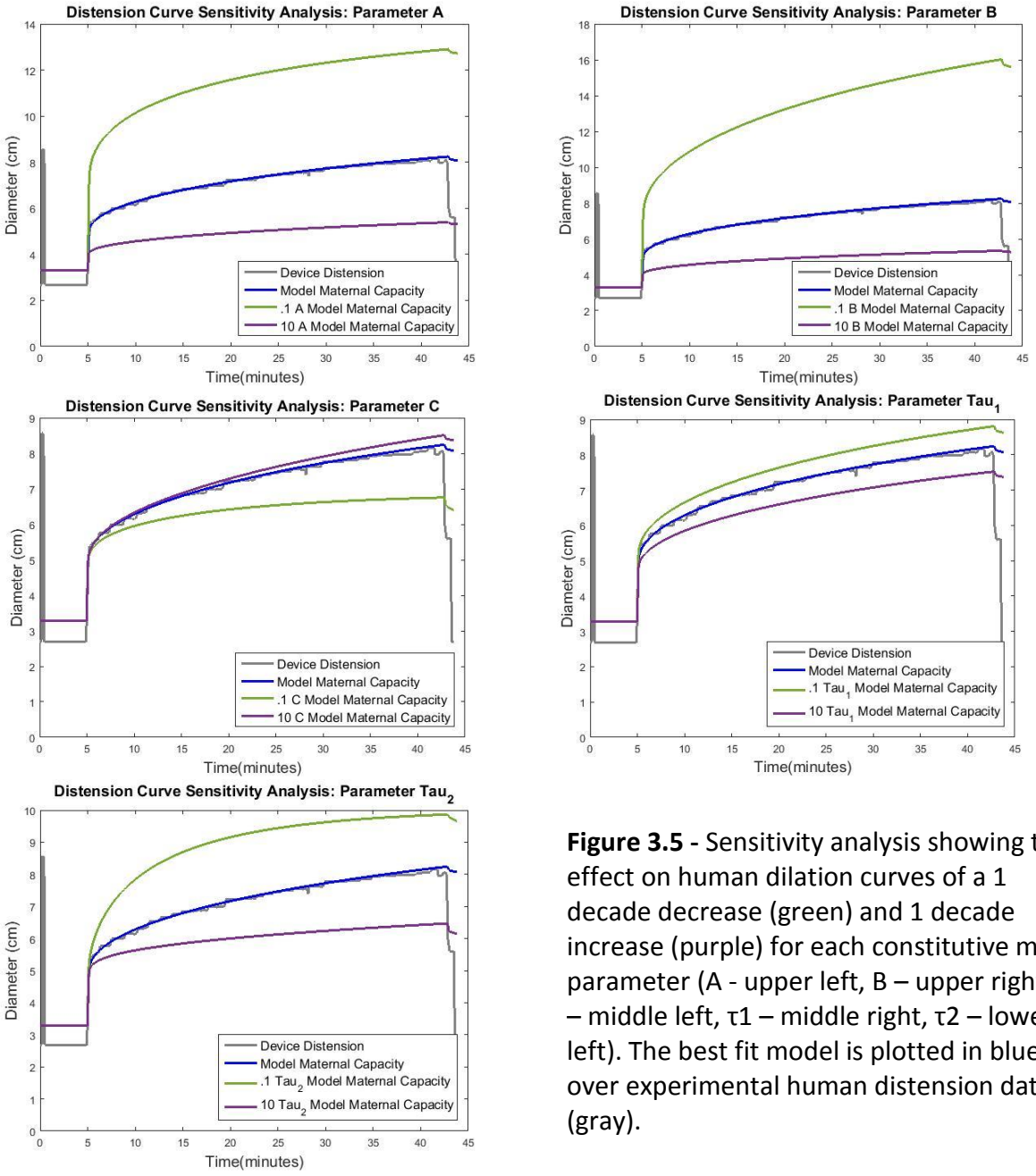

Figure 3.5 - Sensitivity analysis showing the effect on human dilation curves of a 1 decade decrease (green) and 1 decade increase (purple) for each constitutive model parameter (A - upper left, B – upper right, C – middle left, τ1 – middle right, τ2 – lower left). The best fit model is plotted in blue over experimental human distension data (gray).

3.5 Discussion

To our knowledge this is the first *in vivo* and *in situ* quantification of the material properties of the human birth canal at the end of pregnancy. Knowledge of these properties allows the previously unexplored time-dependent relaxation behavior of the human birth canal to be characterized. This quantification may help facilitate a research-based re-evaluation of current

clinical practices concerning how the rate of birth-canal dilation can affect birth outcomes. It also permits investigation into more subtle factors that contribute to a mother's risk for PVM tear, such as asking what would happen if these material properties were not reached due to inadequate hormonal tissue "ripening" [19].

In this study, we have considered three separate species models: squirrel monkey pelvic floor muscle ovine vaginal wall, and human birth canal tissues. Though not identical, these models are similar in the form of their constitutive relationships, and vary primarily in one parameter: the long time constant, τ_2. Here, humans have the shortest of these time constants, with a value of 555 seconds, followed by ovine at 1110 seconds, and squirrel monkeys at 2777 seconds. It would be interesting to explore how this interspecies difference in time constants would affect the duration of second stage of labor for different maternal capacity – to – fetal head demand ratios [6].

The sensitivity analyses revealed that the elastic parameters, A and B, had their greatest effect on the amplitude of the strain response. However, the long time constant, τ_2, is the parameter which had the greatest influence over the temporal response.

The present approach has certain strengths and limitations. A strength is that we were able to study *in vivo, in situ* human tissue during labor and also to demonstrate consistency of the constitutive response across three different species, with differences between species primarily being explained by a single parameter, the long time constant, τ_2. Additionally, the creep and relaxation behavior for these three species is consistent with a relaxation function previously derived for soft tissues [14].

A limitation of the model is that it depends on data from studies of small numbers, generally two, of each species due to the scarcity of tissue, the nature of the methods and resources required. As a result, variations within each species could not be investigated. Additionally, the squirrel monkey and ovine data considered were both excised. However, the pregnant human birth canal distension data was both *in vivo* and *in situ*. Taken as a whole, we believe the model represents a reasonable order of magnitude estimate of human birth canal temporal behavior under distension.

An additional limitation is that the present model describes the temporal behavior of the distal human birth canal. The canal is comprised of the vagina along with the underlying soft tissues, principally the PVM, as presented to the distension device. Our model, therefore, does not reflect only striated muscle or only vaginal wall behavior, but rather the overall response of the combined individual anatomical components that comprise the most distal portion of the canal. This, after all, is the composite structure that is presented to the fetal head, so the properties of this construct are more meaningful than those of any individual component tissue. The stress we calculated by only using the anatomic cross-sectional area of the PVM does not account for the tensile stress of the vaginal wall and adjacent connective tissue. However, considering that the vaginal wall has one sixth the cross sectional area of the PVM [16] and one tenth the elastic modulus of striated muscle [17] [18], the contribution of the vaginal wall tissues to this resistance to stretch are expected to be negligible. When we factored in vaginal properties, there was a 1.6% decrease in stress values.

It is true that the distension we modeled is somewhat different than that which would occur during passage of the fetal head, where downward descent of the pelvic floor during delivery is added to the circumferential deformation induced by this device. This fact limits our ability to conclusively separate out the individual role of each subcomponent, but it does allow us to characterize the overall stress response of the structure, whose individual components lie roughly parallel to the distal circumferential boundary of the birth canal during birth. As a result, if the PVM comprised approximately 80% of the birth canal at the level at which the device is inserted, it could be estimated that 80% of the total force as measured by the distension device is experienced by the PVM as a tensile load. This can be viewed as an extension of laws invoked for elements occurring in parallel in common spring-and-dashpot models.

Acknowledgements

We gratefully acknowledge financial support from the Office for Research on Women's Health SCOR program on Sex Differences in Women's Health (P50 HD 44406). We thank Dr. Mark Juravic of Materna Medical, Inc., for contributing the human birth canal force-displacement data in the absence of any financial support. We thank Drs. Susan Ramin and Francisco J Orejuela at Baylor College of Medicine for conducting the clinical trial that was funded by Materna and resulted in the data we were able to use. We would also like to thank Sharon Edwards and the team at Prince Henry's Institute and the Monash Institute of Medical Research in Melbourne, Australia for their generosity in sharing their ovine specimen data.

3.6 Bibliography

[1] K. Shek and H. Dietz, "Intrapartum risk factors for levator trauma," *BJOG An International Journal of Obstetrics and Gynecology,* vol. 117, no. 12, pp. 1485-1492, 2010.

[2] J. A. Ashton-Miller and J. O. L. DeLancey, "On the Biomechanics of Vaginal Birth and Common Sequelae," *Annual Review of Biomedical Engineering,* vol. 11, pp. 163-176, 2009.

[3] J. Mant, R. Painter and M. Vessey, "Epidemiology of genital prolapse: observations from the Oxford Planning Association Study," *British Journal of Obstetrics and Gynaecology,* vol. 104, no. 5, pp. 579-85, 1997.

[4] G. H. Visser, "Women are designed to deliver vaginally and not by cesarean section: an obstetritian's view," *Neonatology,* vol. 107, no. 1, pp. 8-13, 2015.

[5] C. Zelop and L. J. Heffner, "The downside of cesarean delivery: short- and long-term complications," *Clinical Obstetrics and Gynecology,* vol. 47, no. 2, pp. 386-93, 2004.

[6] P. V. Tracy, J. O. L. DeLancey and J. A. Ashton-Miller, "A Geometric Capacity - Demand Analysis of Maternal Levator Muscle Stretch Required for Vaginal Delivery," *Journal of Biomechanical Engineering,* pp. e1-e54, 2016.

[7] G. Rostaminia, J. D. Peck, K. Van Deft, R. Thakar, A. Sultan and S. A. Shobeiri, "New Measures for Predicting Birth-Related Pelvic Floor Trauma," *Female Pelvic Med Reconstructive Surgery,* vol. 22, no. 5, pp. 292-6, 2016.

[8] K.-C. Lien, J. O. L. DeLancey and J. A. Ashton-Miller, "Biomechanical Analyses of the Efficacy of Patterns of Maternal Effort on Second-Stage Progress," *Obstetrics & Gynecology,* vol. 113, no. 4, pp. 873-880, 2009.

[9] M. E. T. Silva, D. A. Oliveira, T. H. Roza, S. Brandao, M. P. L. Parente, T. Mascarenhas and R. M. Natal Jorge, "Study on the influence of the fetus head molding on the biomechanical behavior of the pelvic floor muscles, during vaginal delivery," *Journal of Biomechanics,* vol. 48, no. 9, pp. 1600-1605, 2015.

[10] P. Zan, G. Yan, H. Liu, B. Yang, Y. Zhao and N. Luo, "Biomechanical modeling of the rectum for the desing of a novel artificial anal sphincter," *Biomedical Instrumentation and Technology,* vol. 44, no. 3, pp. 257-60, 2010.

[11] D. Ulrich, S. L. Edwards, K. Su, J. F. White, J. A. M. Ramshaw, G. Jenkin, J. Deprest, A. Rosamilia, J. A. Werkmeister and C. E. Gargett, "Influence of Reproductive Status on Tissue Composition and Biomechanical Properties of Ovine Vagina," *Public Library of Science,* vol. 9, no. 4, pp. 1 - 8, 2014.

[12] M. Alperin, D. M. Lawley, M. C. Esparza and R. L. Lieber, "Pregnancy-induced adaptations in the intrinsic structure of rat pelvic floor muscles," *American Journal of Obstetrics and Gynecology,* vol. 213, no. 2, pp. 191 - 197, 2015.

[13] D. Jing, "Experimental and Theoretical Biomechanical Analyses of the Second Stage of Labor.," 2010. [Online]. Available: http://deepblue.lib.umich.edu/handle/2027.42/76013. [Accessed 21 August 2015].

[14] Y. C. Fung, Biomechanics: Mechanical Properties of Living Tissues, New York, NY: Springer-Verlag, 1993.

[15] V. C. Morris, M. P. Murray, J. O. L. DeLancey and J. A. Ashton-Miller, "A comparison of the effect of age on levator ani and obturator internus muscle cross-sectional areas and volumes in nulliparous women.," *Neurourology and Urodynamics,* vol. 31, no. 4, pp. 481-6, 2012.

[16] E. Pena, P. Martins, T. Mascarenhas, R. M. Natal Jorge, A. Ferreira, M. Doblare and B. Calvo, "Mechanical Characterization of the Softening Behavior of Human Vaginal Tissue," *Journal of the Mechanical Behavior of Biomedical Materials,* vol. 4, pp. 275-83, 2011.

[17] C. Rubod, M. Boukerrou, M. Brieu, P. Dubois and M. Cosson, "Biomechanical Properties of Vaginal Tissue. Part 1: New Experimental Protocol," *The Journal of Urology,* vol. 178, pp. 320-325, 2007.

[18] M. Silldorff, A. Choo, A. Choi, E. Lin, A. Carr, R. Lieber, J. Lane and S. Ward, "Effect of Supraspinatus Tendon Injury on Supraspinatus and Infraspinatus Muscle Passive Tension and Associated Biochemistry," *The Journal of Bone and Joint Surgery,* vol. 96, pp. e175(1-7), 2014.

[19] S. Makieva, P. T. Saunders and J. E. Norman, "Androgens in pregnancy: roles in parturition," *Human Reproduction Update,* vol. 20, no. 4, pp. 542-59, 2014.

3.7 Appendix

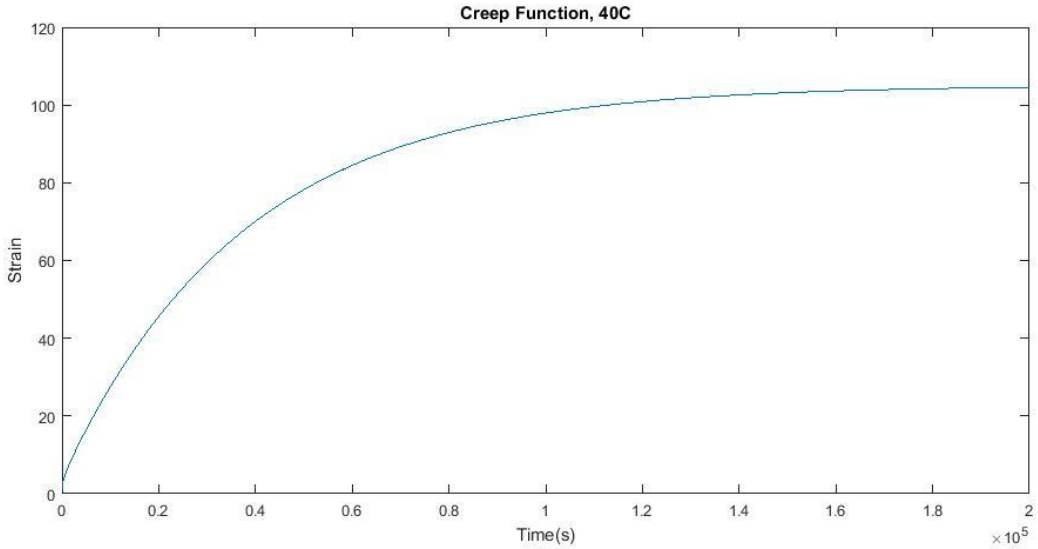

Figure 3.6S - The final human birth canal creep function for the parameter values C = 13.08, τ_1 = 0.973 seconds, τ_2 = 2776.6 seconds.

Chapter 4: On the Variation in Maternal Birth Canal Viscoelastic Properties and Its Effect on Predicted Length of Active Second Stage and Levator Ani Tears

Paige V Tracy[1], Shreya Wadhwani[1], Jourdan Triebwasser[2], Alan S Wineman[3], Francisco J Orejuela[4], Susan M Ramin[4], John O DeLancey[2], James A Ashton-Miller[3]
[1] Department of Biomedical Engineering, University of Michigan
[2] Department of Obstetrics and Gynecology, University of Michigan
[3] Department of Mechanical Engineering, University of Michigan
[4] Department of Obstetrics and Gynecology, Baylor College of Medicine

4.1 Abstract

Exactly why the remarkable elongation of the pubovisceral muscle (PVM) causes the muscle to tear in 13% of vaginal deliveries remains unknown. In this paper we first quantify the variation in *in vivo in situ* data of maternal birth canal viscoelastic properties in healthy women using Fung's Quasilinear Viscoelastic Theory. We tested the hypothesis that no significant inter-individual variation in the long time constant, τ_2, existed. We rejected that hypothesis, finding that τ_2 values ranged 20-fold below and above the median during the first stage of labor. We then used these data in the Tracy et al. (2016) biomechanical model modified to predict how such variations affect both the predicted length of the active second stage of labor and the risk for PVM tears. The results show there was a 100-fold change in the predicted length of active second stage from the shortest to the longest value of τ_2, with a noticeable increase occurring for τ_2 values exceeding 1,000 seconds. However, only 5% of the population's PVM tear risk was

predicted to change due to differences in τ_2. We conclude that τ_2 is a strong theoretical predictor of the time a mother has to push in order to deliver a fetal head whose diameter exceeds that of the maternal birth canal.

Key words: Levator Ani, Birth, Viscoelastic, Constitutive Model, Injury

4.2 Introduction

During labor, the birth canal undergoes remarkable deformation, typically increasing its circumferential length up to three-fold [1] [2] [3]. The most distal part of the birth canal is formed by the pubovisceral muscle (PVM), a subdivision of the levator ani muscles. This region undergoes the most stretch during the second stage of labor, which occurs after the cervix is open and before the baby is born [4] [5]. This portion of the muscle is attached high on the posterior aspect of the pubic symphysis, and forms a U-shaped loop that is dilated and pushed downward by the fetal head during birth (Figure 4.1). It has been predicted to be partially wrapped around the bony pelvis in the parasagittal plane, thereby reducing its capacity to accommodate a fetal head [6]. Due to the large degree of stretch required towards the end of the second stage of labor [4], the PVM tears in approximately 13% of vaginal deliveries [7]. These tears have been linked to the development of pelvic organ prolapse later in life in some individuals [8] [9] [10], a disorder for which 10% of all US women eventually require corrective surgery [8] [11].

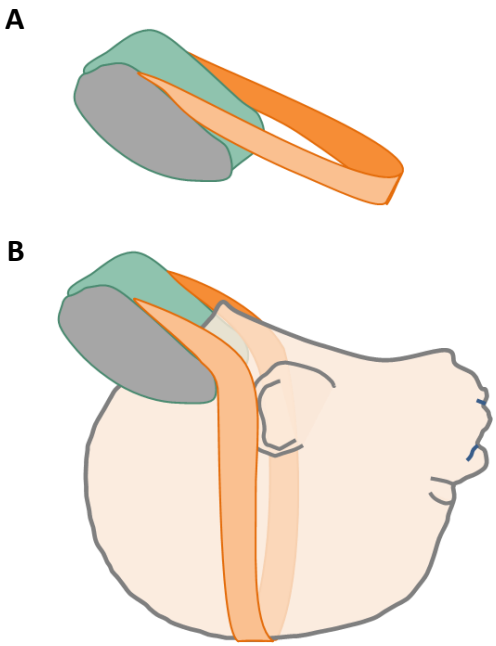

Figure 4.1 - Pubovisceral muscle (orange) anchored onto the anterior pelvis (green) (A) at rest and (B) stretching to accommodate a fetal head.

Some women choose elective Cesarean Section because they are concerned about such complications; however, this operation carries its own immediate and delayed risks [12] [13]. In addition, because there is no current method to predict the risk of a PVM tear prior to birth, the women who would not experience tears during vaginal delivery may be undergoing unnecessary operations, while many women who are at risk fail to avoid PVM tears.

The overall goal of our research has been to develop a framework for predicting levator tear risk as well as the length of the active second stage of labor so that the women at highest risk can be identified for preventative strategies benefitting them without imposing unintended harm on those who are not destined to be injured. In this chapter we will build on the geometric analysis of the fit between the fetal head and maternal birth canal described in Tracy et al. 2016 [6]. Specifically, we will now incorporate the recently characterized viscoelastic

behavior of the term pregnant human birth canal (Chapter 3) into that model in order to simulate the biomechanical interaction between the fetal head and viscoelastic maternal birth canal during the active second stage of labor. Here, the predicted PVM tear outcome will reported in the context of a levator state parameter, based on the product of stress times strain, where a value greater than 1 indicates that a PVM tear is predicted. Since the Tracy et al. (Chapter 3) study characterizing the maternal viscoelastic behavior using a five parameter Quasilinear Viscoelastic Theory (QLV) constitutive model [14] did not consider inter-individual variations, we will first test the null hypothesis that there is no significant variation between term pregnant mothers in their long time constant, τ_2. Then we will test the null hypothesis that the variation in τ_2 will not affect (1) the predicted length of the active second stage of labor, or (2) the risk of a PVM tear.

4.3 Methods

The maternal birth canal force-dilation data for 30 subjects was fit to a previously published five parameter constitutive model based on QLV theory for soft tissues (Chapter 3). These force-distension data were obtained from a device developed by Materna Medical, Inc. to generate a constant outward radial force with the purpose of dilating the lower birth canal prior to delivery. Dilation was limited to a maximum diameter of 8 cm. The force and displacement data were collected as part of a clinical trial and were provided to us by Materna Medical and Baylor College of Medicine. They were analyzed as part of this research. All simulations were run in MATLAB R2015a with a time step size of 0.1 seconds.

4.3.1 Birth Simulations

Stress–strain relationships were assumed to be governed by the QLV constitutive model (Chapter 3).

Maternal capacity and the PVM U-shaped sling length were then calculated from the 2.3rd to the 97.7th female based on the Tracy et al. (2016) geometric model that considered the maternal birth canal capacity to be determined by the subpubic arch angle, PVM origin location, PVM length, while fetal demand was represented by the 2.3rd to the 97.7th fetal head with average molding [6]. Birth simulations were run for each maternal capacity – to – fetal head demand pairing.

PVM strain, ε_{PVM}, was assumed to be related to general birth canal strain, ε_{BC}, based on the ratio between their initial circumferential lengths, l_{PVM} and l_{BC} respectively [6].

$$\varepsilon_{PVM} = \frac{l_{BC}}{l_{PVM}}(\varepsilon_{BC} + 1) - 1$$

It was also estimated, based on anatomical analysis (Chapter 3) of the height of the pubovisceral muscle relative to the distension device, that 83% of the total force as measured by the Materna birth canal distension device was resisted as a tensile load in the PVM.

In the modified Tracy et al. (2016) model, simulations of vaginal birth during the second stage were driven by intrauterine pressure as an input, as measured in previous experiments: this included a 2.6 kPa basal intrauterine pressure, an 8.5 kPa rise during contractions, and an additional 10.5 kPa rise during each volitional push [15]. Contractions and pushes were each modeled as the first half of one period of a cosine wave. Specifically, contractions were

assumed to last for 90 seconds, followed by 90 second rest; three 10 second pushes were assumed per contraction with each followed by 10 seconds of rest [16] [17] [15].

Intrauterine pressure was assumed to be related to circumferential stress in the PVM U-shaped sling, based on the following calculations (Figure 4.2):

$$T = tension\ in\ PVM$$

$$\tilde{T} = \frac{T}{2\pi r} = Tension/length$$

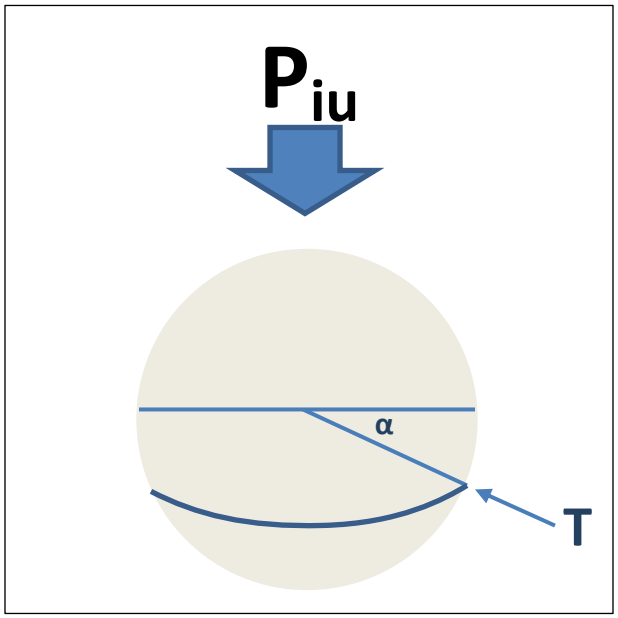

Balancing "Vertical" Forces: $\tilde{T} 2\pi r * sin(\alpha) = P_{ab} \pi * {r_h}^2$

$$\tilde{T} = \frac{P_{ab} * {r_h}^2}{2r * sin(\alpha)}$$

Balancing "Horizontal" Forces: $\sigma_{PVM} 2 * A_{PVM} = \tilde{T} 2r * \cos(\alpha)$

$$\sigma_{PVM} = \frac{\tilde{T} * 2r * \cos(\alpha)}{2A_{PVM}} = \frac{P_{ab} {r_h}^2}{2A_{PVM} \tan(\alpha)}$$

Figure 4.2 - Intrauterine pressure (blue arrow) creates a force distributed over the fetal head (grey circle). The tension (T) in the PVM (dark blue band low on head) was related to intrauterine pressure using the radius of the fetal head (light blue lines) and the angle between the midline of the fetal head and the contact point of the PVM on the fetal head (alpha).

Based on image analysis of deviations of the newborn fetal head from perfectly spherical anatomy, a maximum alpha value of 0.68 radians was assumed.

Simulations of births were run for 2.5th to the 97.5th percentile maternal birth capacity and 2.5th to 97.5th fetal head circumferences for three values of τ_2: the median (555 seconds), the short extreme at 1/20th the median, and the long extreme at 20 times the median. Trials that had a second stage predicted to exceed 24 hours in length were terminated because this would not be allowed clinically and the baby would instead be delivered by cesarean section.

4.3.2 Post analysis in Microsoft Excel 2010

Length of Active Second Stage tables were shaded when a threshold of 3 hours was exceeded because obstetrical guidelines recommend intervening at this point [18].

Likewise, the 'levator state parameter' tables were shaded using 2.7 MPa (levator state parameter equal to 1) as the minimum for shading indicating the threshold for injury, discussed below.

The stress-strain relationship describing the soft tissue injury criterion that was assumed was based on literature available for ligament [19] [20] [21], while the exact value of 2.7 MPa was based on the measured conditions for the ultimate failure of pregnant ovine tissue estimated graphically from [22].

A smoothing function with a width of τ_2 values spanning 100 seconds was used in Figure 4.6. This was done to account for heightened sensitivity to the timing of fetal head delivery during the final contraction for deliveries that require very few contractions, as addressed in the discussion.

4.4 Results

4.4.1 Measured Variations in the Long Time Constant, τ_2

Of the 30 subjects analyzed, variation in viscoelastic responses between 26 of them could be explained by changes in the long time constant, τ_2, alone (Figure 4.3). Therefore, we rejected the null hypothesis that there is no significant variation between term pregnant mothers in the long time constant, τ_2.

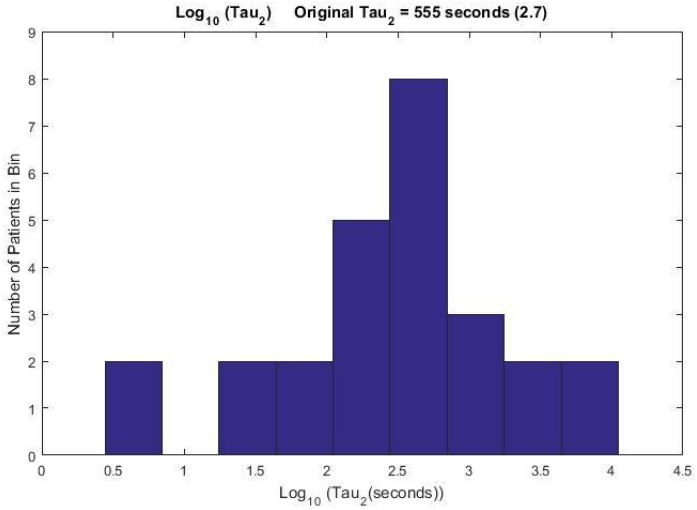

Figure 4.3 - Histogram of long time constant, τ2 values, represented in logarithmic form.

4.4.2 Predicted Length of Active Second Stage

We also rejected the null hypothesis that the variation in τ_2 would not affect the length of the active second stage of labor, showing that values of τ_2 over 1,000 seconds result in predicted active second stages of greater than 1 hour for the 50th percentile maternal capacity and 50th percentile fetal demand (Figure 4.4).

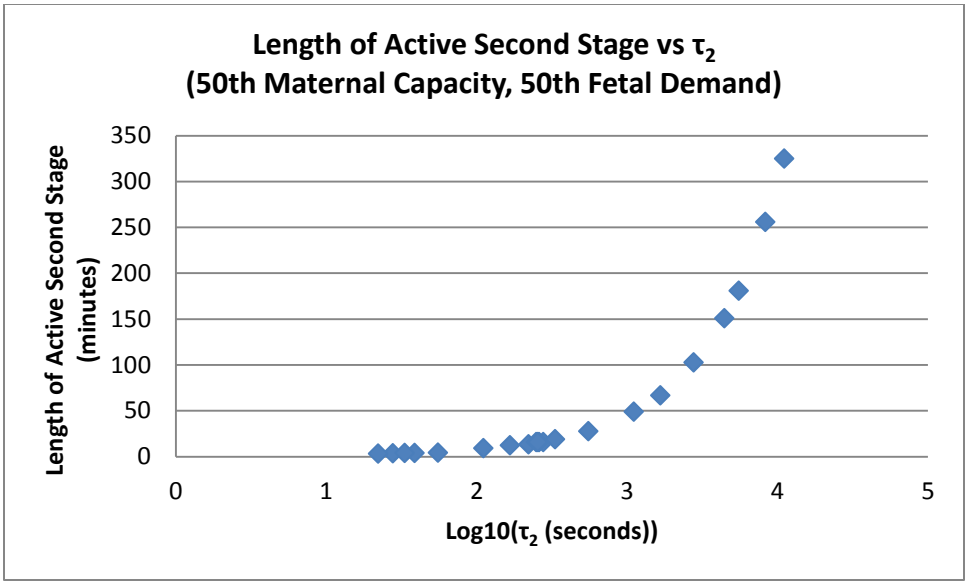

Figure 4.4 - Predicted length of the active second stage for the range of τ2 values observed. Results are for simulations for a single 50th percentile maternal capacity and 50th percentile fetal demand pairing.

Expanding upon this further, we considered a wide range of pairings between maternal capacity and fetal head demand (Figure 4.5). The simulations show that for the lower bound of observed τ_2 values (τ_2= 27 seconds, or 1/20th of the median) only 2% of births exceeded 1 hour of active second stage. Additionally, simulations run for the median observed τ_2 value (550 seconds) resulted in 26% of births exceeding 1 hour of active second stage, with none exceeding 5 hours. However, simulations run for the upper bound (20 times median) of observed τ_2 values (τ_2= 11,000 seconds) resulted in 89% of births being predicted to exceed 1 hour in active second stage.

.05 τ_2 Length of Active Second Stage Table:

CAPACITY (Maternal Circumference, in Percentile)	DEMAND (Fetal Head Circumference, in Percentile)														
	2.3rd	5th	10th	20th	25th	30th	40th	50th	60th	70th	75th	80th	90th	95th	97.7th
2.3rd	19	19	22	25	28	31	34	40	46	58	70	85	***	***	***
5th	10	12	13	13	16	16	16	19	19	22	22	25	28	34	43
10th	7	7	7	10	10	10	10	12	12	13	13	13	16	16	19
15th	6	7	7	7	7	7	7	7	9	10	10	10	10	13	13
20th	4	4	6	6	7	7	7	7	7	7	7	7	9	10	10
25th	4	4	4	4	4	6	6	6	7	7	7	7	7	7	9
30th	4	4	4	4	4	4	4	4	6	6	6	6	7	7	7
40th	3	3	4	4	4	4	4	4	4	4	4	4	4	6	6
50th	1	3	3	3	3	3	3	4	4	4	4	4	4	4	4
60th	1	1	1	1	1	3	3	3	3	3	3	3	4	4	4
70th	1	1	1	1	1	1	1	1	1	1	3	3	3	3	3
75th	1	1	1	1	1	1	1	1	1	1	1	1	1	3	3
80th	1	1	1	1	1	1	1	1	1	1	1	1	1	1	1
85th	1	1	1	1	1	1	1	1	1	1	1	1	1	1	1
90th	1	1	1	1	1	1	1	1	1	1	1	1	1	1	1
95th	0	1	1	1	1	1	1	1	1	1	1	1	1	1	1
97.7th	0	0	0	0	0	0	1	1	1	1	1	1	1	1	1

Median τ_2Table:

CAPACITY (Maternal Circumference, in Percentile)	DEMAND (Fetal Head Circumference, in Percentile)														
	2.3rd	5th	10th	20th	25th	30th	40th	50th	60th	70th	75th	80th	90th	95th	97.7th
2.3rd	118	124	133	148	151	157	166	175	184	196	205	211	235	262	289
5th	82	88	94	103	106	109	115	121	124	133	136	142	154	166	181
10th	61	64	67	73	76	76	82	85	88	91	94	97	106	112	121
15th	49	52	55	58	61	61	64	67	70	73	76	79	82	88	94
20th	40	43	46	49	52	52	55	58	61	61	64	67	70	76	79
25th	37	37	40	43	46	46	49	49	52	55	55	58	61	67	70
30th	31	34	34	37	40	40	43	43	46	49	49	49	55	58	61
40th	25	25	28	31	31	31	34	34	37	37	40	40	43	46	49
50th	19	22	22	25	25	25	28	28	31	31	31	34	37	37	40
60th	16	16	19	19	19	22	22	22	25	25	25	28	28	31	34
70th	13	13	13	16	16	16	19	19	19	19	22	22	22	25	28
75th	10	10	13	13	13	13	16	16	16	19	19	19	19	22	22
80th	7	10	10	10	13	13	13	13	16	16	16	16	19	19	22
85th	7	7	7	10	10	10	10	10	13	13	13	13	16	16	16
90th	4	4	7	7	7	7	7	10	10	10	10	10	13	13	13
95th	1	4	4	4	4	4	4	7	7	7	7	7	7	10	10
97.7th	1	1	1	1	3	4	4	4	4	4	4	4	4	7	7

20 τ_2Table:

CAPACITY (Maternal Circumference, in Percentile)	DEMAND (Fetal Head Circumference, in Percentile)														
	2.3rd	5th	10th	20th	25th	30th	40th	50th	60th	70th	75th	80th	90th	95th	97.7th
2.3rd	1342	1423	1525	1651	***	***	***	***	***	***	***	***	***	***	***
5th	970	1027	1096	1183	1216	1252	1312	1375	1429	1498	1543	1588	***	***	***
10th	697	739	787	850	871	898	937	982	1018	1066	1096	1126	1210	1291	1378
15th	559	592	634	682	703	721	757	790	820	856	880	904	970	1033	1099
20th	472	502	538	580	595	613	643	673	697	727	748	769	826	877	931
25th	409	436	466	505	520	535	559	586	607	637	655	670	721	766	814
30th	352	376	406	439	451	466	487	511	532	556	571	586	631	670	712
40th	274	292	316	346	355	367	385	406	421	442	454	466	502	535	568
50th	211	229	250	274	283	292	307	325	340	355	367	376	406	433	463
60th	160	175	193	214	223	229	244	259	271	286	295	304	328	352	376
70th	118	130	145	160	169	175	187	199	208	220	229	235	259	277	298
75th	94	106	118	133	142	148	157	169	178	190	196	202	223	241	259
80th	76	85	97	112	118	121	133	142	151	160	166	172	190	205	223
85th	55	64	73	85	91	97	106	115	121	130	136	142	157	172	187
90th	34	40	49	61	64	67	76	82	88	97	100	106	118	133	145
95th	13	19	22	31	34	37	40	46	52	58	61	64	76	85	94
97.7th	4	4	7	13	13	16	19	22	28	31	34	37	43	52	61

Figure 4.5 - Predicted length of active second stage (in minutes) across the range of pairings of maternal capacity-to-fetal head demand are shown for τ2 values of 1/20th of the median (27 seconds, Top), median (550 seconds, Middle), and 20X the median (11,000 seconds, bottom). The intensity of the (blue) shading indicates the extent by which each active second stage exceeds 3 hours. The 1 hour (dot-dot-dash line), 2 hour (dot-dash line), 3 hour (dashed line) and 4 hour (solid line) cutoffs are marked in each table.

4.4.3 Predicted Levator Tears

A gradual increase was found in the levator state parameter, used in determining predicted tears, for increasing values of τ_2. This was enough to change whether the 2.7 MPa predicted tear threshold was met for some patients, such as the 20th percentile maternal capacity-to-50th percentile fetal head demand case (Figure 4.6). Therefore, we also rejected the null hypothesis that variation in τ_2 does not affect levator ani tear risk.

Across all maternal capacity and fetal head demand pairings, we demonstrated that for 27 seconds, 550 seconds, and 11,000 seconds τ_2 values, predicted PVM tear rates were 27%, 30%, and 32%, respectively. This relatively narrow variation, represented by dashed lines added to the median table of Figure 4.7, serves as a confidence interval guide when using this table to evaluate the PVM tear risk of a mother for whom viscoelastic properties are unknown.

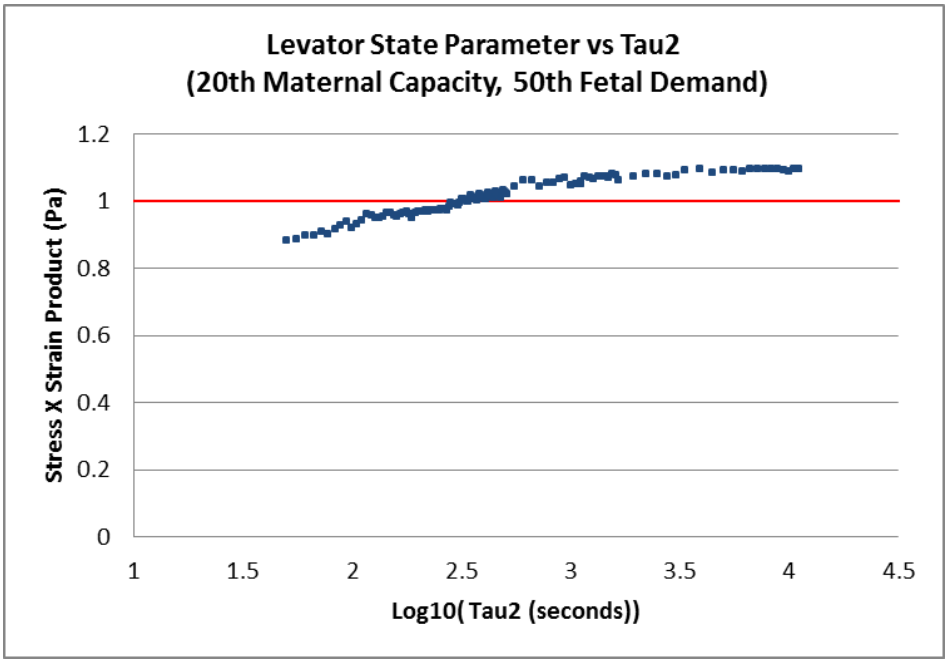

Figure 4.6 - The predicted values of the levator state parameter for the range of τ2 values observed. Results are for simulations for a single 20th percentile maternal capacity and 50th percentile fetal demand pairing. The threshold for predicted injury (2.7 MPa) is shown as the red line.

.05 τ_2Table:

CAPACITY (Maternal Circumference, in Percentile)	DEMAND (Fetal Head Circumference, in Percentile)														
	2.3rd	5th	10th	20th	25th	30th	40th	50th	60th	70th	75th	80th	90th	95th	97.7th
2.3rd	0.8	1.1	0.9	1.5	1.1	1.9	1.7	1.7	2.0	1.7	2.3	2.7	***	***	***
5th	0.8	0.9	1.2	1.2	1.1	1.5	1.4	1.6	1.4	1.9	1.6	1.9	1.8	2.4	2.8
10th	0.8	0.6	0.8	0.8	1.0	1.2	1.3	1.2	1.3	1.4	1.6	1.6	1.3	1.2	2.1
15th	0.6	0.5	0.7	0.9	1.0	0.6	0.9	1.0	1.1	1.0	1.3	1.4	1.3	1.1	1.9
20th	0.5	0.6	0.6	0.7	0.6	0.7	0.9	1.0	1.1	0.7	1.0	1.1	1.2	1.4	1.7
25th	0.6	0.6	0.5	0.7	0.7	0.6	0.8	0.6	0.7	0.9	1.1	1.2	1.2	1.2	1.4
30th	0.4	0.5	0.6	0.7	0.4	0.5	0.7	0.8	0.6	0.8	0.9	0.7	1.0	1.3	1.4
40th	0.4	0.4	0.3	0.5	0.5	0.6	0.7	0.8	0.8	0.8	0.5	0.6	0.9	0.8	1.1
50th	0.3	0.2	0.4	0.5	0.5	0.5	0.4	0.4	0.5	0.6	0.7	0.7	0.9	1.0	0.7
60th	0.2	0.3	0.4	0.4	0.4	0.3	0.4	0.5	0.5	0.6	0.6	0.6	0.5	0.7	0.9
70th	0.3	0.3	0.2	0.3	0.3	0.4	0.4	0.4	0.5	0.5	0.3	0.4	0.6	0.6	0.7
75th	0.3	0.3	0.3	0.3	0.2	0.2	0.3	0.4	0.4	0.4	0.5	0.5	0.5	0.5	0.6
80th	0.2	0.3	0.3	0.3	0.4	0.4	0.4	0.3	0.3	0.3	0.4	0.4	0.5	0.6	0.5
85th	0.2	0.2	0.3	0.3	0.3	0.3	0.4	0.4	0.4	0.4	0.4	0.3	0.4	0.5	0.5
90th	0.1	0.2	0.2	0.2	0.3	0.3	-0.1	0.3	0.4	0.4	0.4	0.4	0.5	0.5	0.3
95th	0.1	0.1	0.1	0.1	0.2	0.2	0.2	0.2	0.3	0.3	0.3	0.3	0.4	0.4	0.5
97.7th	0.1	0.1	0.1	0.1	0.1	0.1	0.1	0.2	0.2	0.2	0.2	0.2	0.3	0.3	0.3

Median τ_2Table:

CAPACITY (Maternal Circumference, in Percentile)	DEMAND (Fetal Head Circumference, in Percentile)														
	2.3rd	5th	10th	20th	25th	30th	40th	50th	60th	70th	75th	80th	90th	95th	97.7th
2.3rd	1.2	1.4	1.6	1.6	1.9	1.9	2.1	2.2	2.4	2.5	2.5	2.8	3.1	3.2	3.7
5th	1.1	1.1	1.3	1.3	1.4	1.5	1.5	1.6	1.9	1.8	2.0	1.9	2.3	2.6	2.7
10th	0.7	0.8	1.0	1.1	1.0	1.2	1.1	1.3	1.4	1.6	1.6	1.7	1.7	2.1	2.2
15th	0.7	0.7	0.8	1.0	0.9	1.0	1.1	1.2	1.3	1.4	1.3	1.3	1.6	1.8	2.0
20th	0.7	0.7	0.8	0.9	0.8	0.9	1.0	1.0	1.0	1.2	1.2	1.2	1.5	1.5	1.7
25th	0.5	0.6	0.7	0.8	0.7	0.8	0.8	1.0	1.0	1.1	1.2	1.1	1.3	1.3	1.5
30th	0.5	0.5	0.6	0.7	0.7	0.8	0.8	0.9	0.9	0.9	1.0	1.1	1.1	1.3	1.4
40th	0.4	0.5	0.5	0.6	0.6	0.7	0.7	0.8	0.8	0.8	0.9	0.9	1.0	1.1	1.2
50th	0.4	0.4	0.5	0.5	0.6	0.6	0.6	0.7	0.6	0.8	0.8	0.8	0.8	1.0	1.1
60th	0.3	0.4	0.4	0.5	0.5	0.5	0.5	0.6	0.6	0.7	0.7	0.7	0.8	0.8	0.9
70th	0.3	0.3	0.4	0.4	0.4	0.4	0.4	0.5	0.5	0.6	0.5	0.6	0.7	0.7	0.7
75th	0.3	0.3	0.3	0.4	0.4	0.4	0.4	0.5	0.5	0.5	0.5	0.6	0.6	0.7	0.8
80th	0.3	0.2	0.3	0.3	0.3	0.3	0.4	0.4	0.4	0.5	0.5	0.5	0.5	0.6	0.6
85th	0.2	0.2	0.3	0.3	0.3	0.3	0.4	0.3	0.4	0.4	0.5	0.5	0.5	0.6	0.6
90th	0.2	0.2	0.2	0.3	0.3	0.3	0.3	0.3	0.3	0.4	0.4	0.4	0.4	0.5	0.6
95th	0.1	0.1	0.2	0.2	0.2	0.2	0.3	0.2	0.3	0.3	0.3	0.4	0.4	0.4	0.5
97.7th	0.1	0.1	0.2	0.2	0.2	0.2	0.2	0.2	0.2	0.3	0.3	0.3	0.3	0.3	0.4

20 τ_2Table:

CAPACITY (Maternal Circumference, in Percentile)	DEMAND (Fetal Head Circumference, in Percentile)														
	2.3rd	5th	10th	20th	25th	30th	40th	50th	60th	70th	75th	80th	90th	95th	97.7th
2.3rd	1.3	1.5	1.6	1.8	***	***	***	***	***	***	***	***	***	***	***
5th	1.1	1.2	1.3	1.4	1.5	1.6	1.7	1.8	1.9	2.0	2.1	2.1	***	***	***
10th	0.9	0.9	1.0	1.1	1.2	1.2	1.3	1.4	1.5	1.6	1.7	1.7	1.9	2.1	2.3
15th	0.7	0.8	0.9	1.0	1.0	1.1	1.1	1.2	1.3	1.4	1.4	1.5	1.6	1.8	2.0
20th	0.7	0.7	0.8	0.9	0.9	1.0	1.0	1.1	1.2	1.2	1.3	1.3	1.5	1.6	1.8
25th	0.6	0.7	0.7	0.8	0.8	0.9	0.9	1.0	1.0	1.1	1.2	1.2	1.4	1.5	1.6
30th	0.5	0.6	0.7	0.7	0.8	0.8	0.9	0.9	1.0	1.0	1.1	1.1	1.2	1.4	1.5
40th	0.5	0.5	0.6	0.6	0.7	0.7	0.7	0.8	0.8	0.9	0.9	0.9	1.1	1.2	1.3
50th	0.4	0.4	0.5	0.6	0.6	0.6	0.6	0.7	0.7	0.8	0.8	0.8	0.9	1.0	1.1
60th	0.4	0.4	0.4	0.5	0.5	0.5	0.1	0.6	0.6	0.7	0.7	0.7	0.8	0.9	1.0
70th	0.3	0.3	0.4	0.4	0.4	0.5	0.5	0.5	0.6	0.6	0.6	0.6	0.7	0.8	0.9
75th	0.3	0.3	0.3	0.4	0.4	0.4	0.4	0.5	0.5	0.5	0.6	0.6	0.7	0.7	0.8
80th	0.3	0.3	0.3	0.4	0.4	0.4	0.4	0.4	0.5	0.5	0.5	0.5	0.6	0.7	0.7
85th	0.2	0.3	0.3	0.3	0.3	0.3	0.4	0.4	0.4	0.5	0.5	0.5	0.6	0.6	0.7
90th	0.2	0.2	0.2	0.3	0.3	0.3	0.3	0.4	0.4	0.4	0.4	0.4	0.5	0.5	0.6
95th	0.2	0.2	0.2	0.2	0.2	0.3	0.3	0.3	0.3	0.3	0.3	0.4	0.4	0.4	0.5
97.7th	0.1	0.1	0.2	0.2	0.2	0.2	0.2	0.2	0.3	0.3	0.3	0.3	0.3	0.4	0.4

Figure 4.7 - Predicted levator state parameter across the full range of pairings of maternal capacity-to-fetal head demand are shown for τ2 values of 27 seconds (Top), 550 seconds (Middle), and 11,000 seconds (bottom). The intensity of the (red) shading indicates the extent by which the predicted injury threshold of 2.7 MPa (levator state parameter of 1) is exceeded. In the median table, the predicted tear cutoffs for each of the other two tables are marked by dashed lines.

4.5 Discussion:

The most surprising new finding was the range in maternal τ_2 values that spanned from 20-fold above to 20-fold below the median value, a 400-fold difference. This is remarkable considering that other conventional biometric measurements of human adults, such as height or blood pressure, vary by a maximum of only two-fold across the population.

A second new finding, related to the first, is that the predicted length of the active second stage ranged from a few minutes to tens of hours depending on the τ_2 value. This high end of this wide range in values is clinically important because long labors are linked to birth complications such as low Apgar scores, low umbilical artery pH, higher rates of resuscitation and ICU admission, higher rates of hypoxic-ischemia encephalopathy, cesarean procedures for non-reassuring fetal heart tones, as well as maternal risk for chorioamnionitis and post-partum hemorrhage [23] [24] [25] [26] [27]. These predicted data may be compared to the results of large clinical studies on the length of the second stage. It is a strength that our results compare favorably with clinical results in that 61% of all active second stage simulations were predicted to take less than 1 hour: for example, a study of 21,991 nulliparous subjects, found that 62% of second stages lasted less than 1 hour [24]. However, for the median τ_2 case, this predicted value was 74%. It should be noted that our simulations did not take into account complicating factors, such as poor maternal effort during the pushing phase, or occiput-posterior fetal head orientation, which can increase the length of the second stage by an average of 45 minutes in nulliparous women with epidurals [23].

It is of clinical interest that women who will experience an active second stage of more than 3 hours can be identified, at least theoretically. For example, using the Materna distension device to dilate the birth canal prior to delivery, it is possible to make two measurements: one at five minutes and one at 20 minutes into device use. Then one can use the increase in distension between these two time points to estimate τ_2 values (Figure 4.8). Using this method, it can be seen that individuals with τ_2 values exceeding 1000 seconds, when the length of active second stage begins to rapidly increase (Figure 4.4), correlate to distension increases of less than 10 mm during this time range.

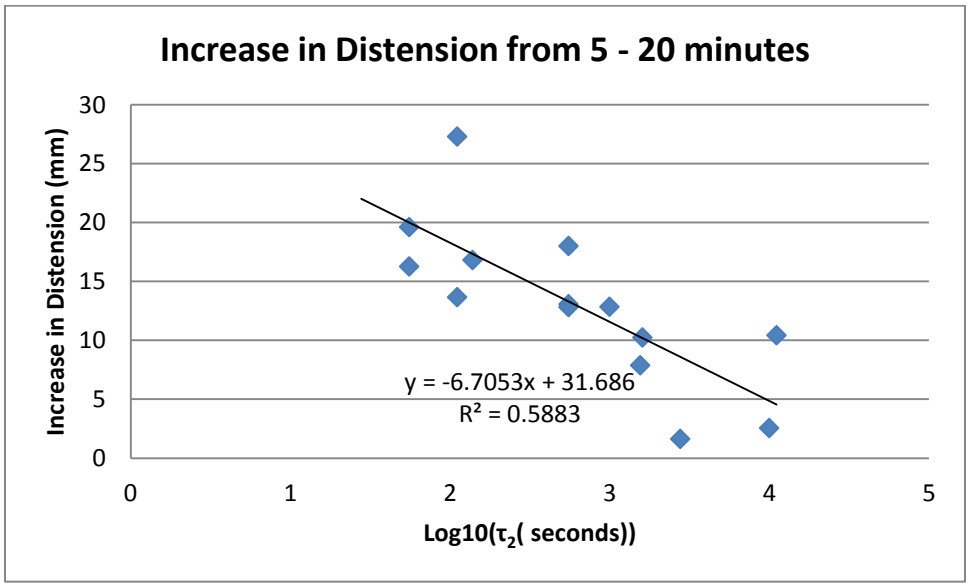

Figure 4.8 - Increases in distension between 5 and 20 minute time points during the Materna distension device use are plotted against τ2 values on a logarithmic scale. Data are correlated with an R2 value of 0.59.

Clinically, if one had knowledge of an impending lengthy active second stage, one could intervene to help alleviate fetal distress. However, when considering Figure 4.5 and Figure 4.7, there are certain scenarios when a woman may experience a very long second stage of labor

while not being at risk for a levator tear, such as a pairing at the 20th percentile for both maternal capacity and fetal head demand, for example. In cases such as these, interventions such as forceps instrumentation, chosen due to the anticipated long length of labor, could result in a levator tear in a mother that was not previously at risk.

Examples of tools that could be developed to guide clinical decisions when the maternal capacity and fetal head demand are made available from ultrasound measurements are shown in Figure 4.5 and Figure 4.7. While the tables in Figure 4.5 do require knowledge of a particular women's τ_2 range, which here was not quantified until the first stage of labor, the narrow variation in PVM tear risk with τ_2 suggests that Figure 4.7, once validated with more clinical information, could actually be employed with reasonable confidence regardless of knowledge of a mother's τ_2 range. Specifically, one can evaluate the effect of this variation in τ_2 values on predicted levator tears from the "confidence intervals" added to the median table in Figure 4.7; so this figure could now be used to evaluate the PVM tear risk in a mother for whom viscoelastic properties are unknown. However, it is noteworthy that effect of τ_2 on predicted PVM tear risk was considerably smaller than the predicted effects on the length of active second stage that we shall discuss next.

A third new finding is that the broad range in maternal τ_2 values found in the first part of this paper did not directly affect the risk of a PVM tear as much as one might have thought. Instead it is the geometric lack of a fit between fetal head and maternal capacity that is the important factor [6], and τ_2 is able to change this risk in only 5% of maternal capacity – to – fetal head demand pairings.

A limitation of our birth simulations is that the birth canal stress values peak depending on when, during the contraction, the birth occurred. For instance, if a mother is near to delivery at the end of a contraction and succeeds in pushing the head out, the stress in the birth canal at birth will be higher than if her tissue can relax until the beginning of the next contraction. The effects of this can be seen in the top table of Figure 4.7, where births are very short and the role of this phenomenon is non-negligible. As the length of active second stage increases, the total amount of time available for tissue relaxation increases, and the effect of adding an additional contraction for relaxation becomes marginal.

A second limitation is that we assumed, for simplicity, that the fetal head had already molded fully; the reason for this was that, to our knowledge, there are no data on the time-dependent molding behavior of the fetal head. In effect, therefore, any viscoelastic behavior of the head during the second stage beyond the 10% molding we had assumed would tend to shorten the delivery times predicted in this paper; likewise, it would also decrease the value of the levator state parameter for the tissue comprising the birth canal, thereby reducing the risk for a tear. Since we did not include fetal head viscoelastic behavior, our current predictions are therefore conservative in terms of the predicted length of second stage and tear risk for fetal heads exceeding maternal capacity [6]. For the cases when the fetal head is smaller than the maternal birth canal then the risk for a tear from delivering the head is, of course, negligible.

A third limitation is that we have considered the PVM as the structure that defines the smallest circumference of the birth canal, namely the urogenital hiatus in this model. While it is possible that the iliococcygeal muscle and the puborectal muscle could tear, our previous studies

suggest that this is unlikely because the stretch in those structures is considerably less than the PVM towards the end of the second stage [5] [4] [6].

In this study, we chose to use the product of stress times strain as the criterion for injury. Some previous models of soft tissue injury have selected purely strain-based criteria [28]. However, we note that literature values for soft tissue failure do show a dependence on both stress and strain [19] [20] [21] [22], hence our choice of failure criterion seems reasonable.

Lastly, the viscoelastic properties of the birth canal were measured on fewer than 30 women. It is possible that an even wider range of maternal tissue behaviors might be found in a larger sample size. So, in that respect, our predictions are conservative for the cases in which the fetal head size exceeds the maternal capacity. Additionally, the Materna data were only recorded during the first stage of labor. We cannot rule out possible hormonal effects continuing to ripen tissue properties in the second stage, when the tissues are placed under stretch. As there is, to our knowledge, no data available on this topic we simply are not able to account for or assess the likelihood of such effects. If further hormonal ripening does occur during the second stage, tissue stresses may reduce even further than those predicted. It is therefore possible that we are overestimating the risk for a tear if such late changes do in fact occur. That brings up the question: how accurate are our predictions of PVM tears?

To address the accuracy of our predicted tear rates, let us compare our models to the approximately 15% PVM tear rates observed clinically. In the present paper we demonstrate that, for a 50^{th} percentile fetal head and the median τ_2 value, mothers larger than the 20^{th} percentile are predicted to deliver without PVM tear. Taking into account the variation in τ_2

values, this cutoff ranges from the 15th to 25th percentile mother which is close to that observed clinically. However, the clinical data do not include women who are unable to deliver without cesarean section, who represent the upper right portion of the tables in Figure 4.7, and who are predicted to experience tears if they were able to deliver vaginally. So, the present predictions appear to be reasonable and not overly conservative.

Acknowledgements

We gratefully acknowledge financial support from the Office for Research on Women's Health SCOR program on Sex Differences in Women's Health (P50 HD 44406). We thank Dr. Mark Juravic of Materna Medical, Inc., for contributing the human birth canal force-displacement data in the absence of any financial support. We thank Drs. Susan Ramin and Francisco J Orejuela at Baylor College of Medicine for conducting the clinical trial that was funded by Materna and resulted in the data we were able to use.

4.6 Bibliography

[1] K.-C. Lien, J. O. L. DeLancey and J. A. Ashton-Miller, "Biomechanical Analyses of the Efficacy of Patterns of Maternal Effort on Second-Stage Progress," *Obstetrics & Gynecology,* vol. 113, no. 4, pp. 873-880, 2009.

[2] M. E. T. Silva, D. A. Oliveira, T. H. Roza, S. Brandao, M. P. L. Parente, T. Mascarenhas and R. M. Natal Jorge, "Study on the influence of the fetus head molding on the biomechanical behavior of the pelvic floor muscles, during vaginal delivery," *Journal of Biomechanics,* vol. 48, no. 9, pp. 1600-1605, 2015.

[3] P. Zan, G. Yan, H. Liu, B. Yang, Y. Zhao and N. Luo, "Biomechanical modeling of the rectum for the desing of a novel artificial anal sphincter," *Biomedical Instrumentation and Technology,* vol. 44, no. 3, pp. 257-60, 2010.

[4] D. Jing, J. A. Ashton-Miller and J. O. L. DeLancey, "A subject-specific anisotropic visco-hyperelastic finite element model of female pelvic floor stress and strain during the second stage of labor," *Journal of Biomechanics,* vol. 45, pp. 455-460, 2012.

[5] K. Lien, B. Mooney, J. O. L. DeLancey and J. Ashton-Miller, "Levator ani muscle stretch induced by simulated vaginal birth," *Obstetrics and Gynecology,* vol. 103, no. 1, pp. 31-40, 2004.

[6] P. V. Tracy, J. O. L. DeLancey and J. A. Ashton-Miller, "A Geometric Capacity - Demand Analysis of Maternal Levator Muscle Stretch Required for Vaginal Delivery," *Journal of Biomechanical Engineering,* pp. e1-e54, 2016.

[7] K. Shek and H. Dietz, "Intrapartum risk factors for levator trauma," *BJOG An International Journal of Obstetrics and Gynecology,* vol. 117, no. 12, pp. 1485-1492, 2010.

[8] J. A. Ashton-Miller and J. O. L. DeLancey, "On the Biomechanics of Vaginal Birth and Common Sequelae," *Annual Review of Biomedical Engineering,* vol. 11, pp. 163-176, 2009.

[9] J. Mant, R. Painter and M. Vessey, "Epidemiology of genital prolapse: observations from the Oxford Planning Association Study," *British Journal of Obstetrics and Gynaecology,* vol. 104, no. 5, pp. 579-85, 1997.

[10] J. O. L. DeLancey, D. M. Morgan, D. E. Fenner, R. Kearney, K. Guire, J. M. Miller, H. Hussain, W. Umek, Y. Hsu and J. A. Aston-Miller, "Comparison of levator ani muscle defects and function in women with and without pelvic organ prolapse," *Obstetrics and Gynecology,* vol. 109, pp. 295-302, 2007.

[11] S. Boyles, A. Weber and L. Meyn, "Procedures for Pelvic Organ Prolapse in the United States, 1979-1997," *American Journal of Obstetrics and Gynecology,* vol. 188, no. 1, pp. 108-15, 2003.

[12] G. H. Visser, "Women are designed to deliver vaginally and not by cesarean section: an obstetritian's view," *Neonatology,* vol. 107, no. 1, pp. 8-13, 2015.

[13] C. Zelop and L. J. Heffner, "The downside of cesarean delivery: short- and long-term complications," *Clinical Obstetrics and Gynecology,* vol. 47, no. 2, pp. 386-93, 2004.

[14] Y. C. Fung, Biomechanics: Mechanical Properties of Living Tissues, New York, NY: Springer-Verlag, 1993.

[15] A. Rempen and M. Kraus, "Pressures on the Fetal Head During Normal Labor," *Journal of Perinatal Medicine,* vol. 19, no. 3, pp. 199-206, 1991.

[16] A. C. J. Allman, E. S. G. Genevler, M. R. Johnson and P. J. Steer, "Head-to-Cervix Force: an Important Physiological Variable in Labour. 1. The Temporal Relation Between Head-to-Cervix Force and Intrauterine Pressure During Labour," *British Journal of Obstetrics and Gynaecology,* vol. 103, pp. 763-768, 1996.

[17] C. S. Buhimschi, I. A. Buhimschi, A. M. Malinow, J. N. Kopelman and C. P. Weiner, "Pushing in Labor: Performance and Not Endurance," *American Journal of Obstetrics and Gynecology,* vol. 186, no. 6, pp. 1339-44, 2002.

[18] C. Spong, V. Berghella, K. Wenstrom, B. Mercer and G. Saade, "Preventing the first cesarean delivery: summary of a joint Eunice Kennedy Shriver National Institute of Child Health and Human Development, Society for Maternal-Fetal Medicine, and American College of Obstetricians and Gynecologists Workshop," *Obstetrics and Gynecology,* vol. 120, no. 5, pp. 1181-93, 2012.

[19] T. J. Bonner, N. Newell, A. Karunaratne, A. D. Pullen, A. A. Amis, A. M. J. Bull and S. D. Masouros, "Strain-rate Sensitivity of the Lateral Collateral Ligament of the Knee," *Journal of the Mechanical Behavior of Biomedical Materials,* vol. 41, pp. 261-70, 2015.

[20] M. Chiba and K. Komatsu, "Mechanical Responses of the Periodontal Ligament in the Transverse Section of the Rat Mandibular Incisor at Various Velocities of Loading In Vitro," *Journal of Biomechanics,* vol. 26, no. 4, pp. 561-70, 1993.

[21] M. M. Panjabi, J. J. Crisco, C. Lydon and J. Dvorak, "The Mechanical Properties of Human Alar and Transverse Ligaments at Slow and Fast Extension Rates," *Clinical Biomechanics,* vol. 13, no. 2, pp. 112-20, 1998.

[22] D. Ulrich, S. L. Edwards, K. Su, J. F. White, J. A. M. Ramshaw, G. Jenkin, J. Deprest, A. Rosamilia, J. A. Werkmeister and C. E. Gargett, "Influence of Reproductive Status on Tissue Composition and Biomechanical Properties of Ovine Vagina," *Public Library of Science,* vol. 9, no. 4, pp. 1 - 8, 2014.

[23] J. Senecal, X. Xiong and W. D. Fraser, "Effect of Fetal Position on Second-Stage Duration and Labor Outcome," *Obstetrics and Gynecology,* vol. 105, no. 4, pp. 763-772, 2005.

[24] A. T. Bleich, J. M. Alexander, D. D. McIntire and K. J. Leveon, "An Analysis of Second-Stage Labor beyond 3 Hours in Nulliparous Women," *American Journal of Perinatology,* vol. 29, no. 9, pp. 717-722, 2012.

[25] K. J. Leveno, D. B. Nelson and D. D. McIntire, "Second-stage labor: how long is too long?," *American Journal of Obstetrics and Gynecology,* vol. 214, no. 4, pp. 484-489, 2016.

[26] S. K. Laughon, V. Berghella, U. M. Reddy, R. Sundaram, Z. Lu and M. K. Hoffman, "Neonatal and Maternal Outcomes With Prolonged Second Stage of Labor," *Obstetrics and Gynecology,* vol. 124, no. 1, pp. 57-67, 2014.

[27] D. Rouse, S. Weiner, S. Bloom, M. Varner, C. Spong, S. Ramin, S. Caritis, A. Peaceman, Y. Sorokin, A. Sciscione, M. Carpenter, B. Mercer, J. Thorp, F. Malone, M. Harper, J. Iams and G. Anderson, "Second-stage Labor Duration in Nulliparous Women: Relationship to Maternal and Perinatal Outcomes," *American Journal of Obstetrics and Gynecology,* vol. 201, no. 4, pp. 357.e1-7, 2009.

[28] W. Li, "Damage Models for Soft Tissues: A Survey," *Journal of Medical and Biological Engineering,* vol. 36, pp. 285-307, 2016.

Chapter 5: Is it Possible for Biomechanical Computer Simulations to Predict the Length of the Second Stage of Labor and/or Pubovisceral Muscle Tears?

Paige V Tracy[1], Francisco J Orejuela[2], Susan M Ramin[2], John O L DeLancey[3], James A Ashton-Miller[4]

[1] Department of Biomedical Engineering, University of Michigan
[2] Department of Obstetrics and Gynecology, Baylor College of Medicine
[3] Department of Obstetrics and Gynecology, University of Michigan
[4] Department of Mechanical Engineering, University of Michigan

5.1 Abstract

The goal of this study was to test the hypothesis that the biomechanical model developed in Chapters 3 and 4 can be used to predict (a) the duration of the second stage of labor and (b) the risk of PVM tear. We conducted a secondary analysis of antenatal ultrasound measurements and post-delivery PVM tear scores from a cohort of 21 nullipara who underwent a Phase I clinical trial of the Materna lower birth canal distension device during the first stage of labor. The results show that the biomechanical model was able to predict up to 55% of the variation in the duration of the second stage of labor for the median age group (29 – 31 years-old), which contained 11 of the 21 women, and 23% of the variation in the second stage for all age groups. The model was also able to predict one of the two major PVM tears, but not the minor PVM tear. The two false negatives were significantly older than the rest of the cohort ($p < 0.001$) and were not at risk anatomically, suggesting that older maternal age may have lowered the

threshold for tissue failure. There were also six false positives, which had significantly longer second stages than the rest of the cohort ($p = 0.02$). This suggests that this biomechanical analysis was able to predict the difficulty of labor, but that this difficulty did not directly correspond to PVM injury.

5.2 Introduction

During labor, the birth canal undergoes remarkable deformation, typically increasing its circumferential length up to three-fold [1] [2] [3]. Due to this distension, the pubovisceral muscle (PVM) tears in approximately 13% of vaginal deliveries [4]. These tears have been linked to the development of pelvic organ prolapse later in life in some individuals [5] [6] [7], a disorder for which 10% of all US women eventually require corrective surgery [5] [8].

Due to a fear of such complications, some women choose to undergo elective cesarean section, which carries its own immediate and delayed risks [9] [10]. Our goal is to help provide the framework necessary to evaluate an individual's risk of experiencing a PVM tear, so that the prevalence of these unnecessary C-sections can be reduced and so that the mothers who are at risk can have the opportunity to evaluate the delivery options.

Toward this goal, we first developed a biomechanical model addressing the fit between the fetal head diameter and the geometric capacity of the lower maternal birth canal (Chapter 2). While it provided the useful insight that 75% of women are not at risk for pubovisceral muscle injury, the model was limited by being simplified to the point that it assumed purely elastic maternal tissue behavior. However, for decades clinicians have intuitively recognized viscoelastic behavior in the tissue comprising the lower birth canal, even if they have not

quantified it. We became aware of the opportunity to quantify it using data from a Phase 1 clinical trial at the Baylor College of Medicine. In this trial we learned that the mechanical distention of the lower birth canal had been accomplished in nullipara during the first stage of their labor using a constant distention force applied by the Materna device (Materna Medical, LLC, San Francisco, CA), while the increase in lower birth canal diameter had been recorded over time. Knowing the relationship between the applied force and the tissue distention provided the unique opportunity to use mathematical modeling to quantify the viscoelastic behavior of the lower birth canal during labor. Then, using that mathematical representation, we could improve the biofidelity of the Chapter 2 model by incorporating viscoelastic behavior (Chapter 3). The result was the set of predictions in Chapter 4 concerning the duration of the second stage of labor and PVM tear risk based on subpubic arch angle, PVM sling length, and fetal head circumference [11]. Moreover, that same clinical trial at Baylor also offered the opportunity to check the sensitivity and specificity of the Chapter 4 predictions of both second stage labor duration and PVM injury risk in a small cohort of about 20 women. This opportunity arose because ultrasound images had been taken of the pre- and post-delivery pelvic floor, and MRI had also been taken of the post-delivery pelvic floor to check for PVM injury. In this Chapter, we use the clinical data kindly provided to us by colleagues at Baylor College of Medicine on second stage of labor duration, subpubic arch angle, fetal head circumference at birth, pre-delivery levator hiatus circumference (as a proxy for the urogenital hiatus), and post-delivery PVM tear status to test the hypothesis that a biomechanical model can be used to predict (a) the duration of the second stage of labor, and (b) the risk of PVM tear. If such a

biomechanical model has veracity it might have considerable utility in the clinical setting when discussing with pregnant women in their third trimester about their delivery options.

5.3 Methods

Maternal capacity was calculated based on the Tracy et al. (2016) geometric model [11]. Stress–strain relationships in the lower birth canal were assumed to be governed by the quasi-linear visco-elastic (QLV) constitutive model (Chapter 3). Birth simulations were run for all subject pairings of fetal head circumference, subpubic arch angle, and PVM sling length. PVM sling length was estimated as 70% of the levator hiatus perimeter, based on optimization such that the shortest simulation required at least two contractions, at which point the longest simulations were exceeding 100 minutes for the duration of the active second stage.

PVM strain, ε_{PVM}, was assumed to be related to general birth canal strain, ε_{BC}, based on the ratio between their initial circumferential lengths, l_{PVM} and l_{BC} respectively [11].

$$\varepsilon_{PVM} = \frac{l_{BC}}{l_{PVM}}(\varepsilon_{BC} + 1) - 1$$

It was also estimated based on image analysis (Chapter 3) that 83% of the total force as applied by the Materna birth canal distension device was resisted as a tensile load in the PVM.

In the modified Tracy et al. (2016) model, simulations of vaginal birth during the second stage were driven by intrauterine pressure as an input, as measured in previous experiments: this included a 2.6 kPa basal intrauterine pressure, an 8.5 kPa rise during contractions, and an additional 10.5 kPa rise during each volitional push [12]. Contractions and pushes were each modeled as the first half of one period of a cosine wave. Specifically, uterine contractions were

assumed to last for 90 seconds, followed by 90 second rest; three volitional 10 second maternal "pushes" to drive the fetal head through the lower birth canal were assumed per uterine contraction, each being followed by 10 seconds of rest [13] [14] [12].

Intrauterine pressure was assumed to be related to circumferential stress in the PVM U-shaped sling, based on the following calculations (Figure 5.1):

$$T = tension\ in\ PVM$$

$$\tilde{T} = \frac{T}{2\pi r} = Tension/length$$

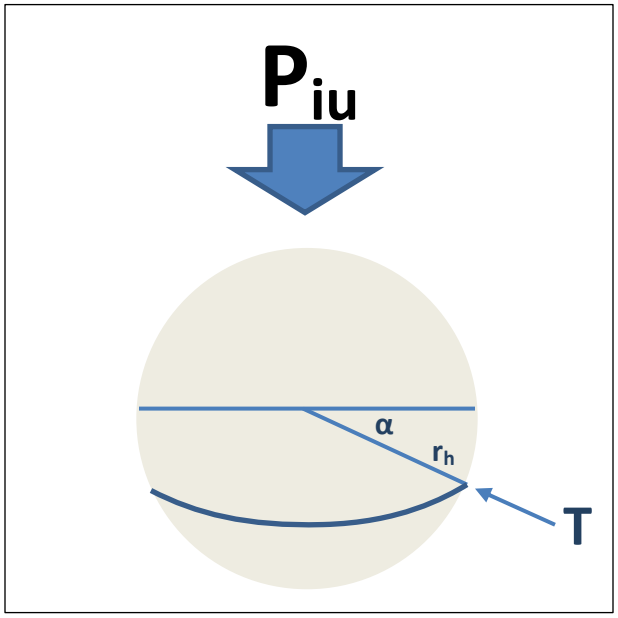

Balancing "Vertical" Forces: $\tilde{T}2\pi r * sin(\alpha) = P_{ab}\pi * {r_h}^2$

$$\tilde{T} = \frac{P_{ab} * {r_h}^2}{2r * sin(\alpha)}$$

Balancing "Horizontal" Forces: $\sigma_{PVM}2 * A_{PVM} = \tilde{T}2r * \cos(\alpha)$

$$\sigma_{PVM} = \frac{\tilde{T} * 2r * \cos(\alpha)}{2A_{PVM}} = \frac{P_{ab}{r_h}^2}{2A_{PVM}\tan(\alpha)}$$

Figure 5.1 - Intrauterine pressure (P_{iu}, blue arrow) creates a force distributed over the area (blue line – normal to uterine pressure) presented by fetal head (grey circle). The tension (T) in the PVM (dark blue band low on head) was related to intrauterine pressure using the radius of the fetal head (light blue lines) and the angle between the midline of the fetal head and the contact point of the PVM on the fetal head (alpha).

Based on image analysis of the non-uniformity of the newborn fetal head, a maximum alpha value of 0.68 radians was assumed.

Based on assumptions in Chapter 4, PVM injury was assumed to occur if the product of PVM stress and strain exceeded the value of 3.2 MPa. This soft tissue injury criterion was based on the literature available for ligament [15] [16] [17], however the exact value of 3.2 MPa was increased from the original value of 2.7 MPa observed for the ultimate failure of pregnant ovine tissue estimated graphically from [18] because the original value resulted in half of the cohort being predicted for injury, and a distinct drop off in predicted tears was observed between 2.7 MPa and 3.2 MPa.

Blinded model predictions of the second stage of labor and PVM injury were sent to a statistician to calculate the sensitivity and specificity of PVM injury predictions.

Duration of second stage analysis was done in Microsoft Excel, using linear regression to calculate R^2 values.

5.4 Results

The duration of second stage was inversely correlated with our capacity-demand based predictions (Figure 5.2). In this cohort, the mean duration of labor was 60 (± 34) minutes. The false positives, or mothers who were predicted to experience a PVM tear, but who did not reveal a tear upon ultrasound examination, had significantly longer second stages than the rest of the cohort ($p = 0.02$) (88 ± 36 vs. 48 ±27 minutes). The geometric capacity – demand ratio, g, predict 55% of the variation in the duration of the second stage for the median maternal age group (Figure 5.2), based on linear regression with a slope of -290 minutes/unit of capacity

demand ratio and a y-intercept of 390 minutes. Therefore, it was possible to predict a significant portion of variation in the duration of the second stage of labor.

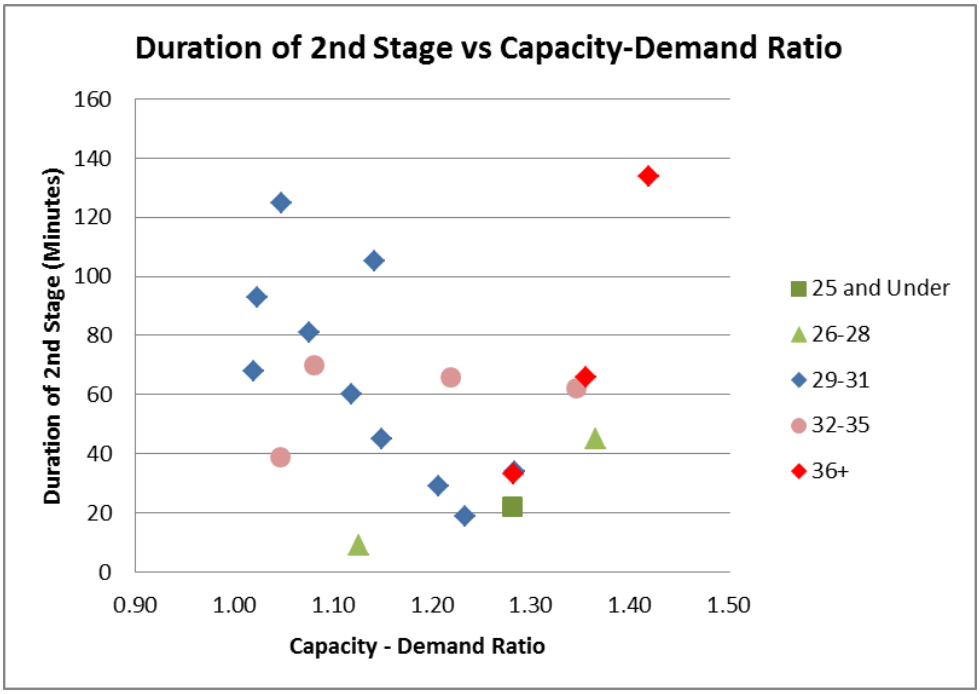

Figure 5.2 – Duration of the second stage plotted against the Capacity-Demand Ratio, g, and partitioned by maternal age group. Note that in this and the next figure these model predictions were based on maternal capacity being derived on the levator hiatus measurements. The R^2 values are 0.22 (y = -140x + 220) and 0.55 (y = -290x + 390) for the entire cohort and the median age group (blue diamonds) respectively.

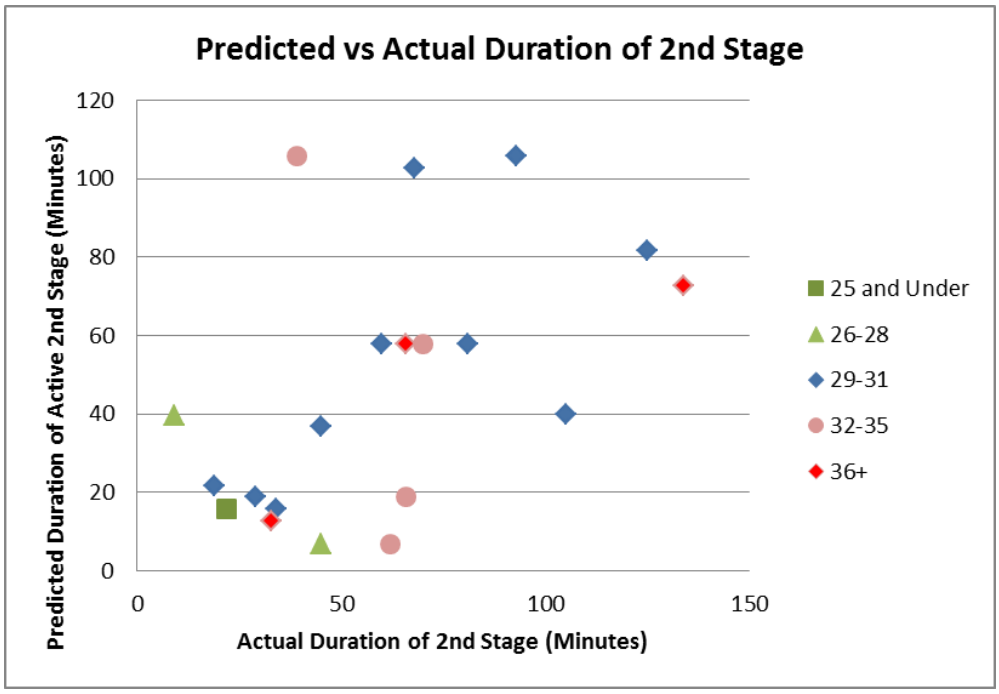

Figure 5.3 – Biomechanical model-predicted duration of active second stage plotted against actual duration of the second stage partitioned by maternal age group. The R^2 values are 0.23 (y = 0.48x + 15) and 0.44 (y = 0.64x + 12) for the entire cohort and for the median age group respectively.

There were three PVM tears observed, two of which were major, and one of which was "very minor" (Table 5.1 and Table 5.2).

		Observed		
		Yes	No	Total
Predicted	Yes	1	6	7
	No	2	12	14
	Total	3	18	21

Table 5.1 –Predicted and observed PVM injuries, including minor tears, based on levator hiatus measurements. Note that in this and the following Tables 5.2-3 the biomechanical model predictions are based on MR measurements of the levator hiatus. .

		Observed		
		Yes	No	Total
Predicted	Yes	1	6	7
	No	1	13	14
	Total	2	19	21

Table 5.2 –Predicted and observed PVM injuries, only including major tears, based on maternal levator hiatus measurements.

	All	Major
Sensitivity	33%	50%
Specificity	67%	68%

Table 5.3 – Sensitivity (true positive) and specificity (true negative) values for the biomechanical model ability to predict all tears (left) and major tears (right) of the PVM using the model based on maternal levator hiatus measurements.

5.5 Discussion

Prediction of Duration of the Second Stage of Labor

A novel finding was that the biomechanical model was able to predict more than half of the variance in the duration of the second stage of labor in the median maternal age group. For the median maternal age range of 29 – 31 years-old, which included 10 out of 21 subjects, the duration of the second stage correlated with our predicted second stage duration with $R^2 = .44$, and with our capacity-demand ratio with $R^2 = .55$ (Figure 5.3 and Figure 5.2). This is a remarkable finding given the biological complexity of the second stage of labor and it confirms that mechanical principles and lower birth canal viscoelastic behavior play an important, and previously unquantified, role in this process. The model was successfully able to predict that an increase in the duration of the second stage was associated with more difficult deliveries associated with greater-than-normal loading of lower birth canal tissues. The question is, why did this increase in loading not result in the PVM tears that would be anticipated for such conditions?

Biomechanical Model Prediction of PVM Tear

The biomechanical model did predict one of the three tears, namely one of the two major tears. For comparison, when considering the ratio of fetal head circumference to levator hiatus circumference, which has recently been reported to correlate to PVM tears [19], all three of these tears would have been missed, as the three subjects had lower values of this ratio (unlikely to experience injury) than over half of the cohort. The two false-negative tear predictions occurred in women who were significantly older than the others ($p<0.001$) and had no geometrical indications for risk (both had larger-than-average levator hiatus, smaller-than-average fetal head circumference, and average or wider subpubic arch angles). The woman with the minor tear had a second stage duration of 33 minutes, the woman with the major tear who was not detected had a second stage of 66 minutes; neither of these lay markedly outside the normal range. Therefore, it appears that these mothers were not subjected to greater loading of the lower birth canal, but rather, their proximal PVM tissue tore at a lower injury threshold than expected. This suggests that these older mothers appear to have had a lower PVM tear threshold than the others in the cohort. This is consistent with studies showing a 48% decrease in the product of stress*strain at failure for aortic tissue between the ages of 20 and 35 years (Table 5.4), which has similar composition to the PVM [20, 21]. The effect of older maternal age on increasing PVM injury risk is well known clinically. For example, odds ratios for PVM injuries of 1.08/year of maternal age have been reported [22, 23, 24, 25, 26, 27]. Our results, while based on a small sample, do suggest that increasing maternal age does decrease the threshold for PVM injury.

	Failure Stress	Failure Strain	Failure Stress*Strain
Decrease from 20 to 35 years	30%	26%	48%
Decrease from 20 to 45 years	49%	43%	71%

Table 5.4 – Decrease in stress, strain, and the product of stress*strain at failure in human aortic tissue between the ages of 20, 35, and 45 years [20].

Most of our predicted tears were false positives. Using our initial injury threshold of 2.7 MPa, there were ten false positives, of which, four were close to a levator state parameter of 1. There was a distinct jump between these four, and the other six (levator state parameters of 1.5 – 2.2). With an adjusted injury threshold of 3.2 MPa, there were six false positives. The true positive lay in the middle of these in levator state parameter value, and they were all grouped fairly closely with values from 1.3 to 1.8 in levator state parameter value (adjusted for 3.2 MPa injury criteria). These false positives had significantly longer second stages than the rest of the cohort ($p = 0.02$; 88 ± 36 vs 48 ±27 minutes). When all 10 false original false positives were included, this difference was still significant at $p = 0.03$ (75 ± 40 vs 46 ± 22 minutes). This suggests that though PVM tears were not observed, deliveries with a low capacity-demand ratio were still difficult, resulting in high loading of the PVM and lower birth canal tissues.

That we are able to predict difficulty of labor (as estimated by the duration of the second stage), but not reliably predict PVM tear outcome, suggests that further research is needed on the injury criteria. That the two false negatives were low in both simulated stress and simulated strain, relative to the cohort, suggests that the distinction is not in the nature of the injury criteria (stress vs strain vs stress*strain), but rather that the actual threshold for injury may vary between individuals. We surmise that older nullipara may have lower PVM tear thresholds and this would be a worthwhile hypothesis to test in the future. If proven true, this should

positively affect how deliveries are handled in older nullipara. Therefore, a next step should be the study of factors affecting variations in injury threshold among mothers.

In designing a study of the effect of maternal age and other factors on the threshold for injury, there are both ethical and sample size limitations to be considered. Though the data provided by the pre-distension device has allowed for the first *in vivo* quantification of the force-distension response of the lower birth canal, it was of course not ethically possible to test the lower birth canal to failure in living women. Therefore it is a limitation that we did not have any data on tissue failure thresholds during the distention conducted in the first stage of labor. Additionally, excising small PVM tissue samples presents concerns about introducing weaknesses to the structure for future deliveries. However, this would not be a concern in women not intending to deliver, such as multiparas who have completed their families, or nulliparas choosing not to have children. However, the ovine data suggest that both non-pregnant parous and virgin tissues exhibit much higher tissue resistance than pregnant tissue. As a result, it appears that any experiments designed to quantify injury criteria in human tissue would need to be limited to pregnant women not planning to deliver vaginally, such as those undergoing elective cesarean sections.

One limitation of the model predictions is that they rely on the Chapter 2 use of the levator hiatus perimeter as the basis for PVM sling length measurements to estimate maternal capacity. This was because the literature contains many reliable data sets on levator hiatus circumference and diameters and it was convenient to use those data. However, a key Chapter 2 finding was that it is the PVM and perineal body that form the main geometric constraint on

maternal capacity, not the levator hiatus. This suggests that the better measurement for the predictive biomechanical model is the urogenital hiatus perimeter, rather than the levator hiatus, because this lies in the plane of the PVM and defines the outlet of the lower birth canal. However, the urogenital hiatus circumference or diameters have not traditionally been measured in a clinical study. So, there is a need to develop a standardized reproducible measurement protocol to quantify the urogenital hiatus on MR images, as well as particularly on ultrasound images. The latter is important because of its widespread availability in maternal fetal medicine and proven safety record with mother and baby.

Other limitations of these biomechanical model predictions include the fact that the birth canal stress values peak depending on when, during the contraction, the birth occurred. For instance, if a mother is near to delivery at the end of a contraction and succeeds in pushing the head out, the stress in the birth canal at birth will be higher than if her tissue is allowed to relax until the beginning of the next contraction. As the length of active second stage increases, the total amount of time available for tissue relaxation increases, and the effect of adding an additional contraction for relaxation becomes marginal. Therefore, for shorter labors, maximum simulated stresses should be adjusted downwards if crowning occurs shortly before the end of a contraction.

A further limitation is that we assumed, for simplicity, that the fetal head had already molded fully. Since we did not include fetal head viscoelastic behavior, our current predictions are conservative in terms of the predicted length of second stage and tear risk for fetal heads

exceeding maternal capacity, as additional dynamic molding would decrease both of these variables [11]. Therefore, we believe these duration and injury predictions are conservative.

5.6 Conclusions

- A) Results support the hypothesis that a viscoelastic biomechanical model can be used to predict the duration of the second stage of labor; this biomechanical model was able to predict a significant and preponderant percentage, 55%, of the variance in the duration of the second stage of labor in healthy median aged (29 – 31 years-old) nullipara.
- B) The results do not yet support the hypothesis that PVM injuries can be reliably predicted, as current predictive methods were only able to predict one of three PVM tears in this cohort. We expect the success rate would be higher had we had time to develop and use repeatable measures of urogenital hiatus size, rather than levator hiatus size.
- C) The results suggest older maternal age in these nullipara decreased the threshold for PVM injury. This effect needs to be explored in more depth in the future. If true, this could be incorporated in future models to improve prediction accuracy.
- D) False positives (predicted injury without actual injury) still had difficult deliveries (long second stages), suggesting that their lack of injuries may be due increased tissue strength, or an increased injury threshold.
- E) This was too small a clinical cohort to reliably test biomechanical model injury prediction accuracy because only 10% of these women were injured. One would ideally need an order of magnitude larger cohort for the clinical trial.

5.7 References

[1] K.-C. Lien, J. O. L. DeLancey and J. A. Ashton-Miller, "Biomechanical Analyses of the Efficacy of Patterns of Maternal Effort on Second-Stage Progress," *Obstetrics & Gynecology,* vol. 113, no. 4, pp. 873-880, 2009.

[2] M. E. T. Silva, D. A. Oliveira, T. H. Roza, S. Brandao, M. P. L. Parente, T. Mascarenhas and R. M. Natal Jorge, "Study on the influence of the fetus head molding on the biomechanical behavior of the pelvic floor muscles, during vaginal delivery," *Journal of Biomechanics,* vol. 48, no. 9, pp. 1600-1605, 2015.

[3] P. Zan, G. Yan, H. Liu, B. Yang, Y. Zhao and N. Luo, "Biomechanical modeling of the rectum for the desing of a novel artificial anal sphincter," *Biomedical Instrumentation and Technology,* vol. 44, no. 3, pp. 257-60, 2010.

[4] K. Shek and H. Dietz, "Intrapartum risk factors for levator trauma," *BJOG An International Journal of Obstetrics and Gynecology,* vol. 117, no. 12, pp. 1485-1492, 2010.

[5] J. A. Ashton-Miller and J. O. L. DeLancey, "On the Biomechanics of Vaginal Birth and Common Sequelae," *Annual Review of Biomedical Engineering,* vol. 11, pp. 163-176, 2009.

[6] J. Mant, R. Painter and M. Vessey, "Epidemiology of genital prolapse: observations from the Oxford Planning Association Study," *British Journal of Obstetrics and Gynaecology,* vol. 104, no. 5, pp. 579-85, 1997.

[7] J. O. L. DeLancey, D. M. Morgan, D. E. Fenner, R. Kearney, K. Guire, J. M. Miller, H. Hussain, W. Umek, Y. Hsu and J. A. Aston-Miller, "Comparison of levator ani muscle defects and function in women with and without pelvic organ prolapse," *Obstetrics and Gynecology,* vol. 109, pp. 295-302, 2007.

[8] S. Boyles, A. Weber and L. Meyn, "Procedures for Pelvic Organ Prolapse in the United States, 1979-1997," *American Journal of Obstetrics and Gynecology,* vol. 188, no. 1, pp. 108-15, 2003.

[9] G. H. Visser, "Women are designed to deliver vaginally and not by cesarean section: an obstetritian's view," *Neonatology,* vol. 107, no. 1, pp. 8-13, 2015.

[10] C. Zelop and L. J. Heffner, "The downside of cesarean delivery: short- and long-term complications," *Clinical Obstetrics and Gynecology,* vol. 47, no. 2, pp. 386-93, 2004.

[11] P. V. Tracy, J. O. L. DeLancey and J. A. Ashton-Miller, "A Geometric Capacity - Demand Analysis of Maternal Levator Muscle Stretch Required for Vaginal Delivery," *Journal of Biomechanical Engineering,* pp. e1-e54, 2016.

[12] A. Rempen and M. Kraus, "Pressures on the Fetal Head During Normal Labor," *Journal of Perinatal Medicine,* vol. 19, no. 3, pp. 199-206, 1991.

[13] A. C. J. Allman, E. S. G. Genevler, M. R. Johnson and P. J. Steer, "Head-to-Cervix Force: an Important Physiological Variable in Labour. 1. The Temporal Relation Between Head-to-

Cervix Force and Intrauterine Pressure During Labour," *British Journal of Obstetrics and Gynaecology,* vol. 103, pp. 763-768, 1996.

[14] C. S. Buhimschi, I. A. Buhimschi, A. M. Malinow, J. N. Kopelman and C. P. Weiner, "Pushing in Labor: Performance and Not Endurance," *American Journal of Obstetrics and Gynecology,* vol. 186, no. 6, pp. 1339-44, 2002.

[15] T. J. Bonner, N. Newell, A. Karunaratne, A. D. Pullen, A. A. Amis, A. M. J. Bull and S. D. Masouros, "Strain-rate Sensitivity of the Lateral Collateral Ligament of the Knee," *Journal of the Mechanical Behavior of Biomedical Materials,* vol. 41, pp. 261-70, 2015.

[16] M. Chiba and K. Komatsu, "Mechanical Responses of the Periodontal Ligament in the Transverse Section of the Rat Mandibular Incisor at Various Velocities of Loading In Vitro," *Journal of Biomechanics,* vol. 26, no. 4, pp. 561-70, 1993.

[17] M. M. Panjabi, J. J. Crisco, C. Lydon and J. Dvorak, "The Mechanical Properties of Human Alar and Transverse Ligaments at Slow and Fast Extension Rates," *Clinical Biomechanics,* vol. 13, no. 2, pp. 112-20, 1998.

[18] D. Ulrich, S. L. Edwards, K. Su, J. F. White, J. A. M. Ramshaw, G. Jenkin, J. Deprest, A. Rosamilia, J. A. Werkmeister and C. E. Gargett, "Influence of Reproductive Status on Tissue Composition and Biomechanical Properties of Ovine Vagina," *Public Library of Science,* vol. 9, no. 4, pp. 1 - 8, 2014.

[19] G. Rostaminia, J. D. Peck, K. Van Deft, R. Thakar, A. Sultan and S. A. Shobeiri, "New Measures for Predicting Birth-Related Pelvic Floor Trauma," *Female Pelvic Med Reconstructive Surgery,* vol. 22, no. 5, pp. 292-6, 2016.

[20] M. Groenink, S. Langerak, E. Vanbavel, E. van der Wall, B. Mulder and A. S. J. van der Wal, "The influence of aging and aortic stiffness on permanent dilatoin and breaking stress of the thoracic descending aorta," *Cardiovascular Research,* vol. 43, no. 2, pp. 471-80, 1999.

[21] R. Okamoto, J. Wagenseil, W. DeLong, S. Peterson, N. Kouchoukos and T. 3. Sundt, "Mechanical properties of dilated human ascending aorta," *Annals of Biomedical Engineering,* vol. 30, no. 5, pp. 624-35, 2002.

[22] H. Dietz and V. Lanzarone, "Levator trauma after vaginal delivery," *Obstetrics and Gynecology,* vol. 106, no. 4, pp. 707-12, 2005.

[23] R. Kearney, J. Miller, J. Ashton-Miller and J. O. L. DeLancey, "Obstetric factors associated with levator ani muscle injury after vaginal birth," *Obstetrics and Gynecology,* vol. 107, no. 1, pp. 144-9, 2006.

[24] H. Dietz and J. Simpson, "Does delayed childbirth increase the risk of levator injury in labour?," *The Australian & New Zealand Journal of Obstetrics & Gynaecology,* vol. 47, no. 6, pp. 491-5, 2007.

[25] H. Dietz and A. Kirby, "Modelling the Likelihood of Levator Avulsion in a Urogynaecological Population," *The Australian & New Zealand Journal of Obstetrics & Gynaecology,* vol. 50, no. 3, pp. 268-72, 2010.

[26] L. Low, R. Zielinski, Y. Tao, A. Galecki, C. Brandon and J. Miller, "Predicting Birth-Related Levator Ani Tear Severity in Primiparous Women: Evaluating Maternal Recovery from

Labor and Delivery (EMRLD)," *Open Journal of Obstetrics and Gynecology,* vol. 4, no. 6, pp. 266-78, 2014.

[27] P. Rahmanou, J. Caudwell-Hall, I. Kamisan Atan and H. Dietz, "The association between maternal age at first delivery and risk of obstetric trauma," *American Journal of Obstetrics and Gynecology,* vol. 215, no. 4, pp. e1-7, 2016.

Chapter 6: Forceps, Vacuum, and Levator Ani Injury: A Biomechanical Analysis

Paige V Tracy[1], Shreya Wadhwani[1], Jourdan E Triebwasser[2], John O L DeLancey[2], James A Ashton-Miller[3]
[1] Department of Biomedical Engineering, University of Michigan
[2] Department of Obstetrics and Gynecology, University of Michigan
[3] Department of Mechanical Engineering, University of Michigan

6.1 Abstract

Objective: Pubovisceral muscle (PVM) tears increase the life-long risk of pelvic organ prolapse. It remains unknown why PVM tear rates are four-times higher in forceps-assisted compared to spontaneous vaginal deliveries, or vacuum assisted deliveries. We hypothesized that, among several possible factors, it is the traction force applied to forceps that results in increased PVM tears.

Study design: Using simulations based on constitutive equations previously fit to the term pregnant human birth canal, we simulated birth and predicted PVM injury risk by varying, traction force applied by forceps or vacuum, space occupied by forceps, timing of forceps application, and length of episiotomy in the context of variable maternal capacity, fetal head size with molding. Force estimates used in the simulation were based on traction force measurements previously reported for vacuum and forceps instrumentation.

Results: Our model predicts a 19% increase in PVM tears for forceps assisted deliveries, when compared to spontaneous and vacuum-assisted deliveries; this was due to an increase in applied traction force. Previous analysis suggested that the space occupying nature of forceps is responsible for no more than a 2% increase in PVM tears. Additionally, the risk of tear is reduced by delaying forceps introduction and by applying partial traction force between contractions. Episiotomy, to a length of at least 1.5 cm reduced the risk of PVM tear. A 50% reduction in maternal effort due to epidural usage resulted in an average increase of 12 minutes in the duration of the active second stage of labor, as well as a 40% reduction in PVM tear rates.

Conclusion: The increase in traction force that can be applied using forceps has a more prominent effect of PVM tears than their space occupying nature. Episiotomy may mitigate that risk. A reduction in maternal pushing effort estimated for epidural usage increases the duration of the second stage of labor, but also decreases predicted PVM tear rates due to increased time available for tissue relaxation.

6.2 Introduction

During labor, the birth canal undergoes remarkable distension [1, 2, 3]. A tissue of interest during this process is the pubovisceral muscle (PVM), a subset of the levator ani muscles that is vulnerable to injury during birth. This muscle is attached high on the anterior pelvis, forming and U-shaped sling, partially wrapping itself around the bony pelvis. This partial wrapping of the PVM around the bony pelvis reduces its capacity to accommodate a fetal head [4]. As a result, the PVM tears in approximately 13% of vaginal deliveries, leading to the later

development of pelvic organ prolapse and incontinence, disorders for which 10% of all US women eventually require corrective surgery [5, 6, 7, 8, 9].

PVM tears occur in over 50% of forceps-assisted deliveries [10, 11, 12, 13, 14, 15]. However, a similar trend has not been observed for vacuum assisted deliveries [16, 17, 5]. There are two competing hypotheses that might explain why injury rates with forceps-assisted deliveries are so high: that tears are due to space around the fetal head that forceps occupy that vacuum does not, or that tears are due to the increased traction force applied to forceps above that of a vacuum device. A previous study demonstrated that the space occupied by Simpson forceps was found to change the PVM tear injuries by no more than 2% in the population (Figure 6.2) [18].

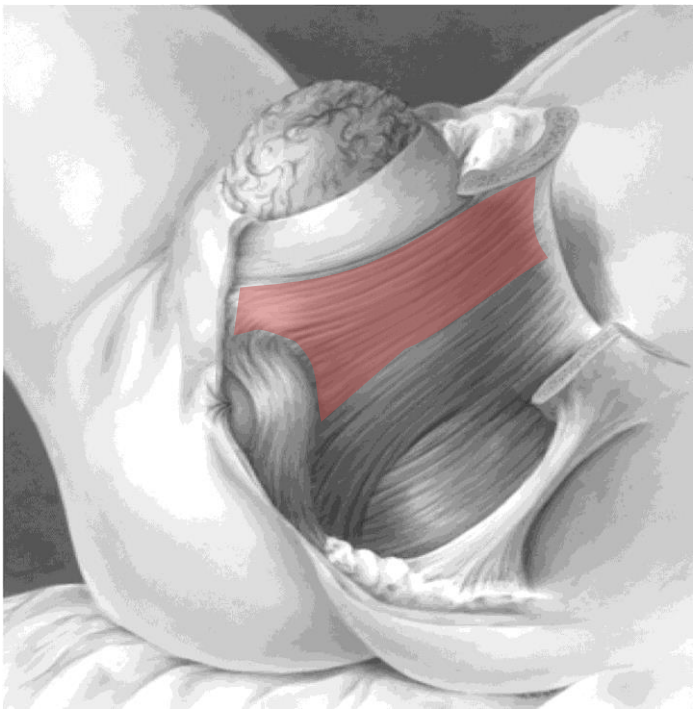

Figure 6.1 - Fetal head crowning during the second stage of labor. The pubovisceral muscle (red) is attached to the anterior pelvis and must wrap around the fetal head. The current perimeter at this level is referred to as the current maternal capacity. Note that the ischium has been removed to show the muscles.

We hypothesize that it is the traction force applied via forceps that increases PVM tears compared to vacuum-assisted deliveries. We are able to test this hypothesis by simulating birth using a viscoelastic model of the term pregnant human birth canal (Chapter 3). Using this model, we ran simulations for a full spectrum of maternal capacity – to –fetal head demand pairings. This allows us to consider the effects of each of these parameters, so that a personalized evaluation of a specific patient's risk for a PVM tear may be evaluated. Varying the traction force applied to the head within values reported in the literature for vacuum and forceps use allowed us to examine the role of this applied traction force on predicted PVM tear risk and duration of the active second stage of labor. We additionally sought to assess the role of episiotomy in reducing PVM tear risk.

6.3 Materials and Methods

Birth Simulations

Our simulations were based upon the quantification of the relationship between the amount of force experienced by the tissue normalized over the tissue cross sectional area (stress) and the current length of the tissue relative to its resting length (strain). This stress–strain relationship was derived from the clinical trial data for the Materna device, which was designed for the purpose of distending the lower birth canal prior to the second stage of labor. Full details on how we quantified this relationship using distension and force data acquired with the device have already been covered in this thesis (Chapter 3). All simulations were run in MATLAB

R2015a with a time step size of 0.1 seconds. This theoretical study was deemed “exempt” by the institutional review board.

Maternal capacity and the U-shaped PVM sling length were calculated from the 2.3rd to the 97.7th percentile female based on the Tracy et al. (2016) geometric model that considered the maternal birth canal capacity to be determined by the subpubic arch angle, PVM origin location, and PVM length. Fetal demand was represented by the 2.3rd to the 97.7th percentile fetal head with average molding [4]. Birth simulations were run for each maternal capacity – to – fetal head demand pairing.

Simulations of vaginal birth during the second stage were driven by intrauterine pressure as an input, as measured in previous experiments: this included a 2.6 kPa basal intrauterine pressure, an 8.5 kPa rise during contractions, and an additional 10.5 kPa rise during each volitional push [19]. Contractions and pushes were each modeled as the first half of one period of a cosine wave. Specifically, contractions were assumed to last for 90 seconds, followed by 90 second rest; three 10 second pushes were assumed per contraction with each followed by 10 seconds of rest [19, 20, 21]. Forceps traction forces were added to the product of fetal head cross sectional area and intrauterine pressure to calculate the net expulsion force on the fetal head.

Simulations of births were run for maternal birth capacities and fetal head circumferences both varying from the 2.3rd to the 97.7th percentile for four values of forceps traction force: 75.6 N – representing average vacuum extraction-induced force, 121 N – representing average forceps extractions force, 226 N – a previous recommendation for maximum forceps traction, and 240 N – average senior clinician forceps traction [22, 23, 24]. Each of these forceps traction forces

was applied for different degrees of fetal head descent through the birth canal. These simulations were performed starting at four levels: the diameter of the birth canal at the level of the PVM (Figure 6.1) being 6 cm, 7 cm, 8 cm, and 9 cm. The nature of our modeling required the use of PVM diameter, rather than fetal head descent, or the amount of fetal head visible during contractions that are more familiar clinical criteria. Because the PVM diameter is above the introitus, these diameters are larger than the diameter of the visible scalp area, as can be seen in Figure 6.1. Additionally, for the application at 6 cm PVM diameter, 240 N traction force case, simulations were run for while maintaining partial traction force between contractions of 0%, 10%, and 50% partial traction force applied between contractions.

Episiotomy was simulated following the 10^{th} contraction. Episiotomy length, as defined by radial length of the incision into the surrounding tissue, was simulated as a 0.5 cm, 1 cm, 1.5 cm, and 2 cm length.

Deliveries with epidural use was simulated as a 50% reduction in intrauterine pressure produced by maternal effort. Intrauterine pressure due to uterine contractions, as well as basal abdominal pressure remained unchanged.

Following Tracy et al. (2016) model-predicted Duration of Active Second Stage tables were shaded, using a threshold of 3 hours as the minimum for shading. Three hours was chosen as arrest of descent could reasonably be diagnosed at that time [25].

Likewise, we assessed the likelihood that a PVM tear occurred using the 'levator state parameter', where a value greater than 1 indicates that the threshold for injury has been exceeded. This parameter is based on the product of stress multiplied by strain as the best

criterion for injury. This criterion is based on data concerning vaginal tissue and ligamentous injury, while the exact value of 2.7 MPa, as the threshold for injury, was based on the measured conditions for the ultimate failure of pregnant ovine tissue estimated graphically [26, 27, 28, 29, 30, 31, 32]. Red shading in the figures indicates the extent by which this injury threshold has been exceeded. This analysis was performed using Microsoft Excel.

6.4 Results

6.4.1 Forceps

The space occupied by forceps, when assuming the forceps do not compress the fetal head, results in a 1.7% increase in predicted PVM tear rates (Figure 6.2) [18].

In simulations, higher forceps traction force produces a higher likelihood of PVM tear, as indicated by higher levator state parameter values in Figure 6.3 (lower left). Here, and throughout this work, the levator state parameter indicates the extent by which the threshold for injury is predicted to be exceeded, with values greater than 1 corresponding to predicted tear occurrence. For example, when no instrumentation is used in a birth involving a 50^{th} percentile fetal head (Figure 6.4, upper panel, center column), a 50^{th} percentile mother, with a levator state parameter of 0.7 (below 1) is unlikely to experience a PVM tear, while a 5^{th} percentile mother, with a levator state parameter of 1.6 (above 1) is particularly likely to experience a PVM tear. For the case of the 20^{th} percentile mother, where the levator state parameter is equal to 1, the mother is on the border-line for injury occurrence.

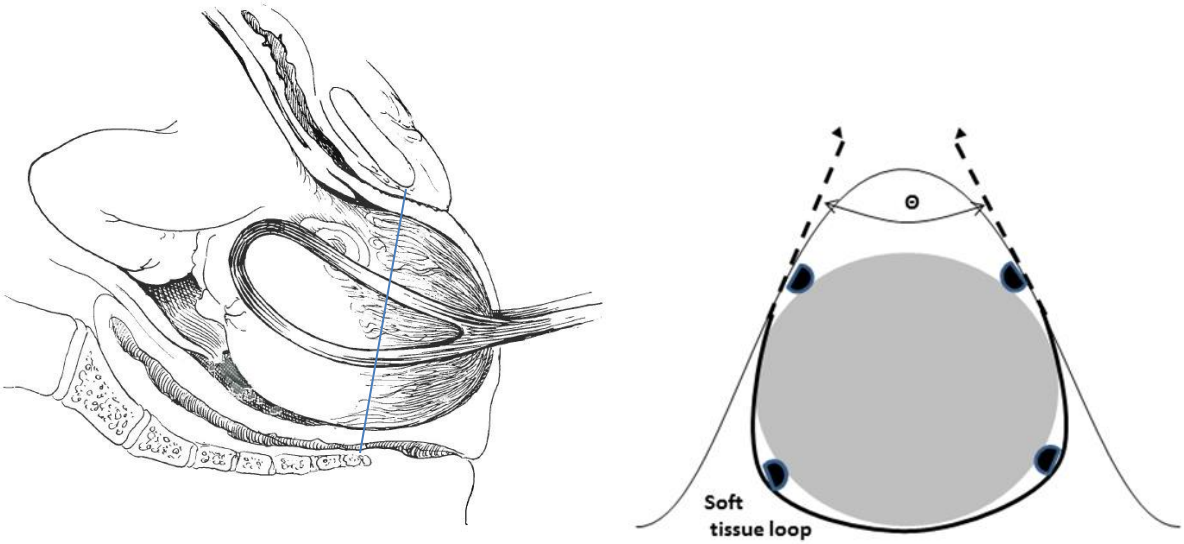

Original (No Forceps)

		DEMAND (Fetal Head Circumference, in Percentile)								
		10	20	30	40	50	60	70	80	90
CAPACITY (Maternal Circumference, in Percentile)	10	0.87	0.86	0.85	0.84	0.83	0.82	0.81	0.80	0.79
	20	1.00	0.98	0.97	0.96	0.95	0.94	0.93	0.92	0.90
	30	1.09	1.07	1.06	1.04	1.03	1.02	1.01	1.00	0.99
	40	1.16	1.14	1.13	1.11	1.10	1.09	1.08	1.07	1.05
	50	1.23	1.21	1.19	1.18	1.17	1.15	1.14	1.13	1.11
	60	1.29	1.27	1.25	1.24	1.23	1.22	1.20	1.19	1.17
	70	1.36	1.33	1.32	1.30	1.29	1.28	1.27	1.25	1.23
	80	1.44	1.41	1.39	1.38	1.37	1.35	1.34	1.32	1.30
	90	1.54	1.51	1.49	1.48	1.46	1.45	1.43	1.42	1.39

Forceps (no indentation of the fetal head)

		DEMAND (Fetal Head Circumference, in Percentile)								
		10	20	30	40	50	60	70	80	90
CAPACITY (Maternal Circumference, in Percentile)	10	0.86	0.84	0.83	0.82	0.82	0.81	0.80	0.79	0.78
	20	0.98	0.97	0.95	0.94	0.93	0.93	0.92	0.90	0.89
	30	1.07	1.05	1.04	1.03	1.02	1.01	1.00	**0.99**	0.97
	40	1.14	1.12	1.11	1.10	1.09	1.08	1.06	1.05	1.03
	50	1.21	1.19	1.17	1.16	1.15	1.14	1.12	1.11	1.09
	60	1.27	1.25	1.23	1.22	1.21	1.20	1.18	1.17	1.15
	70	1.34	1.31	1.30	1.28	1.27	1.26	1.25	1.23	1.21
	80	1.41	1.39	1.37	1.36	1.34	1.33	1.32	1.30	1.28
	90	1.51	1.49	1.47	1.45	1.44	1.43	1.41	1.39	1.37

Figure 6.2 - Inserted forceps shown in lateral (upper left) and in cross section indicated by a line in the left figure (upper right, forceps blades represented as black hemi-spheres) views. Geometric Maternal Capacity – to – Fetal Head Demand ratio is shown for no forceps (middle) and forceps with rigid fetal head case (lower). Because maternal capacity must exceed fetal demand for a safe delivery to be predicted, a value of this ratio below 1 indicates a predicted PVM tear. The intensity of the (red) shading indicates the extent by which the predicted injury threshold is exceeded. These figures have been presented previously [18]. The upper left figure is reproduced with permission from Elsevier [33].

The effect of varying the traction force introduced through use of forceps or vacuum was evaluated by comparing the levator state parameter for the same individual over different traction forces. For example, a 40^{th} percentile mother carrying a 50^{th} percentile fetus had a levator state parameter of 0.8 for spontaneous vaginal birth, predicting a low likelihood of PVM tear occurrence (Figure 6.4, upper panel). When the force used during vacuum delivery is applied in a simulation, this levator state parameter increases to 1.0, placing the mother on the border-line for tear occurrence (Figure 6.4, middle panel). If forceps are simulated with the average traction force measured for a senior obstetrician, this levator state parameter increases to 1.4, indicating a high probability of tear occurrence (Figure 6.4, lower panel). This example illustrates how a mother, who would not naturally be at risk for a PVM tear based on maternal and fetal geometry alone, may experience a PVM tear due to the increase in traction force introduced through forceps instrumentation. This effect can also be visualized by comparing the proportion of red shading in each of the panels in Figure 6.4.

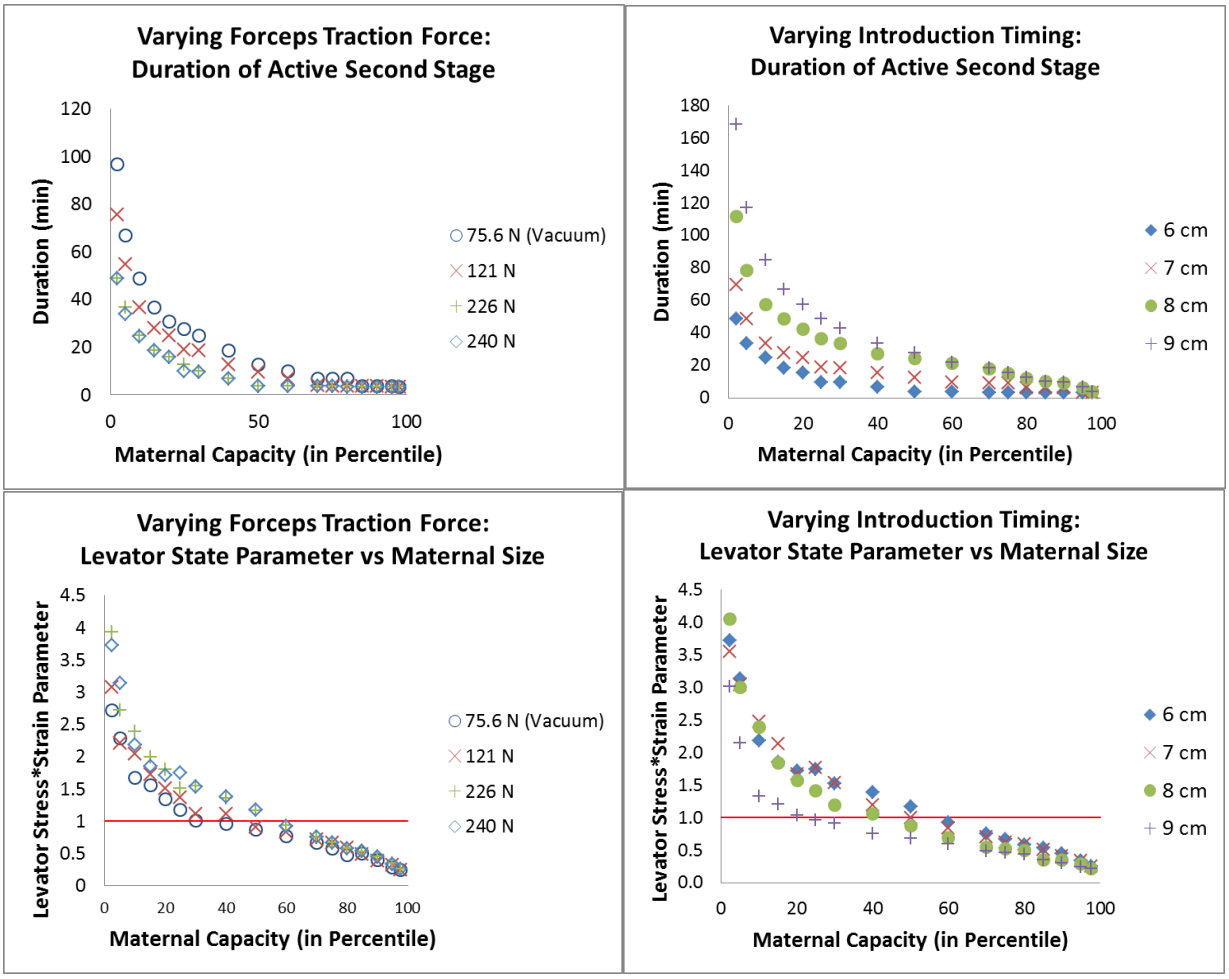

Figure 6.3 - Duration of active second stage (upper) and levator state parameter values (lower) for the range of maternal capacity (in percentile). The left column represents the effect of varying forceps traction force over four different forces, with 75.6 N and 121 N representing vacuum and forceps traction measurements from a single study, 226 N representing a previously proposed forceps limit, and 240 N representing the average forceps traction force measured for senior clinicians [22, 23, 24]. The right column represents the effect of varying forceps application timing over four different birth canal diameters at the level of the PVM. The threshold for injury is a levator state parameter value of 1. A levator state parameter below 1 involves little to no risk whereas a levator state parameter above 1 involves possibility of risk.

Original (no forceps):

CAPACITY (Maternal Circumference, in Percentile)	DEMAND (Fetal Head Circumference, in Percentile)														
	2.3rd	5th	10th	20th	25th	30th	40th	50th	60th	70th	75th	80th	90th	95th	97.7th
2.3rd	1.2	1.4	1.6	1.6	1.9	1.9	2.1	2.2	2.4	2.5	2.5	2.8	3.1	3.2	3.7
5th	1.1	1.1	1.3	1.3	1.4	1.5	1.5	1.6	1.9	1.8	2.0	1.9	2.3	2.6	2.7
10th	0.7	0.8	1.0	1.1	1.0	1.2	1.1	1.3	1.4	1.6	1.6	1.7	1.7	2.1	2.2
15th	0.7	0.7	0.8	1.0	0.9	1.0	1.1	1.2	1.3	1.4	1.3	1.3	1.6	1.8	2.0
20th	0.7	0.7	0.8	0.9	0.8	0.9	1.0	1.0	1.0	1.2	1.2	1.2	1.5	1.5	1.7
25th	0.5	0.6	0.7	0.8	0.7	0.8	0.8	1.0	1.0	1.1	1.2	1.1	1.3	1.3	1.5
30th	0.5	0.5	0.6	0.7	0.7	0.8	0.8	0.9	0.9	0.9	1.0	1.1	1.1	1.3	1.4
40th	0.4	0.5	0.5	0.6	0.6	0.7	0.7	0.8	0.8	0.8	0.9	0.9	1.0	1.1	1.2
50th	0.4	0.4	0.5	0.5	0.6	0.6	0.6	0.7	0.6	0.8	0.8	0.8	0.8	1.0	1.1
60th	0.3	0.4	0.4	0.5	0.5	0.5	0.5	0.6	0.6	0.7	0.7	0.7	0.8	0.8	0.9
70th	0.3	0.3	0.4	0.4	0.4	0.4	0.4	0.5	0.5	0.6	0.5	0.6	0.7	0.7	0.7
75th	0.3	0.3	0.3	0.4	0.4	0.4	0.4	0.5	0.5	0.5	0.5	0.6	0.6	0.7	0.8
80th	0.3	0.2	0.3	0.3	0.3	0.3	0.4	0.4	0.4	0.5	0.5	0.5	0.5	0.6	0.6
85th	0.2	0.2	0.3	0.3	0.3	0.3	0.4	0.3	0.4	0.4	0.5	0.5	0.5	0.6	0.6
90th	0.2	0.2	0.2	0.3	0.3	0.3	0.3	0.3	0.3	0.4	0.4	0.4	0.4	0.5	0.6
95th	0.1	0.1	0.2	0.2	0.2	0.2	0.3	0.2	0.3	0.3	0.3	0.4	0.4	0.4	0.5
97.7th	0.1	0.1	0.2	0.2	0.2	0.2	0.2	0.2	0.2	0.3	0.3	0.3	0.3	0.3	0.4

Vacuum Application at 6 cm PVM Diameter, with a 75.6 N Traction Force:

CAPACITY (Maternal Circumference, in Percentile)	DEMAND (Fetal Head Circumference, in Percentile)														
	2.3rd	5th	10th	20th	25th	30th	40th	50th	60th	70th	75th	80th	90th	95th	97.7th
2.3rd	1.8	1.8	2.1	2.1	2.2	2.2	2.7	2.7	3.1	3.2	3.2	3.5	3.9	3.8	4.6
5th	1.4	1.5	1.4	1.7	1.9	2.0	2.1	2.3	2.4	2.4	2.4	2.7	2.8	3.3	3.5
10th	1.1	1.2	1.3	1.5	1.4	1.6	1.6	1.7	1.9	2.0	1.9	2.2	2.3	2.6	2.9
15th	1.0	1.0	1.2	1.3	1.2	1.3	1.3	1.6	1.6	1.6	1.8	1.6	2.0	2.2	2.4
20th	0.8	0.9	1.0	1.0	1.2	1.2	1.2	1.3	1.4	1.4	1.4	1.6	1.8	2.0	2.2
25th	0.7	0.8	0.9	0.9	0.9	1.0	1.2	1.2	1.3	1.3	1.5	1.5	1.7	1.8	2.0
30th	0.7	0.8	0.7	0.9	1.0	0.9	1.1	1.0	1.2	1.3	1.2	1.4	1.5	1.5	1.6
40th	0.5	0.6	0.7	0.8	0.8	0.9	0.8	1.0	1.0	1.0	1.1	1.2	1.2	1.4	1.5
50th	0.5	0.6	0.6	0.6	0.7	0.7	0.8	0.9	0.8	0.9	1.0	1.0	1.1	1.2	1.3
60th	0.4	0.5	0.5	0.6	0.6	0.6	0.7	0.8	0.7	0.8	0.9	0.9	0.9	1.1	1.0
70th	0.4	0.4	0.5	0.5	0.5	0.6	0.6	0.7	0.6	0.7	0.7	0.8	0.7	0.9	1.0
75th	0.3	0.4	0.4	0.5	0.4	0.4	0.5	0.6	0.6	0.7	0.7	0.6	0.8	0.9	0.9
80th	0.3	0.3	0.4	0.4	0.5	0.5	0.5	0.5	0.5	0.6	0.6	0.7	0.7	0.7	0.9
85th	0.2	0.3	0.3	0.4	0.4	0.4	0.5	0.5	0.5	0.5	0.5	0.5	0.6	0.7	0.6
90th	0.2	0.2	0.2	0.3	0.3	0.3	0.4	0.4	0.4	0.5	0.5	0.5	0.6	0.6	0.7
95th	0.1	0.2	0.2	0.2	0.2	0.3	0.2	0.3	0.3	0.3	0.4	0.4	0.5	0.5	0.6
97.7th	0.1	0.1	0.2	0.2	0.2	0.2	0.2	0.2	0.3	0.3	0.3	0.3	0.3	0.4	0.4

Forceps Application at 6 cm PVM Diameter, with a 240 N Traction Force:

CAPACITY (Maternal Circumference, in Percentile)	DEMAND (Fetal Head Circumference, in Percentile)														
	2.3rd	5th	10th	20th	25th	30th	40th	50th	60th	70th	75th	80th	90th	95th	97.7th
2.3rd	2.3	2.8	2.6	3.1	3.5	3.2	3.2	3.7	3.6	3.9	4.7	4.7	5.2	5.6	6.4
5th	2.0	1.8	2.4	2.6	2.3	2.7	3.0	3.1	2.9	3.6	3.4	3.8	4.0	4.4	4.4
10th	1.4	1.7	1.7	2.1	1.8	2.0	2.4	2.2	2.6	2.8	2.9	3.0	3.4	3.6	3.9
15th	1.4	1.2	1.6	1.5	1.6	1.8	2.0	1.9	2.1	2.4	2.5	2.3	2.9	3.0	3.2
20th	1.2	1.3	1.2	1.5	1.6	1.7	1.8	1.7	1.9	2.2	2.1	2.3	2.2	2.8	2.8
25th	1.0	1.1	1.3	1.4	1.4	1.5	1.6	1.7	1.6	1.9	2.0	2.1	2.2	2.5	2.6
30th	0.9	1.0	1.2	1.3	1.4	1.2	1.3	1.5	1.7	1.8	1.5	1.7	2.1	1.9	2.4
40th	0.7	0.8	0.9	1.0	1.1	1.2	1.3	1.4	1.4	1.3	1.4	1.5	1.8	1.8	2.1
50th	0.6	0.6	0.7	0.8	0.9	0.9	1.1	1.2	1.3	1.3	1.4	1.2	1.4	1.7	1.9
60th	0.5	0.5	0.6	0.7	0.7	0.8	0.9	0.9	1.0	1.1	1.2	1.2	1.4	1.2	1.4
70th	0.4	0.5	0.5	0.6	0.6	0.6	0.7	0.7	0.8	0.9	0.9	1.0	1.1	1.3	1.4
75th	0.4	0.4	0.5	0.5	0.5	0.6	0.6	0.7	0.7	0.8	0.8	0.8	1.0	1.1	1.2
80th	0.3	0.4	0.4	0.5	0.5	0.5	0.5	0.6	0.6	0.7	0.7	0.7	0.8	0.9	1.1
85th	0.3	0.3	0.4	0.4	0.4	0.5	0.5	0.5	0.6	0.6	0.6	0.6	0.7	0.8	0.9
90th	0.2	0.2	0.3	0.3	0.4	0.4	0.4	0.5	0.5	0.5	0.5	0.6	0.6	0.7	0.8
95th	0.1	0.2	0.2	0.2	0.3	0.3	0.3	0.3	0.4	0.4	0.4	0.4	0.5	0.6	0.6
97.7th	0.1	0.1	0.2	0.2	0.2	0.2	0.2	0.3	0.3	0.3	0.3	0.3	0.4	0.4	0.5

Figure 6.4 - Predicted levator state parameter values across pairings of maternal capacity-to-fetal head demand are shown for traction force values of 0 N (Top), 75.6 N (Middle - Vacuum), and 240 N (bottom – Senior Clinician) over a constant 6 cm PVM diameter forceps application. The intensity of the (red) shading indicates the extent by which the predicted injury threshold is exceeded. The dashed line indicates the injury cutoff for the no forceps case.

When varying when forceps are applied (Figure 6.1), we see that earlier application of forceps produces a higher probability of a PVM injury (Figure 6.3 lower right & Figure 6.12S). For instance, the percentage of cells exceeding the injury threshold drops from 56% for forceps application at a 6 cm PVM diameter to 25% for application at a 9 cm PVM diameter, for the 240 N traction force case (Table 6.1). It should be noted that when the forceps were applied at a point where the PVM was at a 9 cm diameter, this forceps application diameter criteria may not be met until the mother is already on her final contraction. Therefore, it is relevant to consider what would happen when the forceps were applied at an 8 cm PVM diameter, in which 42% of cells exceed the predicted injury threshold for the 240 N traction force case.

In simulations where the applied traction force was varied, the 75.6 N (Vacuum) case resulted in fewer predicted PVM tears than any of the forceps cases (Figure 6.3, lower right), with 37% of cells exceeding the predicted injury threshold for the case of vacuum application at 6 cm PVM diameter [22]. In the 121 N (Mishell Forceps Study) traction force case, 43% of cells were predicted to exceed the injury threshold for the application at 6 cm PVM diameter case [22]. This is appreciably below the 56% observed for both 226 N (previous recommendation) and 240 N (senior clinicians), suggesting that the previous guidelines may be too generous and should be modified downwards to be closer to the 120 N mark [23, 24].

		PVM Diameter at Forceps Application (cm)			
		6	7	8	9
Traction Force (N)	76	37	39	35	24
	121	43	43	37	25
	226	56	49	42	25
	240	56	49	42	25

Table 6.1 - This table shows the percentage of individuals with a levator state parameter above 1 (tear predicted) for each traction force and PVM diameter at the time of forceps application pairing. 75.6 N and 121 N represent vacuum and forceps traction measurements from a single study, while 226 N represents a previously proposed forceps limit, and 240 N represents the average forceps traction force measured for senior clinicians [22, 23, 24].

When considering the duration of the active second stage, we see that increased forceps traction force lowers the overall duration of the active second stage (Figure 6.3 upper left, Figure 6.11S, Table 6.2). We also see that a later forceps application is associated with a greater duration of the active second stage (Figure 6.3 upper right & Table 6.2). This can be seen when comparing Figure 6.13S (lower panel) to the lower portion of Figure 6.11S.

		PVM Diameter at Forceps Application (cm)			
		6	7	8	9
Traction Force (N)	76	21	25	32	38
	121	16	21	31	38
	226	10	17	29	38
	240	10	17	29	38

Table 6.2 - This table shows the average duration of the active second stage for each traction force and PVM diameter at forceps application pairing. 75.6 N and 121 N represent vacuum and forceps traction measurements from a single study, while 226 N represents a previously proposed forceps limit, and 240 N represents the average forceps traction force measured for senior clinicians [22, 23, 24].

6.4.2 Partial force between contractions

Simulations suggest that applying a partial traction force between contractions helps to reduce the levator state parameter (Figure 6.5), as well as the duration of active second stage (Figure 6.14S). This effect is more pronounced for higher partial traction forces.

10% traction force between contractions:

CAPACITY (Maternal Circumference, in Percentile)	DEMAND (Fetal Head Circumference, in Percentile)														
	2.3rd	5th	10th	20th	25th	30th	40th	50th	60th	70th	75th	80th	90th	95th	97.7th
2.3rd	2.5	2.5	2.7	3.0	3.4	3.0	3.9	4.1	4.2	4.3	4.0	4.8	5.1	5.0	6.0
5th	1.8	2.1	2.0	2.3	2.6	2.8	2.6	3.2	2.9	3.6	3.3	3.8	3.6	4.1	4.8
10th	1.4	1.7	1.9	2.0	2.1	2.3	2.1	2.5	2.7	2.6	2.9	2.6	3.3	3.6	3.8
15th	1.4	1.5	1.5	1.8	1.9	1.6	1.9	2.1	2.3	2.2	2.4	2.6	2.6	3.1	3.3
20th	1.2	1.3	1.4	1.4	1.5	1.6	1.8	1.9	1.7	2.0	2.2	2.0	2.5	2.4	3.0
25th	1.0	1.1	1.3	1.5	1.3	1.4	1.6	1.7	1.9	1.7	1.8	2.0	2.3	2.3	2.7
30th	0.8	1.0	1.1	1.3	1.4	1.4	1.3	1.4	1.6	1.7	1.8	1.9	1.9	2.3	2.1
40th	0.7	0.8	0.9	1.0	1.1	1.1	1.2	1.4	1.5	1.5	1.3	1.4	1.7	1.6	2.0
50th	0.6	0.6	0.7	0.8	0.9	0.9	1.0	1.1	1.2	1.3	1.4	1.4	1.3	1.6	1.8
60th	0.5	0.6	0.6	0.7	0.7	0.8	0.8	0.9	1.0	1.1	1.1	1.2	1.4	1.5	1.4
70th	0.4	0.5	0.5	0.6	0.6	0.6	0.7	0.7	0.8	0.8	0.9	0.9	1.1	1.2	1.4
75th	0.4	0.4	0.5	0.5	0.6	0.6	0.6	0.6	0.7	0.8	0.8	0.8	0.9	1.0	1.2
80th	0.3	0.4	0.4	0.5	0.5	0.5	0.6	0.6	0.6	0.7	0.7	0.7	0.8	0.9	1.0
85th	0.3	0.3	0.3	0.4	0.4	0.5	0.5	0.5	0.6	0.6	0.6	0.7	0.7	0.8	0.9
90th	0.2	0.2	0.3	0.3	0.3	0.4	0.4	0.4	0.5	0.5	0.5	0.6	0.6	0.7	0.7
95th	0.1	0.2	0.2	0.2	0.2	0.3	0.3	0.3	0.3	0.4	0.4	0.4	0.5	0.6	0.6
97.7th	0.1	0.1	0.2	0.2	0.2	0.2	0.2	0.2	0.2	0.3	0.3	0.3	0.4	0.4	0.5

50% traction force between contractions

CAPACITY (Maternal Circumference, in Percentile)	DEMAND (Fetal Head Circumference, in Percentile)														
	2.3rd	5th	10th	20th	25th	30th	40th	50th	60th	70th	75th	80th	90th	95th	97.7th
2.3rd	2.1	2.6	2.5	3.3	3.0	3.1	3.9	3.8	3.7	4.3	4.0	4.2	4.9	5.6	5.5
5th	1.7	2.0	2.4	2.4	2.7	2.8	2.5	3.0	3.4	3.0	3.4	3.9	4.2	4.2	4.3
10th	1.5	1.5	1.6	1.8	2.1	2.2	2.0	2.1	2.3	2.8	2.5	2.5	3.3	3.0	3.9
15th	1.2	1.3	1.6	1.5	1.6	1.6	1.8	2.1	2.3	2.0	2.1	2.2	2.8	2.7	3.1
20th	1.0	1.1	1.3	1.6	1.7	1.7	1.5	1.6	1.7	1.9	2.2	1.9	2.1	2.6	2.5
25th	1.0	1.0	1.1	1.3	1.5	1.6	1.7	1.4	1.6	1.7	1.8	1.9	2.3	2.2	2.4
30th	0.8	0.9	1.0	1.1	1.2	1.3	1.5	1.6	1.7	1.6	1.6	1.7	1.8	2.2	2.1
40th	0.6	0.7	0.9	1.0	1.0	1.0	1.1	1.2	1.3	1.5	1.5	1.6	1.8	1.7	1.9
50th	0.5	0.5	0.7	0.8	0.8	0.9	0.9	1.0	1.1	1.2	1.2	1.3	1.6	1.7	1.5
60th	0.4	0.5	0.6	0.7	0.7	0.8	0.8	0.9	1.0	0.9	1.0	1.1	1.2	1.4	1.6
70th	0.3	0.3	0.4	0.5	0.5	0.6	0.6	0.7	0.8	0.8	0.9	0.9	1.0	1.1	1.2
75th	0.3	0.3	0.3	0.4	0.4	0.5	0.5	0.6	0.7	0.7	0.8	0.8	0.9	1.0	1.1
80th	0.3	0.3	0.3	0.3	0.4	0.4	0.4	0.5	0.6	0.6	0.7	0.7	0.8	0.9	1.0
85th	0.2	0.3	0.3	0.3	0.3	0.3	0.4	0.4	0.4	0.5	0.5	0.6	0.7	0.8	0.9
90th	0.2	0.2	0.2	0.3	0.3	0.3	0.3	0.3	0.3	0.4	0.4	0.4	0.5	0.6	0.7
95th	0.1	0.2	0.2	0.2	0.2	0.2	0.3	0.3	0.3	0.3	0.3	0.3	0.4	0.4	0.5
97.7th	0.1	0.1	0.2	0.2	0.2	0.2	0.2	0.2	0.2	0.3	0.3	0.3	0.3	0.3	0.4

Figure 6.5 - Predicted levator state parameter values across pairings of maternal capacity-to-fetal head demand are shown for applying a 10% (Top) and 50% (Bottom) traction force between contractions with forceps application at 6 cm PVM diameter, and a traction force of 240 N (senior clinician). The intensity of the (red) shading indicates the extent by which the predicted injury threshold is exceeded. The dashed and solid lines represent the predicted injury cutoffs for the no forceps and forceps without partial traction force between contractions cases respectively.

6.4.3 Episiotomy

When different episiotomy lengths were evaluated, a simulated length of 1.5 cm or greater was necessary to maintain a levator state parameter below 1; a threshold suggesting a low risk of

PVM tear (Figure 6.6). It was also found that episiotomies beyond this length resulted in active second stages below 1 hour in duration.

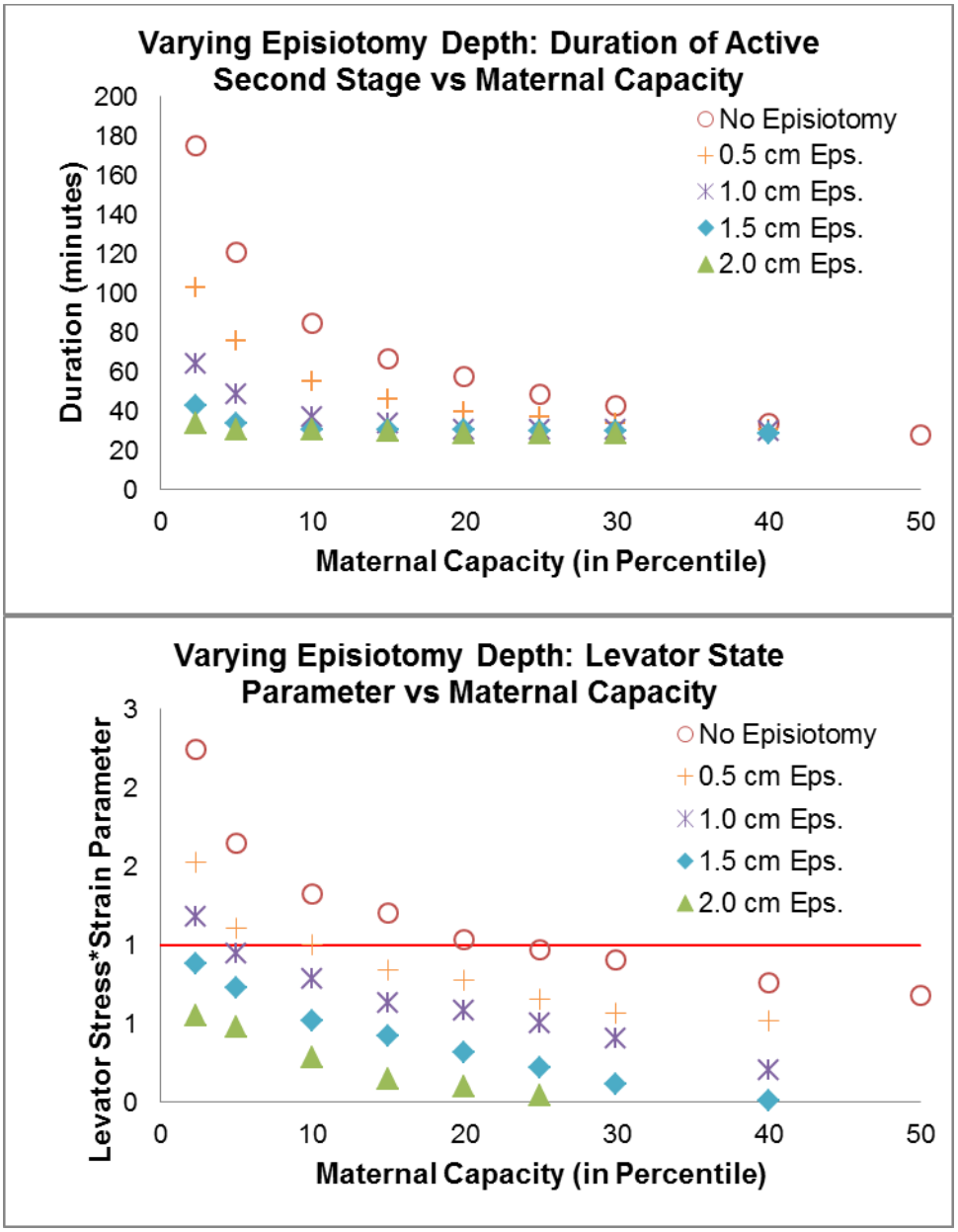

Figure 6.6 - Duration of active second stage (upper) and levator state parameter values (lower) for the range of maternal capacity (in percentile) based on varying episiotomy length. The threshold for injury is a levator state parameter value of 1. A levator state parameter below 1 involves little to no risk whereas a levator state parameter above 1 involves possibility of risk.

6.4.4 Epidural

A 50% decrease in maternal pushing effort was considered to reflect the case of epidural usage. This resulted in an increase in the duration of the active second stage of labor by an average of 12 minutes (Figure 6.7). This increase in the duration of the active second stage corresponded to a 40% decrease in predicted PVM tear rates (Figure 6.8).

		DEMAND (Fetal Head Circumference, in Percentile)														
		2.3rd	5th	10th	20th	25th	30th	40th	50th	60th	70th	75th	80th	90th	95th	97.7th
CAPACITY (Maternal Circumference, in Percentile)	2.3rd	30	33	36	39	42	42	48	51	54	60	60	66	78	87	108
	5th	24	24	24	27	27	27	30	30	33	33	36	36	42	48	51
	10th	15	15	18	18	18	21	18	21	21	24	24	24	27	30	30
	15th	12	12	15	15	15	18	18	18	18	18	18	18	24	24	24
	20th	12	12	12	15	12	15	15	15	15	18	18	15	18	18	21
	25th	9	12	12	12	12	12	12	15	15	15	15	15	18	15	18
	30th	9	9	12	12	9	12	12	12	12	12	12	15	12	15	15
	40th	6	9	9	9	9	12	9	12	9	12	12	12	12	12	12
	50th	6	6	9	9	9	9	9	9	9	9	12	9	9	12	12
	60th	6	6	6	9	9	6	9	9	6	9	9	6	9	9	9
	70th	3	6	6	6	6	6	6	6	6	9	6	6	9	9	6
	75th	6	6	3	6	6	6	6	6	6	6	6	6	9	6	9
	80th	6	3	6	6	3	6	6	6	3	6	6	6	6	6	6
	85th	3	3	6	3	3	6	6	5	3	6	6	6	6	6	8
	90th	3	6	3	3	3	6	6	3	3	6	6	6	3	6	6
	95th	3	3	3	3	3	3	6	3	3	3	3	3	6	3	6
	97.7th	3	3	3	3	0	3	3	3	3	3	3	3	5	3	3

Figure 6.7 - The increase in the duration of the active second stage for epidural usage, relative to control, is reported across pairings of maternal capacity-to-fetal head demand. The intensity of the (blue) shading indicates the magnitude of this increase.

		DEMAND (Fetal Head Circumference, in Percentile)														
		2.3rd	5th	10th	20th	25th	30th	40th	50th	60th	70th	75th	80th	90th	95th	97.7th
CAPACITY (Maternal Circumference, in Percentile)	2.3rd	1.0	1.2	1.3	1.4	1.5	1.6	1.6	1.9	2.0	2.0	2.2	2.3	2.5	2.8	2.9
	5th	0.7	0.8	1.1	1.0	1.2	1.3	1.2	1.5	1.6	1.7	1.7	1.8	1.9	1.9	2.4
	10th	0.6	0.8	0.8	0.9	0.9	1.0	1.1	1.1	1.2	1.3	1.4	1.4	1.4	1.6	1.9
	15th	0.6	0.7	0.6	0.8	0.8	0.8	0.9	1.0	1.0	1.1	1.2	1.2	1.2	1.4	1.6
	20th	0.5	0.6	0.7	0.6	0.8	0.7	0.7	0.9	0.9	1.0	0.9	1.1	1.2	1.3	1.4
	25th	0.5	0.5	0.6	0.7	0.6	0.7	0.8	0.8	0.8	0.8	1.0	0.9	1.0	1.2	1.3
	30th	0.4	0.5	0.5	0.6	0.6	0.6	0.6	0.8	0.8	0.8	0.9	0.9	1.0	1.0	1.2
	40th	0.4	0.4	0.4	0.5	0.5	0.5	0.6	0.6	0.7	0.7	0.6	0.8	0.9	1.0	1.1
	50th	0.3	0.4	0.4	0.3	0.4	0.5	0.5	0.6	0.5	0.6	0.6	0.7	0.7	0.8	0.8
	60th	0.3	0.3	0.3	0.3	0.4	0.4	0.4	0.5	0.5	0.5	0.6	0.6	0.7	0.7	0.7
	70th	0.3	0.2	0.3	0.3	0.3	0.4	0.3	0.4	0.5	0.4	0.5	0.5	0.6	0.5	0.7
	75th	0.2	0.2	0.3	0.3	0.3	0.3	0.3	0.4	0.4	0.4	0.4	0.5	0.5	0.6	0.6
	80th	0.2	0.2	0.2	0.3	0.3	0.2	0.3	0.4	0.4	0.4	0.4	0.4	0.4	0.6	0.6
	85th	0.2	0.2	0.2	0.3	0.3	0.2	0.3	0.3	0.4	0.3	0.4	0.4	0.4	0.5	0.5
	90th	0.2	0.1	0.2	0.2	0.2	0.2	0.2	0.3	0.3	0.3	0.3	0.3	0.4	0.4	0.5
	95th	0.1	0.1	0.2	0.2	0.2	0.2	0.2	0.2	0.2	0.3	0.3	0.3	0.3	0.4	0.3
	97.7th	0.1	0.1	0.1	0.2	0.2	0.1	0.2	0.2	0.2	0.2	0.2	0.3	0.2	0.3	0.3

Figure 6.8 - Predicted levator state parameter values across pairings of maternal capacity-to-fetal head demand are shown for the case of epidural usage. The intensity of the (red) shading indicates the extent by which the predicted injury threshold is exceeded. The dashed and solid lines represent the predicted injury cutoffs for the epidural and control cases respectively.

6.5 Discussion

In our PVM injury simulations, we found that increasing traction force increases risk of PVM tear. Conversely forceps application that occurs later in the birth process with maintained partial traction between contractions is predicted to decrease the risk of tear when other maternal and fetal features remain constant. In terms of the duration of active second stage, both early forceps application, and high traction forces resulted in reduced durations when compared with later forceps application or lower traction force simulations.

Episiotomy of at least 1.5 cm appears protective in terms of injury to the PVM. This depth of incision was enough to reduce the levator state parameter below a value of 1 for all simulated births. This result is interestingly similar to a study in which an obstetric anal sphincter injuries group had an average episiotomy length of 1.3 cm, while a non-injury group had an average episiotomy length of 1.7 cm [34]. We theorize that cuts beyond this length, which is distinctly less than a previously reported average of approximately 4 cm, would cause additional tissue trauma, without added benefit in terms of PVM tear risk or duration of the active second stage [35] and would need to be balanced against the increased risk of anal sphincter tear that occurs in association with midline episiotomies. Some previous studies have suggested that episiotomies are correlated with PVM tears, however, this appears to be a symptom of selective episiotomies being more likely in difficult births, during which PVM tears are also more likely to occur [16, 5, 36, 37]. Additionally, two studies have reported decreases in PVM tear rates in episiotomy groups, including one study which reported a 3-fold reduction in levator damage when forceps were used slowly in conjunction with early episiotomy [38, 39, 40].

Epidural usage is predicted to increase the duration of the active second stage by while also reducing predicted PVM tear rates. This increase in the predicted duration of the active second stage averaged 12 minutes, which is similar to a value of 14 minutes found clinically [41]. This increase in the duration of the active second stage benefited the PVM by allowing additional time for stress relaxation. This resulted in a 40% decrease in predicted PVM tears, which is consistent with a clinically reported odds ratio of 0.42 for PVM tears with the use of epidurals, when compared with controls [5]. The effects of epidural usage on maternal effort were estimated as a 50% decrease in intrauterine pressure due to maternal pushes, with no effect on intrauterine pressure due to uterine contractions. These values were based on observations made by a practicing anesthesiologist, though to our knowledge no published studies report on intrauterine pressure tracings for both epidural and control cases. However, that this assumption results in an increase in the average duration of the active second stage of labor similar to that observed clinically suggests that this assumption may be reasonable [41].

Many, if not most, of the observations in this research will ring true to experienced clinicians. By providing a specific scientific framework based on fundamental biomechanical principles, it allows many complex and often competing factors to be evaluated to establish the degree to which they affect injury risk and how combinations may change outcomes. Obstetricians understand viscoelastic behavior even if they do not know the language of the engineer when they observe that it helps labor to progress if they keep some downward traction on forceps or vacuum between pushes. This allows “stress relaxation” to occur, reducing the resistance of the tissues to elongation. Modeling can say how much and how long this should be done to optimally benefit from this unique property. Of course, the findings of this study need to be

compared with clinical studies. However, it will never be possible to vary each individual parameter in clinical trials in the way that they can be in a model so it will be a combination of biomechanical analysis and applied clinical evidence that can, together, provide a framework for progress.

There are several strengths of this methodology. It allows us to consider a wide variety of maternal and fetal anatomical pairings, for a variety of different traction force and application conditions. This is possible because, by considering the PVM as a single component, rather than a series of individual finite elements, we can increase our computational efficiency so that it was feasible to run the 1,000+ simulations necessary to allow for the analysis conducted here. In this study, we chose to use the product of stress times strain as the criterion for injury. Some previous models of soft tissue injury have selected purely strain-based criteria [42]. However, we note that literature values for soft tissue failure do show a dependence on both stress and strain, hence our choice of failure criterion. [26, 30, 31, 32].

There are several practical limitations to this model for injury. Our threshold for forceps application is based on the diameter of the birth canal at the level of the pubovisceral portion of the levator, which may not be as easily measurable at the time of delivery and is not a familiar anatomic landmark to clinicians. The pubovisceral muscle occupies a location for several centimeters, beginning approximately 1 cm above the hymeneal ring. Therefore, a diameter in this area of 6 cm might correspond to an opening of a few centimeters in the visible introitus. Additionally, due to uncertainty about the overall descent of the pelvic floor during labor, we have been unable to precisely correlate PVM diameter to descent of the fetal head

through the birth canal. A limitation of our birth simulations is that the birth canal stress values peak depending on when, during the contraction, the birth occurred, which could not be predicted prior to delivery for purposes of defining risk of injury.

We also assumed, for simplicity, that the fetal head had already molded fully; the reason for this was that, to our knowledge, there are no data on the time-dependent molding behavior of the fetal head while in the birth canal. Since we did not include fetal head viscoelastic behavior, our current predictions are therefore conservative in terms of the predicted duration of second stage and tear risk for fetal heads exceeding maternal capacity [4].

We have considered the PVM as the structure that defines the smallest circumference of the birth canal, namely the urogenital hiatus in this model. While it is possible that the iliococcygeal muscle and the puborectal muscle could tear, our previous studies suggest that this is unlikely because the stretch in those structures is considerably less than the PVM towards the end of the second stage [4, 43, 44]. Additional clinical factors such as maternal effort and the effect of maternal body habitus are not addressed in this model. It must also be emphasized that these simulations, although powerful because they can analyze a broad range of specific situations would need to be evaluated in the light of clinical trials.

Our simulations suggest that there are maternal, fetal, and operator-dependent characteristics of operative vaginal delivery that affect the risk of PVM tear. With improved understanding of the mechanism of injury, there is the potential to counsel women based on their risk profile for injury as well as other factors that may increase her risk for pelvic organ prolapse later in life. There is also the potential to modify physician behavior in order to minimize risk of PVM injury

by maintaining traction force between contractions while reducing maximum traction on the forceps.

6.6 Bibliography

[1] K.-C. Lien, J. O. L. DeLancey and J. A. Ashton-Miller, "Biomechanical Analyses of the Efficacy of Patterns of Maternal Effort on Second-Stage Progress," *Obstetrics & Gynecology,* vol. 113, no. 4, pp. 873-880, 2009.

[2] M. E. T. Silva, D. A. Oliveira, T. H. Roza, S. Brandao, M. P. L. Parente, T. Mascarenhas and R. M. Natal Jorge, "Study on the influence of the fetus head molding on the biomechanical behavior of the pelvic floor muscles, during vaginal delivery," *Journal of Biomechanics,* vol. 48, no. 9, pp. 1600-1605, 2015.

[3] P. Zan, G. Yan, H. Liu, B. Yang, Y. Zhao and N. Luo, "Biomechanical modeling of the rectum for the desing of a novel artificial anal sphincter," *Biomedical Instrumentation and Technology,* vol. 44, no. 3, pp. 257-60, 2010.

[4] P. V. Tracy, J. O. L. DeLancey and J. A. Ashton-Miller, "A Geometric Capacity - Demand Analysis of Maternal Levator Muscle Stretch Required for Vaginal Delivery," *Journal of Biomechanical Engineering,* pp. e1-e54, 2016.

[5] K. Shek and H. Dietz, "Intrapartum risk factors for levator trauma," *BJOG An International Journal of Obstetrics and Gynecology,* vol. 117, no. 12, pp. 1485-1492, 2010.

[6] J. A. Ashton-Miller and J. O. L. DeLancey, "On the Biomechanics of Vaginal Birth and Common Sequelae," *Annual Review of Biomedical Engineering,* vol. 11, pp. 163-176, 2009.

[7] J. Mant, R. Painter and M. Vessey, "Epidemiology of genital prolapse: observations from the Oxford Planning Association Study," *British Journal of Obstetrics and Gynaecology,* vol. 104, no. 5, pp. 579-85, 1997.

[8] J. O. L. DeLancey, D. M. Morgan, D. E. Fenner, R. Kearney, K. Guire, J. M. Miller, H. Hussain, W. Umek, Y. Hsu and J. A. Aston-Miller, "Comparison of levator ani muscle defects and function in women with and without pelvic organ prolapse," *Obstetrics and Gynecology,* vol. 109, pp. 295-302, 2007.

[9] S. Boyles, A. Weber and L. Meyn, "Procedures for Pelvic Organ Prolapse in the United States, 1979-1997," *American Journal of Obstetrics and Gynecology,* vol. 188, no. 1, pp. 108-15, 2003.

[10] H. U. Memon, J. L. Blomquist, H. P. Dietz, C. B. Pierce, M. M. Wienstein and V. L. Handa, "Comparison of Levator Ani Muscle Avulsion Injury After Forceps-Assisted and Vacuum-Assisted Vaginal Childbirth," *Urogynecology: Original Research,* vol. 125, no. 5, pp. 1080-1087, 2015.

[11] R. Kearney, M. Fitzpatrick, S. Brennan, M. Behan, J. Miller, D. Keane, C. O'Herlihy and J. O. L. DeLancey, "Levator ani injury in primiparous women with forceps delivery for fetal distress, forceps for second stage arrest, and spontaneous delivery," *International Journal of Gynaecology and Obstetrics,* vol. 111, no. 1, pp. 19-22, 2010.

[12] I. Blasi, I. Fuchs, R. D'Amico, V. Vinci, G. La Sala, V. Mazza and W. Henrich, "Intrapartum translabial three-dimensional ultrasound visualization of levator trauma," *Ultrasound in Obstetrics and Gynecology,* vol. 37, no. 1, pp. 88-92, 2011.

[13] J. Cassado Garriga, A. Pessarrodona Isern, M. Espuna Pons, M. Duran Retamal, A. Felgueroso Fabrega, M. Rodriguez Carballeira and I. Jorda Santamaria, "Four-dimensional sonographic evaluation of avulsion of the levator ani according to delivery mode," *Ultrasound in Obstetrics and Gynecology,* vol. 38, no. 6, pp. 701-6, 2011.

[14] J. Cassado Garriga, A. Pessarrodona Isern, M. Espuna Pons, M. Duran Retamal, A. Felgueroso Fabregas and M. Rodriguez-Carballeira, "Tridimensional sonographic anatomical changes on pelvic floor muscle according to the type of delivery," *International Urogynecology Journal,* vol. 22, no. 8, pp. 1011-8, 2011.

[15] S. Chan, R. Cheung, A. Yiu, L. Lee, A. Pang, K. Choy, T. Leung and T. Chung, "Prevalence of levator ani muscle injury in Chinese women after first delivery," *Ultrasound in Obstetrics and Gynecology,* vol. 39, no. 6, pp. 704-9, 2012.

[16] R. Kearney, J. Miller, J. Ashton-Miller and J. O. L. DeLancey, "Obstetric factors associated with levator ani muscle injury after vaginal birth," *Obstetrics and Gynecology,* vol. 107, no. 1, pp. 144-9, 2006.

[17] K. Shek and H. Dietz, "The effect of childbirth on hiatal dimensions," *Obstetrics and Gynecology,* vol. 113, no. 6, pp. 1272-8, 2009.

[18] P. V. Tracy, J. O. L. DeLancey and J. A. Ashton-Miller, "How Much Additional Maternal Spatial Capacity do Forceps Require When Delivering the Fetal Head During Vaginal Birth?," in *Summer Biomechanics, Bioengineering and Biotransport Conference*, National Harbor, MD, 2016.

[19] A. Rempen and M. Kraus, "Pressures on the Fetal Head During Normal Labor," *Journal of Perinatal Medicine,* vol. 19, no. 3, pp. 199-206, 1991.

[20] A. C. J. Allman, E. S. G. Genevler, M. R. Johnson and P. J. Steer, "Head-to-Cervix Force: an Important Physiological Variable in Labour. 1. The Temporal Relation Between Head-to-Cervix Force and Intrauterine Pressure During Labour," *British Journal of Obstetrics and Gynaecology,* vol. 103, pp. 763-768, 1996.

[21] C. S. Buhimschi, I. A. Buhimschi, A. M. Malinow, J. N. Kopelman and C. P. Weiner, "Pushing in Labor: Performance and Not Endurance," *American Journal of Obstetrics and Gynecology,* vol. 186, no. 6, pp. 1339-44, 2002.

[22] D. Mishell and J. V. Kelly, "The Obstetrical Forceps and the Vacuum Extractor: An Assessment of their Compressive Force," *Obstetrics and Gynecology,* vol. 19, pp. 204-6, 1962.

[23] A. Vacca, "Vacuum-assisted delivery: An analysis of traction force and maternal and neonatal outcomes," *Australian and New Zealand Journal of Obstetrics and Gynecology 2006,* vol. 46, pp. 124-127, 2006.

[24] W. H. Pearse, "Electronic recording of forceps delivery," *American Journal of Obstetrics and Gynecology,* vol. 86, pp. 43-51, 1963.

[25] C. Spong, V. Berghella, K. Wenstrom, B. Mercer and G. Saade, "Preventing the first cesarean delivery: summary of a joint Eunice Kennedy Shriver National Institute of Child Health and Human Development, Society for Maternal-Fetal Medicine, and American College of Obstetricians and Gynecologists Workshop," *Obstetrics and Gynecology,* vol. 120, no. 5, pp. 1181-93, 2012.

[26] D. Ulrich, S. L. Edwards, K. Su, J. F. White, J. A. M. Ramshaw, G. Jenkin, J. Deprest, A. Rosamilia, J. A. Werkmeister and C. E. Gargett, "Influence of Reproductive Status on Tissue Composition and Biomechanical Properties of Ovine Vagina," *Public Library of Science,* vol. 9, no. 4, pp. 1 - 8, 2014.

[27] A. Feola, P. Moalli, M. Alperin, R. Duerr, R. Gandley and S. Abramowitch, "Impact of pregnancy and vaginal delivery on the passive and active mechanics of the rat vagina," *Annals of Biomedical Engineering,* vol. 39, no. 1, pp. 549-58, 2011.

[28] M. Alperin, A. Feola, R. Duerr, P. Moalli and S. Abramowitch, "Pregnancy- and delivery-induced biomechanical changes in rat vagina persist postpartum," *International Urogynecology Journal,* vol. 21, no. 9, pp. 1169-74, 2010.

[29] J. L. Lowder, K. M. Debes, D. K. Moon, N. Howden, S. D. Abramowitch and P. A. Moalli, "Biomechanical Adaptations of the Rat Vagina and Supportive Tissues in Pregnancy to Accommodate Delivery," *Obstetrics and Gynecology,* vol. 109, no. 1, pp. 136-143, 2007.

[30] T. J. Bonner, N. Newell, A. Karunaratne, A. D. Pullen, A. A. Amis, A. M. J. Bull and S. D. Masouros, "Strain-rate Sensitivity of the Lateral Collateral Ligament of the Knee," *Journal of the Mechanical Behavior of Biomedical Materials,* vol. 41, pp. 261-70, 2015.

[31] M. Chiba and K. Komatsu, "Mechanical Responses of the Periodontal Ligament in the Transverse Section of the Rat Mandibular Incisor at Various Velocities of Loading In Vitro," *Journal of Biomechanics,* vol. 26, no. 4, pp. 561-70, 1993.

[32] M. M. Panjabi, J. J. Crisco, C. Lydon and J. Dvorak, "The Mechanical Properties of Human Alar and Transverse Ligaments at Slow and Fast Extension Rates," *Clinical Biomechanics,* vol. 13, no. 2, pp. 112-20, 1998.

[33] J. R. Wilson, "Chapter 7: Forceps Delivery," in *Atlas of Obstetric Technique*, Saint Louis, C. V. Mosby Company, 1969, pp. 99 - 105.

[34] M. Stedenfeldt, J. Pirhonen, E. Blix, T. Wilsgaard, B. Vonen and P. Oian, "Episiotomy characteristics and risks for obstetric anal sphincter injuries: a case-control study," *BJOG,* vol. 119, no. 6, pp. 724-30, 2012.

[35] V. Andrews, R. Thakar, A. Sultan and P. Jones, "Are mediolateral episiotomies actually mediolateral?," *BJOG,* vol. 112, no. 8, pp. 1156-8, 2005.

[36] K. Shek, K. Green, J. Hall, R. Guzman-Rojas and H. Dietz, "Perineal and vaginal tears are clinical markers for occult levator ani trauma: a retrospective observational study," *Ultrasound in Obstetrics & Gynecology,* vol. 47, no. 2, pp. 224-7, 2016.

[37] D. Valsky, S. Cohen, M. Lipschuetz, D. Hochner-Celnikier, H. Daum, I. Yagel and S. Yagel, "Third- or Fourth-Degree Intrapartum Anal Sphincter Tears are Associated with Levator Ani Avulsion in Primiparas," *Journal of Ultrasound in Medicine,* vol. 35, no. 4, pp. 709-15, 2016.

[38] H. Gainey, "Post-partum observation of pelvic tissue damage," *American Journal of Obstetrics and Gynecology,* vol. 45, no. 1, p. 457, 1943.

[39] H. Gainey, "Post-partum observations of pelvic tissue damage: Further studies," *American Journal of Obstetrics and Gynecology,* vol. 70, no. 4, pp. 800-7, 1955.

[40] J. Cassado, A. Pessarrodona, M. Rodriguez-Carballeira, L. Hinojosa, G. Manrique, A. Marquez and M. Marcias, "Does episiotomy protect against injury of the levator ani muscle in normal vaginal delivery?," *Neurourology and Urodynamics,* vol. 33, no. 8, pp. 1212-6, 2014.

[41] S. Halpern, B. Leighton, A. Ohlsson, J. Barrett and A. Rice, "Effect of epidural vs parenteral opioid analgesia on the progress of labor: a meta-analysis," *JAMA,* vol. 280, no. 24, pp. 2105-10, 1998.

[42] W. Li, "Damage Models for Soft Tissues: A Survey," *Journal of Medical and Biological Engineering,* vol. 36, pp. 285-307, 2016.

[43] K. Lien, B. Mooney, J. O. L. DeLancey and J. Ashton-Miller, "Levator ani muscle stretch induced by simulated vaginal birth," *Obstetrics and Gynecology,* vol. 103, no. 1, pp. 31-40, 2004.

[44] D. Jing, J. A. Ashton-Miller and J. O. L. DeLancey, "A subject-specific anisotropic visco-hyperelastic finite element model of female pelvic floor stress and strain during the second stage of labor," *Journal of Biomechanics,* vol. 45, pp. 455-460, 2012.

6.7 Appendix

Calculations

PVM strain, ε_{PVM}, was assumed to be related to general birth canal strain, ε_{BC}, based on the ratio between their initial circumferential lengths, l_{PVM} and l_{BC} respectively [4].

$$\varepsilon_{PVM} = \frac{l_{BC}}{l_{PVM}}(\varepsilon_{BC} + 1) - 1$$

Intrauterine pressure was assumed to be related to circumferential stress in the PVM U-shaped sling, based on the following calculations (Figure 6.9S):

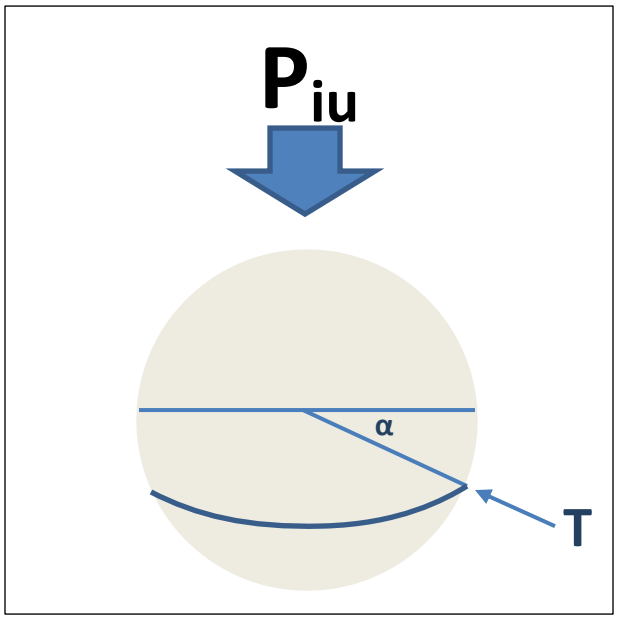

Figure 6.9S - Intrauterine pressure (blue arrow) creates a force distributed over the fetal head (grey circle). The tension (T) in the PVM (dark blue band low on head) was related to intrauterine pressure using the radius of the fetal head (light blue lines) and the angle between the midline of the fetal head and the contact point of the PVM on the fetal head (alpha).

$$T = tension\ in\ PVM$$

$$\tilde{T} = \frac{T}{2\pi r} = Tension/length$$

Balancing "Vertical" Forces:

$$\tilde{T} 2\pi r * sin(\alpha) = P_{ab}\pi * {r_h}^2$$

$$\tilde{T} = \frac{P_{ab} * {r_h}^2}{2r * sin(\alpha)}$$

Balancing "Horizontal" Forces:

$$\sigma_{PVM} 2 * A_{PVM} = \tilde{T} 2r * \cos(\alpha)$$

$$\sigma_{PVM} = \frac{\tilde{T} * 2r * \cos(\alpha)}{2A_{PVM}}$$

$$= \frac{P_{ab}{r_h}^2}{2A_{PVM}\tan(\alpha)}$$

Based on image analysis of the non-uniformity of the newborn fetal head, a maximum alpha value of 0.68 radians was assumed.

		DEMAND (Fetal Head Circumference, in Percentile)								
		10	20	30	40	50	60	70	80	90
CAPACITY (Maternal Circumference, in Percentile)	10	0.86	0.85	0.84	0.83	0.82	0.81	0.81	0.80	0.78
	20	0.99	0.97	0.96	0.95	0.94	0.93	0.92	0.91	0.90
	30	1.08	1.06	1.05	1.04	1.03	1.02	1.01	**0.99**	0.98
	40	1.15	1.13	1.12	1.10	1.09	1.08	1.07	1.06	1.04
	50	1.22	1.19	1.18	1.17	1.16	1.15	1.13	1.12	1.10
	60	1.28	1.26	1.24	1.23	1.22	1.21	1.19	1.18	1.16
	70	1.35	1.32	1.31	1.29	1.28	1.27	1.26	1.24	1.22
	80	1.42	1.40	1.38	1.37	1.35	1.34	1.33	1.31	1.29
	90	1.53	1.50	1.48	1.47	1.45	1.44	1.42	1.41	1.38

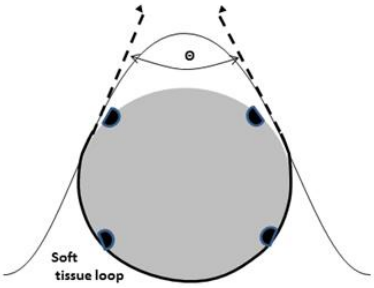

Figure 6.10S - Geometric Maternal Capacity – to – Fetal Head Demand ratio for forceps with a compressible fetal head. Because maternal capacity must exceed fetal demand for a safe delivery to be predicted, a value of this ratio below 1 indicates a predicted PVM tear. The intensity of the (red) shading indicates the extent by which the predicted injury threshold is exceeded. These figures have been presented previously **[18]**.

Original:

CAPACITY (Maternal Circumference, in Percentile)	DEMAND (Fetal Head Circumference, in Percentile)														
	2.3rd	5th	10th	20th	25th	30th	40th	50th	60th	70th	75th	80th	90th	95th	97.7th
2.3rd	118	124	133	148	151	157	166	175	184	196	205	211	235	262	289
5th	82	88	94	103	106	109	115	121	124	133	136	142	154	166	181
10th	61	64	67	73	76	76	82	85	88	91	94	97	106	112	121
15th	49	52	55	58	61	61	64	67	70	73	76	79	82	88	94
20th	40	43	46	49	52	52	55	58	61	61	64	67	70	76	79
25th	37	37	40	43	46	46	49	49	52	55	55	58	61	67	70
30th	31	34	34	37	40	40	43	43	46	49	49	49	55	58	61
40th	25	25	28	31	31	31	34	34	37	37	40	40	43	46	49
50th	19	22	22	25	25	25	28	28	31	31	31	34	37	37	40
60th	16	16	19	19	19	22	22	22	25	25	25	28	28	31	34
70th	13	13	13	16	16	16	19	19	19	19	22	22	22	25	28
75th	10	10	13	13	13	13	16	16	16	19	19	19	19	22	22
80th	7	10	10	10	13	13	13	13	16	16	16	16	19	19	22
85th	7	7	7	10	10	10	10	10	13	13	13	13	16	16	16
90th	4	4	7	7	7	7	7	10	10	10	10	10	13	13	13
95th	1	4	4	4	4	4	4	7	7	7	7	7	7	10	10
97.7th	1	1	1	1	3	4	4	4	4	4	4	4	4	7	7

Vacuum Application at 6 cm PVM Diameter, with a 75.6 N Traction Force:

CAPACITY (Maternal Circumference, in Percentile)	DEMAND (Fetal Head Circumference, in Percentile)														
	2.3rd	5th	10th	20th	25th	30th	40th	50th	60th	70th	75th	80th	90th	95th	97.7th
2.3rd	64	70	73	82	85	88	91	97	100	106	112	115	127	142	154
5th	46	49	55	58	58	61	64	67	70	76	79	79	88	94	103
10th	34	34	37	40	43	43	46	49	49	52	55	55	61	64	70
15th	25	28	28	31	34	34	37	37	40	43	43	46	49	52	55
20th	22	22	25	28	28	28	31	31	34	37	37	37	40	43	46
25th	19	19	22	25	25	25	25	28	28	31	31	31	34	37	40
30th	16	16	19	19	19	22	22	25	25	25	28	28	31	34	37
40th	13	13	13	16	16	16	19	19	19	22	22	22	25	25	28
50th	10	10	10	13	13	13	13	13	16	16	16	16	19	19	22
60th	7	7	7	7	10	10	10	10	13	13	13	13	16	16	19
70th	4	4	4	7	7	7	7	7	10	10	10	10	13	13	13
75th	4	4	4	4	7	7	7	7	7	7	7	10	10	10	13
80th	4	4	4	4	4	4	4	7	7	7	7	7	7	10	10
85th	4	4	4	4	4	4	4	4	4	4	7	7	7	7	10
90th	3	3	4	4	4	4	4	4	4	4	4	4	4	7	7
95th	1	3	3	3	3	3	4	4	4	4	4	4	4	4	4
97.7th	1	1	1	1	3	3	3	3	3	3	3	3	4	4	4

Forceps Application at 6 cm PVM Diameter, with a 240 N Traction Force:

CAPACITY (Maternal Circumference, in Percentile)	DEMAND (Fetal Head Circumference, in Percentile)														
	2.3rd	5th	10th	20th	25th	30th	40th	50th	60th	70th	75th	80th	90th	95th	97.7th
2.3rd	40	43	43	46	49	49	52	55	55	58	64	70	73	73	79
5th	25	28	28	28	31	31	31	34	37	37	40	40	43	46	52
10th	19	16	19	19	22	22	22	25	25	25	25	25	28	31	34
15th	13	16	13	16	16	16	16	19	19	19	19	22	22	25	28
20th	10	10	13	13	13	13	13	16	16	16	16	16	19	19	22
25th	10	10	10	10	10	10	10	10	13	13	13	13	16	16	19
30th	10	7	7	7	7	10	10	10	10	10	13	13	13	16	16
40th	7	7	7	7	7	7	7	7	7	10	10	10	10	10	10
50th	6	6	6	7	7	7	4	4	4	4	4	7	7	7	7
60th	3	3	3	4	4	4	4	4	4	4	4	4	4	7	7
70th	3	3	3	3	3	3	4	4	4	4	4	4	4	4	4
75th	3	3	3	3	3	3	3	3	3	4	4	4	4	4	4
80th	3	3	3	3	3	3	3	3	3	3	3	4	4	4	4
85th	3	3	3	3	3	3	3	3	3	3	3	3	3	4	4
90th	3	3	3	3	3	3	3	3	3	3	3	3	3	3	3
95th	1	3	3	3	3	3	3	3	3	3	3	3	3	3	3
97.7th	1	1	1	1	3	3	3	3	3	3	3	3	3	3	3

Figure 6.11S - Predicted duration of active second stage (minutes) across pairings of maternal capacity-to-fetal head demand are shown for traction force values of 0N (Top), 75.6 N (Middle - Vacuum), and 240 N (bottom – Senior Clinician) over a constant application at 6 cm PVM diameter. The intensity of the (blue) shading indicates the extent by which each active second stage exceeds 3 hours. 1 hour (dot-dot-dash), 2 hour (dot-dash), and 3 hour (dash) are marked by lines in each panel.

Original (no forceps):

CAPACITY (Maternal Circumference, in Percentile)	DEMAND (Fetal Head Circumference, in Percentile)														
	2.3rd	5th	10th	20th	25th	30th	40th	50th	60th	70th	75th	80th	90th	95th	97.7th
2.3rd	1.2	1.4	1.6	1.6	1.9	1.9	2.1	2.2	2.4	2.5	2.5	2.8	3.1	3.2	3.7
5th	1.1	1.1	1.3	1.3	1.4	1.5	1.5	1.6	1.9	1.8	2.0	1.9	2.3	2.6	2.7
10th	0.7	0.8	1.0	1.1	1.0	1.2	1.1	1.3	1.4	1.6	1.6	1.7	1.7	2.1	2.2
15th	0.7	0.7	0.8	1.0	0.9	1.0	1.1	1.2	1.3	1.4	1.3	1.3	1.6	1.8	2.0
20th	0.7	0.7	0.8	0.9	0.8	0.9	1.0	1.0	1.0	1.2	1.2	1.2	1.5	1.5	1.7
25th	0.5	0.6	0.7	0.8	0.7	0.8	0.8	1.0	1.0	1.1	1.2	1.1	1.3	1.3	1.5
30th	0.5	0.5	0.6	0.7	0.7	0.8	0.8	0.9	0.9	0.9	1.0	1.1	1.1	1.3	1.4
40th	0.4	0.5	0.5	0.6	0.6	0.7	0.7	0.8	0.8	0.8	0.9	0.9	1.0	1.1	1.2
50th	0.4	0.4	0.5	0.5	0.6	0.6	0.6	0.7	0.6	0.8	0.8	0.8	0.8	1.0	1.1
60th	0.3	0.4	0.4	0.5	0.5	0.5	0.5	0.6	0.6	0.7	0.7	0.7	0.8	0.8	0.9
70th	0.3	0.3	0.4	0.4	0.4	0.4	0.4	0.5	0.5	0.6	0.5	0.6	0.7	0.7	0.7
75th	0.3	0.3	0.3	0.4	0.4	0.4	0.4	0.5	0.5	0.5	0.5	0.6	0.6	0.7	0.8
80th	0.3	0.2	0.3	0.3	0.3	0.3	0.4	0.4	0.4	0.5	0.5	0.5	0.5	0.6	0.6
85th	0.2	0.2	0.3	0.3	0.3	0.3	0.4	0.3	0.4	0.4	0.5	0.5	0.5	0.6	0.6
90th	0.2	0.2	0.2	0.3	0.3	0.3	0.3	0.3	0.3	0.4	0.4	0.4	0.4	0.5	0.6
95th	0.1	0.1	0.2	0.2	0.2	0.2	0.3	0.2	0.3	0.3	0.3	0.4	0.4	0.4	0.5
97.7th	0.1	0.1	0.2	0.2	0.2	0.2	0.2	0.2	0.2	0.3	0.3	0.3	0.3	0.3	0.4

Forceps Application at 6 cm PVM Diameter, with a 240 N Traction Force:

CAPACITY (Maternal Circumference, in Percentile)	DEMAND (Fetal Head Circumference, in Percentile)														
	2.3rd	5th	10th	20th	25th	30th	40th	50th	60th	70th	75th	80th	90th	95th	97.7th
2.3rd	2.3	2.8	2.6	3.1	3.5	3.2	3.2	3.7	3.6	3.9	4.7	4.7	5.2	5.6	6.4
5th	2.0	1.8	2.4	2.6	2.3	2.7	3.0	3.1	2.9	3.6	3.4	3.8	4.0	4.4	4.4
10th	1.4	1.7	1.7	2.1	1.8	2.0	2.4	2.2	2.6	2.8	2.9	3.0	3.4	3.6	3.9
15th	1.4	1.2	1.6	1.5	1.6	1.8	2.0	1.9	2.1	2.4	2.5	2.3	2.9	3.0	3.2
20th	1.2	1.3	1.2	1.5	1.6	1.7	1.8	1.7	1.9	2.2	2.1	2.3	2.2	2.8	2.8
25th	1.0	1.1	1.3	1.4	1.4	1.5	1.6	1.7	1.6	1.9	2.0	2.1	2.2	2.5	2.6
30th	0.9	1.0	1.2	1.3	1.4	1.2	1.3	1.5	1.7	1.8	1.5	1.7	2.1	1.9	2.4
40th	0.7	0.8	0.9	1.0	1.1	1.2	1.3	1.4	1.4	1.3	1.4	1.5	1.8	1.8	2.1
50th	0.6	0.6	0.7	0.8	0.9	0.9	1.1	1.2	1.3	1.3	1.4	1.2	1.4	1.7	1.9
60th	0.5	0.5	0.6	0.7	0.7	0.8	0.9	0.9	1.0	1.1	1.2	1.2	1.4	1.2	1.4
70th	0.4	0.5	0.5	0.6	0.6	0.6	0.7	0.7	0.8	0.9	0.9	1.0	1.1	1.3	1.4
75th	0.4	0.4	0.5	0.5	0.5	0.6	0.6	0.7	0.7	0.8	0.8	0.8	1.0	1.1	1.2
80th	0.3	0.4	0.4	0.5	0.5	0.5	0.5	0.6	0.6	0.7	0.7	0.7	0.8	0.9	1.1
85th	0.3	0.3	0.4	0.4	0.4	0.5	0.5	0.5	0.6	0.6	0.6	0.6	0.7	0.8	0.9
90th	0.2	0.2	0.3	0.3	0.4	0.4	0.4	0.5	0.5	0.5	0.5	0.6	0.6	0.7	0.8
95th	0.1	0.2	0.2	0.2	0.3	0.3	0.3	0.3	0.4	0.4	0.4	0.4	0.5	0.6	0.6
97.7th	0.1	0.1	0.2	0.2	0.2	0.2	0.2	0.3	0.3	0.3	0.3	0.3	0.4	0.4	0.5

Forceps Application at 9 cm PVM Diameter, with a 240 N Traction Force:

CAPACITY (Maternal Circumference, in Percentile)	DEMAND (Fetal Head Circumference, in Percentile)														
	2.3rd	5th	10th	20th	25th	30th	40th	50th	60th	70th	75th	80th	90th	95th	97.7th
2.3rd	1.2	1.4	1.6	1.6	1.9	1.9	2.4	3.0	3.2	3.7	4.1	4.6	5.3	6.0	6.4
5th	1.1	1.1	1.3	1.3	1.4	1.5	1.8	2.1	2.4	2.7	2.8	3.1	4.0	4.0	4.3
10th	0.7	0.8	1.0	1.1	1.0	1.2	1.1	1.3	1.6	2.0	2.1	2.3	2.7	3.2	3.9
15th	0.7	0.7	0.8	1.0	0.9	1.0	1.1	1.2	1.3	1.5	1.7	1.9	2.2	2.5	2.9
20th	0.7	0.7	0.8	0.9	0.8	0.9	1.0	1.0	1.2	1.2	1.4	1.6	2.0	2.1	2.4
25th	0.5	0.6	0.7	0.8	0.7	0.8	0.8	1.0	1.0	1.2	1.2	1.3	1.7	1.9	2.2
30th	0.5	0.5	0.6	0.7	0.7	0.8	0.8	0.9	0.9	1.0	1.0	1.1	1.5	1.8	1.9
40th	0.4	0.5	0.5	0.6	0.6	0.7	0.7	0.8	0.8	0.8	0.9	0.9	1.2	1.4	1.7
50th	0.4	0.4	0.5	0.5	0.6	0.6	0.6	0.7	0.6	0.8	0.8	0.8	0.9	1.2	1.4
60th	0.3	0.4	0.4	0.5	0.5	0.5	0.5	0.6	0.6	0.7	0.7	0.7	0.8	1.0	1.2
70th	0.3	0.3	0.4	0.4	0.4	0.4	0.4	0.5	0.5	0.6	0.5	0.6	0.7	0.7	0.8
75th	0.3	0.3	0.3	0.4	0.4	0.4	0.4	0.5	0.5	0.5	0.5	0.6	0.6	0.7	0.8
80th	0.3	0.2	0.3	0.3	0.3	0.3	0.4	0.4	0.4	0.5	0.5	0.5	0.5	0.6	0.7
85th	0.2	0.2	0.3	0.3	0.3	0.3	0.4	0.3	0.4	0.4	0.5	0.5	0.5	0.6	0.6
90th	0.2	0.2	0.2	0.3	0.3	0.3	0.3	0.3	0.3	0.4	0.4	0.4	0.4	0.5	0.6
95th	0.1	0.1	0.2	0.2	0.2	0.2	0.3	0.2	0.3	0.3	0.3	0.4	0.4	0.4	0.5
97.7th	0.1	0.1	0.2	0.2	0.2	0.2	0.2	0.2	0.2	0.3	0.3	0.3	0.3	0.3	0.4

Figure 6.12S - Predicted levator state parameter values across pairings of maternal capacity-to-fetal head demand are shown for the no forceps case (upper) as well as forceps application criteria of 6 cm (middle) and 9 cm (lower) over a constant traction force value of 240 N (senior clinician). The intensity of the (red) shading indicates the extent by which the predicted injury threshold is exceeded. The dashed line indicates the injury cutoff for the no forceps case.

Original:

CAPACITY (Maternal Circumference, in Percentile)	DEMAND (Fetal Head Circumference, in Percentile)														
	2.3rd	5th	10th	20th	25th	30th	40th	50th	60th	70th	75th	80th	90th	95th	97.7th
2.3rd	118	124	133	148	151	157	166	175	184	196	205	211	235	262	289
5th	82	88	94	103	106	109	115	121	124	133	136	142	154	166	181
10th	61	64	67	73	76	76	82	85	88	91	94	97	106	112	121
15th	49	52	55	58	61	61	64	67	70	73	76	79	82	88	94
20th	40	43	46	49	52	52	55	58	61	61	64	67	70	76	79
25th	37	37	40	43	46	46	49	49	52	55	55	58	61	67	70
30th	31	34	34	37	40	40	43	43	46	49	49	49	55	58	61
40th	25	25	28	31	31	31	34	34	37	37	40	40	43	46	49
50th	19	22	22	25	25	25	28	28	31	31	31	34	37	37	40
60th	16	16	19	19	19	22	22	22	25	25	25	28	28	31	34
70th	13	13	13	16	16	16	19	19	19	19	22	22	22	25	28
75th	10	10	13	13	13	13	16	16	16	19	19	19	19	22	22
80th	7	10	10	10	13	13	13	13	16	16	16	16	19	19	22
85th	7	7	7	10	10	10	10	10	13	13	13	13	16	16	16
90th	4	4	7	7	7	7	7	10	10	10	10	10	13	13	13
95th	1	4	4	4	4	4	4	7	7	7	7	7	7	10	10
97.7th	1	1	1	1	3	4	4	4	4	4	4	4	4	7	7

Forceps Application at 6 cm PVM Diameter, with a 240 N Traction Force:

CAPACITY (Maternal Circumference, in Percentile)	DEMAND (Fetal Head Circumference, in Percentile)														
	2.3rd	5th	10th	20th	25th	30th	40th	50th	60th	70th	75th	80th	90th	95th	97.7th
2.3rd	40	43	43	46	49	49	52	55	55	58	64	70	73	73	79
5th	25	28	28	28	31	31	31	34	37	37	40	40	43	46	52
10th	19	16	19	19	22	22	22	25	25	25	25	25	28	31	34
15th	13	16	13	16	16	16	16	19	19	19	19	22	22	25	28
20th	10	10	13	13	13	13	13	16	16	16	16	16	19	19	22
25th	10	10	10	10	10	10	10	10	13	13	13	13	16	16	19
30th	10	7	7	7	7	10	10	10	10	10	13	13	13	16	16
40th	7	7	7	7	7	7	7	7	7	10	10	10	10	10	10
50th	6	6	6	7	7	7	4	4	4	4	4	7	7	7	7
60th	3	3	3	4	4	4	4	4	4	4	4	4	4	7	7
70th	3	3	3	3	3	3	4	4	4	4	4	4	4	4	4
75th	3	3	3	3	3	3	3	3	3	4	4	4	4	4	4
80th	3	3	3	3	3	3	3	3	3	3	3	4	4	4	4
85th	3	3	3	3	3	3	3	3	3	3	3	3	3	4	4
90th	3	3	3	3	3	3	3	3	3	3	3	3	3	3	3
95th	1	3	3	3	3	3	3	3	3	3	3	3	3	3	3
97.7th	1	1	1	1	3	3	3	3	3	3	3	3	3	3	3

Forceps Application at a 9 cm PVM Diameter, with a 240 N Traction Force:

CAPACITY (Maternal Circumference, in Percentile)	DEMAND (Fetal Head Circumference, in Percentile)														
	2.3rd	5th	10th	20th	25th	30th	40th	50th	60th	70th	75th	80th	90th	95th	97.7th
2.3rd	118	124	133	148	151	157	165	168	171	178	178	181	187	193	199
5th	82	88	94	103	106	109	114	117	120	123	123	124	127	130	133
10th	61	64	67	73	76	76	82	85	87	87	90	90	91	91	91
15th	49	52	55	58	61	61	64	67	70	72	72	72	75	76	76
20th	40	43	46	49	52	52	55	58	60	61	63	63	63	66	67
25th	37	37	40	43	46	46	49	49	52	54	55	57	57	57	57
30th	31	34	34	37	40	40	43	43	46	48	49	49	51	51	51
40th	25	25	28	31	31	31	34	34	37	37	40	40	42	42	42
50th	19	22	22	25	25	25	28	28	31	31	31	34	36	36	36
60th	16	16	19	19	19	22	22	22	25	25	25	28	28	30	30
70th	13	13	13	16	16	16	19	19	19	19	22	22	22	25	27
75th	10	10	13	13	13	13	16	16	16	19	19	19	19	22	22
80th	7	10	10	10	13	13	13	13	16	16	16	16	19	19	21
85th	7	7	7	10	10	10	10	10	13	13	13	13	16	16	16
90th	4	4	7	7	7	7	7	10	10	10	10	10	13	13	13
95th	1	4	4	4	4	4	4	7	7	7	7	7	7	10	10
97.7th	1	1	1	1	3	4	4	4	4	4	4	4	4	7	7

Figure 6.13S - Predicted duration of active second stage (minutes) across pairings of maternal capacity-to-fetal head demand are shown for the no forceps case (upper) as well as forceps application criteria of 6 cm (middle) and 9 cm (lower) over a constant forceps traction force of 240 N (senior clinician). The intensity of the (blue) shading indicates the extent by which each active second stage exceeds 3 hours. 1 hour (dot-dot-dash), 2 hour (dot-dash), and 3 hour (dash) are marked by lines.

No traction force between contractions:

CAPACITY (Maternal Circumference, in Percentile)	DEMAND (Fetal Head Circumference, in Percentile)														
	2.3rd	5th	10th	20th	25th	30th	40th	50th	60th	70th	75th	80th	90th	95th	97.7th
2.3rd	40	43	43	46	49	49	52	55	55	58	64	70	73	73	79
5th	25	28	28	28	31	31	31	34	37	37	40	40	43	46	52
10th	19	16	19	19	22	22	22	25	25	25	25	25	28	31	34
15th	13	16	13	16	16	16	16	19	19	19	19	22	22	25	28
20th	10	10	13	13	13	13	13	16	16	16	16	16	19	19	22
25th	10	10	10	10	10	10	10	10	13	13	13	13	16	16	19
30th	10	7	7	7	7	10	10	10	10	10	13	13	13	16	16
40th	7	7	7	7	7	7	7	7	7	10	10	10	10	10	10
50th	6	6	6	7	7	7	4	4	4	4	4	7	7	7	7
60th	3	3	3	4	4	4	4	4	4	4	4	4	4	7	7
70th	3	3	3	3	3	3	4	4	4	4	4	4	4	4	4
75th	3	3	3	3	3	3	3	3	3	4	4	4	4	4	4
80th	3	3	3	3	3	3	3	3	3	3	3	4	4	4	4
85th	3	3	3	3	3	3	3	3	3	3	3	3	3	4	4
90th	3	3	3	3	3	3	3	3	3	3	3	3	3	3	3
95th	1	3	3	3	3	3	3	3	3	3	3	3	3	3	3
97.7th	1	1	1	1	3	3	3	3	3	3	3	3	3	3	3

10% traction force between contractions:

CAPACITY (Maternal Circumference, in Percentile)	DEMAND (Fetal Head Circumference, in Percentile)														
	2.3rd	5th	10th	20th	25th	30th	40th	50th	60th	70th	75th	80th	90th	95th	97.7th
2.3rd	34	37	37	40	40	43	43	43	46	49	52	52	58	64	67
5th	25	25	28	28	28	28	31	31	34	34	37	37	40	43	46
10th	19	16	16	19	19	19	22	22	22	25	22	25	25	28	31
15th	13	13	13	13	13	16	16	16	16	19	19	19	22	22	25
20th	10	10	10	13	13	13	13	13	16	16	13	16	16	19	19
25th	10	10	10	10	10	10	10	10	10	13	13	13	13	16	16
30th	10	7	7	7	7	7	10	10	10	10	10	10	13	13	16
40th	6	7	7	7	7	7	7	7	7	7	10	10	10	10	10
50th	6	6	6	7	7	7	4	4	4	4	4	4	7	7	7
60th	3	3	3	3	3	4	4	4	4	4	4	4	4	4	7
70th	3	3	3	3	3	3	3	3	4	4	4	4	4	4	4
75th	3	3	3	3	3	3	3	3	3	3	4	4	4	4	4
80th	3	3	3	3	3	3	3	3	3	3	3	3	4	4	4
85th	3	3	3	3	3	3	3	3	3	3	3	3	3	3	4
90th	3	3	3	3	3	3	3	3	3	3	3	3	3	3	3
95th	1	3	3	3	3	3	3	3	3	3	3	3	3	3	3
97.7th	1	1	1	1	3	3	3	3	3	3	3	3	3	3	3

50% traction force between contractions:

CAPACITY (Maternal Circumference, in Percentile)	DEMAND (Fetal Head Circumference, in Percentile)														
	2.3rd	5th	10th	20th	25th	30th	40th	50th	60th	70th	75th	80th	90th	95th	97.7th
2.3rd	30	31	30	31	33	34	34	34	34	37	37	40	43	46	48
5th	21	22	22	22	22	22	24	25	25	28	28	28	28	31	34
10th	16	13	15	16	16	16	16	18	19	19	18	18	19	22	22
15th	13	13	10	12	12	12	13	13	13	15	15	16	16	18	19
20th	9	10	10	10	10	10	12	12	13	13	10	10	13	13	15
25th	9	9	10	10	7	7	7	9	9	10	10	10	10	12	13
30th	9	6	6	7	7	7	7	7	7	7	9	9	10	10	10
40th	6	6	6	6	6	6	7	7	7	7	7	7	7	7	7
50th	6	6	6	6	6	6	3	3	4	4	4	4	4	4	6
60th	3	3	3	3	3	3	3	3	3	3	3	4	4	4	4
70th	2	3	3	3	3	3	3	3	3	3	3	3	3	3	4
75th	2	2	3	3	3	3	3	3	3	3	3	3	3	3	3
80th	2	2	2	3	3	3	3	3	3	3	3	3	3	3	3
85th	2	2	2	2	2	3	3	3	3	3	3	3	3	3	3
90th	2	2	2	2	2	2	2	2	3	3	3	3	3	3	3
95th	1	2	2	2	2	2	2	2	2	2	2	2	3	3	3
97.7th	1	1	1	1	2	2	2	2	2	2	2	2	2	2	2

Figure 6.14S - Predicted duration of active second stage (minutes) across pairings of maternal capacity-to-fetal head demand are shown for applying no (upper), a 10% (middle), and 50% (lower) traction force between contractions with forceps application at 6 cm PVM diameter, and a 240 N traction force. 1 hour (dot-dot-dash), 2 hour (dot-dash), and 3 hour (dash) are marked by lines in each panel.

Effect of Perineal Fascia Rupture on Duration of the Active Second Stage of Labor and Levator Ani Tear Risk

There is a fascia that lies just superior to the perineal body, which has been observed to have ruptured following birth, but which is not commonly studied. This appendix tests the hypothesis that an intact fascia shields the pubovisceral muscle (PVM) from stress, and that a rupture in the fascia will correspond to a sudden increase in stress in the PVM, resulting in a shorter active second stage and an increased risk of PVM tear.

Methods

Simulation methods used here are the same as those used in Chapters 4, 6, and 7, with the addition of a fascia that experiences loading by the fetal head in parallel with the PVM. This fascia is assumed to have 33% the initial cross sectional area of the PVM, and a failure criteria half that of the PVM, or a stress*strain product of 1.35 MPa. These values were chosen as fractions larger then this allow the fascia to shield the PVM enough to prevent progress on additional pushes in particularly long second stages, and values lower than this become trivial in their effect on forces felt by the PVM. Both the PVM and the fascia were assumed to be incompressible. Due to differences in resting anatomy, strains and resulting changes in cross sectional area were not identical between the PVM and the fascia. Therefore, the ratio between their two cross sectional areas was allowed to change throughout the simulations. This fascia was modeled as a quasilinear visco-elastic material with the same form and co-efficient values as those found in Chapter 3. Using MRI based anatomical measurements, the fascia was assumed to be anchored laterally to the pelvis, near the anterior-posterior midline,

with an initial length of 11.7 cm in the average mother. Initial length was assumed to scale linearly with maternal capacity.

Results and Discussion

We were not able to support our hypothesis that allowing the fascia to rupture would result in an increase in PVM tear rates, as similar results were observed for the “rupture” and “no-rupture” cases (Figure A6.15). This could be the result of an increased viscous relaxation effect following rupture. In the case of rupture, the fascia is no longer able to shield the PVM from tension due to the fetal head, as a result, the stress on pushes subsequent to the rupture are higher on average than in the non-rupture case. This increase in stress in the pushes prior to fetal head crowning increase the magnitude of the viscous relaxation response. For the final contraction, during which the maximum stress*strain product in reached, it appears that the increase in stress due to a reduction in shielding from the fascia is largely balanced out by an increase in viscous relaxation (decreasing stress in the tissue). As a result, we could not support our hypothesis that rupture would result in an increase in PVM tear risk.

Fascia allowed to rupture at 1.35 MPa

CAPACITY (Maternal Circumference, in Percentile)	DEMAND (Fetal Head Circumference, in Percentile)														
	2.3rd	5th	10th	20th	25th	30th	40th	50th	60th	70th	75th	80th	90th	95th	97.7th
2.3rd	1.2	1.4	1.6	1.7	1.6	1.7	2.1	2.1	2.4	2.3	2.4	2.5	3.0	3.4	3.7
5th	1.0	1.0	1.2	1.3	1.4	1.5	1.6	1.8	1.9	1.7	2.1	2.0	2.4	2.6	2.9
10th	0.7	0.8	1.0	1.1	1.1	1.1	1.2	1.4	1.4	1.5	1.5	1.6	1.7	2.1	2.3
15th	0.7	0.7	0.8	0.8	1.0	0.9	1.0	1.1	1.1	1.3	1.2	1.4	1.3	1.8	1.9
20th	0.6	0.6	0.7	0.8	0.8	0.9	0.9	1.0	1.0	1.1	1.2	1.2	1.3	1.5	1.6
25th	0.5	0.6	0.6	0.7	0.8	0.7	0.9	0.9	0.9	1.0	1.1	1.1	1.3	1.2	1.5
30th	0.5	0.5	0.6	0.6	0.7	0.8	0.8	0.8	0.9	1.0	0.9	1.0	1.2	1.3	1.3
40th	0.4	0.5	0.5	0.5	0.6	0.6	0.7	0.7	0.7	0.7	0.8	0.9	1.0	1.1	1.2
50th	0.3	0.4	0.4	0.5	0.5	0.5	0.6	0.6	0.7	0.7	0.7	0.8	0.9	0.9	1.0
60th	0.3	0.4	0.4	0.4	0.4	0.5	0.5	0.5	0.6	0.6	0.6	0.7	0.7	0.7	0.9
70th	0.2	0.3	0.3	0.4	0.4	0.4	0.4	0.5	0.5	0.5	0.5	0.6	0.6	0.7	0.7
75th	0.2	0.3	0.3	0.3	0.4	0.4	0.4	0.4	0.5	0.5	0.5	0.5	0.5	0.7	0.7
80th	0.2	0.2	0.3	0.3	0.3	0.3	0.4	0.4	0.4	0.4	0.5	0.5	0.5	0.6	0.6
85th	0.2	0.2	0.3	0.3	0.3	0.3	0.3	0.4	0.3	0.4	0.4	0.5	0.4	0.5	0.6
90th	0.2	0.2	0.2	0.2	0.2	0.3	0.3	0.3	0.3	0.3	0.4	0.4	0.5	0.5	0.5
95th	0.1	0.2	0.2	0.2	0.2	0.2	0.2	0.3	0.3	0.3	0.3	0.3	0.4	0.4	0.4
97.7th	0.1	0.1	0.1	0.2	0.2	0.2	0.2	0.2	0.2	0.3	0.2	0.3	0.3	0.4	0.4

Fascia not allowed to rupture

CAPACITY (Maternal Circumference, in Percentile)	DEMAND (Fetal Head Circumference, in Percentile)														
	2.3rd	5th	10th	20th	25th	30th	40th	50th	60th	70th	75th	80th	90th	95th	97.7th
2.3rd	1.2	1.3	1.5	1.6	1.7	1.8	2.0	2.1	2.3	2.4	2.4	2.6	3.0	3.2	3.6
5th	1.0	1.0	1.2	1.3	1.4	1.5	1.6	1.7	1.8	1.8	2.0	2.0	2.2	2.6	2.6
10th	0.7	0.8	1.0	1.1	1.1	1.1	1.2	1.3	1.2	1.5	1.5	1.6	1.7	2.0	2.2
15th	0.7	0.7	0.8	0.8	1.0	0.9	1.0	1.1	1.1	1.3	1.2	1.4	1.6	1.7	1.7
20th	0.6	0.6	0.7	0.8	0.8	0.9	0.9	1.0	1.0	1.1	1.2	1.2	1.3	1.5	1.6
25th	0.5	0.6	0.6	0.7	0.8	0.7	0.9	0.9	0.9	1.0	1.1	1.1	1.3	1.2	1.5
30th	0.5	0.5	0.6	0.6	0.7	0.8	0.8	0.8	0.9	1.0	0.9	1.0	1.2	1.3	1.3
40th	0.4	0.5	0.5	0.5	0.6	0.6	0.7	0.7	0.7	0.7	0.8	0.9	1.0	1.1	1.2
50th	0.3	0.4	0.4	0.5	0.5	0.5	0.6	0.6	0.7	0.7	0.7	0.8	0.9	0.9	1.0
60th	0.3	0.4	0.4	0.4	0.4	0.5	0.5	0.5	0.6	0.6	0.6	0.7	0.7	0.7	0.9
70th	0.2	0.3	0.3	0.4	0.4	0.4	0.4	0.5	0.5	0.5	0.5	0.6	0.6	0.7	0.7
75th	0.2	0.3	0.3	0.3	0.4	0.4	0.4	0.4	0.5	0.5	0.4	0.5	0.5	0.7	0.7
80th	0.2	0.2	0.3	0.3	0.3	0.3	0.4	0.4	0.4	0.4	0.5	0.5	0.5	0.6	0.6
85th	0.2	0.2	0.3	0.3	0.3	0.3	0.3	0.4	0.3	0.4	0.4	0.5	0.4	0.5	0.7
90th	0.2	0.2	0.2	0.2	0.2	0.3	0.3	0.3	0.3	0.3	0.4	0.4	0.5	0.5	0.5
95th	0.1	0.2	0.2	0.2	0.2	0.2	0.2	0.3	0.3	0.3	0.3	0.3	0.4	0.4	0.4
97.7th	0.1	0.1	0.1	0.2	0.2	0.2	0.2	0.2	0.2	0.3	0.2	0.3	0.3	0.4	0.4

Figure A6.15 – Predicted levator state parameter across pairings of maternal capacity-to-fetal head demand are shown for scenarios where the fascia is allowed to rupture when the product of stress*strain reaches 1.35 MPa (upper) and when fascia is not allowed to rupture (lower). The intensity of the (red) shading indicates the extent by which the predicted PVM tear threshold is exceeded. The dashed line indicates this threshold for PVM tears.

In simulations where the fascia ruptured, the active second stage of labor did not progress more rapidly than in no-rupture simulations for the same capacity-demand pairing (Figure A6.16). Therefore, we were not able support our hypothesis that allowing the fascia to rupture would result in a decrease in the duration of the active second stage. This could be due to the

fact that the fascia ruptured too late in labor for noticeable duration effects to occur, discussed below.

Fascia allowed to rupture at 1.35 MPa

CAPACITY (Maternal Circumference, in Percentile)	DEMAND (Fetal Head Circumference, in Percentile)														
	2.3rd	5th	10th	20th	25th	30th	40th	50th	60th	70th	75th	80th	90th	95th	97.7th
2.3rd	142	148	160	175	181	187	196	208	217	232	241	250	277	304	340
5th	100	106	112	121	124	127	133	139	145	154	157	163	175	190	205
10th	73	76	79	85	88	91	94	97	100	106	109	112	121	127	136
15th	58	61	64	70	70	73	76	79	82	85	88	88	88	100	106
20th	49	52	55	58	61	61	64	67	70	73	73	76	82	85	91
25th	43	46	49	52	52	55	55	58	61	64	64	67	70	76	79
30th	37	40	43	46	46	46	49	52	52	55	58	58	61	64	70
40th	31	31	34	37	37	37	40	40	43	46	46	46	49	52	55
50th	25	25	28	28	31	31	31	34	34	37	37	38	40	43	46
60th	19	19	22	25	25	25	25	28	28	31	31	31	34	37	37
70th	16	16	16	19	19	19	22	22	22	25	25	25	28	28	31
75th	13	13	16	16	16	16	19	19	19	22	22	22	25	25	28
80th	10	10	13	13	13	16	16	16	16	19	19	19	22	22	25
85th	10	10	10	10	13	13	13	13	16	16	16	16	19	19	19
90th	7	7	7	10	10	10	10	10	10	13	13	13	13	16	16
95th	4	4	4	7	7	7	7	7	7	7	10	10	10	10	13
97.7th	1	1	4	4	4	4	4	4	4	4	7	7	7	7	7

Fascia not allowed to rupture

CAPACITY (Maternal Circumference, in Percentile)	DEMAND (Fetal Head Circumference, in Percentile)														
	2.3rd	5th	10th	20th	25th	30th	40th	50th	60th	70th	75th	80th	90th	95th	97.7th
2.3rd	142	151	160	175	181	187	196	208	217	232	241	250	277	307	340
5th	100	106	112	121	124	127	133	139	145	154	157	163	178	190	208
10th	73	76	79	85	88	91	94	97	103	106	109	112	121	127	136
15th	58	61	64	70	70	73	76	79	82	85	88	88	94	100	109
20th	49	52	55	58	61	61	64	67	70	73	73	76	82	85	91
25th	43	46	49	52	52	55	55	58	61	64	64	67	70	76	79
30th	37	40	43	46	46	46	49	52	52	55	58	58	61	64	70
40th	31	31	34	37	37	37	40	40	43	46	46	46	49	52	55
50th	25	25	28	28	31	31	31	34	34	37	37	37	40	43	46
60th	19	19	22	25	25	25	25	28	28	31	31	31	34	37	37
70th	16	16	16	19	19	19	22	22	22	25	25	25	28	28	31
75th	13	13	16	16	16	16	19	19	19	22	22	22	25	25	28
80th	10	10	13	13	13	16	16	16	16	19	19	19	22	22	25
85th	10	10	10	10	13	13	13	13	16	16	16	16	19	19	19
90th	7	7	7	10	10	10	10	10	10	13	13	13	13	16	16
95th	4	4	4	7	7	7	7	7	7	7	10	10	10	10	13
97.7th	1	1	4	4	4	4	4	4	4	4	7	7	7	7	7

Figure A6.16 - Predicted duration of the active second stage across pairings of maternal capacity-to-fetal head demand are shown for scenarios where the fascia is allowed to rupture when the product of stress*strain reaches 1.35 MPa (upper) and when fascia is not allowed to rupture (lower). The intensity of the (blue) shading indicates the extent by which the clinical threshold for intervention of 180 minutes is exceeded. The dashed, dot-dashed, and dot-dot-dashed lines indicate 3 hour, 2 hour, and 1 hour cutoffs respectively.

In many simulations where the fascia ruptured, it did so on the very last contraction, as the fetal head crowns, when both stress and strain were at their highest. However, in simulations with especially small starting maternal anatomy (low maternal capacities) and large fetal head demands, the stress and strain required for progress to occur early on during labor were large enough that the fascia sometimes ruptured one or two contractions (3 or 6 minutes) before the end of the active second stage (Figure A6.17). Additionally, it will be noted that there are some gaps in Figure A6.17 between predicted fascia ruptures. These gaps corresponded to pairings in which the fetal head just barely failed to deliver by the end of a contraction, allowing for further stress relaxation prior to the final contraction that was sufficient to prevent a fascia rupture.

		DEMAND (Fetal Head Circumference, in Percentile)														
		2.3rd	5th	10th	20th	25th	30th	40th	50th	60th	70th	75th	80th	90th	95th	97.7th
CAPACITY (Maternal Circumference, in Percentile)	2.3rd	100%	100%	100%	100%	98%	98%	100%	99%	100%	99%	99%	99%	99%	99%	98%
	5th	100%	100%	100%	100%	100%	100%	100%	100%	100%	98%	100%	100%	100%	100%	100%
	10th		100%	100%	100%	100%	100%	100%	100%	100%	100%	100%	100%	100%	100%	100%
	15th		100%	100%	100%	100%	100%	100%	100%	100%	100%	100%	100%	100%	100%	100%
	20th				100%	100%	100%	100%	100%	100%	100%	100%	99%	100%	100%	100%
	25th				100%	100%		100%	100%	100%	100%	100%	100%	100%	100%	100%
	30th							100%	100%	100%	100%		100%	100%	100%	100%
	40th						100%			100%			100%	100%	100%	100%
	50th													100%		
	60th															100%
	70th															
	75th															
	80th															
	85th															
	90th															
	95th															
	97.7th															

Figure A6.17 – The time point when the fascia ruptured, as a fraction of the total duration of the active second stage is shown across pairings of maternal capacity-to-fetal head demand.

Conclusions

- Allowing the fascia to rupture does not appear to increase the risk of a PVM tear.

- Fascia ruptured late in the active second stage, at a maximum of six minutes prior to fetal head crowning.
- Due to the late occurrence of fascia rupturing, there was no observable effect on the duration of the active second stage.

Chapter 7: A Biomechanical Simulation of the Effect of Pre-Labor Distension of the Lower Birth Canal on the Predicted Duration of the Active Second Stage and the Risk for Levator Muscle Tear

Paige V Tracy[1], John O L DeLancey[2], James A Ashton-Miller[3]
[1] Department of Biomedical Engineering, University of Michigan
[2] Department of Obstetrics and Gynecology, University of Michigan
[3] Department of Mechanical Engineering, University of Michigan

7.1 Abstract

The goal of this paper was to explore the effect of distension of the lower birth canal to 8 cm diameter during the first stage of labor on both the predicted duration of labor and the risk for levator muscle tear. We used a previously developed viscoelastic model of the lower birth canal to simulate the effects of varying the magnitude and time course of the distension force, final canal diameter, and time between full distension and the beginning of the active second stage (delay duration). The results showed that increasing the distension force decreases the time to reach the target distention by up to 43%, but increased the risk of levator tear by up to 12%, relative to distension with a lower force. Intermittent force application increased the time to target distension. Increasing the target distension diameter decreased both the duration of the active second stage; however, it markedly increased the time needed for distention. We

conclude the primary expected benefit of pre-distending the lower birth canal would be a reduction in the predicted duration of the active second stage of labor.

7.2 Introduction

There have been several attempts to dilate the lower birth canal prior to the second stage of labor in the hopes of easing vaginal birth. For example, gourds of increasing size have traditionally been used in East Africa to gradually distend the perineum [1, 2, 3]. Based on this observation, a product, the Epi-No was developed to pre-dilate the birth canal via a silicon balloon in the weeks leading up to labor [2, 3]. Finally, a recent device has been developed that extends four panels radially outward to expand the lower birth canal using a constant force spring [1]. The ability of the latter device to apply a known distention force opens the way for biomechanical simulations to study the effect of variations in distension force and final distension diameter on the resulting length of the second stage. These simulations can be performed using methods that have previously been used to study biomechanical factors affecting the risk of predicted pubovisceral muscle (PVM) tears as well as labor duration. The PVM forms a U-shaped sling around the lower birth canal which the fetal head must distend and pass through in order to be delivered [4, 5, 6].

The ability to study PVM tears as an outcome is relevant because these tears are linked to the later development of pelvic organ prolapse [7, 8, 9], for which approximately 10% of women eventually require surgery [10, 11, 12, 13, 14]. To simplify predicted PVM tears, we will report results using a score termed the “levator state parameter”. This parameter accounts for the

roles of both stress and strain in predicting when a tear will occur, and is discussed in greater detail in the Methods section. Using this parameter, a value greater than one indicates a predicted PVM tear.

The duration of the active second stage is a clinically important outcome variable because long labors are linked to birth complications such as low Apgar scores, low umbilical artery pH, higher rates of resuscitation and ICU admission, higher rates of hypoxic-ischemia encephalopathy, cesarean procedures for non-reassuring fetal heart tones, as well as maternal risk for chorioamnionitis and post-partum hemorrhage [15, 16, 17, 18, 19]. So if distention of the distal birth canal can shorten the active second stage or result in a higher rate of vaginal birth without operative intervention, this would be a positive outcome, particularly if the risk for levator tears is also reduced. This paper uses biomechanical model simulations to address a knowledge gap: whether lower birth canal distention prior to the active second stage of labor could have beneficial effects, and if so, under what conditions. These models allow specific situations to be manipulated in ways that clinical testing cannot control. Given the viscoelastic nature of the lower birth canal (Chapter 3), we tested the primary hypothesis that increasing the final distension diameter of the lower birth canal reduces the duration of the active second stage. We also tested the secondary hypotheses that increasing the magnitude of the distension force decreases the time to target birth canal diameter, and that the intermittent application of the distension force would reduce the risk of levator tear.

7.3 Methods

Birth Simulations

We have previously quantified the relationship between the amount of force experienced by the birth canal tissue normalized over the wall tissue cross sectional area (stress) and the current length of the canal tissue relative to its resting length (strain). This stress–strain relationship was identified from data resulting from the clinical trial of a device designed for the purpose of distending the lower birth canal prior to the second stage of labor [1]. Full details on how this viscoelastic relationship was quantified using the force -distension data acquired using the device have been published previously (Chapter 3). In brief, we employed a five-parameter Fung model designed for use in characterizing soft tissue response to stretch [20]. The main results showed that most of the variation in canal material properties among mothers was found to be in the long time constant (Chapter 4). In the present simulations, we therefore used the median value of this long time constant for all simulations. All simulations were run in MATLAB R2015a using a time step size of 0.1 seconds. This theoretical study was exempt from institutional review board review.

Birth simulations were run by studying lower birth canal diameter in three phases: the first was a period of birth canal distention using a constant distension force to achieve the target canal diameter (during the first stage of labor), the second was a delay interval characterized by setting the magnitude of the distention force to zero, and the third was simulated active second stage of labor during which the fetal head is actively pushed through the lower birth canal. The duration of time after target distension was achieved and before the beginning of the active

second stage of labor (delay duration) was varied between 0 minutes, 10 minutes, 1 hour, 3 hours, 5 hours and 10 hours, and was controlled at 60 minutes in simulations where delay duration was not the independent variable of study. The magnitude of the distention force was varied between three nominal values corresponding to the settings available on the Materna Dilator Device: 28 N (low force), 35 N (medium force) and 42 N (high force), and was controlled at 28 N in simulations when distention force was not the focus of the simulations. Likewise, the effect of target lower birth canal distension diameter was simulated by varying it from 5 to 10 cm in 0.5 cm increments, but was controlled at 8 cm in simulations in which the target canal distension diameter was not the parameter of interest, as this corresponds to original device parameters. In simulations when an intermittent distention force was employed, intervals of constant force lasting 1, 5, 10, and 20 minutes were employed with correspondingly long intervals of zero force application interposed.

With the exception of the intermittent loading scenario, simulations of birth canal distention were driven by a constant force acting radially outward on the PVM and sub-pubic arch. Due to the configuration of the opposing panels, the force settings described above were divided by two in order to account for the force applied by each panel. This constant force was applied continuously until the target distension threshold was reached whereupon the force was removed. After removal and before the second stage of labor, it was assumed that no distention forces acted on the PVM during the delay interval. For intermittent loading simulations, for each loading cycle, a constant distention force was applied, followed by an interval of the same duration with zero force applied. This loading cycle was repeated until the target birth canal diameter had been achieved.

The initial diameter of the maternal lower birth canal was estimated for the 15th, 20th, and 50th percentile female based on the Tracy et al. (2016) geometric model. The 15th and 20th percentile mothers were chosen as they are close to the threshold for clinically observed PVM tear rates. This model considered the maternal birth canal capacity to be determined by the subpubic arch angle, PVM origin location, and PVM length, with a portion of the PVM wrapping around the pelvis due to descent of tissues during birth [21]. Fetal demand was represented as the 50th percentile fetal head with average molding [21]. The cross sectional area of the molded fetal head in the plane in which it presents to the urogenital hiatus was assumed to be circular. The PVM was modeled as a single incompressible element using a five parameter Fung Quasilinear Viscoelastic model [20]; it was represented with an initial cross-sectional area of 1.2 cm^2 on each side [22], with strain only in the circumferential direction. As a result, uniform stress and strain distributions were assumed.

Simulations of vaginal birth during the second stage were driven by intrauterine pressure as an input, as measured in previous experiments: this included a 2.6 kPa basal intrauterine pressure, an 8.5 kPa rise during contractions, and an additional 10.5 kPa rise during each volitional push [23]. Contractions and pushes were each modeled as the first half of one period of a cosine wave. Specifically, contractions were assumed to last for 90 seconds, followed by 90 second rest; three 10 second pushes were assumed per contraction, each modeled as the first half of a 20 second sinusoidal wave, with each followed by 10 seconds of rest [23, 24, 25]. Tension in the PVM was assumed to be the result of abdominal pressure acting on the cross-sectional area of the fetal head, resulting in a contact force between the fetus and the PVM (Figure 7.6S). Zero friction between the fetal head and the PVM was assumed.

We quantified the likelihood of a PVM tear using a 'levator state parameter', whereby a value greater than 1 indicates that the threshold for injury has been exceeded. This parameter was based on the product of stress multiplied by strain as a reasonable criterion for injury in vaginal tissue and ligamentous injury; an exact value of 2.7 MPa for the threshold for injury was chosen based on the measured conditions for the ultimate failure of pregnant ovine tissue estimated graphically [26, 27, 28, 29, 30, 31, 32].

In the following results section, the outcomes are presented in order that they occur during a birth: the time to reach the target distension diameter, the duration of the active second stage, and the levator tear outcome.

7.4 Results

The time to reach target canal distension was influenced by both the magnitude of the distension force and duty cycle (Figure 7.1). These results support our secondary hypothesis that increasing the distension force decreased the time to target distension, effectively increasing the rate of distension. For example, increasing the distension force from 28 N to 42 N resulted in a 43% decrease in the time to reach target distension, while increasing from 28 N to 35 N resulted in a 27% decrease in this variable.

For the case of intermittent force application, increasing the duration of force application in each loading cycle resulted in a decrease in the time needed to reach the target distension by up to 22%. However, all intermittent loading cases lasted considerably longer than the constant distension simulations, with the duration increasing up to 270% relative to a constant distension control.

The time to reach the target distension increased markedly with target distention diameters greater than approximately 8 cm. The effects observed for varying distension force and intermittent loading scenarios were also most distinct at these larger target distension diameters.

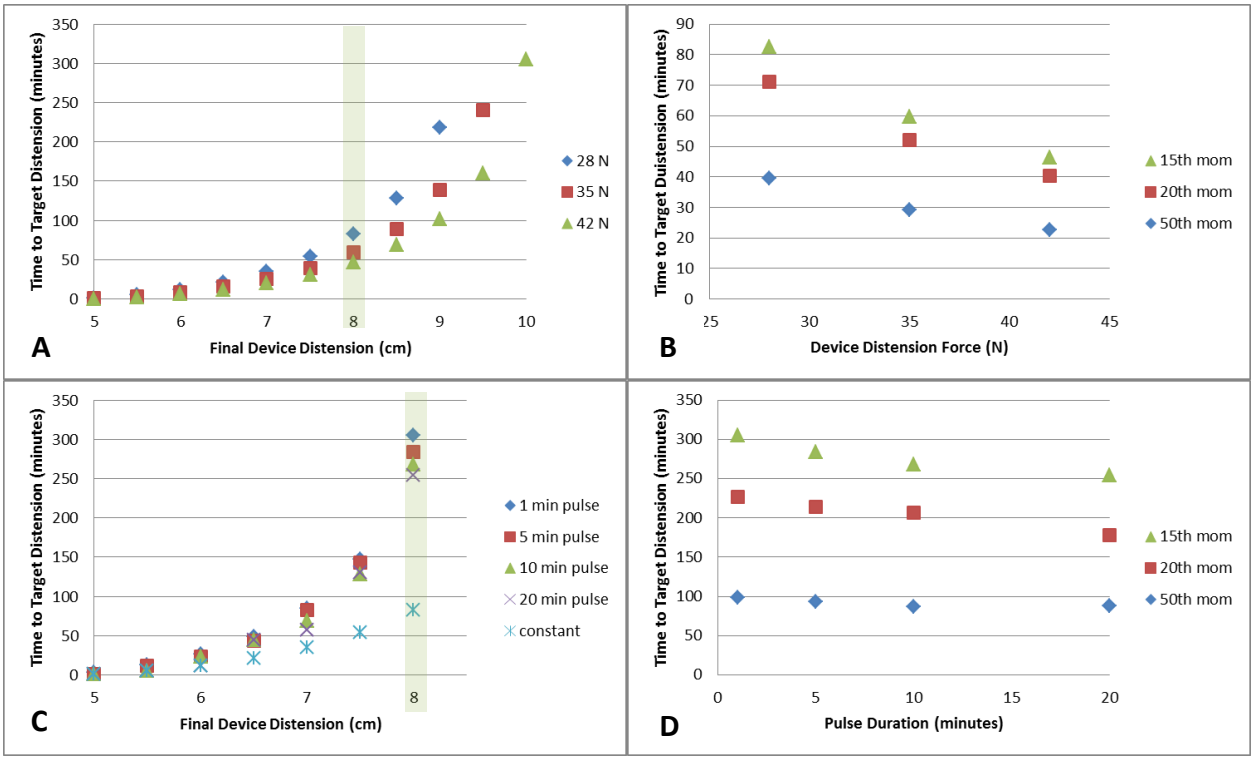

Figure 7.1 - Time to target distension with increasing distension force (upper row – A, B) and intermittent loading cycle duration (lower row – C, D). The plots on the left (A,C) vary the target distension, while in the plots on the right (B,D), target distension was held constant at 8 cm (green bar on left plots – A,C). All results are for the 50th percentile fetal demand. The 15th percentile maternal capacity is reported on the left, while the 15th, 20th, and 50th percentile maternal capacity cases are reported on the right.

The duration of the active second stage decreased proportionately with increasing target distension diameter for the 10 min delay duration case (Figure 7.2), supporting our main hypothesis that increasing the final distension diameter of the lower birth canal reduces the

duration of the active second stage. This effect became less pronounced as the duration of time between device removal and the beginning of the active second stage (delay time) was increased, with almost no benefits on active second stage duration being observed for the 10 hour delay duration case. A reduction in the duration of time between device removal and the beginning of the active second stage resulted in up to a 76% decrease in the duration of the active second stage. This decrease in the duration of active second stage for shorter delay durations resulted in a consistent trend for the 15^{th}, 20^{th}, and 50^{th} maternal capacity cases, when each case was normalized by a no-pre-distension control for each maternal capacity (Figure 7.2, lower left).

Intermittent loading cycle duration also had a small effect on the duration of the active second stage (Figure 7.5S). This effect was primarily apparent only for the 1 minute intermittent loading case, for which there was an approximately 10% decrease in the duration of the active second stage when compared to both constant dilation and longer intermittent loading cycle duration cases.

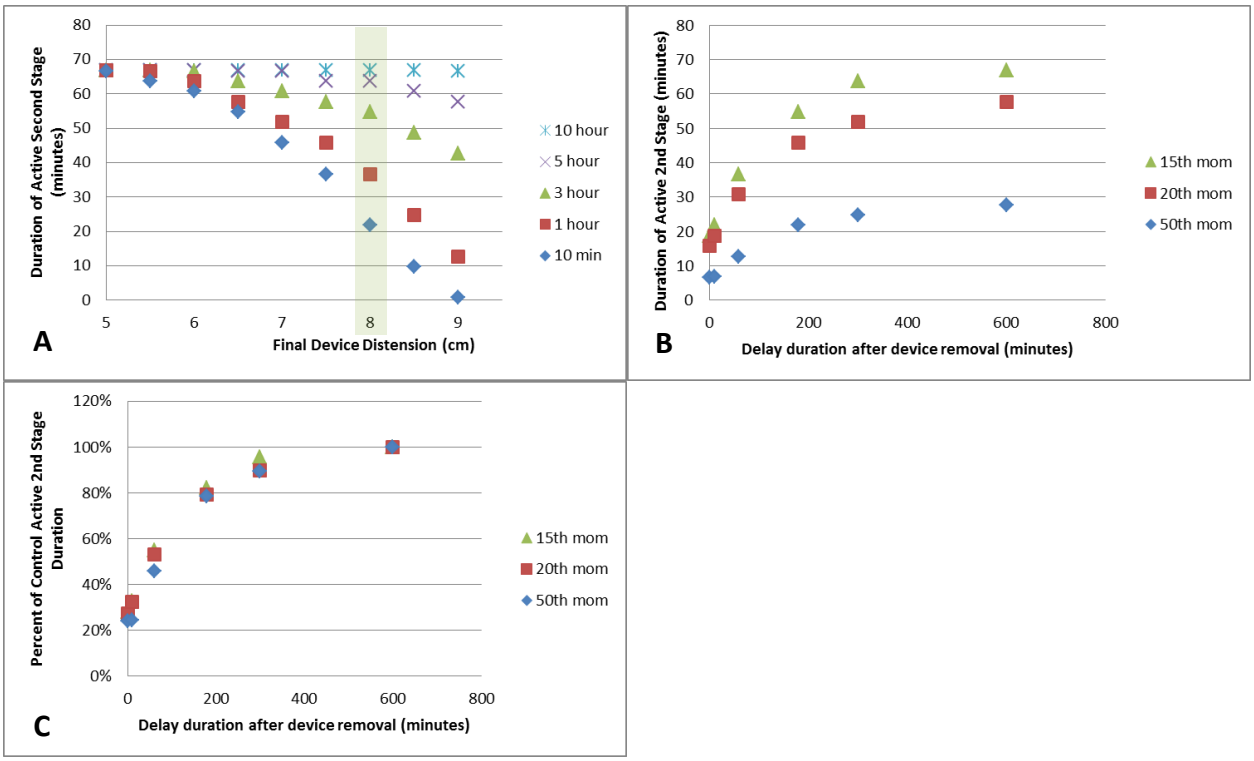

Figure 7.2 - Duration of active second stage with increasing delay interval length. Plot A varies the target distension, while in the remaining plots, target distension was held constant at 8 cm (green bar in A). All results are for the 50th percentile fetal demand. The 15th percentile maternal capacity is reported in plot A, while the 15th, 20th, and 50th percentile maternal capacity cases are reported in the remaining plots. In plot C, duration values are normalized by a no-pre-distension control for each maternal capacity.

The levator state parameter, an indicator for predicted PVM tear risk, showed only a slight dependence on delay duration, distension force as well as intermittent loading cycle duration (Figure 7.3). The most consistent of these was the magnitude of the distension force, with up to a 12% increase in levator state parameter observed when distension force was increased from 28 N to 42 N. Intermittent loading cycles 1 minute in duration increased the levator state parameter by approximately 10%. Loading cycles of longer duration had no distinct effect on the levator state parameter. As a result, we were unable to strongly support our secondary hypothesis that the intermittent application of the distension force would reduce the risk of

levator tear. However, this was primarily a case of the 1 minute intermittent loading case having increased levator state parameter values relative to no-pre-distension controls and longer intermittent loading cycle duration cases. A delay duration of approximately 1 hour led to a decrease in levator state parameter values of approximately 15%.

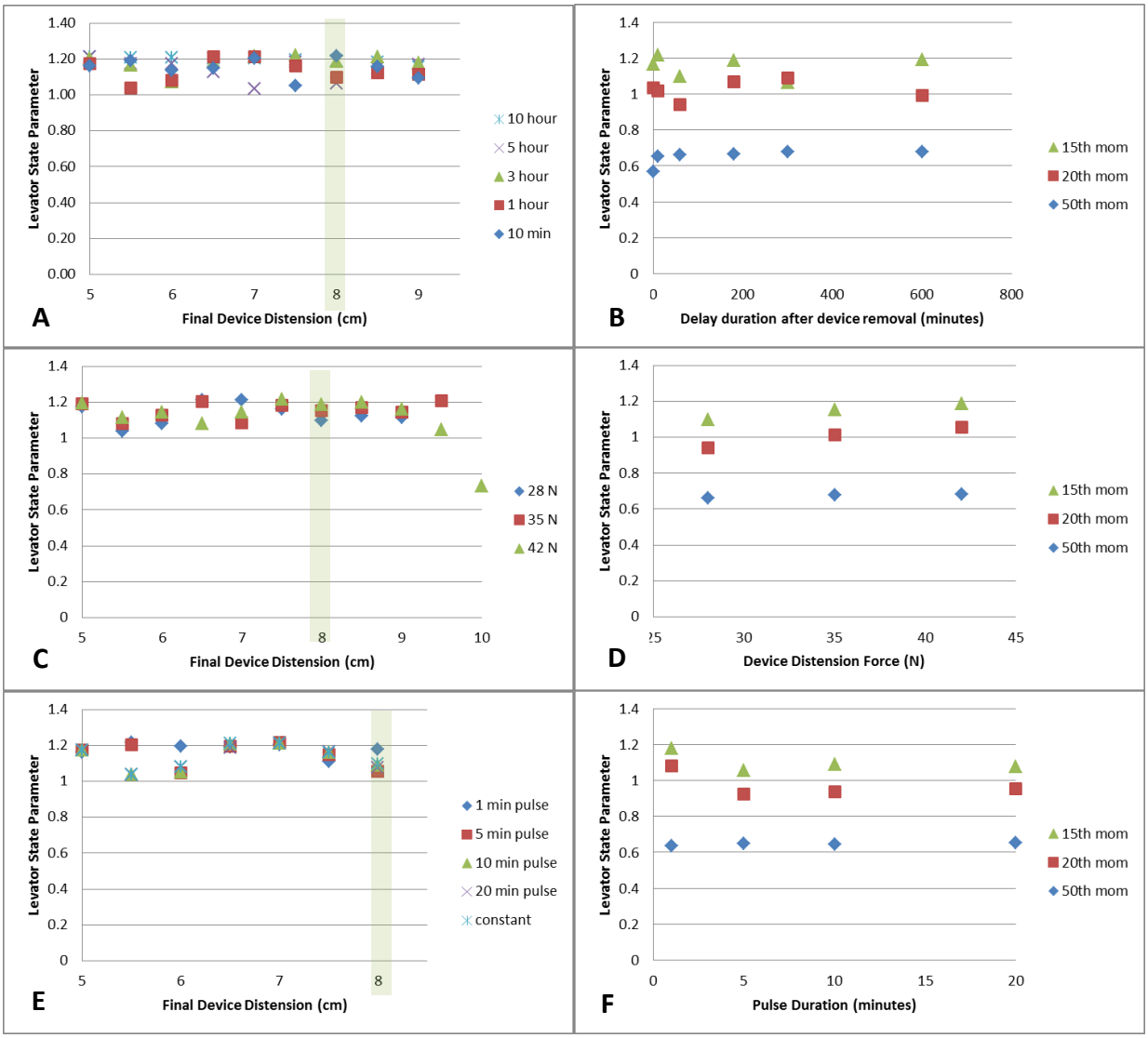

Figure 7.3 - The value for the levator state parameter for increasing delay durations (upper row – A,B), distension force (middle row – C,D), and intermittent loading cycle duration (lower row – E,F). The plots on the left (A,C,E) vary the target distension, while in the plots on the right (B,D,F), target distension was held constant at 8 cm (green bar on left plots). All results are for the 50th percentile fetal demand case. The 15th percentile maternal capacity is reported on the left, while the 15th, 20th, and 50th percentile maternal capacity cases are reported on the right.

7.5 Discussion

To our knowledge, this is the first biomechanical study to consider the effect of the theoretical pre-distension of the birth canal during the first stage of labor and its effects on labor outcomes. A large prospective study varying all of the parameters studied here would not be feasible due to cost and undue subject burden. However, biomechanical modeling lends itself to exploring which parameters might be important without creating risk of physical or psychological harm to the patient.

Our primary hypothesis that increasing the final distension diameter of the lower birth canal reduces the duration of the active second stage was supported when the duration of delay prior to the beginning of the active second stage was around an hour, but this reduction in the duration of the active second stage became less pronounced as the delay phase increased in duration and the tissues had time to recoil towards their original state. Our secondary hypothesis that increasing the magnitude of the distension force decreases the time to target birth canal diameter was also supported. However, the hypothesis that the intermittent application of the distension force would reduce the risk of levator tear was rejected, as this scenario resulted in up to a 270% increase in the time to reach the target distension with no observable benefits to the duration of the active second stage or to levator tear risk.

The maximum achievable target distension varied depending on distension force and loading pattern. For constant force application scenarios, the maximum achievable target distension was 9, 9.5, and 10 cm for the 28, 35, and 42 N distension forces respectfully. Similarly, introducing intermittent loading resulted in the maximum achievable target distension being

reduced to 8 cm for scenarios with a 28 N distension force. Both of these phenomena result from a plateau or halting of progress after a few hours of distension loading. This illustrates that strategic choice of distension force magnitude and loading timing can influence the likelihood of achieving desired distension results.

The case of over-distending the birth canal, so that the target distension went ~ 0.5 cm beyond the diameter of the fetal head, was also simulated. Results showed that this resulted in an average decrease of 2% in the stress*strain metric when compared to control (no-pre-distension) for cases of 3 – 10 hours delay before the beginning of the active second stage. For the case of 60 minutes delay, this average decrease was 50% when compared to control. The reason for this decrease under short delay periods is that the tissue has experienced less recoil, or shortening, prior to the onset of the second stage and, as a result, has very little elongation necessary at the time of birth. It should be noted that the maximum instantaneous stress*strain value is not exceeded during the distension phase because the distension force (28 N, 35 N, or 42 N) is appreciably lower than the approximate force of the intrauterine pressure acting on the fetal head (approximately 150 N, based on 20 kPa intrauterine pressure at peak of contraction and 5 cm fetal head radius). However, if the assumption that the product of stress*strain determines injury is incorrect, and injury is instead purely strain determined, the 10 cm target distension would, in that case, be increasing risk for a levator tear.

A limitation of this study was that the levator state parameter fluctuated depending on the timing of fetal head crowning during a contraction. For example, if a mother is just barely able to deliver late in a contraction, the stress felt in the PVM, which contributes to the levator state

parameter, will be appreciably higher than if the mother waits till the subsequent contraction, allowing for more viscous relaxation of the PVM to occur. For target distension diameters less than 9 cm, levator state parameter dependences on target distension were outweighed by the normal variation observed due to differences in the timing of crowning during a contraction. When the target distension diameter was greater than or equal to 9 cm, a distinct decrease in levator state parameter values was observed for delay times of approximately 1 hour or less, but not for longer delay periods.

A second limitation is that delay duration cannot be controlled. However, its influence on the ability to achieve desired outcomes should be taken into account in planning this intervention. Having the dilation as close to the time a woman starts to push will be important and clinical steps to optimize this timing is important. It also suggests that if labor is slower than anticipated, a second application of the device might be warranted. The decrease in the duration of the active second stage, following pre-distension, which is distinct for 10 minute and 1 hour delay durations, is still noticeable for births after a 3 hour delay period. However, this effect is diminished in the 5 hour delay duration case, and completely absent for the 10 hour delay period case. Similarly, levator state parameter results suggest that a delay duration of approximately 1 hour is optimal; however, it is the effect on the duration of the active second stage of labor that is dominant. In general it would be ideal to wait until a few hours before the onset of the second stage of labor before pre-distension; however, such a timeline cannot be exactly predicted, and final priority should go to ensuring that the device has been safely removed before the second stage begins.

For these simulations, we assumed an inexhaustible mother. Because we did not assess the energy expenditure to deliver the baby, we cannot determine whether the shortened second state would allow more women to deliver vaginally by allowing delivery before maternal exhaustion reduces pushing efforts. It is reasonable to assume that a shorter second stage will allow more women to deliver without the need to resort to forceps or vacuum or to cesarean section. All of these interventions increase risks for mother and infant. Further simulations should allow these important factors to be assessed.

7.6 Conclusions

1) Increasing the target distension diameter of the birth canal was predicted to shorten the active second stage of labor, an effect that could be of particular benefit in reducing complications associated with long labors.

2) Increasing birth canal distension force results in a tradeoff between decreased time to target distension, corresponding to lower patient burden, but a slight increase in predicted PVM tear risk.

3) Intermittent loading increased the time to reach the target distension, with no observable benefit to the duration of the active second stage or levator tear risk.

Acknowledgements

We gratefully acknowledge financial support from the Office for Research on Women's Health SCOR program on Sex Differences in Women's Health (P50 HD 44406). We thank Dr. Mark Juravic of Materna Medical, Inc., for contributing device data and insight in the absence of any

financial support, and colleagues at the Baylor College of Medicine for conducting the clinical trial that gave rise to the Materna data.

7.7 Bibliography

[1] M. Juravik and M. Stewart, "Methods and apparatus for preventing vaginal lacerations during childbirth". United States Patent US 20130053863 A1, 28 February 2013.

[2] K. Shek, V. Chantarasom, S. Langer, H. Phipps and H. Dietz, "Does the Epi-No Birth Trainer reduce levator trauma? A randomised controlled trial," *International Urogynecology Journal,* vol. 22, no. 12, pp. 1521-8, 2011.

[3] T. Kavvadias and I. Hoesli, "The EpiNo Device: efficacy, tolerability, and impact on pelvic floor-implications for future research," *Obstetrics and Gynecology International,* pp. e1-5, 2016.

[4] R. Margulies, M. Huebner and J. O. L. DeLancey, "Origin and insertion points involved in levator ani muscle defects," *American Journal of Obstetrics and Gynecology,* vol. 196, no. 3, pp. 251-255, 2007.

[5] C. Betschart, J. Kim, J. M. Miller, J. A. Ashton-Miller and J. O. L. DeLancey, "Comparison of muscle fiber directions between different levator ani muscle subdivisions: in vivo MRI measurements in women," *International Urogynecology Journal,* vol. 25, no. 9, pp. 1263-1268, 2014.

[6] J. Kim, C. Betschart, R. Ramanah, J. Ashton-Miller and J. O. L. DeLancey, "Anatomy of the pubovisceral muscle origin: Macroscopic and microscopic findings within the injury zone," *Neurourology and Urodynamics,* vol. 34, no. 8, pp. 774-780, 2015.

[7] J. O. L. DeLancey, R. Kearney, Q. Chou, S. Speights and S. Binno, "The Appearance of Levator Ani Muscle Abnormalities in Magnetic Resonance Images After Vaginal Delivery," *Obstetrics and Gynecology,* vol. 101, no. 1, pp. 46-53, 2003.

[8] H. Dietz and A. Steensma, "The prevalence of major abnormalities of the levator ani in urogynaecological patients," *BJOG: an International Journal of Obstetrics and Gynaecology,* vol. 113, no. 2, pp. 225-30, 2006.

[9] H. Dietz, G. AV and P. Phadke, "Avulsion of the pubovisceral muscle associated with large vaginal tear after normal vaginal delivery," *The Australian & New Zealand Journal of Obstetrics & Gynaecology,* vol. 47, no. 4, pp. 341-4, 2007.

[10] A. Olsen, V. Smith, J. Bergstrom, J. Colling and A. Clark, "Epidemiology of surgically managed pelvic organ prolapse and urinary incontinence," *Obstetrics and Gynecology,* vol. 89, no. 4, pp. 501-6, 1997.

[11] F. Smith, C. Holman, R. Moorin and N. Toskos, "Lifetime risk of undergoing surgery for pelvic organ prolapse," *Obstetrics and Gynecology,* vol. 116, no. 5, pp. 1096-100, 2010.

[12] M. Abdel-Fattah, A. Farnilusi, S. Fielding, J. Ford and S. Bhattacharya, "Primary and repeat surgical treatment for female pelvic organ prolapse and incontinence in parous women in the UK: a register linkage study," *BMJ Open,* vol. 1, no. 2, p. e000206, 2011.

[13] T. de Boer, M. Slieker-Ten Hove, B. CW, K. Kluivers and V. ME, "The prevalence and factors associated with previous surgery for pelvic organ prolapse and/or urinary incontinence in a

cross-sectional study in The Netherlands," *European Journal of Obstetrics, Gynecology, and Reproductive Biology,* vol. 158, no. 2, pp. 343-9, 2011.

[14] J. Wu, C. Matthews, M. Conover, V. Pate and M. Jonsson Funk, "Lifetime risk of stress urinary incontinence or pelvic organ prolapse surgery," *Obstetrics and Gynecology,* vol. 123, no. 6, pp. 1201-6, 2014.

[15] J. Senecal, X. Xiong and W. D. Fraser, "Effect of Fetal Position on Second-Stage Duration and Labor Outcome," *Obstetrics and Gynecology,* vol. 105, no. 4, pp. 763-772, 2005.

[16] A. T. Bleich, J. M. Alexander, D. D. McIntire and K. J. Leveon, "An Analysis of Second-Stage Labor beyond 3 Hours in Nulliparous Women," *American Journal of Perinatology,* vol. 29, no. 9, pp. 717-722, 2012.

[17] K. J. Leveno, D. B. Nelson and D. D. McIntire, "Second-stage labor: how long is too long?," *American Journal of Obstetrics and Gynecology,* vol. 214, no. 4, pp. 484-489, 2016.

[18] S. K. Laughon, V. Berghella, U. M. Reddy, R. Sundaram, Z. Lu and M. K. Hoffman, "Neonatal and Maternal Outcomes With Prolonged Second Stage of Labor," *Obstetrics and Gynecology,* vol. 124, no. 1, pp. 57-67, 2014.

[19] D. Rouse, S. Weiner, S. Bloom, M. Varner, C. Spong, S. Ramin, S. Caritis, A. Peaceman, Y. Sorokin, A. Sciscione, M. Carpenter, B. Mercer, J. Thorp, F. Malone, M. Harper, J. Iams and G. Anderson, "Second-stage Labor Duration in Nulliparous Women: Relationship to Maternal and Perinatal Outcomes," *American Journal of Obstetrics and Gynecology,* vol. 201, no. 4, pp. 357.e1-7, 2009.

[20] Y. C. Fung, Biomechanics: Mechanical Properties of Living Tissues, New York, NY: Springer-Verlag, 1993.

[21] P. V. Tracy, J. O. L. DeLancey and J. A. Ashton-Miller, "A Geometric Capacity - Demand Analysis of Maternal Levator Muscle Stretch Required for Vaginal Delivery," *Journal of Biomechanical Engineering,* pp. e1-e54, 2016.

[22] V. C. Morris, M. P. Murray, J. O. L. DeLancey and J. A. Ashton-Miller, "A comparison of the effect of age on levator ani and obturator internus muscle cross-sectional areas and volumes in nulliparous women.," *Neurourology and Urodynamics,* vol. 31, no. 4, pp. 481-6, 2012.

[23] A. Rempen and M. Kraus, "Pressures on the Fetal Head During Normal Labor," *Journal of Perinatal Medicine,* vol. 19, no. 3, pp. 199-206, 1991.

[24] A. C. J. Allman, E. S. G. Genevler, M. R. Johnson and P. J. Steer, "Head-to-Cervix Force: an Important Physiological Variable in Labour. 1. The Temporal Relation Between Head-to-Cervix Force and Intrauterine Pressure During Labour," *British Journal of Obstetrics and Gynaecology,* vol. 103, pp. 763-768, 1996.

[25] C. S. Buhimschi, I. A. Buhimschi, A. M. Malinow, J. N. Kopelman and C. P. Weiner, "Pushing in Labor: Performance and Not Endurance," *American Journal of Obstetrics and Gynecology,* vol. 186, no. 6, pp. 1339-44, 2002.

[26] D. Ulrich, S. L. Edwards, K. Su, J. F. White, J. A. M. Ramshaw, G. Jenkin, J. Deprest, A. Rosamilia, J. A. Werkmeister and C. E. Gargett, "Influence of Reproductive Status on Tissue Composition and Biomechanical Properties of Ovine Vagina," *Public Library of Science,* vol. 9, no. 4, pp. 1 - 8, 2014.

[27] A. Feola, P. Moalli, M. Alperin, R. Duerr, R. Gandley and S. Abramowitch, "Impact of pregnancy and vaginal delivery on the passive and active mechanics of the rat vagina," *Annals of Biomedical Engineering,* vol. 39, no. 1, pp. 549-58, 2011.

[28] M. Alperin, A. Feola, R. Duerr, P. Moalli and S. Abramowitch, "Pregnancy- and delivery-induced biomechanical changes in rat vagina persist postpartum," *International Urogynecology Journal,* vol. 21, no. 9, pp. 1169-74, 2010.

[29] J. L. Lowder, K. M. Debes, D. K. Moon, N. Howden, S. D. Abramowitch and P. A. Moalli, "Biomechanical Adaptations of the Rat Vagina and Supportive Tissues in Pregnancy to Accommodate Delivery," *Obstetrics and Gynecology,* vol. 109, no. 1, pp. 136-143, 2007.

[30] T. J. Bonner, N. Newell, A. Karunaratne, A. D. Pullen, A. A. Amis, A. M. J. Bull and S. D. Masouros, "Strain-rate Sensitivity of the Lateral Collateral Ligament of the Knee," *Journal of the Mechanical Behavior of Biomedical Materials,* vol. 41, pp. 261-70, 2015.

[31] M. Chiba and K. Komatsu, "Mechanical Responses of the Periodontal Ligament in the Transverse Section of the Rat Mandibular Incisor at Various Velocities of Loading In Vitro," *Journal of Biomechanics,* vol. 26, no. 4, pp. 561-70, 1993.

[32] M. M. Panjabi, J. J. Crisco, C. Lydon and J. Dvorak, "The Mechanical Properties of Human Alar and Transverse Ligaments at Slow and Fast Extension Rates," *Clinical Biomechanics,* vol. 13, no. 2, pp. 112-20, 1998.

7.8 Appendix:

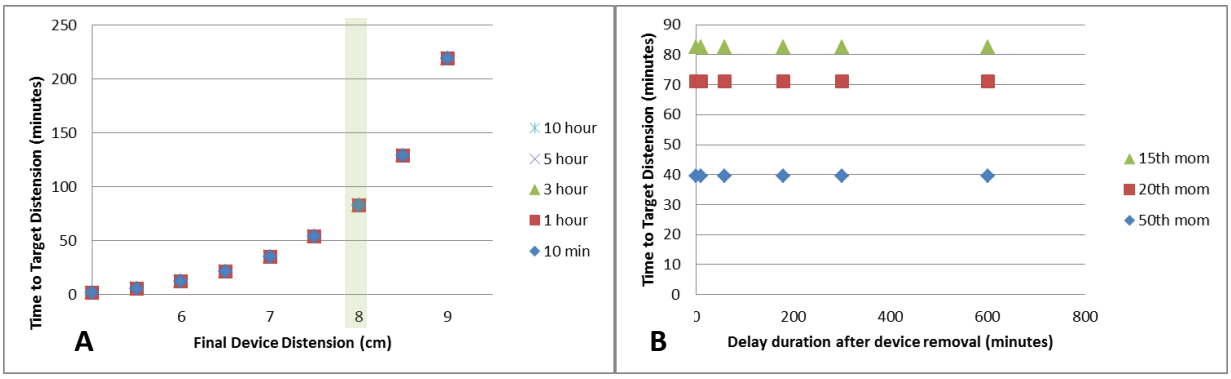

Figure 7.4S - Time to target distension with increasing delay duration. Plot A varies the target distension, while in plot B, target distension is held constant at 8 cm (green bar on left plot). All results are for the 50th percentile fetal demand. The 15th percentile maternal capacity is reported in plot A, while the 15th, 20th, and 50th percentile maternal capacity cases are reported in plot B.

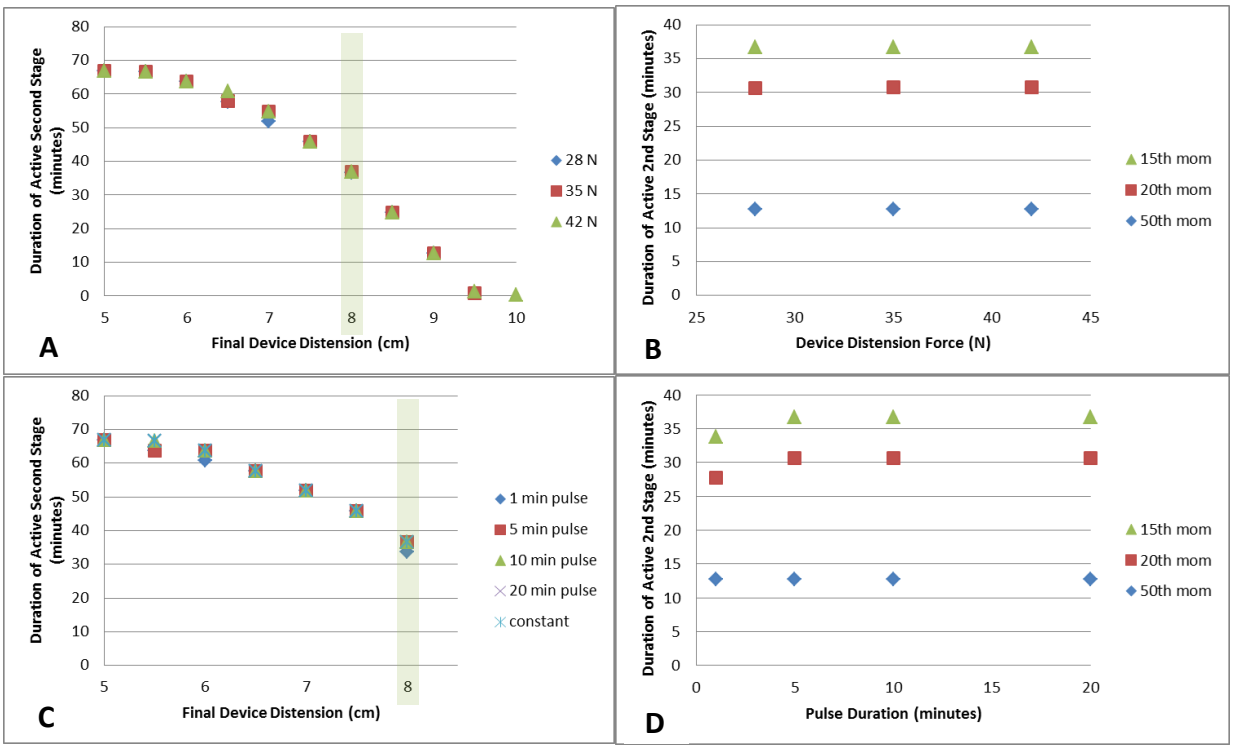

Figure 7.5S - Duration of active second stage with increasing distension force/rate (upper row – A,B) and intermittent loading cycle duration (lower row – C,D). The plots on the left (A,C) vary the target distension, while in the plots on the right (B,D), target distension was held constant at 8 cm (green bar in left plots). All results are for the 50th percentile fetal demand. The 15th percentile maternal capacity is reported on the left, while the 15th, 20th, and 50th percentile maternal capacity cases are reported on the right.

7.9 Calculations

PVM strain, ε_{PVM}, was assumed to be related to general birth canal strain, ε_{BC}, based on the ratio between their initial circumferential lengths, l_{PVM} and l_{BC} respectively [21].

$$\varepsilon_{PVM} = \frac{l_{BC}}{l_{PVM}}(\varepsilon_{BC} + 1) - 1$$

Intrauterine pressure was assumed to be related to circumferential stress in the PVM U-shaped sling, based on the following calculations (Figure 7.4S):

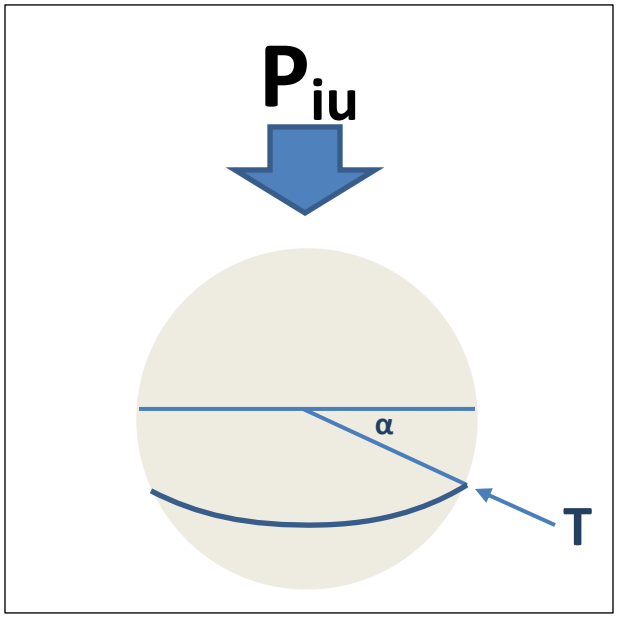

Figure 7.6S - Intrauterine pressure (blue arrow) creates a force distributed over the fetal head (grey circle). The tension (T) in the PVM (dark blue band low on head) was related to intrauterine pressure using the radius of the fetal head (light blue lines) and the angle between the midline of the fetal head and the contact point of the PVM on the fetal head (alpha).

$$T = tension\ in\ PVM$$

$$\tilde{T} = \frac{T}{2\pi r} = Tension/length$$

Balancing "Vertical" Forces: $\tilde{T}2\pi r * sin(\alpha) = P_{ab}\pi * {r_h}^2$

$$\tilde{T} = \frac{P_{ab} * {r_h}^2}{2r * sin(\alpha)}$$

Balancing "Horizontal" Forces:

$$\sigma_{PVM}2 * A_{PVM} = \tilde{T}2r * \cos(\alpha)$$

$$\sigma_{PVM} = \frac{\tilde{T} * 2r * \cos(\alpha)}{2A_{PVM}}$$

$$= \frac{P_{ab}{r_h}^2}{2A_{PVM}\tan(\alpha)}$$

Based on image analysis of the non-uniformity of the newborn fetal head, a maximum alpha value of 0.68 radians was assumed.

Chapter 8: General Discussion

Levator ani muscle tears continue to affect approximately 15% of women delivering vaginally, and have been linked to the later development of pelvic organ prolapse [1, 2, 3], for which approximately 10% of women later need surgery (See Chapter 1 for review) [4, 5, 6, 7, 8]. Apart from older maternal age [9], clinicians have not had any reliable predictors, prior to the onset of labor, with which to predict who is at highest risk for levator tears during the second stage of labor. The use of computer simulation to predict, a priori, several outcomes of the second stage of labor is a novel aspect of this dissertation. These include both the duration of the second stage of labor and the risk for a levator tear. Due to the quasi-unidimensional nature of our modeling approach, we have been able to greatly reduce simulation generation and computational time, making it possible to assess outcomes for a large variety of maternal and fetal geometric pairings. Additionally, the tabular form of the simulation results harnesses the predictive capabilities of the simulations without maternal fetal medicine personnel, or midwives needing to invest in the training necessary to run such simulations or wait for the computations to run. Essentially, a clinician needs an ultrasound machine, with which they are already familiar, and the ability to make three key measurements: subpubic arch angle, urogenital hiatus sagittal diameter, and fetal head circumference. Armed with these three numbers, they can then locate the cell in our results “look up” table that best represents the

maternal and fetal geometric pairing before them. Admittedly, since these measurements are presently new for this purpose, some training will be necessary to help these clinicians identify the correct planes in which to measure the subpubic arch angle and the urogenital hiatus, which presently are confused in the literature with the more common measurements of the retropubic arch angle and the levator hiatus, respectively. But once trained, these measurements could become as routine as the measurement of fetal head circumference is currently.

In Chapter 2, a novel framework was introduced for guiding a conversation about how we may better evaluate personalized maternal levator tear risk. In a capacity-demand analysis, we started with population data for the range in fetal head diameters and then considered the main factors that affect maternal birth canal diameter calculating how well a fetal head of any given size will fit through the range of available birth canal diameters. The resulting predictions revealed that maternal capacity plays a larger role than fetal head demand in determining levator tear risk. Therefore, any ultrasound measurements should focus first on maternal measurements, as fetal head measurements may only provide added insight if the mother is near the 20^{th} percentile. Additionally, a novel insight concerned the reason that levator tears are primarily observed in the pubovisceral muscle (PVM) portion and not in the puborectal (PRM) portion of the muscle. This difference is the result of the PVM having to wrap about the lower pelvic rami during the second stage of labor, because the PVM origins are higher on the pelvis. Our anthropometric analysis reveals that this wrapping shortens the length of the PVM available to pass around the fetal head as it descends along the Curve of Carus. The PRM, having a different line-of-action because it originates lower down from the perineal membrane,

is able to swing down in a manner similar to a bucket handle without needing to wrap around any bone that would cause a loss in the length of the loop of muscle available for the fetal head to pass through. Additionally, it is possible that friction involved in the PVM wrapping around the pelvis could affect injury risk, though we have not been able to assess this using our current modeling approach, which neglect friction. A limitation of Chapter 2 was the slight over-prediction of PVM tear prevalence in smaller women. This limitation was directly addressed in the next Chapter.

In Chapter 3, we hypothesized that the inclusion of viscoelastic effects in our Chapter 2 analysis would lead to a reduction in tear rates due to the tissue relaxation that occurs over the multiple pushes and resting periods of the second stage of labor. In order to accurately account for viscoelastic effects, it was necessary to develop a way to validate a viscoelastic constitutive model for the term pregnant human birth canal. As discussed in Chapter 3, previously data on this topic were limited to *ex vivo* data for pregnant rats, squirrel monkeys, and sheep, but as of yet no human data were available. Fortuitously, the very force-displacement data necessary to quantify the material properties of the term pregnant human birth canal had recently been collected as part of a clinical trial for a device designed to pre-distend the birth canal to 8 cm prior to the second stage of labor. The temporal relationship between the force and the displacement data was not part of the trial outcome, which instead focused on standard clinical factors such as levator tear but also the temporal rate at which the canal distended. Our realization that a constant force had been used to cause the canal distention meant that these were unique and scientifically very valuable data describing the force-displacement-time behavior of the lower birth canal in healthy human nulliparas. We therefore asked the

company and clinical team whether they would share the data for a secondary data analysis on viscoelasticity under a data use agreement, to which they graciously agreed. Using birth simulations based on this constitutive model, we were able to refine the geometric predictions in Chapter 2 to not only consider risk of PVM tear; we now also could estimate the duration of the active second stage of labor. This latter variable is clinically relevant as an indicator for interventions such as forceps or vacuum instrumentation, as well as cesarean section. A primary limitation to Chapter 3 was that our results were only based upon data from only one subject. That limitation is removed in the next Chapter, where we consider a cohort of 26 participants.

In Chapter 4, we used the force-length-time data to conduct the first analysis of the viscoelastic response of the lower birth canal to distention in 26 nulliparous women during the first stage of labor. We found marked variation across these women, especially in the long time constant, τ_2, of our Chapter 3 constitutive model. This variation among the 26 woman cohort took the form of a lognormal distribution. We then simulated births for the median, as well as the lower and upper extrema, corresponding to $1/20^{th}$ and 20X the median long time constant value. From these simulations, we were able to identify a narrow uncertainty region for the cutoff for levator tear predictions depending upon a specific mother's long time constant value (τ_2). However, the more distinct effect was on the duration of the active second stage, with a larger value of the long time constant corresponding to longer labors. Using the original *in vivo* distension data, we found that measuring the net increase in distension from the 5 minute time point to a point approximately 10 minutes later provided a reasonable correlation with this long time constant, τ_2. This information has practical importance because it could be used to

estimate an individual's long time constant, τ_2, value during the first stage of labor, allowing for a more informed delivery plan. A primary limitation is that it may not be meaningful to measure this prior to the onset of labor, because the measurement requires distension of the birth canal, and it has been hypothesized that the material properties of the birth canal may only change shortly before the onset of labor [10]. In the following chapter, we consider how our simulation-based PVM tear predictions compare to clinical occurrence.

In Chapter 5, we employed antenatal ultrasounds, paired with postnatal PVM tear diagnoses, to evaluate our model's ability to predict the duration of the second stage of labor as well as PVM tears. Our results showed that we were able to predict up to 55% of the variation in the duration of the second stage of labor for the median age group, and 22% of this variation when considering outlying age groups. This is remarkable considering that there are many factors such as fetal head presentation, maternal discomfort, and clinician instruction which affect the duration of the second stage and which are not able to be predicted prior to labor. When considering PVM tears, we were only to predict one of two major tears, and failed to predict the only minor tear observed. The two false negatives, or tears which we failed to predict, were both above the mean for maternal capacity, and below the mean for fetal head demand, indicating no anatomical risk for injury. However, these subjects had significantly older maternal age than the rest of the cohort. Additionally, the false positives, or subjects who were predicted to experience injuries, but who did not display an injury upon ultrasound examination, had significantly longer durations of the second stage than the rest of the cohort. This suggests that we are able to predict the difficulty of labor, assuming that a long labor is indicative of resistance to the passage of the fetal head. When considering the ratio of fetal

head circumference to levator hiatus circumference, which has recently been shown to correlate to PVM tears [11], none of the three subjects who experience a PVM tear were predicted to be at risk. This suggests that, with a larger cohort, our prediction methods would be expected to perform at least to the level of this previously reported correlation. That the difficult labors in the present study did not correspond to PVM tears, and that PVM tears occurred in older mothers with no anatomical risk factors, suggests that the threshold for injury may not be constant across subjects. Investigation into factors affecting injury threshold is therefore a fruitful area for future research. In the following chapter, we return to biomechanical simulations to consider the cause of high PVM tear rates when forceps instrumentation is employed.

In Chapter 6, we investigated why PVM tear rates of up to 60% are observed in forceps-assisted deliveries, but not in vacuum-assisted deliveries. Using the Chapter 2 geometric analysis techniques, we were able to reject the hypothesis that the additional space occupied by the forceps “blades” are responsible for this increase, because they had less than a 2% effect on predicted levator tear rates. We then showed that the traction force applied by forceps had a more distinct effect, with up to 54% tear prevalence when simulating with traction forces exerted by senior clinicians. It is therefore suggested that future forceps designs include an alert to the clinician when a traction force of 76 N, the average measured for vacuum instrumentation, is exceeded [12]. Birth simulations were also used to evaluate the effect of the length of episiotomy of levator tear rates. It was concluded that 1.5 cm is the minimum cut depth sufficient to keep the levator state parameter below 1 (no tears predicted) for all mothers.

In Chapter 7, we evaluated the effect of pre-distension of the birth canal during the first stage of labor on the duration of the active second stage as well as levator tear outcomes. We found that effects on levator tear outcomes were only observed for distensions of ~9 cm or greater, with an approximately 10% effect dependent upon the distension force chosen. The more distinct effect of the pre-distension was on the duration of the active second stage of labor, which was reduced by as much as an hour for the 15th percentile mother in the case of distension finishing less than 1 hour before the onset of the active second stage of labor. However, a primary limitation here was that the onset of the active second stage is difficult to predict clinically. The achievement of a reduction in the second stage of labor, which is predicted to occur if the second stage of labor begins within ~1 hour of distension completion, may be less apparent for distensions that are completed a longer duration before the beginning of the active second stage, which is difficult to predict. Additionally, waiting too long to begin pre-distension would also be a valid concern because the distension device should be removed prior to the descent of the fetal head into the lower birth canal.

PVM tears may not be the only factor at play in determining the development of pelvic organ prolapse. For this reason, in Appendix 1, we have considered a second observed injury, involving fascia rupture, that has not been commonly studied.

The streamlined nature of these simulations has allowed us to efficiently investigate many scenarios that are clinically relevant, circumventing the many financial and ethical barriers posed by using clinical studies to investigate such matters. It is true, however, that in streamlining our simulation framework, we have had to make simplifying assumptions. One

such assumption is that the cross section of the fetal head, in the plane that it is presented to the birth canal, is circular. This assumption is reasonable for occiput anterior deliveries, which are the most common and least associated with complications. However, a more complex finite element-based modeling framework might better allow for the investigation of the geometric complexities associated with other presentations, such as occiput posterior and breach positions.

Additionally, though these simulation models are the first to be validated using *in vivo* data from a small cohort of term pregnant nulliparous women, model predictions would clearly benefit from validation through a large scale prospective randomized clinical trial because of the variability in tissue behavior we have identified. The larger prospective clinical trial is needed to determine the selectivity and specificity of the computer simulation predictions of levator tear risk and length of second stage. An additional challenge anticipated is the acceptance of such framework by the broader clinical culture and the integration of such framework into regular labor planning and assessment. Such paradigm transitions can take a decade or more because Phase II and Phase III clinical trials are required to prove the clinical effectiveness and reliability of the method. But it is heartening that we do see an increase in interest when our results are presented at clinical meetings.

Overall, this dissertation provides the first biomechanical framework for assessing PVM tear risk prior to delivery. Additionally, our results help to evaluate debates in clinical culture regarding the usage of episiotomies and forceps instrumentation. Specifically, we were able to show that an episiotomy cut to at least 1.5 cm can have a protective effect on the PVM, which will seem

counterintuitive to many clinicians who have seen studies that report a correlation between episiotomies and PVM tear risk, but which fail to control variables that would increase both the risk of PVM injury and the need to an intervention such as episiotomy. Additionally, the result that it is the traction force applied by forceps, and not the space that they occupy, that is responsible for PVM injuries, will surprise some clinicians. However, knowledge of the role of traction force, which can be controlled through intentional use, suggests that with education and awareness of this variable, PVM tear rates may be reduced for this type of instrumentation.

8.1 Bibliography

[1] J. O. L. DeLancey, R. Kearney, Q. Chou, S. Speights and S. Binno, "The Appearance of Levator Ani Muscle Abnormalities in Magnetic Resonance Images After Vaginal Delivery," *Obstetrics and Gynecology,* vol. 101, no. 1, pp. 46-53, 2003.

[2] H. Dietz and A. Steensma, "The prevalence of major abnormalities of the levator ani in urogynaecological patients," *BJOG: an International Journal of Obstetrics and Gynaecology,* vol. 113, no. 2, pp. 225-30, 2006.

[3] H. Dietz, G. AV and P. Phadke, "Avulsion of the pubovisceral muscle associated with large vaginal tear after normal vaginal delivery," *The Australian & New Zealand Journal of Obstetrics & Gynaecology,* vol. 47, no. 4, pp. 341-4, 2007.

[4] A. Olsen, V. Smith, J. Bergstrom, J. Colling and A. Clark, "Epidemiology of surgically managed pelvic organ prolapse and urinary incontinence," *Obstetrics and Gynecology,* vol. 89, no. 4, pp. 501-6, 1997.

[5] F. Smith, C. Holman, R. Moorin and N. Toskos, "Lifetime risk of undergoing surgery for pelvic organ prolapse," *Obstetrics and Gynecology,* vol. 116, no. 5, pp. 1096-100, 2010.

[6] M. Abdel-Fattah, A. Farnilusi, S. Fielding, J. Ford and S. Bhattacharya, "Primary and repeat surgical treatment for female pelvic organ prolapse and incontinence in parous women in the UK: a register linkage study," *BMJ Open,* vol. 1, no. 2, p. e000206, 2011.

[7] T. de Boer, M. Slieker-Ten Hove, B. CW, K. Kluivers and V. ME, "The prevalence and factors associated with previous surgery for pelvic organ prolapse and/or urinary incontinence in a cross-sectional study in The Netherlands," *European Journal of Obstetrics, Gynecology, and Reproductive Biology,* vol. 158, no. 2, pp. 343-9, 2011.

[8] J. Wu, C. Matthews, M. Conover, V. Pate and M. Jonsson Funk, "Lifetime risk of stress urinary incontinence or pelvic organ prolapse surgery," *Obstetrics and Gynecology,* vol. 123, no. 6, pp. 1201-6, 2014.

[9] H. Dietz and J. Simpson, "Does delayed childbirth increase the risk of levator injury in labour?," *The Australian & New Zealand Journal of Obstetrics & Gynaecology,* vol. 47, no. 6, pp. 491-5, 2007.

[10] D. Liao, L. Hee, P. Sandager, N. Uldbjerg and H. Gregersen, "Identification of biomechanical properties in vivo in human uterine cervix," *Journal of the Mechanical Behavior of Biomedical Materials,* vol. 39, no. 1, pp. 27-37, 2014.

[11] G. Rostaminia, J. D. Peck, K. Van Deft, R. Thakar, A. Sultan and S. A. Shobeiri, "New Measures for Predicting Birth-Related Pelvic Floor Trauma," *Female Pelvic Med Reconstructive Surgery,* vol. 22, no. 5, pp. 292-6, 2016.

[12] D. Mishell and J. V. Kelly, "The Obstetrical Forceps and the Vacuum Extractor: An Assessment of their Compressive Force," *Obstetrics and Gynecology,* vol. 19, pp. 204-6, 1962.

Chapter 9: Conclusions

Chapter 2

A. In our geometric capacity-demand analysis, initial pubovisceral muscle (PVM) loop length had the greatest impact on maternal capacity, followed by non-contact length, then subpubic arch angel (SPAA), and finally levator origin separation (Chapter 2).
B. The PVM and puborectal muscle (PRM) loops had the capacity to accommodate 75% of vertex presentation births without injury. But for injury to occur in only 15% of births, as observed clinically, there must be either more fetal head molding than was allowed for, or creep relaxation behavior of the PVM loop under strain, both of which are possible (Chapter 2).
C. Relative to that of the PVM, it is the more caudal origin of the PRM portion of the levator muscle that reduces its stretch ratio at crowning, thereby helping to protect it from the stretch injuries commonly observed in the PVM portion (Chapter 2).
D. The numeric value of the capacity – demand ratio, g, indicates the level of risk for PVM injury during the late stage of vaginal delivery. A g value of 1.0 or more suggests a low probability of cephalolevator muscle disproportion and hence risk of PVM injury due to the conservative assumptions employed in Chapter 2.

Chapter 3

E. In this first *in vivo* and *in situ* quantification of the material properties of the lower human birth canal at the end of pregnancy, the results conclusively demonstrate and quantify the time-dependent relaxation (viscoelastic) behavior of the lower birth canal in nullipara(Chapter 3).

F. The elastic parameters, A and B, had their greatest effect on the amplitude of the lower birth canal strain response. However, the longer of the two time constants, $\tau 2$, was the parameter which had the greatest influence over the temporal response of the lower birth canal to distention (Chapter 3).

Chapter 4

G. For a practical two-step antenatal procedure in the clinic, it is most logical to first measure maternal capacity in order to establish whether it near the 20^{th} percentile, in which case, the fetal head should be measured to gain the additional insight (Chapter 4). In maternal capacity measurements, it is the urogenital hiatus, and not the levator hiatus that should be used (Chapter 2).

H. In certain circumstances, a woman may experience an extended second stage of labor while not being at risk for a levator tear. These include a pairing at the 20th percentile for both maternal capacity and fetal head demand. However, in this case the use of forceps, chosen due to the anticipated long length of labor, could result in a PVM tear in a mother not previously at risk (Chapters 4 and 6).

I. The large range in maternal τ2 values found in Chapter 4 only had a 5% effect on the risk of a PVM tear. Instead it was the geometric lack of fit between fetal head and maternal capacity that was the more important factor (Chapter 4).

Chapter 5

J. Our model was able to predict up to 55% of the variation in the duration of the second stage for the median maternal age group, and 23% of the variation in this duration when considering outlying maternal age groups.

K. We accurately predicted one major PVM tear, and failed to predict a second major tear, as well as the only minor tear observed.

L. The false negatives, or mothers diagnosed with PVM tears but who were not predicted to experience them, were not anatomically at risk for injury, and were significantly older than the rest of the cohort. This suggests that their tissue tore more readily than others in the cohort.

M. The false positives, or those predicted to experience a PVM tear but who did not display a tear upon ultrasound examination, had significantly longer duration of the second stage of labor than the rest of the cohort. This suggests that we were able to accurately predict the difficulty of labor; however, these mothers did not display an injury, despite experiencing a difficult labor, suggesting that the injury criteria may not be constant between subjects.

Chapter 6

N. In simulations of forceps traction force application, risk of a PVM tear increased with the magnitude of traction force (Chapter 6).

O. The application of forceps later in the second stage as well as maintaining partial traction between contractions was predicted to decrease the risk of PVM tear when other maternal and fetal factors remained constant (Chapter 6).

P. In terms of the duration of active second stage, both early forceps application and large traction forces were predicted to result in reduced durations when compared with later forceps application or lower traction forces (Chapter 6).

Q. The addition of a traction-force limiting handle to forceps is predicted to reduce PVM injury risk.

Chapter 7

R. In the pre-distension of the lower birth canal simulations, increasing the target distension diameter of the birth canal was predicted to shorten the active second stage of labor. This effect could be of particular benefit in reducing complications associated with long labors (Chapter 7).

S. Increasing lower birth canal distension force resulted in a tradeoff between the large decrease in time to target lower birth canal distension, corresponding to lower patient burden, but a slight increase in predicted PVM tear risk (Chapter 7).

T. Intermittent distention loading increased the time to reach the target lower birth canal distension value, with no observable benefit to the duration of the active second stage or PVM tear risk (Chapter 7).

Chapter 10: Suggestions for Future Research

1) The primary suggestion for future work is a large scale prospective randomized clinical trial with the goal of validating these model predictions. Outcomes of this trial would be the specificity and selectivity of the pubovisceral muscle (PVM) tear predictions. Predictions for the duration of the active second stage could also be scored. However, due to the variability in tissue behavior identified in Chapter 4, it would be difficult to make these predictions without quantification of the long time constant, τ_2, in each individual. The goal of these clinical trials would be to prove the clinical effectiveness and reliability of this method for predicting levator ani muscle tears.
2) It is also recommended that the quantification of viscoelastic properties be conducted for subject populations not represented by the Chapter 4 subject pool. Such quantification could be done using the Chapter 4 methods, but would require new clinical trials designed to target more diverse subject populations. Of particular interest are multiparas. All of the subjects represented in Chapter 4 were nullipara. As it is anecdotally noted that an obstetrician can tell immediately if a woman has given birth, it is clear that the tissues do not completely recover back to the same resting status that they held prior to the first delivery. Observations also show that multiparas, on average, have shorter labors than nulliparas [1, 2]. It would be interesting to quantify which

components of the viscoelastic relationship reflect these changes. For example, one could test the null hypothesis that all reduction in the duration of labor is due to the enlarged resting anatomy, and not due to changes in the viscoelastic constitutive relationship.

3) An additional subject pool deserving of special attention are the older nullipara because older maternal age at first delivery is linked with increased risk for PVM tears [3, 4]. The reason is presently unknown. It would therefore be interesting to use the Chapter 4 methodology to quantify the viscoelastic material properties of the lower birth canal in older nullipara. This would permit the hypothesis to be tested as to whether the effects of "hormonal ripening" on tissue properties are less pronounced in older mothers because of longer birth canal tissue relaxation time constants, less elastic tissue behavior, or both.
4) A related analysis that would not require a new clinical trial would be the secondary analysis of data collected for increases in levator hiatus during pregnancy [5, 6]. If the extant data were re-segmented by maternal age, it would be possible to test if there are any differences between younger and older mothers in the amount of change in the levator hiatus during pregnancy, or in the final levator hiatus achieved at the 37 week gestation measurement.
5) Given the results suggesting that increased tension force is responsible for the increase in levator tear rates observed in forceps, but not in vacuum assisted deliveries (Chapter 6), the development of force-limiting forceps may be warranted.

6) Future research could also involve improvements in our current modeling technique. For example, maternal fatigue could be incorporated into our current model as a gradual reduction in intrauterine pressure. Our group has attempted to quantify the specific time course of this fatigue in the past by asking non-pregnant volunteers to push with the same strength observed for laboring mothers. However, in that study, pushing alone was not enough to fatigue the volunteers. The high oxygen demand by the uterus during labor may account for the distinct increase in fatigue observed in laboring mothers. In order to properly represent these effects in simulations, it would be best to acquire intrauterine pressure readings over a long enough duration to capture the threshold for fatigue as well as the nature of the decline (i.e., rapid or gradual, and the magnitude of change). The inclusion of maternal fatigue in the analysis would allow one to account for the added benefits of being able to deliver before the onset of fatigue limits further progress. In studies where the duration of the active second stage is an outcome of interest, knowledge of a fatigue point would allow us to directly compare if variations in an intervention reduce the duration of labor enough to avoid distinct maternal fatigue. Incorporation of maternal fatigue would also itself affect the predicted duration of the active second stage, because a reduction in maternal effort (pushing force) later in labor would be anticipated to increase the duration of labor.
7) Our modeling technique could also be improved once results are available for a current study of the histologic and material property changes observed in the perineal body during late pregnancy. It has previously been hypothesized that the perineal body forms

a “fusible link” in the birth canal, and that it may be able to reduce the strains in surrounding tissues through an increase in its own extensibility [7]. The data currently being collected could be used to validate and help to quantify the nature of this phenomenon, so that it may be incorporated into future birth simulations.

8) The levator hiatus is often used as the traditional measure of the soft tissue aperture in the female pelvic floor, and has been the focus of studies tracking anatomical changes during pregnancy [8, 9, 10, 11, 5, 6]. But insights from Chapter 2 made us realize that it is the urogenital hiatus that is the true outlet aperture in the second stage of labor. So, future studies should focus on the change in the urogenital hiatus diameter in preparation for birth as well as during birth.
9) Given the results of our clinical validation attempts in Chapter 5, a study into the factors affecting injury threshold, such as older maternal age, may be merited. Due to ethical concerns, it is difficult to test tissue from pregnant humans to failure. However, in the case of mothers delivering by planned Cesarean, with no plans for future vaginal deliveries, the acquisition of tissue samples at the time of Cesarean delivery may be possible. In such an experiment, it is recommended that, prior to testing to failure, the tissue be cyclically loaded to mimic the strain environment experienced during labor. Additionally, it is recommended that multiple samples be collected from the same subject, if possible, so that micro-failure, or failure on the single muscle fiber level can be quantified in tissue that has not reached ultimate failure. As this damage may accumulate over loading cycles, it is recommended that an analysis be conducted in which the number of loading cycles is considered as the independent variable. We

expect an experiment on failure criteria to reveal an accumulation of damage prior to ultimate failure, which may be responsible for some cases of pelvic organ prolapse for which PVM tears are not observed.

10.1 Bibliography

[1] J. Piper, D. Bolling and E. Newton, "The second stage of labor: factors influencing duration," *American Journal of Obstetrics and Gynecology,* vol. 165, no. 4 Pt 1, pp. 976-9, 1991.

[2] A. Vahratian, M. Hoffman, J. Troendle and J. Zhang, "The impact of parity on course of labor in a contemporary population," *Birth,* vol. 33, no. 1, pp. 12-7, 2006.

[3] H. Dietz and J. Simpson, "Does delayed childbirth increase the risk of levator injury in labour?," *The Australian & New Zealand Journal of Obstetrics & Gynaecology,* vol. 47, no. 6, pp. 491-5, 2007.

[4] R. Kearney, J. Miller, J. Ashton-Miller and J. O. L. DeLancey, "Obstetric factors associated with levator ani muscle injury after vaginal birth," *Obstetrics and Gynecology,* vol. 107, no. 1, pp. 144-9, 2006.

[5] F. Siafarikas, J. Staer-Jensen, G. Hilde, K. Bo and M. Ellstrom Engh, "The levator ani muscle during pregnancy and major levator ani muscle defects diagnosed postpartum: a three- and four- dimensional transperineal ultrasound study," *BJOG: an International Journal of Obstetrics and Gynaecology,* vol. 122, no. 8, pp. 1083-91, 2015.

[6] J. Staer-Jensen, F. Siafarikas, G. Hilde, J. Benth, K. Bo and M. Engh, "Postpartum recovery of levator hiatus and bladder neck mobility in relation to pregnancy," *Obstetrics and Gynecology,* vol. 125, no. 3, pp. 531-9, 2015.

[7] J. A. Ashton-Miller and J. O. L. DeLancey, "On the Biomechanics of Vaginal Birth and Common Sequelae," *Annual Review of Biomedical Engineering,* vol. 11, pp. 163-176, 2009.

[8] J. Staer-Jensen, F. Siafarikas, G. Hilde, K. Bo and M. Engh, "Ultrasonographic evaluation of pelvic organ support during pregnancy.," *Obstetrics and Gynecology,* vol. 122, no. 2 Pt 1, pp. 329-36, 2013.

[9] G. van Veelen, K. Schweitzer and C. van der Vaart, "Ultrasound imaging of the pelvic floor: changes in anatomy during and after first pregnancy," *Ultrasound in Obstetrics & Gynecology,* vol. 44, no. 4, pp. 476-80, 2014.

[10] S. Oliphant, I. Nygaard, W. Zong, T. Canavan and P. Moalli, "Maternal adaptations in preparation for parturition predict uncomplicated spontaneous delivery outcome.," *American Journal of Obstetrics and Gynecology,* vol. 211, no. 6, pp. 630.e1-7, 2014.

[11] S. Chan, R. Cheung, K. Yiu, L. Lee, T. Leung and T. Chung, "Pelvic floor biometry during a first singleton pregnancy and the relationship with symptoms of pelvic floor disorders: a prospective observational study," *BJOG: an International Journal of Obstetrics and Gynaecology,* vol. 121, no. 1, pp. 121-9, 2014.